Tissue expression and functional insights into HIF prolyl hydroxylase domain enzymes

A thesis submitted for the degree of doctor of philosophy

University of Oxford

J. Bhathiya Wijeyekoon

Wolfson College

Trinity Term 2013

DEDICATION

In loving memory of my grandparents, 'Archchi and Seeya' Wijeyekoon

ABSTRACT

Bhathiya Wijeyekoon *D.Phil. Thesis*

Wolfson College *Trinity 2013*

TISSUE EXPRESSION AND FUNCTIONAL INSIGHTS INTO HIF PROLYL HYDROXYLASE DOMAIN (PHD) PROTEINS

This research programme investigated the expression of prolyl hydroxylase (PHD) proteins in rodent tissues. The importance of PHD enzymes lies in their ability to render oxygen sensitivity to Hypoxia inducible factor (HIF), the principal mediator of intracellular oxygen homeostasis. The first part of this study focused on developing and validating anti-sera capable of detecting PHD proteins in rodent tissues. With these reagents, it was possible to assess the relative expression of each PHD protein in a number of different rat tissues. PHD2 was the most abundant isoform in all tissues studied. In contrast, an abundance of PHD1 was observed only in testis and skeletal muscle. A number of different tissue species of PHD3 were identified and their abundance was found to vary between different tissues.

These observations provide further evidence of the principal role of PHD2 in regulating HIF in vivo, but also point towards additional roles for PHD1 and PHD3 in selected tissues. They highlight the potential for there being a complex interplay between different PHD enzymes which could, in the future, prove potential targets for therapeutic manipulation. This study also provides additional insights into the mechanisms underlying the phenotypes observed in PHD deletional mouse models which appear, in many cases, to be directly related to the abundance of a given PHD isoform.

The emerging role of PHD3 as a promoter of sympathetic lineage apoptosis prompted further study of PHD3 expression in rat neuronal tissues. An abundance of PHD3 was demonstrated throughout the rat sympathetic nervous system, a finding which appeared at odds with its known role as a promoter of neuronal apoptosis and resulted in a series of collaborative studies which demonstrated a sympatho-adrenal phenotype in wild type compared to PHD3-/- mice. Further collaborative studies utilising wild type mice and those deleted of specific PHD isoforms, were carried out to assess the significance of the abundance of PHD3 and PHD1 noted here in rat hippocampus and testis respectively. While neither study demonstrated statistically significant phenotypes, these observations remain of interest and areas for future research.

ACKNOWLEDGMENTS

I am indebted to my supervisor, Professor Chris Pugh for his guidance, encouragement, tutorage and patience throughout this work. I also wish to thank all members of the Ratcliffe group for their support and help, in particular Professor Peter Ratcliffe, Dr Tammie Bishop, Dr Ya-Min Tian and Lynn Nichols. I am grateful to Dr Keith Buckler, Dr Robert Deacon and Professor Zoltan Molnar in the departments of Physiology, Psychology and Anatomy respectively for their tutorage. I wish also to thank Wolfson College for accepting me as a graduate student and the MRC for funding my work. Last but not least I wish to thank my wife Anju, without whose support none of this would have been possible.

LIST OF ABBREVIATIONS USED IN THIS THESIS

ABC, Avidin-Biotin complex

APS, ammonium persulfate

BSA, bovine serum albumin

CIP, calf intestinal phosphatase

COS, African green monkey kidney cell line

dNTP, deoxcynucloside triphosphate

DAB, diaminobenzidine

DAPI, 4', 6-diamidion-2-phenylindole

DMEM, Dulbecco's modified eagle's medium

DMSO, dimethyl sulphoxide

DTT, 1,4-dithiothreitol

EDTA, ethylenediaminetetraacetic acid

EGTA, ethylene glycol tetraacetic acid

FITC, fluorescein isothiocyanate

HEPES, 4-(2-hydoxyethyl)-1-piperazineethanesulfonic acid

HRP, horseradish peroxidase

IHC, immunohistochemistry

IPTG, isopropyl-β-D-thiogalactoside

IVTT, in vitro transcription and translation

LB, Lysogeny broth

MOPS, 3-(N-morpholino)-propanesulfonic acid

Na3VO4, sodium orthovanadate

NaAc, sodium acetate

NaCl, sodium chloride

NaF, sodium fluoride

NaOH, sodium hydroxide

NEB, New England Biolabs

OCT, optimal cutting temperature

PAF, paraformaldehyde

PBS, phosphate buffered saline

PBST, PBS containing 0.1% Tween 20

PCR, polymerase chain reaction

PMSF, phenylmethanesulphonylfluoride

SCG, superior cervical ganglion

SDS, sodium dodecyl sulfate

TAQ, Thermous aquaticus

TBE, Tris borate EDTA

TEA, triethanolamine

TEMED, tetramethylethylenediamine

TABLE OF CONTENTS

Section 1: Introduction

Chapter1. Background to this study 1

1.1 Hypoxia inducible factor (HIF) 2

1.1.1 HIF and its regulation in vitro 2

1.1.2 The importance of HIF in vivo 3

1.1.3 Hypoxic regulation of HIF in tissues 8

1.2 PHD enzymes, an overview of their biology and related topics 11

1.2.1 The discovery of prolyl hydroxylase domain (PHD) enzymes 11

1.2.2 Characteristics of HIF prolyl hydroxylases domain (PHD) enzymes 12

1.2.3 Characteristics of sympathetic lineage cell types and the autonomic nervous system 16

1.2.4 PHD3 and neuronal apoptosis 21

1.2.5 Tumours of the autonomic nervous system and the putative role of PHD3 in their aetiology 24

1.2.6 The importance of PHD1 and 2 in the whole animal 28

1.3 Reasons to study the expression of PHD enzymes 32

1.3.1 In relation to previous mRNA studies of PHD tissue abundance 32

1.3.2 In relation to drug design and therapeutics 34

1.4 Studies relating to protein abundance of PHD enzymes in tissues at the time of commencing this doctoral thesis 37

1.5 Aims of this doctoral thesis 38

Section 2: Methods

Chapter 2. Overview of methods 39

2.1 Recombinant DNA techniques 40

2.1.1 Generic recombinant DNA techniques 40

2.1.1.1 Bacterial culture for plasmid DNA mini preparation 40

2.1.1.2 Mini preparation of plasmid DNA from bacterial culture 40

2.1.1.3 Agarose gel electrophoresis 41

2.1.1.4 Purification of DNA 41

2.1.1.5 Purification of DNA from solution 42

2.1.1.6 Subcloning DNA into pGEX plasmids 43

2.1.2 Design and generation of recombinant protein immunogens to mouse PHD isoforms 43

2.1.2.1 Rationale 43

2.1.2.2 Recombinant DNA techniques used to generate new PHD1 Immunogens 45

2.1.2.3 Recombinant DNA techniques used to generate new antibodies to mouse PHD2 50

2.1.2.4 Recombinant DNA techniques used to generate new antibodies to mouse PHD3 52

2.1.3 Recombinant DNA techniques used to generate T7 promoter driven cDNA for each mouse PHD 1 and 3 54

2.1.3.1 Rationale 54

2.1.3.2 Restriction endonuclease and reaction conditions used to generate T7 promoter driven cDNA for mouse PHD1 and 3 55

2.1.4 Generating a cDNA containing the full length mouse PHD2 open reading frame 56

2.2 Protein Expression in bacteria / IVTT / COS cells 60

2.2.1 Expression of recombinant mouse PHD protein in bacteria 60

2.2.1.2 Bacterial transformation 60

2.2.1.3 Expression of recombinant protein in bacteria 60

2.2.1.4 Extracting recombinant protein from bacteria 61

2.2.1.5 Determining the concentration of expressed recombinant bacterial protein 62

2.2.2 Methods used to express full length mouse PHD proteins 62

2.2.2.1 Rationale 62

2.2.2.2 IVTT expression and normalisation of PHD proteins 62

2.2.3 Expression of PHD isoforms in COS cells 63

2.2.3.1 COS-7 cell culture 63

2.2.3.2 COS-7 Cell transfection 64

2.3 Antibodies 65

2.4 Conjugation of Fluorescein isothyocyanate (FITC) to anti-PHD3 mouse monoclonal antibody (188e) 68

2.4.1 Rationale 68

2.4.2.1 Protein G bead based purification of 188e mouse monoclonal antibody 68

2.4.3 FITC conjugation 69

2.4.4 Isolation of FITC conjugated antibody 69

2.5 Immunoblot 70

2.6 In situ hybridisation 73

2.6.1 Rationale 73

2.6.2 PHD3 mRNA probes 73

2.6.3 In situ hybridisation 74

2.7 Animal hypoxia and tissue preparation 75

2.7.1 Animal hypoxia studies 75

2.7.2 Whole tissue protein preparation for immunoblot 76

2.7.3 Preparation of nuclear proteins from tissues for immunoblot 77

2.7.4 Perfusion fixation and processing of tissues for IHC 78

2.7.5 Embedding and sectioning of tissues 79

2.7.6 Processing of frozen tissues 80

2.7.7 COS cell pellet synthesis for IHC 80

2.7.8 Identifying brain regions 81

2.8 Immunohistochemistry 81

2.8.1 Generic immunohistochemistry methods 81

2.8.2 Streptavidin-biotin-peroxidase based IHC 83

2.8.3 HRP-conjugated polymer based IHC 83

2.8.4 Avidin-Biotin complex method based IHC 84

2.8.5 Immunofluorescence 84

2.8.6 Quantitation of IHC PHD3 signal in tissues of the peripheral nervous system 85

2.9 Determining the sequence of PHD3 in PC12 cells 85

2.9.1 Rationale 85

2.9.2 Designing primers to rat PHD3 86

2.9.3 RNA extraction from PC12 cells 87

2.9.4 Synthesis of first strand cDNA from PC12 cell RNA 89

2.9.5 Polymerase chain reaction (PCR) amplification of segments of PHD3 from PC12 cells using first strand cDNA as template 90

2.10 Psychometric tests 90

2.10.1 Rationale 90

2.10.2 T- maze alternation 91

2.10.3 Burrowing 92

2.10.4 Nest building 93

2.10.5 Hoarding 94

Section 3: Results

Chapter 3. Identification and generation of antibodies with the ability to recognize rodent PHD isoforms specifically at endogenous levels in tissues 96

3.1 Generating recombinant protein immunogens to mouse PHD isoforms 97

3.2 Generating full length mouse and rat PHD proteins by IVTT 103

3.3 Testing the sensitivity and specificity of antibodies to mouse PHD proteins 106

Chapter 4. Determining the relative expression of PHD protein in a range of different rodent tissues from healthy animals exposed to normal atmospheric oxygen levels 117

4.1 Characterising the expression of PHD protein in mouse tissues 118

4.1.1 Characterising the expression of PHD1 in mouse tissues 118

4.1.2 Characterising the expression of PHD2 in mouse tissues 122

4.1.3 Characterising the expression of PHD3 in mouse tissues 124

4.2 Characterising the expression of PHD isoforms in rat tissues 130

4.2.1 Characterising the expression of PHD1 in rat tissues 130

4.2.2 Characterising the expression of PHD2 in rat tissues 134

4.2.3 Characterising the expression of PHD3 in rat tissues 136

4.2.4 Relative expression of different PHD isoforms in rat tissues 148

Chapter 5. Characterising the expression of PHD3 protein in tissues of the sympatho-adrenal axis 153

5.1. Testing the ability of rat anti-PHD3 antibodies to detect tissue PHD3 by immunohistochemistry 156

5.2 Characterising the cellular expression of PHD3 in sympathetic tissues of the peripheral nervous system 157

5.2.1 Superior cervical ganglion and carotid body 157

5.2.2 Assessing PHD3 mRNA in the rat SCG 159

5.2.3 Co-localisation studies of PHD3 and TH in rat SCG 161

5.2.4 Characterising PHD3 expression in the adult rat carotid body 163

5.2.5 Characterising PHD3 expression in the adult rat adrenal gland 165

5.3 Assessing the subcellular expression of PHD3 in different sympathetic lineage cell populations of the adult rat 169

5.4 Characterising the expression of PHD3 in extra-adrenal chromaffin cells 171

Chapter 6. Establishing if neuronal populations apart from those of the sympatho-adrenal axis also expressed PHD3 173

6.1 Expression of PHD3 in non-sympathetic ganglia of the peripheral nervous system 174

6.1.1 Characterising the expression of PHD3 in the nodose ganglion 174

6.1.2 Characterising the expression of PHD3 in the trigeminal ganglion 177

6.1.3 Characterising the expression of PHD3 in the dorsal root ganglion 178

6.2 Relative PHD3 abundance in sympathetic and non-sympathetic rat ganglia 179

6.3 Characterising the expression of PHD3 in the CNS 181

6.3.1 Characterising the expression of PHD3 in tyrosine hydroxylase expressing cell populations of the CNS 183

6.3.1.1 PHD3 expression in the substantia nigra 183

6.3.1.2 Assessing PHD3 expression in other CNS sympathetic lineage cell types 186

6.3.2 PHD3 expression in other regions of the CNS 187

6.3.2.1 PHD3 expression in the trigeminal and facial cranial nuclei 187

6.3.2.2 PHD3 expression in the hippocampus 189

6.4 Reconciling the expression of PHD3 in adult sympatho-adrenal lineage tissues with its role as a promoter of apoptosis 191

6.5 PHD3 expression in rat lung 198

6.5.1 Characterising the expression of PHD3 in adult rat lung 198

6.5.2 Characterising the expression of PHD3 in developing rat lung 201

6.6 Putative relationships between PHD3 expression and tumourigenesis within the sympatho-adrenal lineage 202

6.6.1 Differences in the species of PHD3 expressed in PC12 cells and sympathetic lineage tissues and possible implications for tumour biology 202

Chapter 7. Understanding the relationship between expression and function of PHD isoforms in tissues 206

7.1 Phenotypic studies of mice with constitutional deletion of individual PHD isoforms 207

7.1.1 Assessing the significance of PHD3 expression within the rat sympatho-adrenal axis 207

7.1.2 Psychometric studies of hippocampal function 208

7.1.2.1 Psychometric assessment of food hoarding 209

7.1.2.2. 'T' maze spontaneous alternation 211

7.1.2.3 Psychometric study of nest building 212

7.1.2.4 Psychometric assessment of burrowing behaviour 212

7.2.3 Characterising the testicular phenotype of PHD1-/- mice 215

Section 4: Discussion

Chapter 8. Discussion 217

8.1 Discussion relating to the relative expression of PHD isoforms in rodent tissues 218

8.1.1 Relationship between the abundance of tissue PHD protein and mRNA 220

8.1.2 Discussion relating to the different protein species of each PHD isoform 222

8.1.3 Implications of differences in the abundance of each PHD isoform for PHD deletional mouse models 228

8.1.3.1 Direct versus indirect nature of deletional models 228

8.1.3.2 Implications of PHD abundance for 'true' and 'functional' PHD levels 232

8.1.3.2.1 Insights gained into the 'true' and 'functional' amounts of tissue PHD2 from the study of PHD2 deletional phenotypes 233

8.1.3.2.2 Insights gained into the 'true' and 'functional' amounts of tissue PHD1 and PHD3 from the study of corresponding deletional mouse models 237

8.1.3.3 Implications of PHD abundance for 'hidden' tissue phenotypes 239

8.1.4 Speculation regarding the impact of tissue PHD abundance on tissue HIF regulation 242

8.1.4.1 PHD2 abundance and tissue HIF regulation: a speculative analysis 242

8.1.4.2 Impact of PHD2 abundance in relation to tissue HIF2: a speculative analysis 243

8.1.4.3 Impact of PHD1 and PHD3 abundance on tissue HIF: a speculative analysis 244

8.1.5 Implications of PHD abundance for drug design and therapeutics 245

8.2 Discussion relating to the expression of PHD3 in rat sympatho-adrenal tissues 248

8.2.1 Discussion relating to stable expression of adult forms of PHD3 during the period of naturally occurring neuronal death 249

8.2.2 Discussion relating to the developmental expression of additional bands in proximity to the 50KDa species of PHD3 250

8.2.3 Discussion relating to the expression of 109KDa species in PHD3 immunoblots of developing tissues 251

8.2.4 Discussion relating to changes in the subcellular expression of PHD3 during development 253

8.3 Insights gained into the development of sympatho-adrenal neoplasia from the study of PHD3 expression 255

8.3.1 Insights gained into the biology of sympatho-adrenal neoplasia from the study of PC12 cell PHD3 257

8.3.2 Insights gained into the predisposition of different autonomic nervous system tissues to neoplastic transformation through the study of PHD3 expression 258

8.3.2.1 PHD3 expression in relation to neoplasms of parasympathetic tissues and carotid body 258

8.3.2.2 PHD3 expression in relation to syndromic neoplasm's of the autonomic nervous system 259

8.3.2.3 PHD3 expression in relation to development of adrenal and extra-adrenal phaeochromocytomas 260

8.3.2.4 PHD3 expression in relation to syndromic tumour predispositions of tissues outside those of the sympatho-adrenal axis 261

8.4 Functional insights gained through collaborative animal studies into PHD3's role in the sympatho-adrenal axis 262

8.5 Other emerging roles for PHD3 within the sympatho-adrenal axis 263

8.6 The study of PHD3 expression in lung 263

8.7 Insights gained from the study of PHD3 expression in other peripheral nervous system tissues 264

8.8 Insights gained from the study of PHD3 expression in the CNS 265

8.9 Achievements of this doctoral study and where they lead 266

Bibliography 269

Section 1: Introduction

Chapter 1. Background to this study

1.1 Hypoxia inducible factor (HIF)

1.1.1 HIF and its regulation in vitro

Hypoxia inducible factor (HIF) is an oxygen sensitive transcription factor which consists of a heterodimer of α and β subunits (Wang et al., 1995). Oxygen regulation is mediated by the α-subunit of which there are three forms termed HIF-1α (Wang et al., 1995), HIF-2α (Tian et al., 1997; Hogenesch et al., 1997; Ema et al., 1997) and HIF-3α (Hara et al., 2001). In normoxia, the HIF-α subunit is degraded thorough interaction with the von Hippel-Lindau protein (pVHL) E3 ubiquitin ligase complex (Maxwell et al., 1999) while in hypoxia, it is stabilised and dimerises with the constitutively expressed β-subunit to form a heterodimeric complex which binds to hypoxia response elements (HREs) of target genes (Huang and Bunn., 1995). Through this mechanism, HIF is able to activate genes involved in the adaptive response to reduced oxygen tensions. These genes include erythropoietin, glucose transporters, glycolytic enzymes, vascular growth factors as well as nitric oxide synthase (Bunn and Poyton., 1996; Wenger and Gassmann., 1997).

These studies demonstrated the ability of HIF to promote a large number of hypoxically inducible genes but the mechanism by which oxygen sensitivity is rendered to HIF remained obscure until the discovery of a novel group of oxygen sensing prolyl hydroxylase domain (PHD) enzymes (Epstein et al., 2001) termed PHD1, 2 and 3. A further enzyme which mediates hydroxylation of a conserved HIF-α subunit asparagine residue has also been identified and termed factor inhibiting HIF (FIH) because of its negative regulatory effects on HIF gene transcription (Lando et al., 2002; Lando et al., 2002; Mahon et al., 2001).

The study of PHD enzymes will form a central part of this doctoral thesis and will be discussed in detail at a later stage of this introduction. The importance of PHD enzymes stems from their ability to render oxygen sensitivity to HIF and in order to appreciate the need to study these enzymes it is first necessary to gain a clear understanding of the importance of HIF.

1.1.2 The importance of HIF in vivo

Perhaps the most convincing evidence of the importance of HIF *in vivo* was provided by genetic deletional studies of different HIF isoforms in rodents. Constitutive deletion of HIF-1α in mice resulted in early embryonic death from neural tube defects, cardiovascular malformations, and cephalic growth arrest (Iyer et al., 1998). Several different HIF-2α constitutional deletional phenotypes have been described. Initial studies demonstrated intrauterine death of HIF-2α-/- mice at day 12.5 post-conception either from reduced circulating catecholamine and severe bradycardia or marked vascular abnormalities (Tian et al., 1998; Peng et al., 2000; Compernolle et al., 2002). Other HIF-2α constitutional deletional studies produced viable animals which went on to develop a syndrome of multiple-organ pathology characterised by retinopathy, hepatic steatosis, cardiac hypertrophy, skeletal myopathy, hypocellular bone marrow, azoospermia and mitochondrial abnormalities (Scortegagna et al., 2003).

Of late, more targeted gene deletions have been achieved and these conditional deletional models have allowed for a greater finesse when matching genotype to phenotype. Conditional deletion of HIF-1α in the myeloid lineage was found to result in profound impairment of myeloid cell aggregation, motility, invasiveness and bacterial killing, a consequence of reduced cellular ATP pools (Cramer et al., 2003).

A similar reduction in cellular ATP levels was noted in cardiomyocytes conditionally deleted of HIF-1α; these rodents demonstrated a phenotype characterised by reduced myocardial contractility, diminished cardiac vascularisation and cardiac hypertrophy (Huang et al., 2004).

The study of solid tumours complemented these genetic studies and provided additional insight into the importance of HIF. Von Hippel-Lindau (VHL) disease is a hereditary cancer syndrome characterised by CNS and retinal haemangioblastomas, clear–cell renal carcinomas and phaeochromocytomas. Germline inactivation of the VHL gene causes a hereditary cancer syndrome while somatic mutations of this gene have been linked to the development of sporadic haemangioblastomas and clear-cell renal carcinomas (Kim and Kaelin., 2004). The demonstration that the HIF-α subunit was stabilised in cells devoid of wild type pVHL (Maxwell et al., 1999) linked HIF to these hereditary and sporadic cancer syndromes.

Furthermore, the study of tumour biology has demonstrated that tumour hypoxia is associated with a poorer prognosis. HIFα isoforms were found to be expressed in the hypoxic regions of a number of different solid tumours (Onita et al., 2002), in both tumour parenchyma and tissue macrophages (Talks et al., 2000). There is evidence to show that HIF-1α is associated with tumour growth and progression as demonstrated in studies of embryonic stem (ES) cell derived from HIF-1α null tumours (Ryan et al., 1998) and mouse tumour xenografts (Maxwell et al., 1997). Paradoxically, there is also evidence to suggest that HIF-1α may slow tumour progression as demonstrated in a study of astrocytomas (Blouw et al., 2003). When HIF-1α deletional astrocytomas

were injected into the brains of mice they showed a more aggressive phenotype compared to wild type.

The pro-tumourigenic and anti-tumourigenic properties of HIF highlighted in these studies appears to be influenced by tissue environment as demonstrated when subcutaneous injection of the same HIF-1α deletional astrocytomas, produced a less aggressive phenotype (Blouw et al., 2003). Other studies demonstrated that over-expression of HIF-2α but not HIF-1α promoted growth of renal cell carcinoma (RCC) cell-lines (Maranchie et al., 2002), yet inhibited growth of breast carcinoma cell-lines (Blancher et al., 2000), suggesting that these HIFα isoforms had distinct functions in tumour biology. Further studies in VHL-defective RCC cell lines demonstrated that the expression of pro-tumourigenic genes such as cyclin D1, transforming growth factor alpha (TGFα), and vascular endothelial growth factor (VEGF) was promoted by HIF-2α while expression of pro-apoptotic genes such as BNIP3, while being promoted by HIF-1α, were negatively regulated by HIF-2α (Raval et al., 2005). These studies serve to demonstrate the complex nature of the interplay between different HIF isoforms and the tissue milieu in tumour biology.

Recent studies have demonstrated additional roles for HIF in other human diseases as exemplified by studies of hereditary polycythaemia syndromes. Polycythaemia is defined as a condition in which the red cell mass is greater than 125% of predicted (McMullin et al., 2005). Broadly speaking, primary polycythaemia can be divided into three groups. In the first group, an increase in red cell mass occurs due to clonal expansion of a neoplastic red cell precursor, a condition called polycythaemia rubra vera. This condition is usually associated with low serum

erythropoietin (Epo) levels. In the second, suppressed Epo levels are associated with a defect of Epo signalling, usually due to enhanced Epo receptor (EpoR) function. In the third group, termed hereditary polycythaemia syndromes, Epo levels tend to be abnormally elevated and associated with a defect of oxygen sensing. Chuvash polycythaemia (CP) is a form of hereditary polycythaemia named after the Chuvash Republic of the former Soviet Union where the recessive form of the disease is endemic. In a diseased cohort, a VHL recessive mutation was identified different to the dominant mutations known to causes the VHL syndrome of phaeochromocytoma's, renal cell carcinoma and CNS haemangioblastomas. CP affected individuals have a homozygous germline mutation in exon 3 of the VHL gene resulting in Adenine to Thymine substitution at nucleotide 598 which impairs the binding of the VHL gene product to HIF-2α. This impairment reduces the rate of HIF-2α degradation, stabilises HIF and increases expression of HIF target genes in normoxic. Other mutations of *VHL* have since been described in adult and childhood polycythaemia syndromes (Percy et al., 2003; Pastore et al., 2003). Recently a gain-of-function missense mutation of HIF-2α resulting from glycine to tryptophan substitution at amino acid 537 of human HIF-2α was demonstrated in kindred with another hereditary polycythaemia (Percy et al., 2008). The impact of CP on human physiology was assessed and demonstrated to result in exercise induced skeletal muscle phosphocreatine depletion, elevated blood lactate and a reduction in maximum exercise capacity, further emphasising the importance of HIF (Formenti et al., 2010). Familial polycythaemia due to mutations of PHD2 have also been identified and these will be discussed later in this thesis.

In contrast to HIF-1α and HIF-2α the role of HIF-3α in human disease has yet to be established. Three of the six HIF-3α splice forms are subject to oxygen dependent degradation in a PHD and VHL dependent manner (Maynard et al., 2003). Therefore dis-regulation of HIF-3α splice forms 1, 2 and 3 may have implications for normal physiology and pathological states.

These studies demonstrated the importance of HIF in the context of complex mammalian tissues as a master regulator of hypoxic genes, playing a central role in a range of normal and disease processes which include angiogenesis, energy metabolism, tumour biology as well as disorders of inflammation. Importantly they highlighted the need for tight control of HIF and demonstrated that both over and under expression of HIF can cause significant pathology in the complex environment of mammalian tissues.

The dual effects of HIF on cell survival pose important questions for treating human disease. In tumour biology, it would clearly be beneficial to shift the balance towards apoptosis and cell death, the opposite is true for conditions such as stroke and ischaemic heart disease. The importance of HIF is therefore clear and it has been proposed that modulating HIF may provide new approaches to managing these and other conditions (Giaccia et al., 2004).

In order to consider manipulating the HIF system, it was necessary to have an understanding of HIF regulation in complex mammalian tissues and studies pertaining to this will now be described.

1.1.3 Hypoxic regulation of HIF in tissues

The distribution of HIF-1α in mice subjected to varying concentrations of inspiratory oxygen was determined (Stroka et al., 2001). Immunohistochemical analysis of normoxic tissues which included brain, kidney, liver, heart and skeletal muscle revealed that HIF-1α was expressed at low levels in specific normoxic cell types. HIF-1α expression was found to be markedly enhanced by hypoxia. In hypoxic brain, HIF-1α was detected in neurons of the cerebral cortex, dentate gyrus and Purkinje cells of the cerebellum. In hypoxic kidney, staining was seen in the distal convoluted tubule, and was in keeping with known renal hypoxic gradients. Wide spread nuclear staining of hepatocytes was seen in hypoxic liver, which despite the presence of a known liver oxygen gradient, did not follow a zonal distribution. In heart, staining was demonstrated in the nuclei of myocytes, arterial endothelial and smooth muscle cells.

This study (Stroka et al., 2001), also demonstrated that 1 hr hypoxic exposure (FiO2 8%) was sufficient to increase HIF-1α expression in brain and that a maximum level was achieved after 4 to 5 hr exposure. Despite on-going hypoxia, HIF-1α expression decreased and returned to normoxic levels by 12 hr. In the kidney and liver, little effect was seen with 8% FiO2 but with 6% FiO2 exposure, HIF-1α expression again quickly increased after 1 to 2 hr and declined to undetectable levels 2 to 4 hr later.

A subsequent study in rats explored the expression of HIF-2α under different oxygen tensions (Wiesener et al., 2003). Unlike HIF-1α, HIF-2α was not detectable in normoxia but was induced by hypoxia (FiO2 8%) in all organs investigated which included the brain, heart, lung, kidney, liver, pancreas and intestine. While HIF-1α

expression in kidney and liver was only transient and returned to baseline at 3 hours, the expression of HIF-2α in these organs was sustained for more than 6 hours. Further comparison of the two studies showed that a more severe hypoxic stimulus was needed to induce HIF-1α compared to HIF-2α. The type of cells expressing HIF-1α and 2α also appeared to vary between organs. In kidney, HIF-2α was expressed in glomerular and peritubular endothelial cells compared to HIF-1α which was expressed in the renal tubule. In brain, HIF-2α was expressed in endothelial and glial cells, while HIF-1α was expressed in neuronal cells. In liver, HIF-2α expression in hepatocytes followed a zonal distribution in keeping with known liver oxygen gradients which was in contrast to HIF-1α. Although some of these differences could be accounted for by different experimental conditions including different rodent species and specificity / sensitivity of the assay procedures, overall they demonstrate that hypoxia does regulate HIF *in vivo* and that there are similarities as well as differences between HIF-1α and HIF-2α in terms of expression kinetics, cell populations, and required hypoxic drive. Importantly they demonstrate that HIF-1α and 2α appear to be expressed in different cell populations. Of particular relevance is the predominant expression of HIF-1α in neuronal cells, cardiac myocytes and renal tubule, which may pre-condition such cells to apoptotic cell death under conditions of hypoxic stress. Indeed, either suppression of HIF-1α or promotion of HIF-2α before, during or after a hypoxic insult may help to improve tissue survival.

It is intriguing that low levels of HIF-1α were detected in normoxic brain, kidney, liver and heart. In reality oxygen gradients exist within tissues which arise from factors such as blood oxygen content, distance between a region of tissue and blood vessel, the permeability of the tissue to oxygen and the rate of tissue oxygen consumption. Therefore even in normal ambient oxygen many tissues exist in relative

hypoxia and oxygen tensions of between 4% and 5% have been recorded in liver (Wolfle et al., 1983); 3% to 4% in the renal cortex (Epstein et al., 1994; Schurek et al., 1990); 3% in the myocardium and epicardium (Rumsey et al., 1994) and 3% in regions of the cerebral cortex during stroke (Whalen et al., 1970). Occlusion of a distal branch of the left anterior descending artery for 1 min resulted in myocardial oxygen tension of near 0% (Rumsey et al., 1994).

These studies clearly demonstrate that hypoxia effects the expression of HIF not only in cultured cells but also in the setting of complex mammalian tissues. A number of cell-line based studies however have demonstrated that HIF expression can also be influenced by non-hypoxic regulatory processes which include growth factors (Feldser et al., 1999; Richard et al., 2000); cytokines (Hellwig-Burgel., 1999), vascular hormones (Gorlach et al., 2001; Richard et al., 2000), lipoplysaccharides derived from macrophages (Blouin et al., 2004) and viral proteins (Moon et al., 2004). Non-hypoxic HIF regulatory processes are also likely to influence the expression of HIF in complex mammalian tissues, indeed the overall level of tissue HIF is likely to be a product of the interplay between hypoxic and non-hypoxic HIF regulatory pathways.

A complex picture of HIF regulation at the whole animal level is emerging. What is important to this doctoral thesis is the establishment through the work of Stroka and Wiesener that hypoxic regulation of HIF takes place in many complex mammalian tissues. This together with the knowledge that HIFα chain abundance is a function of PHD enzyme activity (Epstein et al., 2001), a concept that will be further developed in the next section, makes the study of PHD enzymes important, particularly when

considering ways to manipulate the HIF system. Studies relating to PHD enzymes will be discussed next.

1.2 PHD enzymes, an overview of their biology and related topics

1.2.1 The discovery of prolyl hydroxylase domain (PHD) enzymes

It was observed that in von Hippel Lindau (VHL) disease derived renal cell-lines, HIF-1α and HIF-2α were expressed at a high level in both normoxic and hypoxic conditions (Maxwell et al., 1999). This study went on to demonstrate that reintroduction of VHL into these cell-lines was able to restore oxygen sensitivity, reducing HIFα subunit abundance to undetectable levels in normoxia. Further studies demonstrated that HIF-1α was targeted for degradation in normoxia by a multi-protein ubiquitin E3 ligase complex and that VHL was needed to allow this complex to interact with HIF-1α (Cockman et al., 2000; Ohh et al., 2000). The demonstration that HIF-1α degradation in normoxia could be inhibited by iron chelators such as cobalt chloride and desferrioxamine (DFO) (Wang and Semenza., 1993), implied that a ferro-protein was also necessary for HIF targeting. Mass spectrometric analysis of a synthetic HIF-1α containing the minimal oxygen degradation domain demonstrated hydroxylation of proline residue 564, when treated with normoxic but not hypoxic cell extracts (Ivan et al., 2001 ; Jaakkola et al., 2001). Taken together these results pointed towards the function of a ferro-protein with hydroxylase activity. The only know ferro-hydroxylases able to hydroxylate proline were the collagen-4-prolyl hydroxylases. The active site of these enzymes is formed by a β barrel jelly-roll motif. A bioinformatics search using this conserved region led to the identification of the *egl-9* gene in *Caernorhabditis elegans* and three mammalian homologs termed ‘prolyl

hydroxylase domain containing' (PHD) enzymes 1, 2 and 3 (Epstein et al., 2001). In a series of experiments carried out under controlled oxygen tensions it was demonstrated that the activity of recombinant human PHD1 was sensitive to graded levels of hypoxia suggesting that the PHD's were primary oxygen sensing enzymes (Epstein et al., 2001).

1.2.2 Characteristics of HIF prolyl hydroxylases domain (PHD) enzymes

The three PHD's form part of the 2-oxoglutarate dependent dioxygenase family of ferro-proteins (Epstein et al., 2001). Secondary structure analysis demonstrates that this family of enzymes fold to produce a common jelly roll structure that positions a non-haem iron coordinating HXD….H motif at the catalytic site. Studies have indicated that this class of enzymes function by ordered binding of iron II, 2-oxoglutarate, and substrate (Zhang et al., 2000; Zhou et al., 1998). An important aspect of the enzymatic hydroxylation reaction is that it is predicted to be unidirectional. The specific activities of PHD 1, 2 and 3 have been shown to be roughly comparable (Tuckerman et al., 2004). This means that changes in the abundance of PHD enzyme significantly alters the reaction rate at any given oxygen tension, and provides a mechanism to control the degree of HIF hydroxylation.

It was demonstrated that PHD's were able to hydroxylate human HIF-1α at pro-564 and pro-402 (Ivan et al., 2001; Jaakkola et al., 2001; Masson et al., 2001). Human *PHD1* is located on chromosome 19q13.2 and encodes a protein of 407aa (Bruick and McKnight., 2001; Epstein et al., 2001). A further study identified PHD1 as a protein termed Falkor, the C-terminal of which conferred resistance to cisplatin induced growth arrest in cultured mouse embryonic fibroblasts (MEFs) (Erez et al.,

2002). When over-expressed as an epitope tagged protein, human PHD1 was found to localise to the nucleus (Metzen et al., 2003 ; Oehme et al., 2002).

Human *PHD2* is located on chromosome 1q42-43 and was originally identified as a gene associated with major psychosis (C10RF12) (Dupuy et al., 2000). It encodes a 426aa protein (Bruick and McKnight., 2001; Epstein et al., 2001), which localises to the cytoplasm as an epitope tagged over-expressed form (Metzen et al., 2003). *PHD3* is located on chromosome 14q13.1 and was originally identified as a rat smooth muscle growth factor responsive gene termed SM-20 (Wax et al., 1994). In this study its expression was found to be promoted by angiotensin II and platelet derived growth factor as well as forskolin and the catecholamine, isoproterenol. PHD3 (SM-20) was later detected after activation of a temperature-sensitive p53 protein in fibroblasts (Madden et al., 1996). Human PHD3 encodes a 230aa protein (Taylor et al., 2001) which is expressed in the nucleus and cytoplasm as an epitope tagged over-expressed form (Metzen et al., 2003).

The advent of small inhibitory RNA technology (siRNA) enabled a detailed study of individual PHD isoform expression and function in cell lines. These studies measured the effect of individual PHD isoform suppression against induction of HIF-1α and its target genes. In all cell lines examined, PHD2 mRNA was the most abundantly expressed isoform and its suppression in normoxia was sufficient to induce HIF-1α and its target genes (Berra et al., 2003). A study of PHD proteins in cell lines found that normoxic levels of PHD1 and 3 were far less than that of PHD2. Suppression of PHD1 and 3 isoforms in normoxia was found to have no discernible effect on the expression of HIF-1α or its target genes (Appelhoff et al., 2004). These

results highlighted the central role played by PHD2 in regulating the abundance of normoxic HIF-1α. However the role played by other PHD's in regulating the abundance of HIF-α subunits needed to be clarified. In particular, it needed to be established if reducing the abundance of PHD1 and 3 failed to influence normoxic HIF-1α levels due to too little of these isoforms being expressed in the cell-lines under study or due to a reduction in their enzyme activity.

For PHD1, this issue was addressed by using a previously characterised BT-474 cell line in which PHD1 could be induced by oestrogen (Seth et al., 2002). Oestrogen induction significantly increased normoxic PHD1 expression to a level comparable with that of PHD2. In this setting, suppression of PHD2 alone was compared with suppression of both PHD1 and 2, demonstrating that PHD1 also had the ability to increase the abundance of HIF-1α in normoxia (Appelhoff et al., 2004). Assessing the impact of PHD3 required a different approach. PHD2 and 3 were found to be induced by hypoxia, with relatively more PHD3 expressed under similar degrees of hypoxia (Appelhoff et al., 2004). This difference allowed PHD3 protein to be hypoxically induced to a level comparable to PHD2. Having established comparable levels, an assay was designed to determine the rate of HIF-1α decay following re-oxygenation. Suppression of PHD2 in this setting allowed PHD3 expression to dominate and showed a greater rate of HIF-1α decay compared to that achieved by suppression of all three isoforms (Appelhoff et al., 2004). This study demonstrated that all three PHDs were able to regulate HIF-1α and its target genes in cell-lines and that the activity of each isoform was principally determined by their protein abundance.

It is important to emphasise that although PHD enzymes have in common the ability to degrade HIF, they differ from one another in a number of different ways. Cell-line based studies demonstrated clear differences in the abundance of each protein isoform (Appelhoff et al., 2004). In this study, PHD2 was found to be the most abundant in normoxic cell types; PHD3 was virtually absent under the same conditions and PHD1 expressed at an intermediate but low level compared to the other two. PHD enzymes also differ in size (Epstein et al., 2001), subcellular distribution (Metzen et al., 2003) and inducibility (Appelhoff et al., 2004; Seth et al., 2002). They also differ in their ability to degrade each of the different HIF isoforms with PHD1 and 3 having a greater influence on the abundance of HIF-2α compared to HIF-1α (Appelhoff et al., 2004). Differences in the selectivity of each enzyme for the N- terminal oxygen dependent degradation domain (NODD) and C- terminal oxygen dependent degradation domain (CODD) of HIF-1α have also been found. All PHDs are more active on the CODD than NODD (Hirsila et al., 2003). PHD3 was found to have the least activity against the NODD (Hirsila et al., 2003). Further studies have demonstrated that the abundance of PHD1 and 3 but not PHD2 can be influenced by the E3 ubiquitin ligase *Drosophila* Seven in Absentia homolog's (Siah) 1 and 2 (Nakayama et al., 2004). The heterogeneous nature of PHD enzymes is thus clear and gives rise to the possibility that in addition to their shared ability to hydroxylate HIF they may also have other non-overlapping functions.

A number of studies which emerged at the start of this doctoral thesis helped to focus our interest on PHD3. These studies indicated a role for PHD3 in mediating apoptosis of sympathetic lineage cell types. The implication of this finding was profound, giving rise to the possibility that PHD3 may have a role in development of

sympatho-adrenal tissues as well as the formation of neoplasms of the sympatho-adrenal axis. These studies will be described in detail later in this introduction. In order to understand their significance, it is first necessary to gain a clear understanding of sympathetic lineage cell types as well as the structure and function of the autonomic nervous system. This will be discussed next.

1.2.3 Characteristics of sympathetic lineage cell types and the autonomic nervous system

The sympathetic nervous system forms part of the involuntary or autonomic nervous system, the other part of which is the parasympathetic nervous system. The function of these two systems occurs without conscious control and is hence termed involuntary. A series of reflex loops allows sensory information to be relayed via primary visceral afferent sensory neurons to central neurons located in the brain and spinal cord. Here, efferent motor neurons are triggered to mediate responses in target organs. Traditionally the two systems were considered to have opposing effects with the sympathetic half mediating a 'fight or flight' response and the parasympathetic, mediating 'rest and digest' (reviewed by Oppenheim et al., 1984). The two systems have different embryological origins with the sympathetic nervous system being derived from the neural crest (Loring et al., 1987), while the parasympathetic is derived from neural placodes (Verwoerd and Oostrom., 1979).

Sympathetic lineage cell types express enzymes required for the synthesis of catecholamines, namely tyrosine hydroxylase and dopamine β-hydroxylase (Ernesberger et al., 2000). There are a number of morphologically distinct cell types in the sympathetic lineage which are expressed in different regions of the sympathetic nervous system. During development, some sympathetic lineage cell types migrate

from the neural crest to finally differentiate into sympathetic neurons of the sympathetic chain. Sympathetic neurons have typical neuronal morphology and express neuronal markers such as neurofilament 68 and SCG10. Other precursor cells migrate to adrenal and extra-adrenal sites where they form the adrenal medulla and extra-adrenal chromaffin cell clusters. In extra-adrenal sites, chromaffin cells can form discrete structures known as paraganglia located adjacent to sympathetic ganglia and great vessels. The largest of these paraganglia is the organ of Zukerkandl located at the bifurcation of the aorta (Coupland et al., 1968). In contrast to sympathetic neurons, chromaffin cells lack neuronal morphology and are characterised by large chromaffin granules which are required for storage and release of catecholamines. Extra-adrenal chromaffin cells contrast with those of the adrenal gland by undergoing atrophy during the post-natal period (Partanen et al., 1984). A diagram depicting the anatomical organisation of the autonomic nervous system is indicated in figure 1.

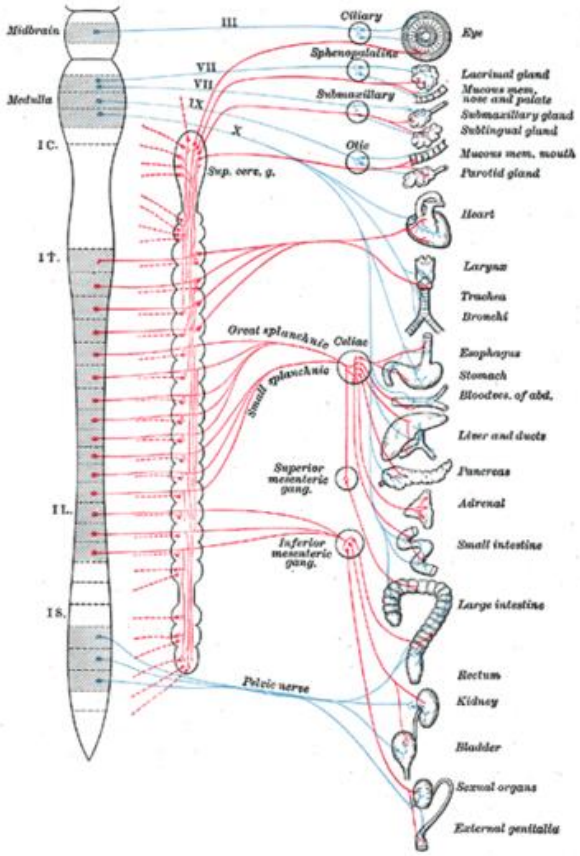


Fig 1. Diagram of the autonomic nervous system (Gray's Anatomy of the Human Body). Red: sympathetic nervous system, blue: parasympathetic nervous system

Sympathetic efferent neurons originate within the intermediolateral column of the spinal segments T1 to L3. The axons of these nerves leave the spinal cord through the anterior horn where they enter the paravertebral sympathetic chain via the white, myelinated, rami communicans. Once inside the sympathetic chain, one of four outcomes can occur. Axons can either synapse at the level of the corresponding spinal nerve with post-synaptic sympathetic neurons, they can ascend in the sympathetic chain before forming synapses at a level above that of the corresponding spinal nerve or they descend to synapse below the corresponding spinal nerve. Alternatively, they may leave the paravertebral sympathetic chain to synapse in a series of paravertebral sympathetic ganglia. These include the coeliac, superior and inferior mesenteric ganglia which supply sympathetic out-flow to the gut. The superior cervical ganglion

(SCG) is the largest of these and is located in close proximity to the carotid body and internal carotid artery. Sympathetic outflow to the head, neck and heart is derived from it. Its relatively large size and anatomical position mean that it has been widely used in the study of sympathetic lineage tissues (Gray. H, *Gray's Anatomy of the Human Body*, Arcturus Ltd, 2008).

Sympathetic efferent axons from the spinal cord are generally short and the majority form synapses in the sympathetic chain and paravertebral ganglia which are located in close proximity to the spinal column. In contrast, axons of post synaptic sympathetic neurons are much longer having further to travel in order to reach their target organs. The sympathetic outflow to the adrenal gland is a notable exception and here presynaptic axons extend from the intermediolateral column and travel through the sympathetic chain all the way to the adrenal medulla where they synapse directly with 'pseudo-neuronal' chromaffin cells which secrete their neurotransmitter directly into the circulation. In the sympathetic nervous system acetylcholine is secreted by pre-synaptic nerve endings which bind to muscarinic receptors on post-synaptic membranes as demonstrated in figure 2. Post-synaptic neurons release noradrenaline which binds to α and β receptors on target organs. The adrenal medulla is a modified sympathetic ganglion and releases adrenaline rather than noradrenaline into the circulation (Gray. H, *Gray's Anatomy of the Human Body*, Arcturus Ltd, 2008).

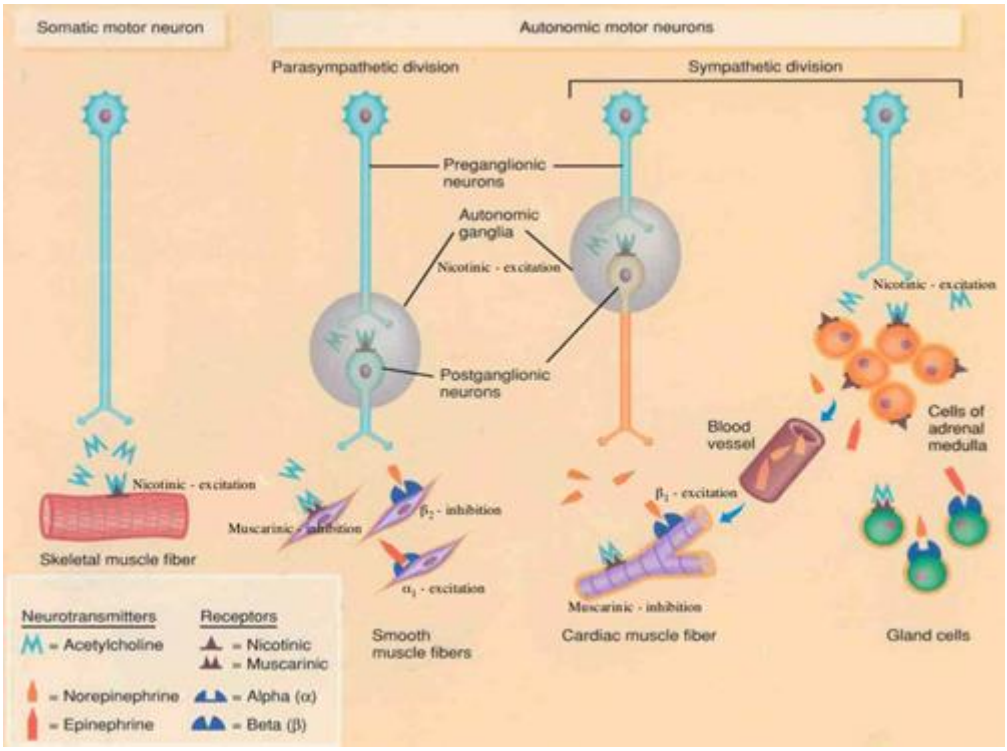


Fig 2. Major neurotransmitters and receptors of the nervous system

The parasympathetic system is organised in a similar manner to the sympathetic nervous system with sensory and motor limbs. The efferent outflow arises from the brain stem nuclei of cranial nerves III (occulomotor), VII (facial), IX (glossopharyngeal), and X (vagus). While those of cranial nerves III, VII and IX supply the head and neck, those of the vagus extend to most organs in the body and constitute the main parasympathetic outflow. 70% of vagus nerve fibres are in fact sensory visceral, the cell bodies of which are located in the nodose ganglion. While the nodose ganglion receives information from the gut and the carotid sinus, afferents which go via the petrosal ganglion originate in the carotid body (Finley and Katz., 1992). The carotid body is itself considered to be a modified ganglion which is located in the neck at the bifurcation of the carotid artery. It contains neural crest derived oxygen and pH sensing type I (chief) cells as well as supporting type II (sustentacular) cells. Type I cells release a variety of neurotransmitters which include

acetylcholine, dopamine, noradrenaline and ATP. Visceral afferents from the carotid body and aortic body traverse their respective ganglia to reach the brain stem where they synapse in the nucleus tractus solitarii (NTS) (Beckstead et al., 1980). The NTS controls autonomic outflow through integrating pathways with other brainstem cardio-respiratory centres in the medulla oblongata as well as influencing parasympathetic outflow via the nuclei of the vagus and hypoglossal nerves.

Other parasympathetic efferents arise from spinal sacral segments S2, S3 and S4 and are referred to as the pelvic splanchnic nerves. The parasympathetic efferent neurons differ from those of the sympathetic nervous system by being relatively long. In the head and neck, they form synapses in a series of parasympathetic ganglia where short post-synaptic neurons arise to supply target organs. The ciliary ganglion provides parasympathetic out-flow to the pupil, the sphenopalatine ganglion innovates the lacrimal gland and mucus membranes of the nose and palate. The submaxillary ganglion innervates the submandibular and sublingual salivary glands while the otic ganglion innervates the parotid gland and mucus membranes of the mouth. In the parasympathetic nervous system acetylcholine is secreted from both pre- and post-synaptic nerve terminals, as indicated in figure 2.

1.2.4 PHD3 and neuronal apoptosis

During development, sympathetic neurons compete for increasingly limited amounts of nerve growth factor (NGF). Those neurons that fail to secure an adequate supply of NGF undergo death by apoptosis, a process termed ‘naturally occurring neuronal cell death’ (Levi-Montalcini., 1968; Oppenheim., 1991). As will now be discussed, a series of studies indicated that PHD3 had a role as a mediator of apoptosis in sympathetic lineage neurons. Furthermore, these studies indicated that

this property was not shared by either PHD1 or PHD2. These studies were carried out in primary sympathetic neurons derived from rat superior cervical ganglion (SCG) but also in a rat PC12 phaeochromocytoma cell line which can differentiate to a neuronal phenotype. In these studies the expression of PHD3 was found to be increased in PC12 cells following nerve growth factor (NGF) withdrawal as well as by treatment with the anti-tumour drug AraC and the PI 3-kinase inhibitor, LT294002 indicating that PHD3 expression was increased in response to a number of different apoptotic stimuli (Lipscomb et al., 1999). In the same study, microinjections of rat PHD3 (SM-20) cDNA into the nuclei of cultured primary rat sympathetic neurons was compared with vector-only control and found to be sufficient to promote apoptosis indicating a causative role for PHD3 in neuronal apoptosis. Further studies demonstrated that induction of PHD3 (SM-20) in PC12 cells led to an increase in cytochrome c levels and accumulation of cytochrome c in the cytosol indicating that PHD3-mediated apoptosis occurred through a cytochrome c dependent pathway (Straub et al., 2003). The role of other PHD isoforms in this process remained unknown until it was demonstrated that apoptosis was promoted by over-expressing PHD3 but not PHD1 or PHD2 in PC12 cells, suggesting this pro-apoptotic function in sympathetic lineage cells was unique to PHD3 (Lee et al., 2005).

Because of the link between PHD3 and apoptosis, researchers went on to explore PHD3's role in development and tumour biology. These studies will be discussed next.

The development of mice with constitutional deletion of PHD3 provided a means to explore its role at the whole animal level. In work carried out in Oxford in parallel

with my thesis, it was found that PHD3-/- animals had reduced apoptosis and increased cell numbers within the adrenal medulla, SCG and carotid body (Bishop et al., 2008). This work confirmed that PHD3 did play an important role in development of the sympathetic nervous system.

This study, in which I participated, went on to demonstrate a number of important functional outcomes of PHD3 deletion. Interestingly it was found that despite an increase in cell number, the sympatho-adrenal system appeared hypo-functional with decreased adrenal medullary secretory capacity, target organ innervation, sympatho-adrenal reflex responses and reduced systemic blood pressure. The reduction in blood pressure was felt to be primarily due to reduced basal circulating catecholamine levels secondary to reduced catecholamine secretion from the adrenal gland. PHD3-/- animals were also noted to have a reduction in innervation density of organs innervated by sympathetic ganglia. This was an unexpected finding as in addition to its role in survival, NGF also promotes neurite outgrowth, a process which determines tissue innervation density (Crowley et al., 1994; Seagal and Greenberg., 1996). Despite innervation density being reduced, the overall number of target organ innervating neurons was increased and it was speculated that this may have been due to increased retrograde transport of NGF from target organs to a level below that necessary to promote neurite formation. This abnormality of target organ innervation was felt to account for why PHD3-/- mice demonstrated abnormal pupillary responses despite increased numbers of sympathetic neurons.

This study went on to provide further insights into PHD3 mediated apoptosis by demonstrating that SCG derived primary sympathetic neurone cultures exhibited

resistance to apoptosis, not only under conditions of NGF deprivation but also when deprived of neurotrophin 3 (NT-3), another growth factor know to impact on neuronal survival (Karavanov et al., 1995). Sensory cell populations of the dorsal root ganglion and trigeminal ganglion are also known to be NGF sensitive (Crowley et al., 1994). However these ganglia, on a PHD3-/- background were found to be no different from those of wild types suggesting their sensitivity to NGF was mediated through pathways independent of PHD3.

Finally this study demonstrated reversal of phenotype when PHD3-/- mice were crossbred onto a HIF-2α but not HIF-1α heterozygous background, thereby strengthening the link between PHD3 and HIF-2α (Bishop et al., 2008).

1.2.5 Tumours of the autonomic nervous system and the putative role of PHD3 in their aetiology

A number of different tumour types occur in the autonomic nervous system. The nomenclature used to describe these tumours is variable and no clear consensus exists (Martin and Maher., 2007). Some authors use anatomical terminology such as 'carotid paraganglioma' or 'jugulotympanic paraganglioma' while others use histological features such as 'chemodectoma', 'carotid body tumour', or 'non-chromaffin-staining paraganglioma'. Phaeochromocytomas arise from chromaffin cells, which are present primarily in the adrenal medulla but also in scattered extra-adrenal sites. Tumours arising from sympathetic neurons are termed neuroblastomas while those arising from sympathetic ganglia are termed ganglioneuromas. Some have features of both sympathetic neurons and ganglia and are termed ganglioneuroblastomas (Shimada et al., 1999). The term 'paraganglioma' has also been used to describe tumours which

arise from head and neck ganglia of both the sympathetic and parasympathetic nervous systems.

Such tumours can occur spontaneously or as part of a tumour syndrome. In the latter, tumour formation is linked to mutations of specific genes and Von Hippel Lindau protein (VHL), succinate dehydrogenase (SDH), receptor tyrosine kinase (RET) and neurofibromin 1 (NF1) are currently recognised as such syndromic tumour genes (Bryant at al., 2003; Maher and Eng., 2002). Each is associated with a particular cluster of tumour types (Maher et al., 2002). Phaeochromocytomas are however common to all syndromic forms suggesting that the pathway leading to their formation is linked. Indeed recent studies have demonstrated the existence of such a pathway and gone on to demonstrate the central role of PHD3 within it. Studies relating to this will be discussed next.

Succinate dehydrogenase (SDH) is a mitochondrial enzyme and the observation that PHD3 in rat sympathetic neurons localised to mitochondria and required intact mitochondrial function to promote apoptosis (Lipscomb et al., 2001; Straub et al., 2003) gave rise to the possibility of interplay between PHD3 and SDH. This hypothesis was supported by the fact that succinate was common to both enzymes, being a by-product of PHD3 mediated HIF-α subunit hydroxylation and the substrate for SDH in the tri-carboxylic-acid (TCA) cycle. The link between the two was tested in a VHL binding assay which demonstrated that the activity of PHD3 on HIF's ability to bind VHL could be influenced by succinate accumulation (Lee et al., 2005). Accumulation of succinate had been shown to occur following pharmacological inhibition of SDH (Selak et al., 2006) and it therefore seemed possible that

abnormalities of SDH could, through accumulation of succinate, lead to inhibition of PHD activity. Indeed the same study demonstrated that pharmacological inhibitors of SDH could limit apoptosis of PC12 cells transfected with PHD3. It was also demonstrated that transfection of two different siRNA sequences against SDH subunit D was sufficient to suppress apoptosis of PC12 cells following nerve growth factor withdrawal, an effect mirrored by the use of pharmacological SDH blockade in the same cell culture setting. In this way it was demonstrated that defects in SDH could lead to an accumulation of succinate which in turn was sufficient to suppress the activity of PHD3 and thereby inhibit PHD3 mediated apoptosis of sympathetic precursors.

This study went on to explore the link between PHD3, neuronal apoptosis and other genes implicated in syndromic phaeochromocytoma formation. The function of elements of the AP-1 transcription factor became important as a first step to defining PHD3's role in this process. AP-1 is not a single protein but a menagerie of dimeric basic region-leucine Zipper (bZIP) proteins which belong to the Jun, Fos, Maf and ATF sub-families (Shaulian et al., 2002). Previous studies had established that Jun B antagonises the function of C-Jun in a wide variety of settings (Gelberblom et al., 2004; Herdegen and Leah., 1998). C-Jun was shown to promote apoptosis in sympathetic neurons following NGF withdrawal (Estus et al., 1994; Ham et al., 1995). Therefore a process that promotes Jun B expression would lead to suppression of c-Jun mediated apoptosis. Lee et al. explored the interplay between Jun B, c-Jun and these syndromic tumour genes. In relation to VHL, Lee et al demonstrated that Jun B levels were increased in renal cell carcinoma (RCC) cells deficient in VHL as well as in HeLa cervical carcinoma cells treated with siRNA to VHL. Based on these findings

further studies were carried out demonstrating that Jun B was increased following siRNA mediated knockdown of VHL in PC12 cells, resulting in suppression of apoptosis. Furthermore this effect on apoptosis was reversed by transfecting human VHL but not appropriate control siRNA, confirming the effect was VHL specific and establishing a link between VHL and apoptosis in the sympathetic lineage.

This study went on to explore the effect of RET, another tumour syndrome related gene and Jun B. It was demonstrated that transfection of mutant, but not wild type, RET was sufficient to increase Jun B and suppress PC12 cell apoptosis under NGF deficient conditions indicating that RET could also suppress sympathetic lineage apoptosis by increasing Jun B. Although the relationship between Jun B and NF1 was not examined in this study, a link between the two had been established previously in work which demonstrated that loss of NF1 promoted survival of embryonic neurons under NGF poor conditions (Vogel et al., 1995). Overall, the work by (Lee et al., 2005) demonstrated that mutations of genes linked to syndromic forms of sympathetic lineage tumours could inhibit apoptosis in a pathway dependent on PHD3, thus providing a mechanism by which rogue neurons could survive under conditions of limited NGF. These findings are summarised in figure 3.

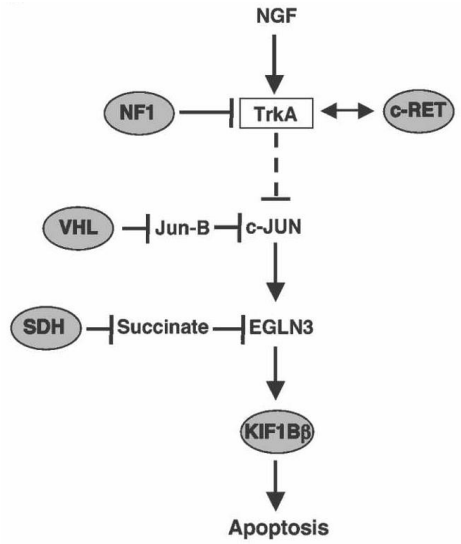


Fig 3. Relationship between familial phaeochromocytoma and paraganglioma genes with PHD3 (EGLN3).

Suppression of PHD3 function in sympathetic lineage cell types is purported to allow rogue neurites capable of undergoing neoplastic transformation to survive normal developmental apoptosis.

1.2.6 The importance of PHD1 and 2 in the whole animal

During the course of this doctoral thesis further studies emerged demonstrating phenotypes related to deletion or mutation of PHD1 and 2. Homozygous deletion of PHD2 in adult animals {using tamoxifen-inducible Cre-recombinase (*Rosa26 CreERT2)*} resulted in a phenotype of exaggerated angiogenesis associated with increased levels of normoxic tissue HIF and its target gene VEGF-A (Takeda et al., 2007). Importantly the vasculature of these animals demonstrated a number of properties of normal blood vessels in terms of being patent, normally perfused with blood and the appropriate recruitment of vascular smooth muscle cells. This work taken together with that of previous studies demonstrating embryonic lethality from abnormal placental vasculature in mice with constitutive PHD2 but not PHD1 or 3 deletional (Takeda et al., 2006) was in keeping with earlier *in vitro* studies suggesting

that PHD2 holds primacy in regulating normoxic HIF-1α levels. Although it is highly likely that the phenotypes observed in these animals was a consequence of normoxic HIF, reversal of phenotypes by breeding onto a HIF null background has yet to be studied. Therefore it is currently only possible to say with certainty that normoxic animals with PHD2 deletion manifest a significant pro-angiogenic phenotype in developing as well as adult tissues and that the HIF dependency of this phenotype is highly likely although yet to be proven. It is interesting to note that in these animals PHD2 deletion was not universal to all tissues. Further evidence supporting the primacy of PHD2 in normoxic function comes from the observation that siRNA to PHD2 but not PHD1 or 3 protected against mouse myocardial ischaemic-reperfusion injury (Natarajan et al., 2006).

Overall, evidence is accumulating which indicates that deletion of PHD2 in the whole animal promotes HIF dependent gene expression under conditions where such genes would not normally be expressed. Recent studies of other PHD2 deletional models have allowed this phenomenon of normoxic HIF expression to be explored further and revealed unexpected findings in the field of tumour biology (Mazone et al., 2009). In this study, heterozygous deletion of PHD2 was associated with reduced tumour hypoxia, vascular invasion and metastasis through a process of tumour vascular endothelial cell normalisation. Importantly this study also demonstrated reduced levels of vascular endothelial derived growth factor receptor 1 (VEGFR1 also known as FLT1) and VE-cadherin following in vitro deletion of HIF-1α and HIF-2α in cultured PHD2 +/- primary vascular endothelial cells, suggesting that reversal of phenotype was likely to occur. It is also of interest that when PHD2 homozygous and heterozygous deleted animals from these studies were compared, the former favoured

the full spectrum of angiogenesis while the latter influenced vascular endothelial cell function alone. Further evidence demonstrating the importance of the PHD2 heterozygous state and its ability to influence normoxic HIF comes from the study of hereditary forms of human polycythaemia. A Pro-317 to Arg mutation of PHD2 was demonstrated to cause a high Epo polycythaemia (Percy et al., 2006). In this study over expression of mutated PHD2 was unable to reverse wild type PHD2 inhibition of a HRE reporter, implying that a dominant negative effect was unlikely, suggesting that haploinsufficiency was the most likely cause of polycythaemia in this kindred.

These studies demonstrated that deletion or mutation of PHD2 had significant effects at the whole animal level in the setting of normoxia. The absence of correspondingly severe phenotypes in animals with deletion of PHD1 (Aragones et al., 2007) and PHD3 (Bishop et al 2008) would suggest that PHD2 holds primacy in determining the normoxic HIF phenotype of many tissues.

A phenotype relating to PHD1 was also demonstrated during the time of my doctoral work in animals with constitutional PHD1 deletion (Aragones et al., 2008). In this study, constitutional deletion of PHD1 was shown to re-programme basal metabolism resulting in a phenotype in which skeletal muscle was resistant to hypoxic stress. PHD1 loss was associated with an increase in HIF-1α but not HIF-2α in ischaemic skeletal muscle. When these animals were interbred onto a HIF-1α heterozygous background, the phenotype was reversed demonstrating that the PHD1 phenotype was dependent on HIF-1α. In contrast, similar phenotypes were not observed in PHD3 deletional animals or from PHD2 heterozygous animals available at the time of study. Given the results of more recent studies demonstrating the

prominent role of PHD2 and the presence of phenotypes even in the PHD2 heterozygous state, the absence of protection from ischaemia in PHD1 deletional animals would argue in favour of their phenotypes being independent of PHD2. It is also of interest that the PHD1 deletional phenotype of ischaemic resistance was not associated with an increase in red cell mass or neovascularisation, but instead was due instead to changes in mitochondrial metabolism, indicating a mechanistically different process from that governed by PHD2. These observations provided further evidence supporting the concept that despite their shared ability to regulate HIF, there were significant differences in the molecular pathways governed by different PHD enzymes in complex animal tissues.

Further studies of mice with PHD1 and 3 double constitutional deletions demonstrated a phenotype characterised by polycythaemia and hepatosplenomegaly (Takeda et al., 2008). It is of interest that a phenotype which showed parallels to this was observed in PHD2-/- conditional adult animals. While both backgrounds were associated with polycythaemia as well as enlargement of liver and spleen, these changes were less pronounced with combined PHD1 and 3 deletions. Furthermore, while PHD2-/- mice had significantly elevated serum Epo levels, combined deletional animals had reduced Epo levels compared to wild types. Elevated levels of HIF-1α was noted in the kidney of PHD2-/- animals which contrasted with elevated HIF-2α but not HIF-1α in the liver of combined PHD1 and 3 deletional animals. This study suggested that although PHD2 had a dominant role in setting normoxic HIF it was unable to compensate for the combined loss of PHD1 and 3 with regards to haemopoiesis.

Through these studies a picture was emerging where in tissues, PHD2 held primacy of HIF regulation in normoxia while PHD3 was linked to hyperplasia of the sympatho-adrenal axis and PHD1 with skeletal muscle resistance to ischaemic stress.

1.3 Reasons to study the expression of PHD enzymes

1.3.1 In relation to previous mRNA studies of PHD tissue abundance

A number of studies assessed the expression of PHD mRNA in tissues. Such studies suggested that each PHD had a distinct pattern of tissue expression with PHD2 being widely expressed in many different tissues while PHD1 and 3 mRNA appeared more restricted. There were nonetheless differences between these studies; the expression of PHD2 in liver being one such example with some studies indicating relatively low liver PHD2 (Oehme et al., 2002; Willam et al., 2004; Willam et al., 2006) while others detected more PHD2 in liver (Lieb et al., 2002; Cioffi et al., 2003). Furthermore, PHD1 was consistently found to be expressed in testis (Erez et al., 2004; Lieb et al., 2002; Oehme et al., 2002) but its expression in other tissues was more variable; several studies indicated intermediate levels of PHD1 mRNA in brain, liver, kidney and heart (Erez et al., 2004; Lieb et al., 2002) while others indicated generally low levels in these and other tissues (Oehme et al., 2002; Hirsila et al., 2003). The expression of PHD3 mRNA was also found to vary between different studies with some reporting an abundance in heart with relatively less in other tissues (Lieb et al., 2002; Hirsila et al., 2003; Coiffi et al., 2003) while others reported an abundance in liver (Lieb et al., 2002), Brain (Oehme et al., 2002) and skeletal muscle (Coiffi et al., 2003).

This variability meant that despite the insights gained from these studies, there remained questions relating to the exact expression of tissue PHD isoforms, highlighting the need for additional studies such as those aimed at characterising tissue PHD protein. Furthermore, the function of a gene is determined through protein expression and although often representative of one another, protein and mRNA abundance can be disproportionate. Induction of PHD protein and mRNA has been described in a number of different settings. These include PHD2 and 3 induction by hypoxia (Appelhoff et al., 2004), PHD1 by oestrogen (Seth et al., 2002), PHD3 by temperature sensitive P53 in smooth muscle cells (Wax et al., 1994) and in sympathetic lineage cell type's following nerve growth factor withdrawal (Lipscomb et al., 1999; Lipscomb et al., 2001; Straub et al., 2003). In these settings, differences in fold-induction between protein and mRNA were observed.

Differences in the subcellular distribution of PHD proteins have also been described; PHD1 being predominantly nuclear, PHD2 cytoplasmic and PHD3 present in both (Metzen et al., 2003; Oehme et al., 2002). The ability of such difference to impact on PHD function was recently demonstrated for PHD2 (Yasumoto et al., 2009). Insights into how these changes in protein subcellular expression may affect tissue function require an assessment of tissue protein rather than mRNA.

Alternative methionine translation initiation has been described for human PHD1 (Tian et al., 2006) and this together with post-translational modification and the formation of protein-protein complexes could also impact on protein function, yet remain undeclared, in studies of mRNA.

1.3.2 In relation to drug design and therapeutics

The development of mice with deletion of individual PHD isoforms served to take the study of PHD enzymes to the whole animal level. These studies demonstrated that PHD enzyme, despite their shared ability to regulate HIF, have non-redundant tissue functions allowing distinct phenotypes to develop in the context of individual PHD deletion. Many of these phenotypes occurred in viable animals and as such were encouraging from the perspective of using targeted PHD deletion as a future therapeutic strategy.

Despite the advances made by these studies important questions remained regarding the mechanisms underlying development of individual phenotypes particular, the role of PHD protein abundance. The relationship between protein abundance and a corresponding deletional phenotype could be considered to be either 'direct' or 'indirect in nature. A direct relationship is one where the gene under study is abundantly expressed in those tissues which manifest the deletional phenotype. In contrast, in an indirect phenotype, the gene is expressed in another tissue to that which manifests the phenotype. An appreciation for the direct versus indirect nature of a phenotype is important for a number of different reasons. From the perspective of basic science, a direct phenotype would promote study of a single tissue or organ while indirect phenotypes would require additional study of humeral, cardiovascular, and developmental factors. The direct versus indirect relationship is also likely to have implications for putative drug design and therapeutics allowing for targeting of therapies to specific organs or tissues.

In the complex environment of tissues it is also possible that factors apart from protein abundance could impact on a given deletional phenotype. In this context

recent cell line based studies demonstrated that the activity of PHD's could be altered through an accumulation of succinate (Lee et al., 2006) and/or fumarate (Koivunen et al., 2007), thereby providing potential for differences between the abundance of PHD protein in a given tissue and its corresponding deletional phenotype. Other factors which could impact on this relationship include cellular compartmentalisation, the compensatory effects of other PHD isoforms or indeed novel non-HIF target proteins. The study of PHD tissue protein abundance may help to provide insights into such process. For example, if a given PHD isoform was dominantly expressed in a particular tissue and its deletion was linked to development of a specific tissue phenotype, there would be a clear relationship between the abundance of that isoform and the corresponding tissue phenotype. Alternatively, if despite being the most abundant tissue isoform, its loss failed to manifest a specific tissue phenotype there would be grounds to consider the relationship between abundance and phenotype to be altered by factors such as those described above. Indeed it is possible that such factors may serve to either suppress or enhance the activity of PHD isoforms resulting in a difference between the 'true' and 'functional' amount of tissue PHD protein isoform abundance.

The possibility of phenotypes which remain 'hidden' in the context of PHD deletional models needs also to be considered in relation to drug design and therapeutics. Such phenotypes may remain undetected by virtue of their subtle nature or alternatively, may fail to manifest due to the compensatory effects of remaining PHD enzymes. They may have the potential to become prominent either in the context of combined PHD isoform deletion or when tissues are subject to specific stressors. Putative PHD modulators may result in such 'hidden' phenotypes declaring

themselves in either a therapeutic or pathological way. Indeed it is possible that tolerable therapeutic effects may only be demonstrated in those tissues in which PHD enzymes are expressed but in which their phenotype is hidden under standard conditions.

In humans, a number of other factors are of relevance from a therapeutic perspective. These include the use of multiple therapeutic agents, senescence as well as disease. In disease states such as those leading to tissue hypoxia, the effects of PHD modulation may be more profound in certain tissues and therefore determining the expression of PHD proteins in both diseased and healthy tissues is of importance. The use of multiple therapeutic agents, a phenomenon known as ‘polypharmacy’, may also have implications for putative PHD modulators impacting on the expression or activity of tissue PHD’s. An appreciation for the expression of PHD isoforms in tissues may help to identify those tissues likely to manifest a hidden phenotype of therapeutic or detrimental significance. The effect of senescence is again unpredictable. Vessel hardening and tissue ischaemia which occurs with aging may have an impact on PHD enzyme expression, increasing the importance of potential 'hidden' phenotypes with age.

The need to establish the abundance of PHD proteins in tissues is thus clear. A limited number of studies have gone onto determine the expression of PHD isoforms in tissues. These will be discussed next.

1.4 Studies relating to protein abundance of PHD enzymes in tissues at the time of commencing this doctoral thesis

A few studies have assessed the expression of PHD protein isoforms in tissues. In one study, PHD2 and 3 were detected in rat myocardium and their expression was demonstrated to increase following myocardial ischaemia in the peri-infarct zone (Willam et al., 2006). In a separate study, PHD3 protein expression was found to increase with age in mouse myocardium, although it is not clear how the reagents used in this study to detect PHD3 were validated (Rohrbach et al., 2005). An immunohistological study of PHD isoforms in a variety of normal and diseased human tissues has also been carried out (Soilleux et al., 2005). This study demonstrated generally weak PHD1 staining in most tissues including the testis. Interestingly the majority of PHD1 staining in this study was cytoplasmic in nature, which contrasted with the predominantly nuclear staining pattern observed in over-expression studies of PHD1 in cell lines. In this study, PHD2 was found in to be expressed in a similar tissue distribution to PHD1 but was of greater abundance and predominantly cytoplasmic. PHD3 was also found to be widely expressed in this study producing both nuclear and cytoplasmic staining patterns. Importantly, the antibodies used in this study to detect each PHD isoform were validated by demonstrating specific signal in COS cells transfected with cDNA for each isoform and processed as a cell pellet in a manner parallel to the histological preparation of tissues. Despite the insight gained from this study, factors such as species differences, tissue age, method of preparation, genetic variability and the impact of disease and treatment meant that it was difficult to draw firm conclusions about patterns of PHD protein expression. A quantitative assessment of all three PHD proteins in normal tissues remained an outstanding goal.

1.5 Aims of this doctoral thesis

The central aims of this doctoral thesis are listed below and will be expanded upon in the relevant future sections.

- To identify or generate antibodies with the ability to recognize rodent PHD isoforms specifically at endogenous levels in tissues.
- To determine the relative expression of PHD proteins in a range of different rodent tissues, from healthy animals, exposed to normal atmospheric oxygen levels.
- To characterise the expression of PHD3 protein in tissues of the sympatho-adrenal axis.
- To establish if neuronal populations apart from those of the sympatho-adrenal axis also expressed PHD3.
- To carry out individual and collaborative studies with the aim of better understanding the relationship between expression and function of PHD isoforms in tissues.

Section 2: Methods

Chapter 2. Overview of methods

2.1 Recombinant DNA techniques

2.1.1 Generic recombinant DNA techniques

2.1.1.1 Bacterial culture for plasmid DNA mini preparation

Using a sterile spreader, transformed bacteria were spread on to ampicillin plates and cultured overnight at 37ºC. The following day, single colonies were isolated with a sterile disposable pipette tip and cultured separately in a shaking incubator overnight in 5 ml of LB (Sigma, UK) medium supplemented with 100 µg/ml of ampicillin (Sigma, UK) at 37ºC.

2.1.1.2 Mini preparation of plasmid DNA from bacterial culture

DNA mini preparation was carried out using a QIAprep Spin Miniprep Kit (Qiagen) as follows: 5 ml of bacterial culture were centrifuged at 2000g for 2 min, the supernatant discarded and the pellet resuspended in 250 µl of P1 buffer supplemented with RNase A and transferred to a 1.5 ml microcentrifuge tube. Care was taken to completely resuspend the pellet in P1 buffer by vortex until no cell clumps were visible. Next, 250 µl of P2 buffer were added and mixed by inverting the tube until the solution became viscous and slightly clear. The lysis reaction was not allowed to proceed for more than 5 min. Next, 350 µl of N3 buffer was added and immediately and thoroughly mixed by inverting the tube 6 times. The mixture was centrifuged for 10 min at 14500g and the supernatant transferred into a pre-assembled QIAprep spin column taking care to avoid pelleted debris. The column was centrifuged at 14500g for 1 min and the flow-through discarded. Trace nuclease activity was removed from the column by adding 0.5 ml of PB buffer and centrifuging at 14500g for a further 1 min. The flow through was discarded. The column was washed by adding 0.75 ml of PE buffer and centrifuging at 14500g for 1 min and the flow-through discarded. The

column was centrifuged again for 1 min at 14500g to remove any residual wash buffer and the column transferred to a fresh 1.5 ml microcentrifuge tube. Next 30 µl of EB buffer was pipetted to the centre of the spin column and allowed to stand at room temperature for 1 min. DNA was eluted by centrifuging at 14500g for 1 min, and the flow-through stored at -20ºC until further use.

2.1.1.3 Agarose gel electrophoresis

A 2% agarose gel was made by dissolving 2g of agarose (Sigma, UK) in 100 ml of 0.5% TBE buffer by heating at maximum power in a microwave (Cookworks) until fully dissolved then allowed to cool at room temperature for 5 min before adding 1 µl of ethidium bromide (10 mg/ml) (Sigma, UK) and swirling to mix while taking care to avoid inhalation of vapour. The Gel was poured slowly into a preassembled 8 x 10 cm mini gel tank taking care to avoid forming bubbles. Any bubbles which did form were pushed away from combs towards the edge of the tank using a disposable pipette tip. After allowing 30 min for the gel to set, the comb was removed taking care not to damage the gel. The gel was submerged with 0.5% TBE buffer. DNA samples in 6x DNA loading dye {25 mg bromophenol blue (Sigma, UK) and 3 ml glycerol (Sigma, UK) dissolved in 10 ml distilled water and stored as a stock solution at -20ºC}, boiled for 5 min and allowed to cool for 2 min before loading on to the gel, taking care to avoid over flow. DNA ladder (Sigma, UK) diluted with 6x loading dye was loaded into one lane. The gel tank was closed and run at a 100V. When the bromophenol blue marker had advanced ¾ of the length of the tank, the gel was removed and digestion products visualised under UV light with appropriate eye and skin protection.

2.1.1.4 Purification of DNA

A GFX PCR and Gel Band DNA purification kit (Amersham Bioscience) was used. GFX columns were placed in collection tubes for each sample to be purified.

The PCR product was transferred to the GFX column. The sample was mixed thoroughly by pipetting the sample up and down 6 times in 500 µl of capture buffer. The sample was centrifuged at 14500g for 1 min and the flow through discarded. 500 µl of wash buffer was added to the column and centrifuged at 14500g for 1 min. The collection tube was discarded and the column transferred to a fresh microcentrifuge tube. 30 µl of elution buffer was applied directly onto the glass fibre matrix in the GFX column and incubated at room temperature for 1 min before centrifuging at 14500g for 1 min to recover purified DNA which was stored at -20ºC.

2.1.1.5 Purification of DNA from solution

DNA was resolved by agarose gel electrophoresis. DNA bands were visualised under long wave length (365 nm) UV light and cut from the gel with a clean scalpel before storing in a DNase free 1.5 ml microcentrifuge tube at -20ºC. Care was taken to ensure minimal exposure of DNA to UV light. DNA was extracted from bands and purified using a GFX DNA purification kit (Amersham Biosciences) as follows. Gel bands were weighed and an equivalent volume of capture buffer added, before incubating at 60ºC with frequent vortexing until the agarose was completely dissolved. Up to 800 µl of dissolved agarose in capture buffer was transferred to an assembled GFX spin column and incubated at room temperature for 1 min before centrifuging at 14500g for 30 seconds. The flow through was discarded by emptying the collection tube and the process repeated until all sample has been loaded onto the column. Next 500 µl of wash buffer was added to the column and centrifuged at 14500g for 30 seconds, the collection tube discarded and the column transferred to a fresh DNase free 1.5 ml microcentrifuge tube. 30 µl of elution buffer was pipetted onto the centre of the GFX membrane and the column left at room temperature for 1

min before centrifuging at 14500g for 1 min to recover purified DNA in the flow through which was then stored at -20ºC until further use.

2.1.1.6 Subcloning DNA into pGEX plasmids

The concentration of insert and vector DNA were calculated by spectrophotometry (NanoDrop 1000, Thermo Scientific) and samples diluted in capture buffer to achieved similar final DNA concentrations. Ligation reactions were carried out with insert to vector molar ratios of 1:1 and 3:1. The 1:1 molar ligation reaction was set up as follows: 2 µl of insert DNA, 2 µl of vector DNA, 2 µl of 10x T4 DNA ligation buffer (NEB) and 13 µl of distilled water to which 1 µl of T4 DNA ligase (NEB) was added immediately before use in a 1.5 ml microcentrifuge tube. After a brief vortex the reaction mixture was incubated at room temperature for 2 hr. For a 3:1 insert to vector reaction ratio, 6 µl of insert was used with 2 µl of vector DNA and 2 µl of 10x T4 DNA ligation buffer (NEB), 9 µl of distilled water and 1 µl of T4 DNA ligase (NEB) was added immediately before use.

2.1.2 Design and generation of recombinant protein immunogens to mouse PHD isoforms

2.1.2.1 Rationale

To generate antibodies to mouse PHD isoforms two strategies were used. Firstly regions of each PHD isoform of a size between 200 and 300 amino acids were subcloned into pGEX vectors (Pharmacia) thus allowing for IPTG driven expression of recombinant protein through the pGEX lac promoter.

The second approach was used to generate additional recombinant immunogens for mouse PHD1 and 3 with improved solubility. Hydrophilic regions of PHD1 and 3 were identified on the basis of Kyte-Dolittle hydropathy analysis. Next, a strategy was

developed whereby regions identified were PCR amplified with flanking SacII / AscI sites and subcloned into modified pGEX vectors bearing these sites in the appropriate reading frame in the multiple cloning site such that a GST – peptide fusion protein would be expressed on IPTG induction of transformed bacteria. This approach was not required for PHD2 as an anti-mouse PHD2 antibody able to recognise tissue PHD2 became available during the course of this doctoral thesis.

The recombinant proteins generated were used to immunise New Zealand white rabbits commercially (Eurogentec). Initially 100 µg of recombinant protein was used to immunise rabbits followed by three boosts of 100 µg at day 14, 28 and 50.

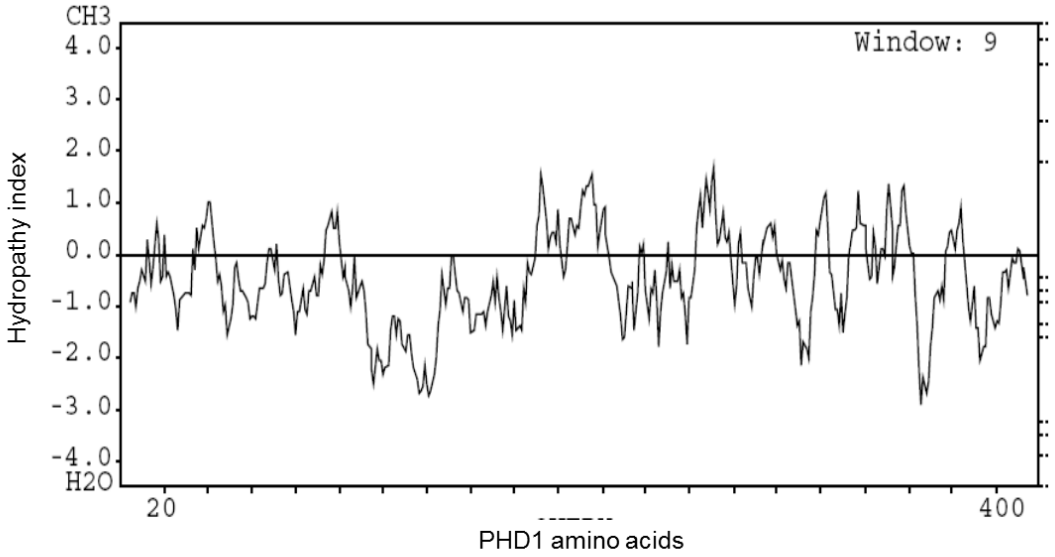
2.1.2.2 Recombinant DNA techniques used to generate new PHD1 immunogens

For mouse PHD1, Nco1 / Nco1 and Nco1 / Not1 restriction endonuclease derived fragments of mouse PHD1 cDNA (IMAGE clone: 5135579) were cloned in-frame into a pGEX vector and used to express amino acids 1 to 294 and 295 to 419 respectively. Restriction endonuclease digests were carried out as indicated in table 1.

DNA	Restriction endonuclease	Restriction endonuclease reaction conditions	Size of DNA band of interest
PHD1 (IMAGE:5135579)	Nco1	2 µl of 10x reaction buffer 3 (NEB), 2 µl of mini prep DNA, 5 µl of distilled water, immediately prior to use 1 µl of Nco1 restriction endonuclease was added to the reaction mix and incubated in a water bath for 2 hr at 37ºC. The reaction was stopped by heat inactivation at 65ºC for 5 min.	882 bp
PHD1 (IMAGE:5135579)	Nco1 / Not1	Restriction enzyme digests were carried out simultaneously. 2 µl of 10x reaction buffer 3, 2 µl of BSA 10 µl of distilled water, 2 µl of mini prep DNA. Immediately prior to use 2 µl of Nco1 and 2 µl of Not1 restriction endonucleases were added to the reaction mix and incubated in a water bath for 2 hr at 37ºC. The reaction was stopped by heat inactivation at 65ºC for 5 min.	982 bp
pGEX vector	The same restriction enzyme or enzyme pairs indicated above.	The same restriction endonucleases and reaction conditions used above. In addition 1 µl of CIP was added at the end of the digest for 30 min before heat inactivation at 65ºC for 10 min.	Not subject to agarose gel electrophoresis

Table 1. Restriction endonucleases and reaction conditions used in the generation of recombinant PHD1 protein immunogens.

Kyte-Dolittle hydropathy plot analysis of the PHD1 peptide sequence was used to identify hydrophilic regions as indicated in fig 1.



Hydrophobic: +ve, Hydrophilic: -ve

Fig 1. Kyte-Dolittle hydropathy plot of mouse PHD1

Based on this analysis, the following four hydrophilic regions of mouse PHD1 were identified corresponding to amino acids: 1 to 30; 50 to 91; 110 to 178; 300 to 340 and 360 to 400.

In order to generate new recombinant proteins these regions were PCR amplified to incorporate flanking SacII / AscI sites with the primer pairs indicated in table 2.

PHD1 hydrophilic regions:	Primer pairs incorporating SacII / AscI restriction sites
Amino acid 1 to 30	Forward 5'-TCCCCGCGGGGAGCATCTGGGGAG-3' Reverse 5'-GGCGCGCCTCATGGCCAAGCTCACCACC-3'
Amino acid 50 to 91	Forward 5'-TCCCCGCGGCAGGGTGCCCGGCCTGAG-3' Reverse 5'-GGCGCGCCTCACTCCCTCAGCCTAGC-3'
Amino acid 110 to 178	Forward 5'-TCCCCGCGGCCAGGCTGCCGGAGC-3' Reverse 5'-GGCGCGCCTCACACCATGGCCTTTGGGCG-3'
Amino acid 300 to 340	Forward 5'-TCCCCGCGGGGCAATGGGCTCGGGTACGTG-3' Reverse 5'-GGCGCGCCTCACTAGAAGATCTGCAGCAG-3'
Amino acid 360 to 400	Forward 5'-TCCCGCGGATTTTCTGGTCTGAC-3' Reverse 5'- GGCGCGCCTCACTATTTCTGTCCCGATGC-3'

Table 2. Primer pairs used to amplify hydrophilic regions of mouse PHD1

PCR amplification was carried out in 100 µl of reaction buffer (Stratagene, UK) {20 mM Tris-HCl (pH 8.8), 10 mM KCl, 2 mM $MgSO_4$, 10 mM $(NH_4)_2SO_4$ and 0.1% Triton X-100}, 200 µM of each nucleotide, 0.8 µM of each primer, 1 µl (50 ng of plasmid DNA) and 0.8 µl (2 units) of TAQ DNA polymerase. Temperature cycling was carried out on a DNA Thermal Cycler (Perkin Elmer). An initial 'Hot-start' for 4 min at 94ºC was carried out to reduce elongation of non-specifically primed sequences. 30 cycles of amplification were carried out with each cycle consisting of denaturing for 45 seconds at 94ºC, annealing for 50 seconds at 50ºC and extension for 1 min at 72ºC. A final incubation for 2 min at 72ºC ensured all amplification products

were of full length. A 5 µl aliquot of each PCR product was resolved by 2% agarose gel electrophoresis to confirm the presence of DNA fragments of the correct size.

Next, PCR products and pGEX vector were digested with the restriction endonuclease pairs indicated in table 3.

DNA	Restriction endonuclease	Restriction endonuclease reaction conditions	Size of DNA band of interest
PCR products	SacII / AscI	2 µl of 10x restriction enzyme buffer 4, 2 µl of DNA, 11 µl of distilled water. Immediately prior to use 2 µl of SacII and 2 µl of AscI restriction endonucleases were added to the reaction mix and incubated in a water bath at 37ºC for 1 hr then heat inactivated at 65ºC for 5 min.	Digestion products not subject to gel electrophoresis
pGEX vector	The same restriction endonucleases indicated above.	The digestion conditions used above. In addition 1 µl of CIP was added at the end of the digest for a further 30 min before heat inactivation as previously described.	As above

Table 3. Restriction endonucleases and reaction conditions used in the generation of recombinant PHD1 immunogens based on Kyte-Doolittle hydropathy analysis

Strategies used to generate mouse PHD1 immunogens are summarised in figure 3.

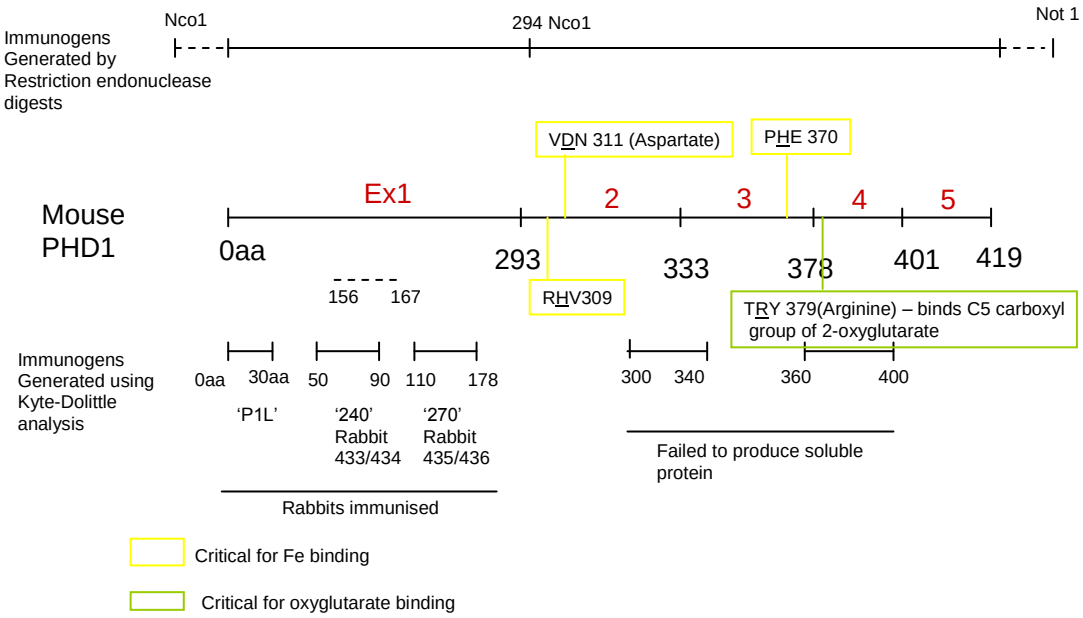


Fig 3. Summary of strategies used to generate new mouse PHD1 immunogens

2.1.2.3 Recombinant DNA techniques used to generate new antibodies to mouse PHD2

To generate mouse PHD2 antibodies, a Nco1/Not1 restriction endonuclease derived fragment of mouse PHD2 cDNA (IMAGE clone: 6312638) was cloned in-frame into a modified pGEX plasmid and used to express amino acids 295 to 400. Restriction endonuclease digests were carried out as indicated in table 4.

DNA	Restriction endonuclease	Restriction endonuclease reaction conditions	Size of DNA band of interest when digest resolved by agarose gel electrophoresis
PHD2 (IMAGE:6312638)	Nco1 / Not1	Restriction endonuclease digests were carried out simultaneously. 2 µl of 10x reaction buffer 3, 2 µl of BSA 10 µl of distilled water, 2 µl of mini prep DNA. Immediately prior to use 2 µl of Nco1 and 2 µl of Not1 restriction endonucleases were added to the reaction mix and incubated in a water bath for 2 hr at 37ºC. The reaction was stopped by heat inactivation as previously described.	2.5 Kb
pGEX vector	The same restriction enzymes or enzymes pairs indicated above.	The digestion conditions used above. In addition 1 µl of CIP was added at the end of the digest for a further 30 min before heat inactivation as previously described.	Not subject to agarose gel electrophoresis

Table 4. Restriction endonucleases reactions used to synthesise recombinant PHD2 protein immunogens

Purification and subcloning of the products of restriction enzyme digestion into pGEX plasmids was carried out as previously described. Strategies to generate mouse PHD2 immunogens are indicated in figure 4.

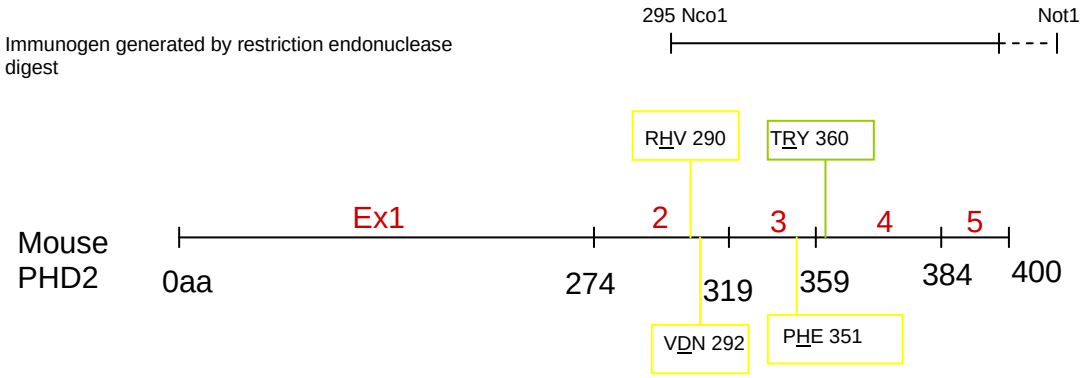


Fig 4. Summary of strategy used to generate new immunogens to mouse PHD2

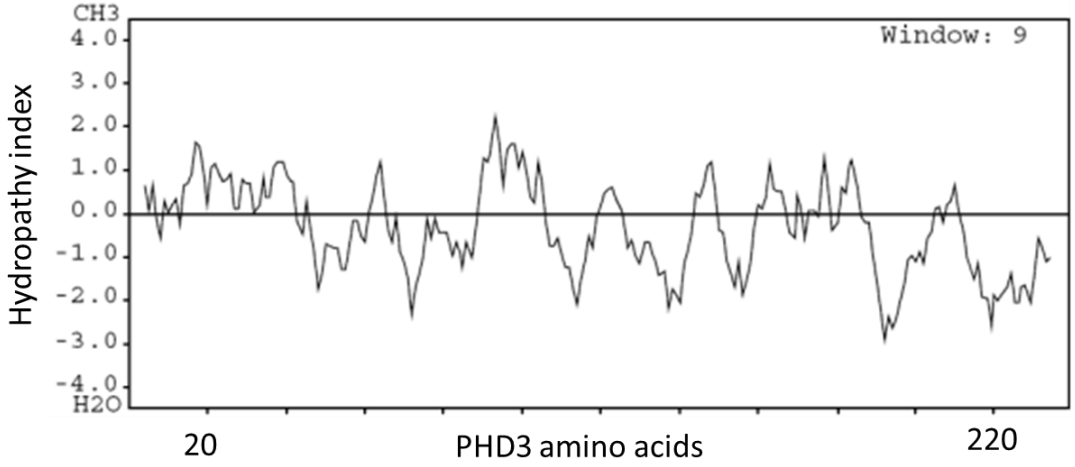
2.1.2.4 Recombinant DNA techniques used to generate new antibodies to mouse PHD3

For mouse PHD3, a blunt end restriction enzyme digest was required for in-frame translation of PHD3. Therefore PvuII / Not1 restriction endonuclease fragment of mouse PHD3 cDNA (IMAGE clone: 5373240) was cloned in-frame into a pGEX plasmid digested with Sma1 / Not1 restriction enzymes, thus allowing expression of amino acids 135 to 239. Restriction enzyme digests were carried out as indicated in table 5.

DNA	Restriction endonuclease	Restriction endonuclease reaction conditions	Size of DNA band of interest
PHD3 (IMAGE:5373240)	PvuII / Not1	2 µl of 10x restriction endonuclease buffer 3, 2 µl of DNA, 2 µl of BSA was added to 10 µl of distilled water. Immediately prior to use 2 µl of PvuII and 2 µl of Not1 restriction endonucleases were added and incubated in a water bath at 37ºC for 2 hr before heat inactivating as previously described	1583 bp
pGEX vector	Sma1 / Not1	2 µl 10x restriction endonuclease buffer 4, 2 µl of DNA, 2 µl of BSA, 12 µl of distilled water. Immediately prior to us 1 µl of Not1 and 1 µl of Sma1 restriction endonucleases were added to the reaction mix and incubated in a water bath at 37ºC for 4 hr. In addition, 1 µl of CIP was added at the end of the digest for a further 30 min before heat inactivation as previously described.	Not subject to agarose gel electrophoresis

Table 5. Restriction endonuclease reactions used to synthesise recombinant PHD3 protein immunogens

Kyte-Dolittle hydropathy plot analysis was used to identify hydrophilic regions of PHD3 as indicated in figure 5.



Hydrophobic : +ve, Hydrophilic: -ve

Fig 5. Kyte-Dolittle hydropathy plot of mouse PHD3

For mouse PHD3, hydrophilic regions corresponding to amino acids 50 to 90; 110 to 160, 190 to 239 were identified by this analysis and PCR amplified with flanking Sac II/ Asc I sites using the primer pairs indicated in table 6.

PHD3 hydrophilic regions:	Primer pairs incorporating SacII / AscI restriction sites
Amino acid 50 to 90	Forward 5'-*TCCCCGCGGCTGCACTACAACGGGGCC*-3' Reverse 5'-*GGCGCGCCTCAGATGGCCTCGCAGCCC*-3'
Amino acid 110 to 160	Forward 5'-*TCCCCGCGGTATGTCAAGGAGCGG*-3' Reverse 5'-*GGCGCGCCTCATCCGTGTAACTTGGC*-3'
Amino acid 190 to 239	Forward 5'-*TCCCCGCGGTGGTCAGACCGCAGG*-3' Reverse 5'-*GGCGCGCCTCAGTCTTTAGCAAGAGC*-3'

Table 6. Primer pairs used to amplify hydrophilic regions of mouse PHD3

PCR products were digested with SacII / AscI restriction endonuclease pairs as previously described. Purification and subcloning of the products of restriction endonuclease digests, into pGEX plasmids was carried out as previously described. Strategies used to generate mouse PHD3 immunogens are summaries in figure 6.

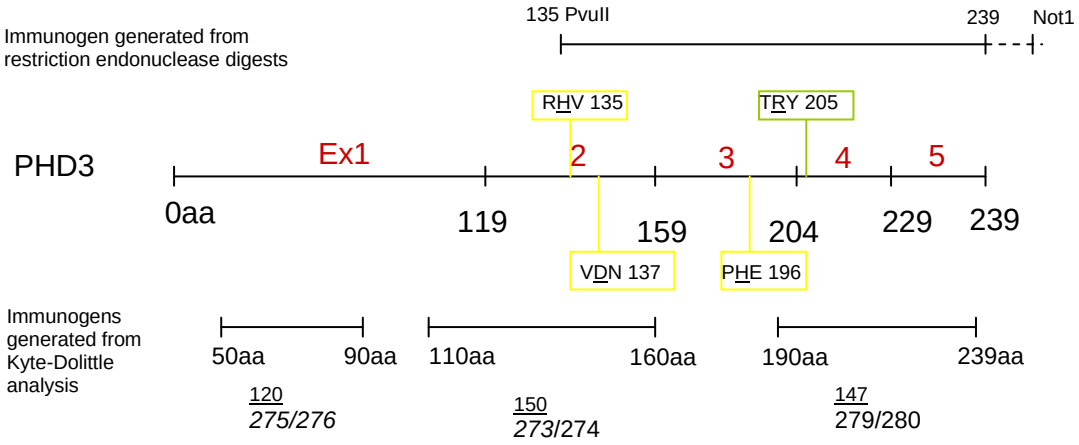


Fig 6. Summary of strategies used to generate new mouse PHD3 immunogens

2.1.3 Recombinant DNA techniques used to generate T7 promoter driven cDNA for each mouse PHD 1 and 3

2.1.3.1 Rationale

Full length mouse PHD isoforms were required to test the sensitivity and specificity of existing and new antibodies to each respective PHD isoform. PHD proteins were generated using a quick couple IVTT system (Promega), programmed with cDNA to each mouse PHD isoform and empty vector control. Full length cDNA for mouse PHD1 and 3 was commercially obtained within a pCMV sport 6 vector. Full-length mouse PHD2 cDNA was not commercially available at the start of this doctoral thesis and was generated as part of this doctoral study by methods to be described later.

The IVTT system allowed for generation of protein through either SP6 or T7 RNA polymerase promoters. cDNA for each isoform was used to programme either rabbit reticulocyte lysate or wheat germ lysate to generate full length PHD isoform. cDNA for pCDNA3 empty vector was used as a negative control, while cDNA for human PHD isoforms served as positive controls. ^{35}S methionine was used in the reaction mix to generate radio-labelled proteins, which were resolved on a 10% SDS-PAGE gel. The ^{35}S signal generated allowed the molecular weight of each product to be assessed. The number of methionine residues in each PHD protein sequence allowed for normalising the quantities of each PHD isoform at a molar level thus enabling direct comparison of signal generated by different antibodies.

We found that the SP6 promoter driven transcription of mouse PHD1 and 3 to be very weak. Therefore to enhance transcription, these cDNA sequences were subcloned from pCMV sport 6 vector into a pCDNA3 vector to allow T7 promoter driven transcription.

2.1.3.2 Restriction endonuclease and reaction conditions used to generate T7 promoter driven cDNA for mouse PHD1 and 3

Full length mouse PHD1 cDNA was digested with Not1 and EcoR1 restriction endonuclease pair and the fragment generated subcloned into pCDNA3 vector digested with the same restriction enzyme pair. For mouse PHD3, the Sma1 EcoR1 restriction endonuclease pair was used and the fragment generated subcloned into pCDNA3 vector digested with the same enzyme pair. Restriction endonucleases and reaction conditions are indicated in table 7.

DNA	Restriction endonuclease	Restriction endonuclease reaction conditions	Predicted fragment size
PHD1 (IMAGE:3600176)	Not1 / EcoR1	2 µl of min prep DNA , 2 µl of restriction endonuclease buffer 3, 2 µl of BSA, 10 µl of distilled water, 2 µl of Not1 and 2 µl of EcoR1 were incubated at 37ºC for 2 hr. The reaction was heat inactivated as previously described	1.8 Kb
PHD3 (IMAGE:5373240)	Sma1 / EcoR1	2 µl of mini prep DNA, 2 µl of 10x restriction endonuclease buffer 4, 12 µl of distilled water, 2 µl of Sma1 and 2 µl of EcoR1 were incubated at 35ºC for 2 hr before being heat inactivated as previously described.	1.9 Kb
pCDNA3	Restriction enzyme pairs indicated above	The digestion conditions used above. In addition, 1 µl of CIP was added at the end of the digest for a further 30 min before heat inactivation.	Not subject to agarose gel electrophoresis

Table 7. Restriction endonucleases and reaction conditions used to generate T7 promoter driven PHD1 and PHD3 isoforms

PHD1 and 3 cDNA fragments were subcloned into pCDNA3 in a ligation reaction as previously described.

2.1.4 Generating a cDNA containing the full length mouse PHD2 open reading frame

A mouse PHD2 cDNA containing the entire open reading frame was not commercially available at the start of this doctoral thesis. In order to generate it, a bioinformatics search was carried out to identify the longest PHD2 fragment

commercially available. This was identified to be a 1091 bp sequence which had missing, 107 bp of coding sequence from its 5' end incorporated in a PT73TD vector. We chose to commercially synthesis the missing 107 bp and subcloned it into the PT73TD vector using flanking HindIII and Not1 restriction endonuclease sites, thereby generating a full length mouse PHD2 sequence.

In order to create T7 promoter driven transcription, the full length PHD2 cDNA was next subcloned into pCDNA3 vector using HindII and EcoR1 restriction sites. A second T7 driven cDNA was generated using HindIII and Xho1 restriction sites as summarised in figure 7.

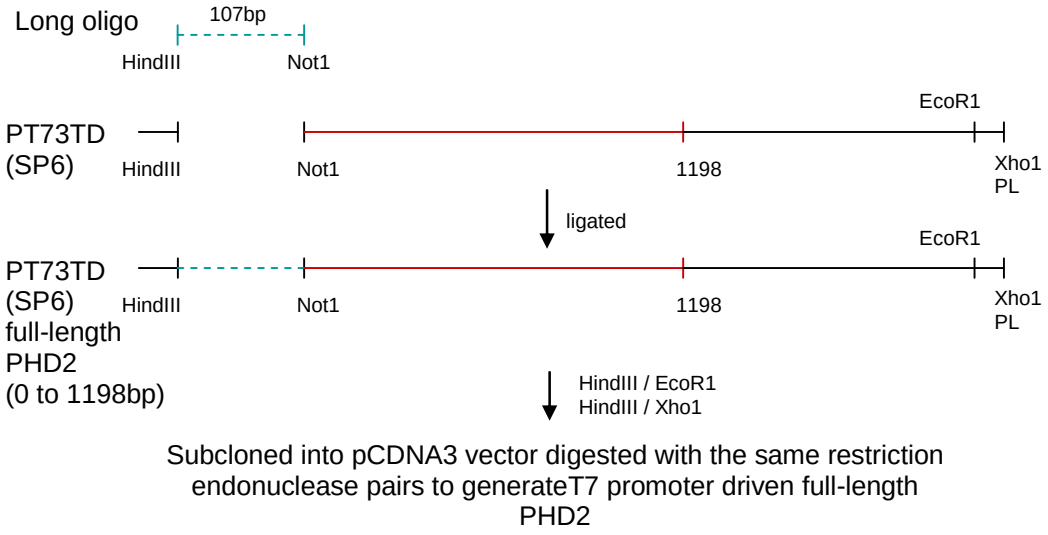


Fig 7. Schematic representation of the strategy used to generate full length mouse PHD2 cDNA

Long oligonucleotide sequence flanked by ends compatible with HindIII and Not1 restriction enzyme sites was designed to bridge the missing region of mouse PHD2 as indicated in table 8.

Forward strand:	5'- AGC TTA CCA TGG CCA GTG ACA GCG GCG GGC CCG GCG TGC TGA GCG CCA GCG AGC GCG ACC GGC AGT ACT GCG AGC TGT GCG GGA AGA TGG AGA ACC TGC TGC GCT GC -3'
Reverse strand:	5'- AT GGT ACC GGT CAC TGT CGC CGC CCG GGC CGC ACG ACT CGC GGT CGC TCG CGC TGG CCG T CA TGA CGC TCG ACA CGC CCT TCT ACC TCT TGG ACG ACG CGA CGC CGG – 3'

Table 8. Long oligonucleotide pair used to generate full-length mouse PHD2

The oligonucleotide pair was commercial obtained (Sigma Genosis). Each was diluted to 1 µM in TE buffer {10 mM Tris-HCL (pH 7.5), 1 mM EDTA} and 100 µl of each solution was placed in a 1.5 ml microcentrifuge tube and mixed by agitation. The tube was placed on a float in a water bath and heated at maximum power in a microwave cooker (Sanyo microwave oven, 750W) until the water bath boiled. Samples were annealed by cooling overnight at room temperature.

The PT73TD vector expressing partial mouse PHD2 cDNA was commercially obtained (IMAGE: 3375423) and used to produce mini preparation cDNA as previously described. This cDNA was digested with HindIII and Not1 restriction endonucleases under conditions indicated in table 9. The digestion products were purified as previously described and ligated to the long oligonucleotide pair to generate full length mouse PHD2 within the PT73TD vector.

DNA	Restriction endonuclease	Restriction endonuclease reaction conditions	DNA fragment size
Partial PHD 2 in PT73TD vector (IMAGE clone: 3375423)	HindIII / Not1	2 µl of DNA, 2 µl of 10x NEB buffer 2, 2 µl of BSA, 8 µl of distilled water, 2 µl of HindIII and 2 µl of Not1 restriction endonucleases in a water bath at 37ºC for 4 hr. A longer digest was used as Not1 activity in buffer 3 is reduced by 50%. Heat inactivation was carried out as previously described.	Not subject to agarose gel electrophoresis
Full length PHD2 in modified PT7T3 vector	HindIII / EcoR1	2 µl of DNA, 2 µl of 10x NEB buffer 2, 12 µl of distilled water, 2 µl of HindIII and 2 µl of EcoR1 were added immediately prior to use, and incubated at 37ºC for 2 hr and heat inactivated as previously described.	1.4 Kb
pCDNA3	HindIII / EcoR1	As indicated above, with additional 1 µl of CIP for 30 min before heat inactivation	Not subject to agarose gel electrophoresis
Full length PHD2 in modified PT7T3 vector	HindIII / Xho1	2 µl of DNA, 2 µl of 10x restriction enzyme buffer 2, 2 µl of BSA, 8 µl of distilled water, 2 µl of Hind III and 2 µl of Xho1 in a water bath at 37ºC for 2 hr. Enzymes were heat inactivated at 65ºC for 5 min.	1.5 Kb
pCDNA3	HindIII / Xho1	Reaction conditions indicated above with additional 1 µl of CIP for 30 min before heat inactivation	Not subject to agarose gel electrophoresis

Table 9. Restriction endonucleases reactions used to synthesise full-length mouse PHD2

Ligation reactions were carried out as previously described.

2.2 Protein Expression in bacteria / IVTT / COS cells

2.2.1 Expression of recombinant mouse PHD protein in bacteria

2.2.1.2 Bacterial transformation

For bacterial transformation, *E. coli* strain DH5α were thawed from -80ºC and a 50 µl aliquot transferred into a 1.5 ml microcentrifuge tube pre-chilled on ice, with unused cells being returned immediately to -80ºC. 1 µl of subcloned pGEX plasmid was added to DH5α *E.coli* bacteria and left to incubate for 30 min on ice. Heat shock was carried out by heating to 37ºC in a water bath for 15 seconds and returning to ice for a further 2 min. 950 µl of LB medium was added to the transformed bacteria and incubated on a shaker at 37ºC for 1 hr, before centrifuging at 2000g for 1 min, discarding the supernatant and resuspending the pellet in 20 µl of LB medium and transferring onto ampicillin containing LB agar plates and spreading under flame. Plates were allowed to dry for 10 min before incubating overnight at 37ºC. Single colonies were cultured and used to generate DNA mini preparations as previously described. These were sequenced at the Department of Biochemistry Oxford University and mini preparations incorporating recombinant PHD DNA stored at -20ºC until further use.

2.2.1.3 Expression of recombinant protein in bacteria

Plasmid incorporating recombinant PHD cDNA was used to transform *Escherichia coli* strain BL21 as previously described for transformation of DH5 α. A single colony was picked and grown overnight in 20 ml of LB medium (Sigma) supplemented with 100 µg/ml of ampicillin (Sigma). The overnight culture was added to 1l of fresh LB-ampicillin medium and allowed to culture while measuring its optical density at 600 nm (OD600) at ½ hr intervals using a spectrophotometer

(Perkin Elmer). When the bacterial culture had reached the exponential phase of growth as indicated by an OD600 of 0.7, T7 promoter driven protein expression was induced by the addition of IPTG (Sigma, UK) to a final concentration of 100 µM. After 2 hr of IPTG induction, cells were pelleted at 154000g for 30 min in a refrigerated centrifuge (Beckman Coulter) in a SW32 T1 rotor at 4ºC.

2.2.1.4 Extracting recombinant protein from bacteria

After centrifuging, the supernatant was removed and pellet resuspended in 100 ml lysis buffer (1% Triton-X-100, 0.5 mM EDTA in PBS). The resuspended bacteria were lysed by sonication on ice with a large probe (Vibra-cell, Sonics) at 16 µm amplitude for 20 seconds. Care was taken to avoid frothing. The lysate was centrifuged at 3273g for 20 min at 4ºC in a refrigerated centrifuge (Beckman Coulter) and the supernatant removed. Next 500 µl bed volume of glutathione sepharose 4B (Amersham) was washed 3 times with ice cold PBS to remove ethanol storage buffer and incubated with the lysate for 4 hr at 4ºC. The supernatant was then centrifuged at 3273g for 4 min at 4ºC in a refrigerated centrifuge (Beckman Coulter), the bead pellet transferred to a 1.7 ml microcentrifuge tube. After washing the beads three times in ice cold PBS, bead bound protein was eluted by agitating for 2 min at room temperature in 200 µl of reduced glutathione (10 mM glutathione in 50 mM Tris-HCl, pH 8.0). The elution step with reduced glutathione was repeated twice to maximise yield. Final elutes and 500µl aliquots taken at each stage of the expression process were diluted in 5x sample buffer {10% w/v SDS, 10 mM DDT (Sigma, UK), 20% w/v Glycerol, 0.2M Tris-HCl (Sigma UK) pH 6.8, 0.05% Bromophenol blue (Sigma, UK)}, boiled for 5 min and allowed to cool at room temperature for 2 min before being stored at -20ºC until further use.

2.2.1.5 Determining the concentration of expressed recombinant bacterial protein

The concentration of recombinant protein was determined by SDS-PAGE electrophoresis. The gels were next stained with Coomassie blue {0.4g of Coomassie blue (Sigma) dissolved in 200 ml of 40% v/v methanol and 200 ml of 20% v/v acetic acid} for 5 min before being washed in Coomassie distain (50% v/v methanol and 10% v/v acetic acid). Protein concentration was determined by comparing to an albumin dilution series run on a parallel gel.

2.2.2 Methods used to express full length mouse PHD proteins

2.2.2.1 Rationale

To tests the sensitivity and specificity of antisera, two strategies were used in parallel to express full length PHD proteins. One approach involved using full length T7 promoter driven cDNA generated during this doctoral thesis to programme rabbit reticulocyte IVTT. The other strategy involved transfecting these cDNAs into COS cells. PHD protein generated by this method was resolved by SDS-PAGE gel electrophoresis and used in an immunoblot to test the sensitivity and specificity of antibodies as will be described later in this methods section.

2.2.2.2 IVTT expression and normalisation of PHD proteins

^{35}S labelled methionine (Amersham biosciences) was used in the following IVTT reaction to generate radio labelled IVTT proteins. 40 µl of rabbit reticulocyte lysate, 2 µl of ^{35}S labelled methionine, 7 µl of nuclease free water and 2 µl of cDNA (0.5 µg/µl) was incubated at 30ºC for 90 min. IVTT products were diluted in 6x sample buffer and resolved by sodium dodecyl sulphate (SDS)- polyacrylamide gel electrophoresis (PAGE).

To fix proteins, SDS-PAGE gels were incubated on a rocker at room temperature for 30 min in fixative {10% acetic acid (Sigma), 50% methanol (Sigma), 40% distilled water} before being mounted on 3MM filter paper (Whatmen), covered with plastic wrap and dried at 80ºC for 90 min under vacuum using a gel vacuum drier (Biorad).

Next, the mounted gel was exposed to a phosphor screen (Cyclone storage phosphor screen, Packard) for 1 hr and the ^{35}S signal intensity of each PHD protein determined with a phosphor imager (Cyclone, Packard), and Optiquant software (Packard).

Equimolar amounts of ^{35}S labelled IVTT PHD protein was calculated on the basis of their ^{35}S signal intensities and adjusted according to the number of labelled methionine residues present in each PHD isoform.

2.2.3 Expression of PHD isoforms in COS cells

2.2.3.1 COS-7 cell culture

COS-7 cells were cultured under the following conditions: DMEM (Sigma) supplemented with 10% foetal calf serum, L-glutamine (1 mM) (Sigma), penicillin (100 µl/ml) (Sigma) and streptomycin (100 µg/ml) (Sigma) at 37ºC in an atmosphere of 5%CO_2, balance air. Cells were passaged every 4 days.

2.2.3.2 COS-7 Cell transfection

658 µl of serum free medium (Invitrogen) was added to a 5 ml centrifuge tube. Next, 7 µl of FuGENE 6 Transfection Reagent (Roche) was added to the serum free medium, taking care not to touch the sides of the tube. FuGENE and serum free medium were mixed by flicking and left to stand for 5 min at room temperature. 100 µl of FuGENE and serum free medium mixture were then added drop-wise to 2 µg (2 µl) of each cDNA to be transfected, mixed by flicking and incubated at room temperature for 15 min. During this incubation, cells were washed twice with serum free medium and washed wells filled with 800 µl of the same medium. Next, cDNA diluted in the FuGENE-serum free medium mix was added drop-wise to each well and returned to the incubator for 2 hr to allow transfection of cDNA to take place. After 2 hr, 100 µl of BSA (Sigma) was added and cells cultured for a further 48 hr before cells were harvested.

To harvest, cells were washed 3 times with ice cold PBS and detached by scrapping into 300 µl of urea SDS/buffer {6.7M urea, 10 mM Tris-HCl (pH 6.8), 1 mM DTT, 10% glycerol and 1% SDS supplemented with Complete Protease Inhibitor Cocktail (Roche)}.

The protein concentration of cell extracts was determined using a Detergent Compatible Protein Assay Kit (Bio-Rad) as follows. 5 µl of protein sample was pipetted into individual wells of a 96-well plate (Falcon). 20 µl of reagent 'S' (surfactant solution) was added to 980 µl of reagent 'A' (alkaline copper tartrate solution) in 1.7 ml microcentrifuge tube. After a brief vortex, 20 µl of this mixture was added to each well followed by 160 µl of reagent 'B' (dilute Folin reagent). After incubating at room temperature for 15 min, absorbance at 650 nm was determined

using a microplate Reader (Bio-Rad) and microplate manager '5' software (Bio-Rad). The average obtained from triplicate samples was corrected for background by subtracting averaged values for lysis buffer from that of cell extracts. Protein concentration was determined by comparing to a BSA dilution series made up with the same lysis buffer. Samples were diluted in 6x sample buffer {1M Tris-HCL (pH 6.8), 30% glycerol, 10% SDS, 0.6M DTT, 0.02% bromophenol blue} and heated for 5 min at 95ºC. After a brief vortex samples were allowed to cool at room temperature before being stored at -20ºC.

2.3 Antibodies

Antibodies identified to be capable of detecting PHD1 to 3 in rat tissues and PHD1 and 2 in mouse tissues are summarised in tables 10 and 11.

Antibody	Species generated in	Optimal dilution (IB)	Incubation time (IB)	Rodent Species	Note
PHD3: 188e	Mouse monoclonal (in house)	1/10	6 hr at room temperature	Rat	Used with isotype matched secondary antibody rabbit anti-mouse IgG1 (cat # 04-6120, Zymed) at 1:1000 for 1 hr at room temperature
PHD3: NB100-137	Rabbit polyclonal to human PHD3	1:1000	6 hr at room temperature	Good signal in rat cell lines only	Used with conventional secondary anti-rabbit antibody at 1:2000 for 1 hr at room temperature
PHD3 NB 100-303	Rabbit polyclonal to human PHD3	1:1000	6 hr at room temperature	Good signal in rat cell lines only	as above
PHD2	Rabbit polyclonal generated by Professor Patrick Maxwell to mouse PHD2	1:3000	6 hr at room temperature	Rat Mouse	as above
PHD2 Novus NB100-2219	Rabbit polyclonal to human PHD2	1:1000	6 hr at room temperature	Rat	as above
PHD1 (R1)	Rabbit polyclonal to rat PHD1, in house generated by Dr. Ya-Min Tian	1:2000	6 hr at room temperature	Rat	as above
PHD1 (Af 1.3)	Rabbit polyclonal to human PHD1, in house generated by Dr. Ya-Min Tian	1:500	4ºC overnight	Rat	as above
PHD1 (Af 1.1)	Rabbit polyclonal to human PHD1 generated by Dr. Ya-Min Tian	1:250	4ºC overnight	Mouse	As above

Table 10. Antibodies used for immunoblot of rodent tissues

Antibody	Species of origin	Optimal dilution (IHC)	Incubation time (IHC)	Kit	Chromogen	Development time (IHC)	Rodent species
188e	mouse monoclonal to full length human PHD3	5x	Overnight at 4ºC	Envision mouse	DAB, Vector grey Vector blue	1 min	Rat
Novus NB100-303	affinity purified rabbit polyclonal to PHD3	1:1000	Overnight at 4ºC	Envision rabbit	DAB, Vector grey	1 min	Rat
Af 1.1 to PHD1	Affinity purified rabbit polyclonal to human PHD1	1:500	Overnight at 4ºC	CSA method only	DAB	3 min	mouse
Tyrosine hydroxylase (ImmunoStar :22806)	Mouse monoclonal	1:2000	6 hr at room temperature	Envision (mouse) Vector ABC with mouse Alkaline phos	DAB Vector blue	30 seconds	rat
Tyrosine hydroxylase (Abcam : 112)	Affinity purified rabbit polyclonal	1:1000	6 hr at room temperature	Vector ABC with rabbit alkaline phos	Vector blue	1 min	rat
NeuN (Chemicon: MAB377)	mouse monoclonal to neuronal nuclei	1:1000	6 hr at room temperature	Vector ABC with mouse alkaline phos	Vector blue	1 min	rat
Mouse IgG1 Kappa monoclonal control (Abcam: MG1-45; ab 18448)	Mouse monoclonal to Trinitrophenol conjugated to KLH	1:500	Overnight at 4ºC	Envision mouse	DAB, Vector grey Vector blue	1 min	rat

Table 11. Antibodies used for IHC of rodent tissues

2.4 Conjugation of Fluorescein isothyocyanate (FITC) to anti-PHD3 mouse monoclonal antibody (188e)

2.4.1 Rationale

Using rabbit reticulocyte IVTT, it was established that the anti-human PHD3 mouse monoclonal antibody, 188e was able to also detect mouse PHD3. However when it was used to immunoblot mouse tissue extracts, the signal from this antibody was found to be obscured by cross reacting mouse immunoglobulin. In an attempt to overcome this, antibody 188e was conjugated to FITC and an anti-FITC secondary antibody used instead of an anti-mouse secondary to detect PHD3 bound antibody.

2.4.2.1 Protein G bead based purification of 188e mouse monoclonal antibody

500 µl of protein G beads (Sigma) was washed 3 times in ice cold PBS to remove storage buffer and incubated overnight at 4ºC with 50 ml of 188e antibody hybridoma supernatant on a rocker. Next, beads were separated from supernatant by centrifugation at 2000g for 5 min and the isolated beads washed 3 times in ice cold PBS. Antibody was eluted from beads by washing three times in 500 µl of elution buffer (0.1M glycine pH 2.8). Eluted antibody was brought to a neutral pH by the drop-wise addition of neutralisation buffer (Tris 1M pH 8.0). PH was monitored with pH strips (Whatman).

In order to remove Tris, glycine and sodium azide the antibody concentrate was dialysed at 4ºC with a 20 KDa MWCO membrane (Millipore) for 48 hr with 4 changes of water bath. To produce the correct concentration of antibody for conjugation, 2 ml of dialysed antibody was centrifuged at 2000g for 20 min in a 30,000 KDa MWCO concentrator (Vivaspin 2, Sartorius Stedim Biotech). A final

volume of 300 µl of immunoglobulin at a concentration of 5 mg/ml was achieved in 0.1M sodium carbonate-bicarbonate buffer (Sigma).

2.4.3 FITC conjugation

Conjugation to FITC was carried out using a FluroTag FITC conjugation kit (Sigma) according to the manufacturer's instructions. 250 µl of antibody concentrate was pipetted into a microcentrifuge tube and wrapped in foil. Immediately prior to use, a FITC vial was dissolved in 2 ml of 0.1M sodium carbonate-bicarbonate buffer (Sigma). 50 µl of this solution was added drop-wise to the antibody concentrate and incubated at room temperature for 2 hr with gentle stirring. In order to optimise the binding of FITC to concentrated 188e, two further conjugation reactions were carried out in parallel with different amounts of FITC to antibody ratios in accordance with the manufacturer's instructions. In the first reaction, 500 µl of FITC and concentrated antibody were conjugated while in the second reaction, 250 µl of FITC was conjugated with 750 µl of concentrated antibody.

2.4.4 Isolation of FITC conjugated antibody

Labelled antibody was isolated using a Sephadex G-25M column. Briefly, the column was emptied of storage buffer taking care not to allow beads to dry. Any remaining storage buffer was removed from the bead column with 6 x 2 ml washes of PBS. The conjugated antibody was next applied to the column. Two bands were visible in the column, with the conjugated fraction present in the upper band. Conjugated antibody was eluted by adding 2.5 ml aliquots of PBS to the column and collecting the flow through. The absorbance of each aliquot at 280 nm was assessed

and those with an absorbance of greater than 0.2 were pooled, the remainder discarded. Pooled samples were protected from light with foil wrap and stored in a cold room at 4ºC until further use.

The molar FITC to antibody ratio (F/P) was calculated using a spectrophotometer (ND-1000, NanoDrop) by determining the absorbance of FITC at 495 nm (A495) and immunoglobulin at 280 nm (A280) according to the following formula:

$$\text{Molar F/P} = \frac{2.77 \times A_{495}}{A_{280} - (0.35 \times A_{495})}$$

Optimum conjugation of FITC to immunoglobulin occurred at F/P ratios of <6.

2.5 Immunoblot

Sodium dodecyl-sulphate polyacrylamide gel electrophoresis (SDS-PAGE) were synthesised as follows. Running gels were made up according to the molecular weight of the protein of interest as indicated in tables 12 and 13.

Molecular weight range	% acrylamide in running gel
50 to 500 KDa	7
20 to 300 KDa	10
10 to 200 KDa	12
3 to 100 KDa	15

Table 12. Percentage of acrylamide per running gel and corresponding molecular weight range of protein to be resolved

Reagent	Percentage gel and reagent volume (ml)			
	7%	10%	12%	15%
H2O	15.3	12.3	10.2	7.2
1.5M Tris-HCl, pH 8.8	7.5	7.5	7.5	7.5
20% (w/v) SDS	0.15	0.15	0.15	0.15
Acrylamide/Bis-acrylamide (30%/0.8% w/v)	6.9	9.9	12	15
10% (w/v) APS	0.15	0.15	0.15	0.15
TEMED	0.02	0.02	0.02	0.02

Table 13. Composition of running gel according to required percentage of acrylamide

A Mini-Protean Vertical Gel Electrophoresis Apparatus (Bio-Rad) was assembled according to the manufacturer's instructions taking care to ensure that glass plates were thoroughly cleaned and dried prior to assembly. A 10% running gel was cast first and amounts of reagent chosen according to this percentage as indicated above. Polymerisation was initiated by adding APS and TEMED immediately prior to pouring the gel. The gel was cast with sufficient space to allow for a 1 cm gap between comb and running gel. 100 µl of water saturated butanol (Sigma, UK) was pipetted onto the gel after pouring to minimise formation of a meniscus. Polymerisation occurred at room temperature over a 30 min period, after which the butanol layer was removed by tipping the cassette and absorbing any residual butanol with tissue.

Next the stacking gel was poured using reagents indicated in table 14 and a 15 well comb sited. After 20 min, the comb was carefully removed to avoid damaging the stacking gel and the glass plates encompassing the gel removed from its cassette and placed in the electrophoresis tank. Next the tank was filled with running buffer {25 mM Tri-HCl (Sigma, UK), 200 mM Glycine (Sigma, UK), 0.1% (w/v) SDS

(Sigma, UK)}. Individual wells were flushed with running buffer using a needle and syringe to remove debris before loading samples. Equal amounts of protein samples were loaded per well and resolved at 100v until the sample dye marker had reached the bottom of the gel.

Reagent	Volume (ml)
H2O	3.075
0.5M Tris-HCl, pH 6.8	1.25
20% (w/v) SDS	0.025
Acrylamide/Bis-acrylamide (30%/0.8% w/v)	0.67
10% (w/v) APS	0.025
TEMED	0.005

Table 14. Composition of staking gel

Immobilon-P membranes (Millipore) membranes were prepared by immersion for 2 min in methanol followed by a further 2 min in distilled water and a final immersion in transfer buffer (10 mM Tris, 100 mM glycine, 10% methanol, 0.005% SDS).

After electrophoresis, gels were removed from the gel tank and separated from glass plates by use of a scalpel. Gels were next equilibrated in transfer buffer before being placed against the prepared Immobilon-P membrane and sandwiched between an inner, 3MM chromatography paper (Whatman) and outer fibre pads before being placed in a cassette and loaded into the Mini-Protean II tank (Bio-Rad). Transfer of proteins took place over 1 hr at 100V.

After transfer, gels were discarded and the membranes blocked for 20 min with 5% fat-free milk (Marvel) and probed with primary antibody as indicated in table 10. The membrane was next washed 5 x PBST for 3 min each.

Next, membranes were incubated with HRP conjugated anti-rabbit or anti-mouse secondary antibody (DAKO) at a concentration of 1:1000 in 5% fat-free milk (Marvel) for 30 min and the membrane washed 3 x for 5 min with PBST.

The ECL Plus system (Amersham Biosciences) was used to visualise immunoreactive species by a chemiluminescence reaction. 5 µl of reagent A was added to 995 µl of reagent B and incubated in the dark for 3 min. During this period the washed membrane was placed onto an acetate sheet, and care taken to avoid the membrane from drying. After 3 min the ECL Plus mix was pipetted evenly onto the membrane and covered with a further acetate sheet, taking care to avoid air trapping. Chemiluminescent signal was detected either by X-OMAT LS film (Kodak) or chemiluminescent camera (AutoChemi System, UVP) and analysed with Labworks software (UVP).

2.6 In situ hybridisation

2.6.1 Rationale

In tissues where PHD3 signal was demonstrated by IHC, in-situ hybridisation was also carried out to confirm the presence of PHD3 mRNA.

2.6.2 PHD3 mRNA probes

The following primer pairs, designed and generated by Willam et al, were used in a PCR reaction using rat PHD3 cDNA as template. The anti-sense probe generated protected a 167 bp region of rat PHD3 exon 1 as indicated in table 15.

Forward primer	5′-GGAATTCGGCTCTGTGAGCGAGATGCC – 3′
Reverse primer	5′-CGGGATCCAGCTGCTTGACTCGCTCCAG -3'
Region protected	5'-TCGGCTCTGTGAGCGAGATGCCTCTGGGACACATCATGAGGCTGGATC TGGAGAAGATCGCCCTGGAGTACATCGTGCCCTGTCTGCACGAGGTCGGT TTCTGCTACCTGGACAACTTCCTAGGCGAGGTGGTGGGCGACTGCGTACT GGAGCGAGTCAAGCAGCTG-3'

Table 15. Primer pair used to generate RNA probe to rat PHD3 and region protected

Sense and anti-sense probes were generated and labelled with [^{35}S]-UTP (Amersham) as described by Willam et al., 2006.

2.6.3 In situ hybridisation

10 µm frozen tissue sections were cut onto coated slides (Vector Laboratories), air dried for 10 min and stored at – 80ºC. Next, sections were fixed for 20 in 4% PAF in PBS then two 2 min washes in PBS, before being treated with proteinase K (0.0005%) in 0.1M Tris/0.05 M EDTA, pH 8.0 for 5 min at room temperature.

Slides were next rinsed in 0.2% glycine in water and post-fixed with 4% PAF/ 0.1M NaOH/0.1M NaAc for 5 min, rinsed in 0.1M TEA, pH 8.0 for 3 min, acetylated for 10 min in 0.25% acetic anhydride/ 0.1 M TEA, pH 8.8, and dehydrated by immersing sequentially in 50%, 75% and 100% ethanol baths for 3 min each. RNA probe was then hybridized to the sections at 60ºC for 16 hr in 50% formamide/10% dextran sulphate/ 0.15 M NaCl/1x Denhardt's solution/0.01M Tris, pH 8.0/0.01 M DTT with 0.5 mg/ml tRNA.

Sense probes were processed in parallel as a specificity control. The slides were next rinsed in 4x SSC and incubated at 37ºC for 30 min with 0.1 mg/ml RNase A in 0.5M NaCl/0.01 M Tris, pH 8.0/l mM EDTA and dehydrated though graded ethanol washes as previously described.

Next slides were coated with emulsion (Kodak NTB-2, Eastman Kodak), in a dark room and the emulsion allowed to develop in the dark for 10 days at 4ºC. Next the emulsion was developed (Kodak D19 developer) and fixed (Kodak Fixer). Sections were then stained with haematoxylin and eosin.

2.7 Animal hypoxia and tissue preparation

2.7.1 Animal hypoxia studies

All studies were carried out in keeping with local animal welfare policies. Animals were placed in a Perspex air sealed chamber (Harvard Apparatus) measuring 31 x 30.5 x 45.5 cm. The chamber had a perforated aluminium floor with one gas inlet below the floor and one gas outlet above. The floor of the chamber was lined with wet-bed absorbent flooring (Harlen) and animals provided access to food, water and environmental stimuli *ad libitum.* Animals were acclimatised by graded reduction in oxygen tensions over a period of 30 min to a steady state of 8% O_2 and the remainder N_2 (BOC gases), and maintained at this level for either 1 ½ hr, 8 hr or 24 hr. Animals were sacrificed by cervical dislocation. Organs were rapidly harvested before being stored in liquid nitrogen.

2.7.2 Whole tissue protein preparation for immunoblot

Organs were rapidly harvested and larger organs (liver, kidneys, brain) divided into smaller sections before being rapidly frozen in liquid nitrogen. The small size of sympatho-adrenal tissues necessitated skills to be developed in micro-anatomy, micro-dissection, as well as handling and processing of delicate tissue which included those of the adrenal gland, SCG and carotid body (CB). The size of these tissues meant that generating sufficient extracts for immunoblot purposes proved to be technically challenging. This was particular true of the carotid body, which in adult rat was of 0.5mm x 0.3mm x 0.15mm in size (Korkala et al., 1973). Similarly the adrenal medulla has a volume of 1.3mm3 (Tomlinson et al., 1987) and although marginally larger than the carotid body, lacked clear demarcation from the adrenal cortex under dissecting light microscope. This meant that only whole adrenal gland extracts were generated.

Harvested tissues were weighed and homogenised in 20x v/w urea-SDS lysis buffer {10 ml 8M urea; 1 ml glycerol (Sigma), 0.5 ml 20% SDS (Sigma); 100 µl 1M Tris/HCl pH 7.5 supplemented with complete protease inhibitor cocktail (Roche)} e.g. 20 ml lysis buffer for every 1g of tissue. Samples were homogenised for 30 seconds with a large tissue homogeniser (10G, Ika-Werke) and left on ice for 10 min. The lysate was next centrifuged at 3230g for 5 min and supernatant removed taking care to avoid both pellet and meniscus.

The small size of the rat SCG meant that it could not be processed in this way without causing significant sample loss. Therefore whole SCG's were micro-dissected from their normal anatomical position using a stereo microscope (M80, Leica) and

fibre optic light source (L2, Leica). The dissected SCG was suspended in ice cold PBS solution with fine insect pins (Agar Scientific) in a polymer coated Petri dish (Agar Scientific) and residual connective tissue quickly dissected under microscope guidance. SCGs devoid of connective tissue were frozen in liquid nitrogen and stored at -80ºC until further use.

At the time of processing whole SCGs were placed in a dry ceramic mortar (Stratech Scientific) which had been pre-chilled for 10 min with dry ice. SCG's were immersed in liquid nitrogen and ground to a fine powder using a pre-chilled pestle (Stratech Scientific). Care was taken to retain all ground tissue within the mortar. Powdered tissue was next transferred quickly into a pre-chilled microcentifuge tube using a pre-chilled metal spatula (Stratech Scientific) and the tube immersed in ice until the powder had thawed, to a pulp. Next 200 µl of urea SDS buffer was added to the sample and left on ice for a further 5 min with intermittent vortexing, before centrifuging at 3230g for 5 min. The supernatant was removed and stored in 6x sample buffer until further use.

A Protein Assay Kit (DC; Bio-Rad) was used to determine tissue protein content as previously described. Samples were normalised at the time of immunoblot by loading 10 µl of the most dilute homogenate, and adjusting the volumes of more concentrated tissue extracts accordingly.

2.7.3 Preparation of nuclear proteins from tissues for immunoblot

500 mg of frozen tissue was rapidly ground into a fine powder with a ceramic pestle and mortar (Stratech Scientific) whilst in a liquid nitrogen bath. Ground tissues

were transferred to a Dounce homogenizer (loose) (VWR) and 1 ml of lysis buffer {10 mM HEPES pH 7.9; 10 mM KCl; 0.1 mM EDTA pH 8.0; 0.1 mM EGTA to which 0.5 mM PMSF; 1 mM Na_3VO_4; 1 mM NaF and 1x 'complete' protease inhibitor (Roche) was added immediately before use}. Ground tissues were homogenised using 10 strokes of the Dounce homogeniser. 10 µl of 10% NP-40 was added to the homogenate and vortexed for 30 seconds before being placed on ice for 10 min. The tissue was homogenised again with a further 5 strokes and transferred into a 1.5 ml microcentrifuge tube. Samples were centrifuged for 5 min at 3273g at 4ºC for 5 min.

Next, the top and middle layers were discarded and the pellet washed 3 times with 1 ml of lysis buffer. The washed pellet was centrifuged at 3273g for 5 min to remove residual lysis buffer. Next the pellet was resuspended in 400 µl of nuclear extraction buffer {20 mM HEPES pH 7.9, 400 mM NaCl, 1 mM EDTA pH 8.0, 1 mM EGTA; 10% glycerol; 0.5 mM PMSF 1 mM Na_3VO_4; 1 mM NaF; 4M KCl and 'complete' protease inhibitor (Roche) was added immediately before use}, before incubating on ice for 30 min. Next, the homogenate was centrifuged at 3273g for 5 min at 4ºC and the supernatant removed and stored in aliquots at -80ºC in 6x sample buffer.

2.7.4 Perfusion fixation and processing of tissues for IHC

Rats were deeply anaesthetised with 300 µl intraperitoneal pentobarbital (Harlen), the heart and the left ventricle was cannulated. Ice cold PBS infused into the systemic circulation via this cannula from a glass chamber suspended 1m above the animal and perfusate drained by puncture of the right atrium. After 3 min of PBS infusion, the fluid drained from the right atrium became clear indicating that the circulation was

devoid of blood. At this stage, PBS was replaced with 4% ice cold PAF (Sigma) fixative which was perfused into the circulation for 5 min. During this period tissues were noted to stiffen as tissue fixation took place.

After fixation, tissues were removed and immersed in a 4% PAF bath overnight. The next day, tissues were washed twice in 70% ethanol and placed into processing cassettes (Tissue Tek) before being processed sequentially as indicated in table 16.

Step	Reagent	Duration in hours
1	70% ethanol in distilled water	1
2	70% ethanol in distilled water	1
3	90% ethanol in distilled water	1
4	90% ethanol in distilled water	1
5	100% ethanol	1 ½
6	100% ethanol	1 ½
7	Histo-clear	1 ¾
8	Histo-clear	1 ¾
9	Histo-clear	1 ¾
10	molten wax at 65ºC	2 ½
11	molten wax at 65ºC	2 ½
12	molten wax at 65ºC	2 ½

Table 16. Tissue fixation protocol

2.7.5 Embedding and sectioning of tissues

Tissue embedding was carried out using a tissue embedding station (Leica). Tissues were placed into moulds (Tissue Tek) and orientated in molten wax. Next molten wax was allowed to cool by placing on a cold plate.

Once hardened, tissue blocks were detached from their moulds and mounted on a rotary microtome and 8 µm sections cut. The ribbon of sections was carefully placed in a floatation bath at 40ºC and mounted onto a glass slide (Surgipath). Slides were

dried in an oven (Leica) at 35ºC for 1 hr. Dried slides were left at room temperature overnight and then placed in a slide box (Agar Scientific) until further use.

2.7.6 Processing of frozen tissues

Tissues were harvested as previously described and orientated in OCT mounting medium (Sakura) before being frozen in a liquid nitrogen bath. For sectioning, frozen tissues were mounted on a chuck with OCT (Sakura) and placed in a cryostat (Leica) at -20ºC. OCT embedded tissues, slides (Surgipath), microtome blades (Surgipath), forceps and tissue brushes were allowed to equilibrate for 20 min to cryostat temperature before sectioning. Next, 8 µm tissue sections were cut and up to 4 sections mounted per slide. Slides were allowed to dry at room temperature before being stored at -80ºC.

2.7.7 COS cell pellet synthesis for IHC

COS cells were transfected with pCDNA3 expression vector containing cDNA for each PHD isoform as well as empty vector as previously described. Cells were detached from the culture dish with 250 µl per well of trypsin-EDTA solution (Sigma). Detached cells were washed 3 times in ice cold PBS solution before being centrifuged at 2000g for 1 min to form a cell pellet which was fixed overnight in 4% PAF. The pellet was then embedded in paraffin, sections cut and mounted on a slide for use in immunohistochemical studies as previously described.

2.7.8 Identifying brain regions

A brain stereotactic matrix (Zivic instruments) was used to section brain into anatomical regions according to validated co-ordinates (Rat brain atlas, Paxinos and Watson). Representative sections from each anatomical region of interest were stained with an anti-tyrosine hydroxylase antibody (Stratech Scientific) under conditions indicated in table 11, to confirm the presence of catecholamine expressing cell populations at the expected co-ordinates.

2.8 Immunohistochemistry

2.8.1 Generic immunohistochemistry methods

Sections were de-waxed in 2 x 3 min baths of xylene and re-hydrated in a series of ethanol washes as follows: 2 x 3 min baths of 100% ethanol followed by 2 x 3 min baths of 70% ethanol and then 2 x 5 min distilled water baths. Next, antigen retrieval solution (DAKO) was heated at maximum setting in a microwave oven (Sanyo, 750v) until the solution became cloudy and started to boil. It was then removed from the microwave oven and allowed to cool for 1 min at room temperature.

Slides were mounted on a glass rack and placed into the boiled antigen retrieval solution and the whole container transferred to a pressure cooker (Delico, Tefal) which had been pre-heated for 5 min on a hot plate (Cookworks). Next sections were heated at pressure setting ‘2’ for 15 min at maximum temperature after which the pressure cooker was removed from the hot plate and allowed to cool at room temperature until the pressure release valve had opened.

Slides were removed from the pressure cooker and allowed to cool further at room temperature until the antigen retrieval solution became clear and sections ringed with a wax-pen (Pap Pen, Zymed Laboratories). All incubations were performed in a humidified chamber (Raymond Lamb) and care taken to prevent drying of sections. All incubations apart from the normal serum block were followed by two 5 min washes with TBST {300 mM NaCl, 50 mM Tris (pH 7.5), 0.1% Tween-20}. Residual TBST was dabbed off the slide with tissue paper (Kimwipe) taking care not to disrupt sections.

Primary antibodies were used as indicated in table 11. For mouse monoclonal antibodies, sections adjacent to those treated with primary antibody were treated with an isotype matched antibody of the same dilution as a control. For rabbit primary, antibodies normal rabbit serum of the same dilution was used as a control.

For peroxidase conjugated secondary antibodies, antigen bound antibody was visualised as a brown colour change by reaction with H_2O_2 using DAB chromogen. The reaction was stopped by washing in copious amounts of warm tap water at the times indicated in table 11. Where indicated, sections were counter stained for 2-5 seconds with Hematoxylin (Raymond and Lamb) and de-stained (70% ethanol, 1% HCl) when appropriate to optimise resolution.

Next, slides were dehydrated in a series of ethanol washes (ethanol 70% 2 x 3 min, 100% 2 x 3 min), de-waxed in Xylene (2 x 3 min) to remove wax-pen boarders and mounted using mounting medium (DPX, Raymond and Lamb) and 22 x 50 mm cover glass (VWR) before being stored in a slide box (VVR) until further use.

Stained sections were analysed by bright field microscopy, using a differential interference contrast microscope (Leica) and digital image capture software (Visitron).

2.8.2 Streptavidin-biotin-peroxidase based IHC

For mouse tissues, a commercial catalysed signal amplification kit (CSA, DAKO), based on the streptavidin-biotin-peroxidase reaction was used according to the manufacturer's instructions. Endogenous tissue avidin, biotin, peroxidase, and background proteins were blocked with specific blocking agents for 10 min, 10 min, 5 min and 30 min respectively. To identify PHD1, Af1.1 rabbit polyclonal antibody was dilute to 1:500 in background reducing agent (DAKO) and incubated overnight in a humidified chamber. Next, sections were incubated with a biotinylated anti-rabbit secondary antibody, streptavidin-biotin complex, amplification reagent and streptavidin-peroxidase each for 15 min. Antigen bound antibody was visualised with DAB.

2.8.3 HRP-conjugated polymer based IHC

For rat tissues, a HRP-conjugated polymer based kit (Envision, DAKO) was used according to the manufacturer's instructions. After treatment for 5 min with peroxidase block, sections were incubated with primary antibody. Next, sections were incubated for a further 30 min at room temperature with either anti-rabbit or anti-mouse HRP-conjugated polymer. DAB chromogen was used to visualise antigen bound antibody as above.

2.8.4 Avidin-Biotin complex method based IHC

For those tissues indicated in table 11, an ABC-alkaline phosphatase kit (Vector Laboratories) was used according to the manufacturer's instructions. Sections were incubated at room temperature for 20 min with 5% goat serum block. Next primary antibody was added and incubated as indicated in table 11. Biotinylated anti-mouse or anti-rabbit secondary antibody was added to each section and incubated for a further 1 hr at room temperature. The Avidin-biotin complex was applied to each section and incubated at room temperature for a further 30 min. Vector Blue alkaline phosphatase substrate (Vector Laboratories) was added to each section and incubated in the dark for 10 min. The reaction was stopped by washing in copious amounts of warm tap water for the times indicated. Where indicated, sections were counter stained for 2-5 seconds with Hematoxylin (Raymond and Lamb) and de-stained (70% ethanol, 1% HCl) when appropriate to optimise resolution.

2.8.5 Immunofluorescence

Sections were blocked with 5% goat serum in TBST at room temperature for 20 min followed by incubation with a combination of anti-PHD3 and TH antibodies at concentrations and durations indicated in table 11. After washing, slides were incubated with fluorochrome conjugated anti-mouse {Alex Fluor 488, green (Invitrogen)}, and anti-rabbit {Alex Fluor 635, red (Invitrogen)} antibodies at a concentration of 1:1000 for one hour at room temperature, protected from light by foil. Sections were mounted with DAPI containing mounting medium (Vectorshield, Vector laboratories), covered with a 22 x 50 mm cover slip (VVR) before sealing with nail varnish. Fluorochrome labelled antigens were visualised using a confocal microscope (LSM5, Zeiss).

2.8.6 Quantitation of IHC PHD3 signal in tissues of the peripheral nervous system

High power (1000x) images of PHD3 immunostained tissues with DAB chromogen were converted to grey scale images using ImageJ software (NIH, USA). The total amount of grey scale units in a $3\mu m^2$ unit area was determined for the nuclear and cytoplasmic compartment of 5 randomly selected cells. Mean grey scale values were obtained from each peripheral nervous system tissue and graphically expressed as mean + SEM after correction for background. Signal from SCG sections immunostained in parallel with each peripheral nervous system tissue was used to standardise this signal. Semi-quantitative comparisons were made between signal from different tissues. The large size of sympathetic neurons, even in the immediate post-natal period, allowed for a similar approach to be used to assess and standardise PHD3 signal at different developmental time points.

2.9 Determining the sequence of PHD3 in PC12 cells

2.9.1 Rationale

To explore the link between PHD3 and apoptosis further, we assessed the amino acid sequence of PHD3 in the rat phaeochromocytoma derived PC12 cell line. Our immunoblot analysis demonstrated that the 25 KDa species of PHD3 was strongly expressed in this cell line (see results section). We therefore chose to assess the sequence of this smaller form of PHD3 to determine if it varied at the nucleic acid level from that of known rat PHD3.

2.9.2 Designing primers to rat PHD3

The rat PHD3 mRNA sequence corresponding to NM_019371 was used in primer output 3 software to design oligonucleotide primers in accordance with a melting temperature of 63ºC, primer size of 20 bp, and product size of between 150 and 300 bp. Primers were subjected to BLAST analysis on the NCBI data base to confirm specificity to rat PHD3 and further analysed using DNA calculator software (Santa Cruz) to exclude those forming primer dimers. Ten final primer pairs were selected as indicated in table 17. These primers allowed full sequence coverage of the smaller species of rat PHD3 as indicated in figure 8.

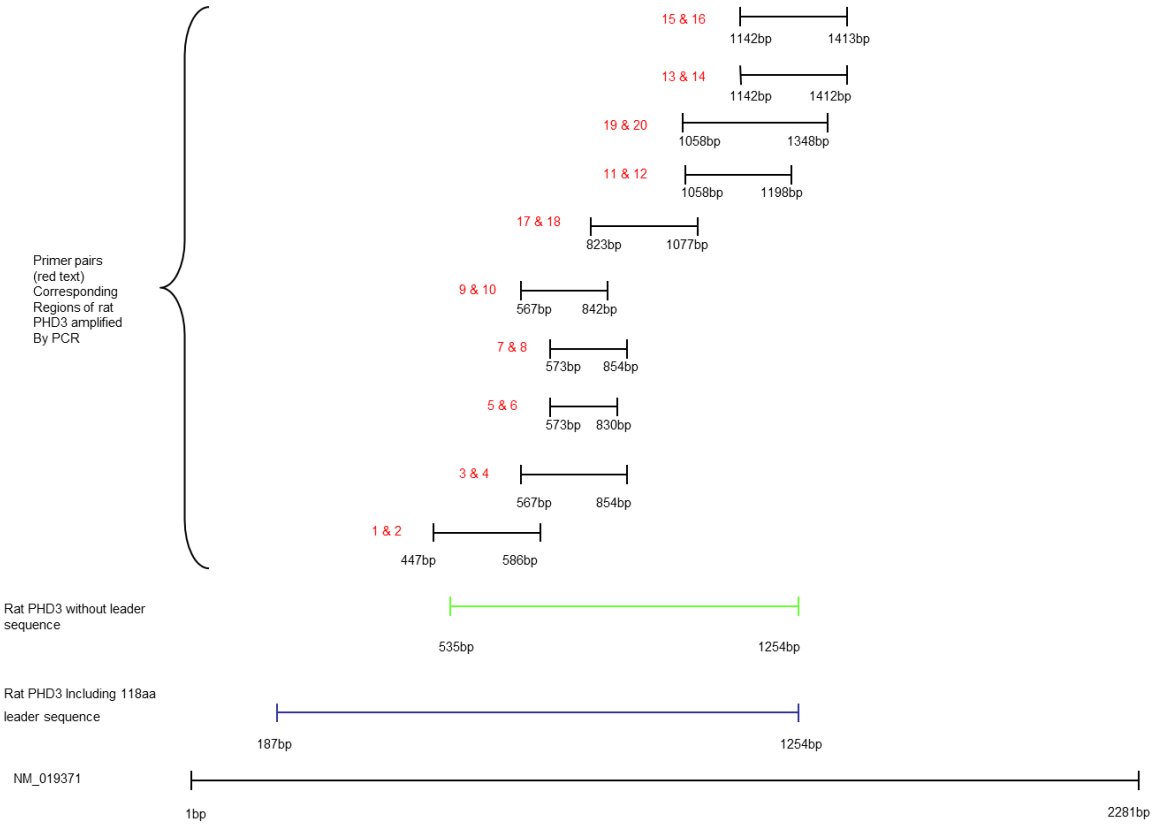


Fig 8. Schematic indicating primers used and corresponding PCR amplified regions during sequencing of the dominantly expressed form of PHD3 detected in PC12 cells

Primer pairs	Primer sequences	Size of amplified region in bp	Region of rat amplified (correspond to sequence NM_019371) in bp
1 (forward) 2 (reverse)	5'-GCTCTCTGCATCTCCGCTGT-3' 5'-ACTCCAGGGCGATCTTCTCC-3'	140	447-586
3 (forward) 4 (reverse)	5'- GGAGAAGATCGCCCTGGAGT-3' 5'- CTCCCGCAGTACAGGACCAG-3'	288	567-854
5 (forward) 6 (reverse)	5'- GATCGCCCTGGAGTACATCG-3' 5'- TCGATGAGGGACAGGAGGAA-3'	258	573-830
7 (forward) 8 (reverse)	5'- GATCGCCCTGGAGTACATCG-3' 5'- CTCCCGCAGTACAGGACCAG-3'	282	573-854
9 (forward) 10 (reverse)	5'- GGAGAAGATCGCCCTGGAGT-3' 5'- AGGACCAGCCTGTCGATGAG-3'	276	567-842
17 (forward) 18 (reverse)	5'- CTCATCGACAGGCTGGTCCT-3' 5'- AATGGGCTCCACGTCTGCTA-3'	255	823-1077
11 (forward) 12 (reverse)	5'- TAGCAGACGTGGAGCCCATT-3' 5'- TGGCTTCTGCCCTTTCTTCA-3'	141bp	1058-1198bp
19 (forward) 20 (reverse)	5'- TAGCAGACGTGGAGCCCATT-3' 5'- TAGGCAGGGGATTGGACAGA-3'	291	1058-1348
13 (forward) 14 (reverse)	5'- CCACCAGGTACGCCATGACT-3' 5'- CGCATTCCCAGCAAGAAAAC-3'	271	1142-1412
15 (forward) 16 (reverse)	5'- CCACCAGGTACGCCATGACT-3' 5'- ACGCATTCCCAGCAAGAAAA-3'	272	1142-1413

Table 17. Primer pairs used to amplify regions of rat PHD3

The following Glut 1 primer pair, which was homologous in rat and mouse PHD3 was used as an internal positive control for PCR reactions:

5'-CCATCCACCACACTCACCAC-3'; 5'-GCCCAGGATCAGCATCTCAA-3' to amplify a 206bp segment.

2.9.3 RNA extraction from PC12 cells

PC12 cells were cultured as previously described. 3 days after passage, 20 ml of cultured PC12 cells were pelleted by centrifugation at 3273g in a refrigerated centrifuge at 4ºC for 10 min. The pellet was washed twice in ice cold PBS and resuspended in 1 ml of TRIzol reagent (Invitrogen) for 15 min.

An RNeasy kit (Qiagen) was used to extract RNA and the procedure carried out using RNase free reagents and conditions. The TRIzol homogenate was centrifuged at 3273g for 10 min at 4ºC and the supernatant transferred to a fresh 1.7 ml microcentrifuge and shaken vigorously by hand for 15 seconds. Next the supernatant and TRIzol mix was centrifuged at 10000g for 10 min at 4ºC and the upper aqueous phase carefully transferred to a fresh microcentrifuge tube, care being taken not to include any material from the aqueous/organic interface. An equal volume of 70% ethanol was then added drop wise to avoid localised precipitation of RNA. The solution was then loaded into an RNeasy column (Qiagen) and centrifuged for 30 seconds at 10000g. The column was transferred into a new collection tube and 500 µl of RPE buffer was added and centrifuged for 30 seconds at 10000g and the flow through discarded. A further 500 µl of RPE buffer was added to the column and spun for 2 min at 10000g. The column was transferred to a new collection tube and spun for 2 min at 10000g to dry the membrane. The dried column was next transferred to a 1.5 ml collection tube to which 30 µl of RNase free water was added directly to the membrane of the RNase easy column. The sample was allowed to sit at room temperature for 1 min and centrifuged for 1 min at 10000g to elute RNA.

Purity of extracted RNA was assessed by RNase free agarose gel electrophoresis as follows. 1.5g of agarose (Sigma) was mixed in 92 ml of autoclaved water and 5 ml of 20 x MOPS (Sigma), 3 ml of formaldehyde (Sigma) and heated in a microwave oven (Cookworks) until the solution became clear. The mixture was placed in a fume hood and after being allowed to cool for 5 min and then poured into a mould, pre-cleaned with 0.1M NaOH in ethanol solution.

The following loading buffer was used: 0.5 µl of 20 x MOPS, 10 µl of formamide (Sigma), 3.5 µl formaldehyde, 0.2 µl of ethidium bromide, 3.8 µl of RNase free water for each 2 µl of RNA. This mixture was heated at 65ºC for 10 min and samples were resolved by electrophoresis at 100V for 1 hr and visualised under UV light.

2.9.4 Synthesis of first strand cDNA from PC12 cell RNA

The SuperScript First-Strand Synthesis System for RT-PCR (Invitrogen) was used.

Contaminating DNA was first removed by mixing 1 µg of RNA (0.5 µl), 1 µl of DNase, 1 µl of 10x DNase buffer, 7.5 µl RNase free water and incubating in a DNA Thermal Cycler (Perkin Elmer) at 25ºC for 15 min. Synthesis of first strand cDNA was carried out as follows: 1 µl of 25 mM EDTA was added to the reaction mix and incubated at 65ºC for 10 minutes, then chilled on ice. 9 µl of master mix (1 µl of random hexamers (50 ng/µl), 1 µl of 10 mM dNTP's, 2 µl 10x reverse transcriptase buffer, 2 µl of 50 mM $MgCl_2$, 2 µl of 0.1 µM DTT, 1 µl RNaseOUT) was added to each sample while still on ice. The sample was next incubated for 2 min at 25ºC. 0.25 µl of Superscript II reverse transcriptase was added to each sample and incubated for a further 10 min at 25ºC, followed by 50 min at 42ºC and finally 15 min at 70ºC. Samples were stored at -20ºC until further use.

2.9.5 Polymerase chain reaction (PCR) amplification of segments of PHD3 from PC12 cells using first strand cDNA as template

A series of pilot PCR studies were carried out to optimise error free PCR amplification. Initial reactions were carried out as previously described with TAQ DNA polymerase (Roche). In order to minimise error rates, *Pyrococcus furiosus* (PFU) DNA polymerase (Stratagene) which incorporates a proof-reading function was used. Reaction conditions were further optimised by varying the concentration of $MgSO_4$ and addition of DMSO as indicated in the results section of this thesis. Next, a 5 µl aliquot of PCR product was resolved by agarose gel electrophoresis as previously described to confirm the presence of a PCR product of the predicted molecular weight. The remainder was purified using a GFX PCR DNA purification kit (Amersham Biosciences) as previously described. In order to obtain maximum sequence coverage PCR products were sequenced using the same forward and reverse primer pairs indicated in table 17.

2.10 Psychometric tests

2.10.1 Rationale

A number of psychometric tests were carried out using PHD3-/- mice with wild type litter mate controls. These studies were based on the observation that IHC staining of rat brain had demonstrated PHD3 signal in regions of the rat hippocampus. The hippocampus is involved in learning, memory and behaviour and to assess the significance of this finding, advice was sought from Dr Robert Deacon, Department of Experimental Psychology at Oxford University. As a first step, a panel of simple psychometric tests aimed at discriminating significant differences in hippocampal function between wild type and PHD3-/- mice were carried out using protocols

established by Deacan and Rawlins (Nature Protocols, 2006) within the Department of Experimental Psychology. Each study was carried out in triplicate with 8 wild type and 8 PHD3-/- animals of 3 months of age.

2.10.2 T- maze alternation

T-maze alternation is a test of short term memory. Animals with normal hippocampal function are able to recall which goal arm they visited on their first run and most times choose the opposite side during the second run. The T maze alternation apparatus is illustrated in figure 9.

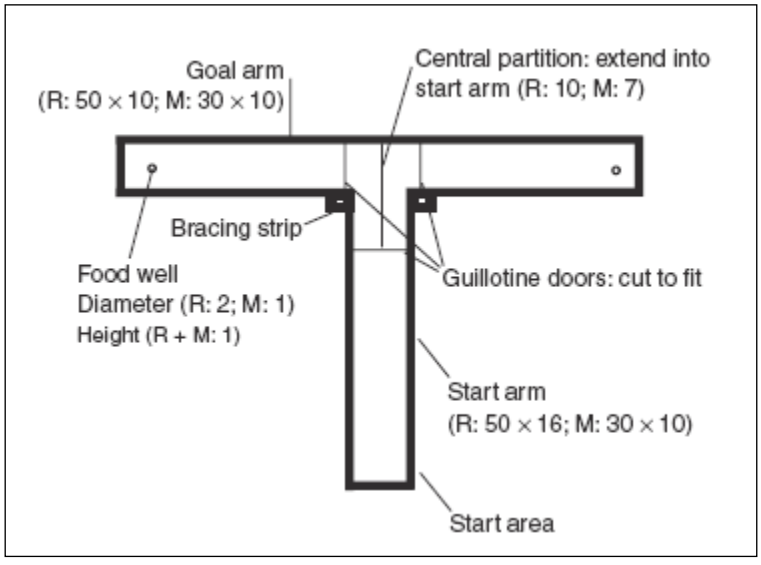


Fig 9. Schematic of T maze alternation apparatus

All material was obtained from the Department of Experimental Psychology, University of Oxford. The T-maze was assembled with the central partition in place and all guillotine doors raised. The animal was placed in the start area facing away from the goal arms and allowed to choose a goal arm. The animal was confined to the chosen arm by quietly sliding down a guillotine door. After 30 seconds all doors were raised and the procedure repeated. Each run was completed within 2 min. As PHD3-/-

and wild type mice were well motivated, food incentives were not required in the goal arms of our study.

2.10.3 Burrowing

Burrowing is a rodent behaviour which involves co-ordinated digging and kicking movements which is affected by lesions of the hippocampus. The apparatus used in the burrowing study is indicated in figure 10.

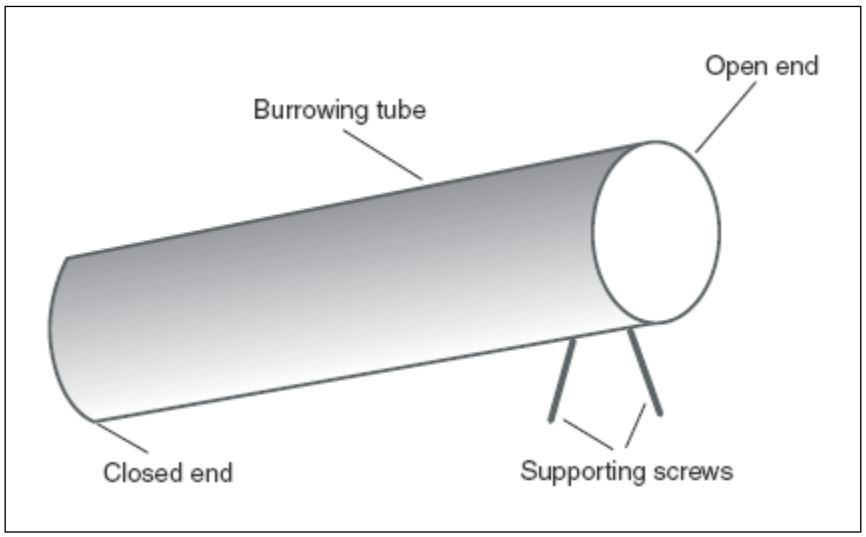


Fig 10. Apparatus used in burrowing study

Burrows were obtained from the Department of Experimental Psychology, University of Oxford and were filled with 200g of food pellets for mice and placed against the longer wall of a clean cage with a thin layer of bedding. The study was started 3 hr before the mouse sleep cycle. Water was provided but no extra food. As burrowing drive differs between mouse strains, data was taken at an early (2 hr) and late (overnight) time point with the amount of material displaced from the burrow measured at each time point.

2.10.4 Nest building

Nest building is a rodent behaviour influenced by hippocampal function. Approximately 1 hr before the dark phase, mice were transferred to individual testing cages with wood-chip bedding but no environmental enrichment items such as cardboard houses or tunnels. One nestlet was placed in each cage. The next morning nests were scored as indicated in figure 11 and Table 18.

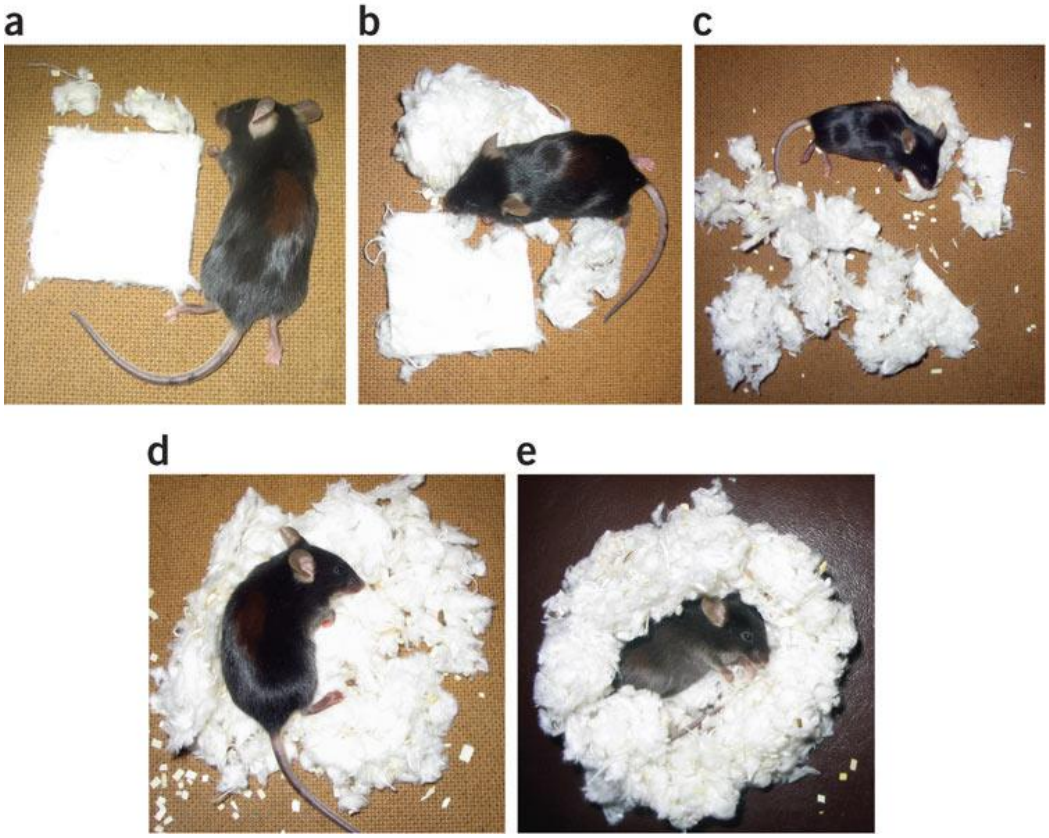


Fig 11. Photographs depicting nest building behaviour in mice

(Deacon RM., Nature Protocols)

Fig	Description	Score
a	Nestlet not noticeably touched	1
b	Nestlet partially torn	2
c	Nestlet mostly shredded but often no identifiable nest site	3
d	An identifiable but flat nest	4
e	A near perfect nest: more than 90% of the nestlet is torn and the nest is a crater with walls higher than mouse body height for more than 50% of its circumference.	5

Table 18. Rating scale for nest building

2.10.5 Hoarding

Hoarding is a behaviour which involves a process of collecting food and storing it in one or more locations for later use. Hoarding behaviour is influenced by hippocampal function. The hoarding apparatus was assembled as indicated in figure 12. The wooden home box was filled with cardboard shelter and soiled bedding from the animal's normal cage to encourage normal behaviour. 100g of food pellets were place at the distal end of the hoarding tube and a bung put at its entrance. Early in the day, the mouse was placed in the home box to habituate it to its new environment. At 5 pm the bung was removed. The following morning the amount of food hoarded in the home box was measured. Mice eat on average 3g of food during a 24hr cycle and as all the mice ate similar amounts and our subject animals were successful hoarders, this did not require correcting for.



Fig 12. Hoarding apparatus

Section 3: Results

Chapter 3. Identification and generation of antibodies with the ability to recognize rodent PHD isoforms specifically at endogenous levels in tissues

A central aim of this doctoral study was to establish the expression of PHD proteins in mammalian tissues. The development of mice with constitutive deletion of PHD isoforms allowed for an added specificity control and as such, initial efforts were focused on establishing a panel of antibodies able to detect PHD isoforms in mouse tissues. Two approaches were adopted in parallel, with efforts being placed into generating new antisera to mouse PHD proteins and testing of existing anti-human PHD antisera for their ability to detect rodent counterparts.

3.1 Generating recombinant protein immunogens to mouse PHD isoforms

In order to generate new antibodies to mouse PHD isoforms, the pGEX expression system was used to generate a series of fusion proteins as described in the methods section of this thesis. Of the fusion proteins generated, several were soluble and of the correct predicted size. In addition to full length protein products, several of the final eluates contained smaller sized proteins which were felt to represent fragmented full-length fusion proteins which were considered to be potentially useful immunogens. These fusion proteins were used to immunise New Zealand white rabbits from a commercial source (Eurogentec, Liege, Belgium).

For mouse PHD1, two fusion proteins produced soluble protein products (fig 1 and 2). For mouse PHD2, one produced soluble protein (fig 3) and for mouse PHD3 three soluble proteins were generated (fig 4 and 5).

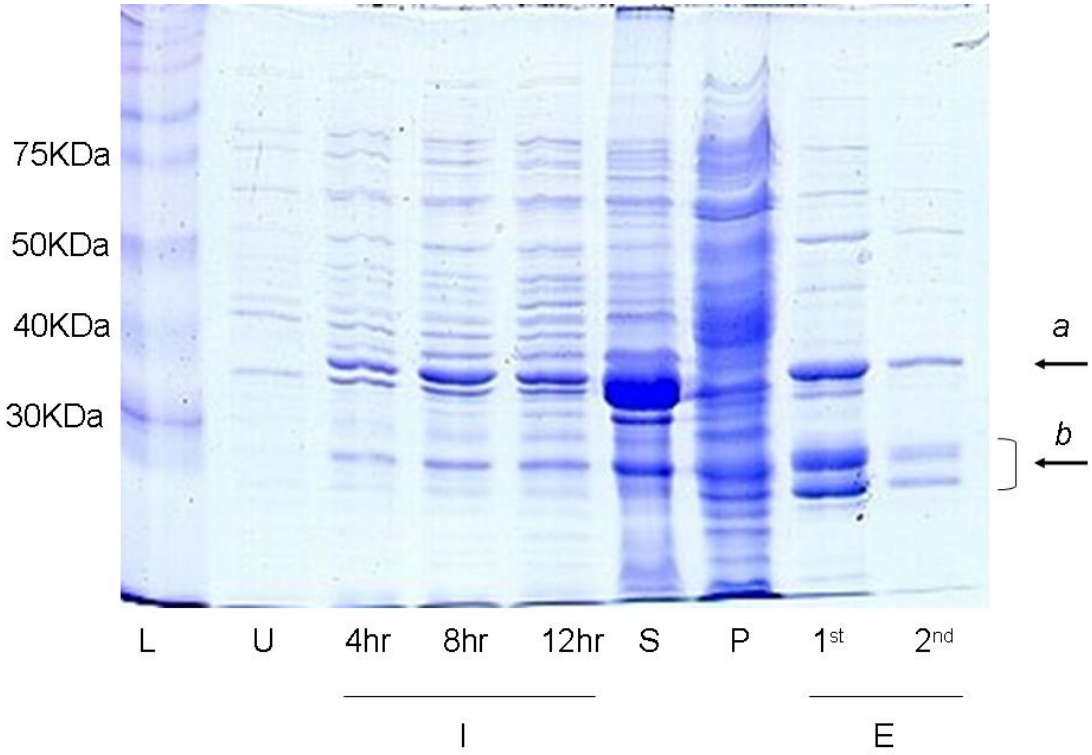


Figure 1. Expression of a fusion protein of GST and PHD1 (amino acids 294 to 419)

Expression of a fusion protein of GST and 125 amino acid fragment of mouse PHD1 (amino acids 294 to 419). This fusion protein was induced and produced soluble protein of the predicted size of 39KDa (13KDa for PHD1 peptide + 26 KDa for GST), (arrow, a) which was eluted and used to immunise rabbits. Further bands were noted in the region of 26KDa which were likely to represent GST and / or fragmented fusion protein (arrow, b). 10µl aliquots from each stage of the extraction process were run on a 10% SDS-PAGE gel. Fractions were labelled as follows: Ladder, L; uninduced bacteria, U; IPTG induced bacteria I; post-lysis bacterial supernatant, S; post-lysis bacterial pellet, P; recombinant fusion proteins eluted from GST beads, E.

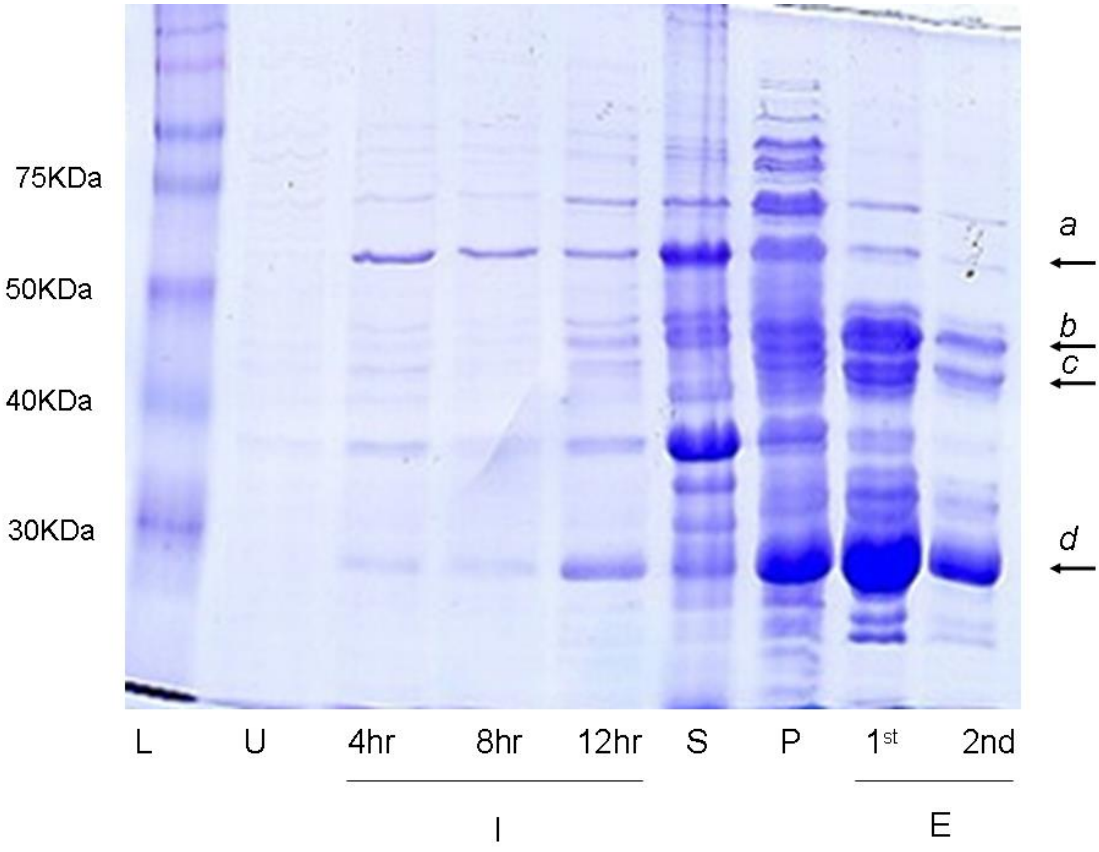


Figure 2. Expression of a fusion a protein of GST and PHD1 (amino acids 1 to 294)

A fusion protein of GST and a 294 amino acid fragment of mouse PHD1 (amino acids 1 to 294 of mouse PHD1) with a predicted molecular weight of 56KDa (30KDa for PHD1 peptide + 26 KDa for GST) was expressed. Although the induced sample was of the predicted size (arrow, a), the eluted sample was found to contain a number of dominant smaller bands (arrows, b and c), which were likely to represent fragmented fusion protein. As discussed, these were considered to have immunogenic potential and as such were used to immunise rabbits. GST (arrow, d). Fractions were labelled as follows: Ladder, L; uninduced bacteria, U; IPTG induced bacteria I; post-lysis bacterial supernatant, S; post-lysis bacterial pellet, P; recombinant fusion proteins eluted from GST beads, E.

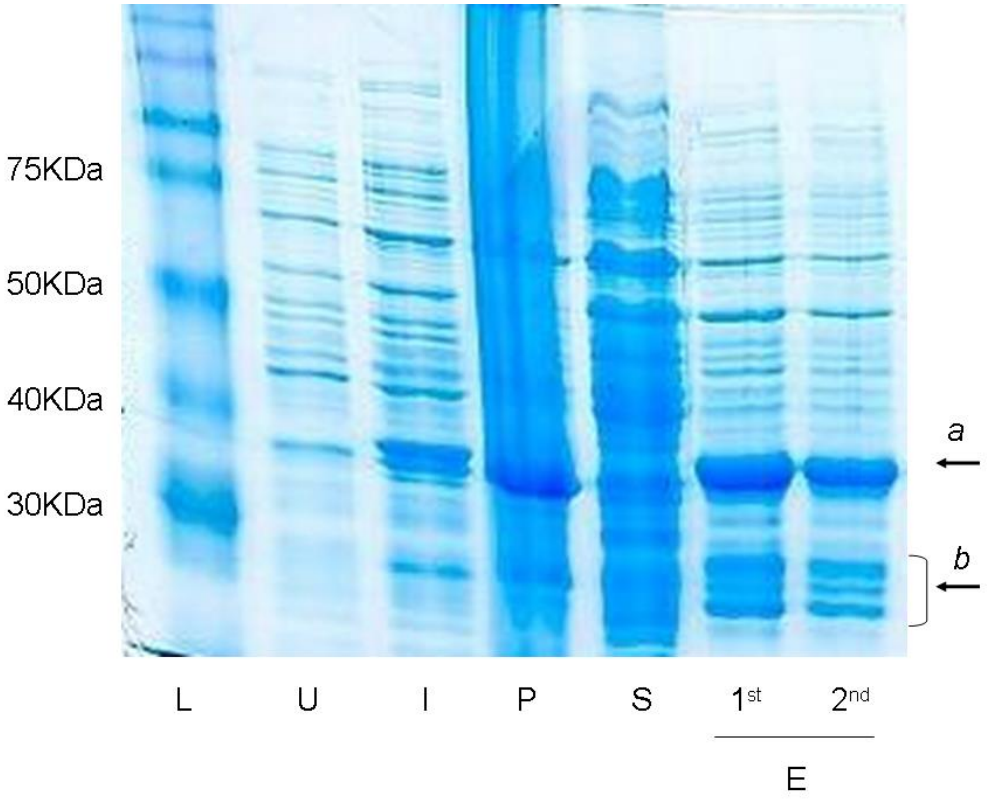


Figure 3. Expression of a fusion protein of GST and PHD2

Expression of a fusion protein of GST and 105 amino acid fragment of mouse PHD2 (amino acids 295 to 400). This protein was induced (arrow, a) and produced a fusion peptide of the predicted size of 36KDa (10KDa for PHD2 peptide + 26KDa for GST) which was eluted intact and used to immunise rabbits. Further bands were noted in the region of 26KDa which were likely to represent GST or possibly a fragmented fusion protein (arrow, b). Fractions were labelled as follows: Ladder, L; uninduced bacteria, U; IPTG induced bacteria I; post-lysis bacterial supernatant, S; post-lysis bacterial pellet, P; recombinant fusion proteins eluted from GST beads, E.

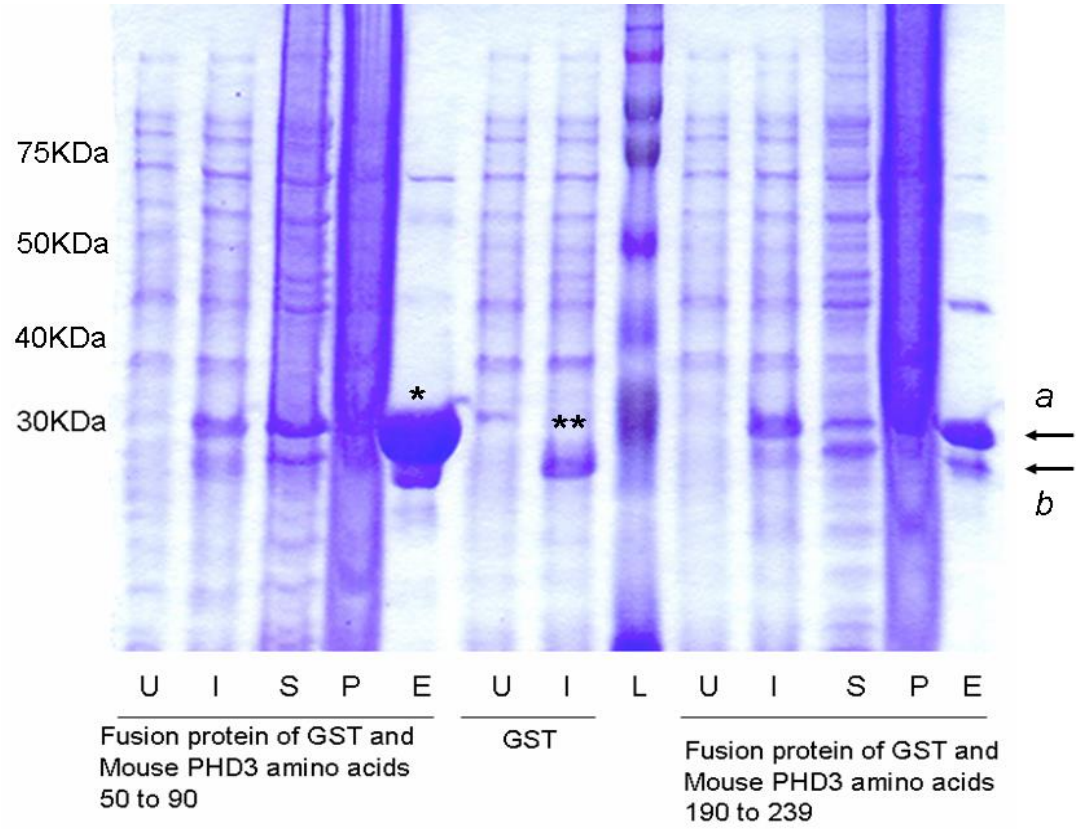


Figure 4. Expression of fusion proteins of GST and mouse PHD3 (amino acids 50 to 90; amino acids 190 to 239)

Left hand panel: Expression of a fusion protein of GST and 40 amino acid fragment of mouse PHD3 (amino acids 50 to 90) is indicated in the left hand panel. This protein was induced and produced a fusion peptide of the predicted size of 30KDa (*) (4KDa for PHD3 peptide + 26KDa for GST) which was eluted intact and used to immunise rabbits. When the expressed fusion protein was of a relatively small size, a 10µl aliquot of GST alone (**) was run in parallel to allow fusion protein and GST to be clearly distinguished. *Right hand panel:* This fusion protein consisted of GST and a 49 amino acid fragment of mouse PHD3 (amino acids 190 to 239). When induced, a fusion protein of the predicted size of 31KDa was generated (arrow, a) (5KDa for PHD3 peptide + 26KDa GST), which was distinct from GST (arrow, b), and used to immunise rabbits. Fractions were labelled as follows: Ladder, L; uninduced bacteria, U; IPTG induced bacteria I; post-lysis bacterial supernatant, S; post-lysis bacterial pellet, P; recombinant fusion proteins eluted from GST beads, E.

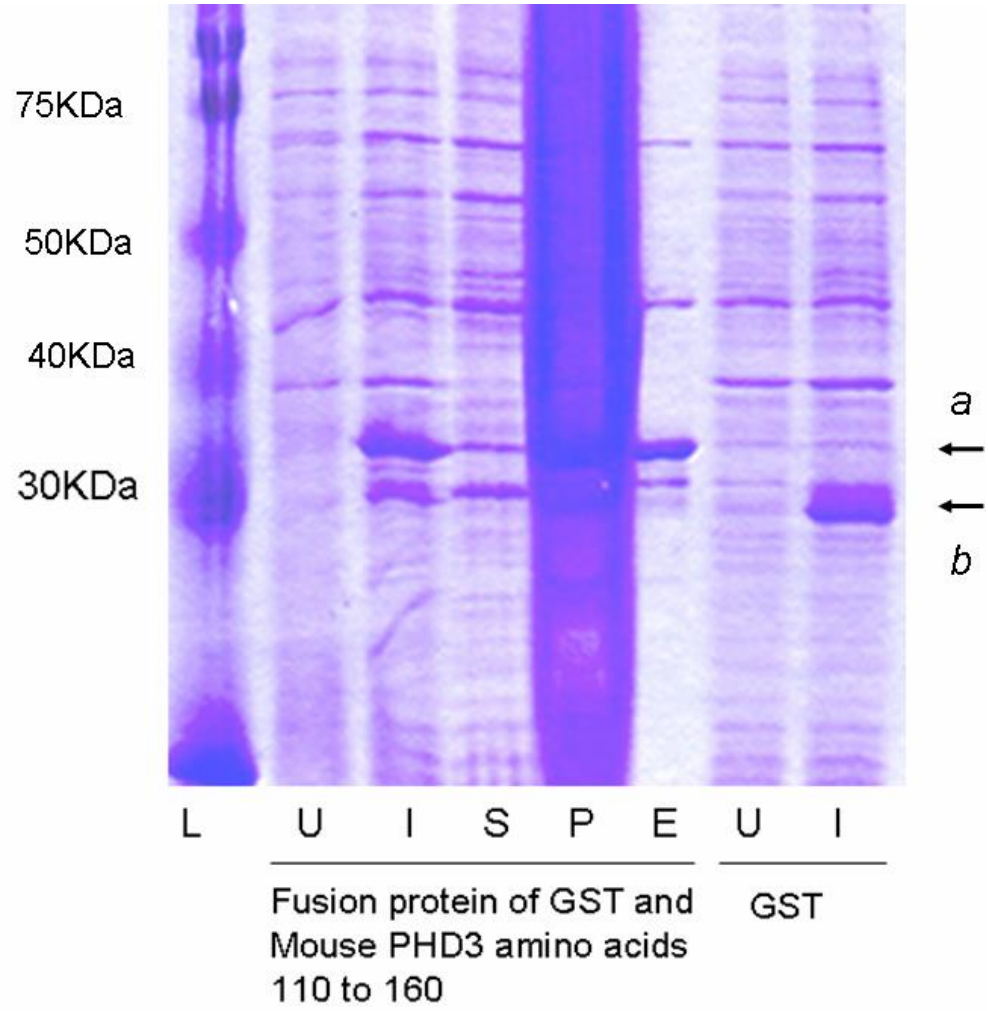


Figure 5. Expression of a fusion protein of GST and PHD3 (amino acids 110 to 160)

Expression of a fusion protein of GST and 50 amino acid fragment of mouse PHD3 (amino acids 110 to 160). This protein was induced and produced a fusion peptide of the predicted size of 31KDa (arrow, a) (5KDa for PHD3 peptide + 26KDa for GST) which was eluted intact. This peptide was also distinct from GST alone (arrow, b), and was used to immunise rabbits. Fractions were labelled as follows: Ladder, L; uninduced bacteria, U; IPTG induced bacteria I; post-lysis bacterial supernatant, S; post-lysis bacterial pellet, P; recombinant fusion proteins eluted from GST beads, E.

3.2 Generating full length mouse and rat PHD proteins by IVTT

An IVTT approach was used to generate each rodent PHD protein to allow assessment of the sensitivity and specificity of antibodies to each rodent PHD isoform. Predictive molecular weights of mouse and rat PHD proteins are indicated in table 1.

PHD isoform	Mouse	Rat
PHD1	45KDa	44KDa
PHD2	43KDa	42KDa
PHD3	27KDa	40KDa

Table 1. Predictive molecular weights of mouse and rat PHD isoforms

Full length cDNA IMAGE clones for mouse PHD1 and 3 were obtained in vector, pCMV-Sport 6. Restriction enzyme analysis indicated that these cDNA's were correctly orientated to be transcribed through the internal SP6 promoter of vector pCMV-Sport 6. Full-length mouse PHD2 cDNA was not commercially available at this stage and as will be described later in this methods section, was generated during the course of this doctoral study.

Mouse PHD1 and PHD2 were known to contain six methonines each while mouse PHD3 contained only 3. Initially, IVTT's programmed with mouse PHD1 and PHD3 cDNA's and labelled with ^{35}S methionine, were used to generate respective full-length radio-labelled proteins. Human PHD proteins served as positive controls and were generated in parallel using a panel of validated T7 promoter driven human PHD cDNA's (Appelhoff et al., 2004) (fig 6). Only mouse PHD1 cDNA produced a protein product (fig 6), which was of lesser abundance compared to its human counterpart. A number of different species of mouse PHD1 were noted to be present and their significance will be discussed later in this thesis.

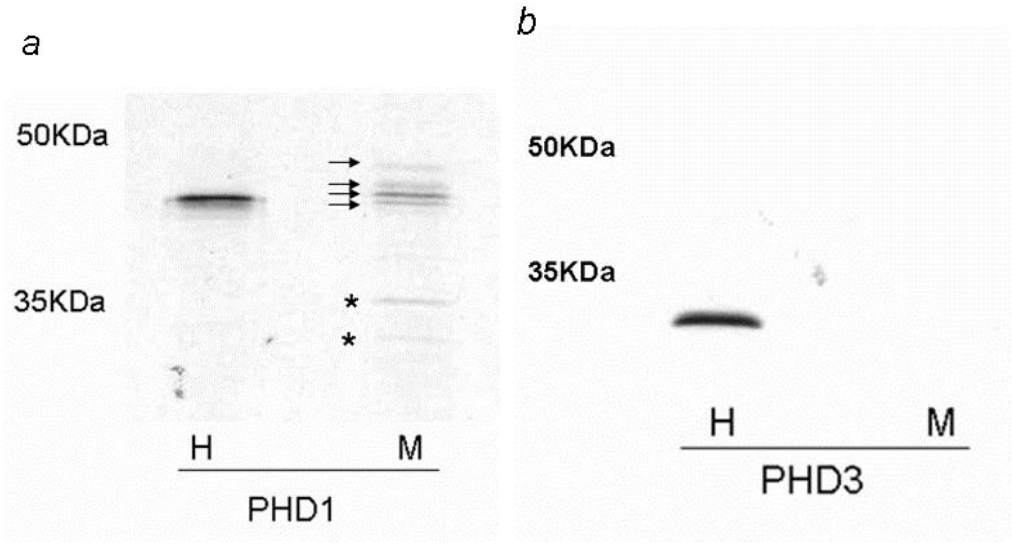


Figure 6. Human and mouse PHD1 and 3 IVTT's

Rabbit reticulocyte IVTT programmed with T7 promoter driven human (H) and SP6 promoter driven mouse (M) cDNA for PHD1 and 3. Expression of mouse PHD protein through the SP6 promoter was found to be generally weaker than its T7 promoter generated human counterpart. Despite this, several species of mouse PHD1 were noted (fig 6, arrows). A number of smaller bands were also noted in this lane (fig 6, *) which were too small to represent PHD1 and were likely to be degradation products. SP6 promoter driven full-length mouse PHD3 cDNA did not produce any signal. Full-length mouse PHD2 cDNA was not available at this stage of study. (Representative of 2 immunoblots).

SP6 is a weaker transcriptional promoter compared to T7. Therefore in order to optimise IVTT based protein synthesis, mouse PHD1 and 3 cDNA's were subcloned into vector pcDNA3 in an orientation to allow T7 promoter driven transcription. By this stage, I had generated full-length mouse PHD2 cDNA and had sub-cloned it into vector pcDNA3 to allow T7 promoter driven transcription to take place.

IVTT's programmed with these new cDNA's and labelled with ^{35}S methionine produced PHD proteins of the correct sizes (fig 7). A strong ^{35}S methionine signal

was generated from IVTT's programmed with mouse PHD1 and 2 cDNA while that generated from mouse PHD3 remained weak despite manoeuvres which included using wheat germ instead of rabbit reticulocyte IVTT, maxi-preparation of cDNA as well as increasing the duration of the ethanol evaporation step in order to reduce ethanol contamination of cDNA.

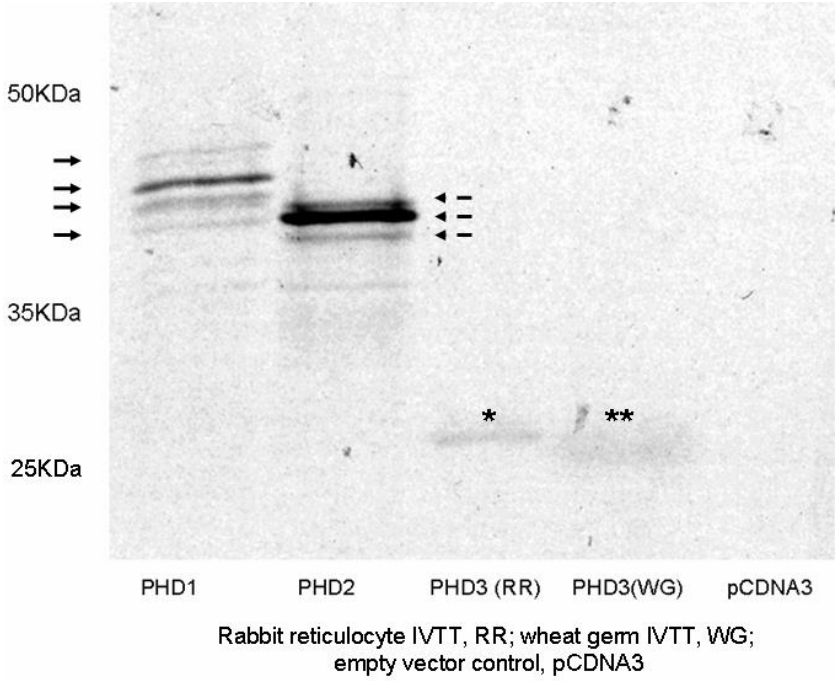


Figure 7. T7 promoter driven mouse PHD IVTT's

IVTT's programmed with cDNA for mouse PHD1 to 3 and labelled with ^{35}S methionine produced signal of the predicted size for PHD1 and 2. Several PHD1 species were again noted (Fig 7, full arrows). Several species of mouse PHD2 were also noted (Fig 7, hatched arrows). A single species of mouse PHD3 was generated by subcloning mouse PHD3 cDNA into a T7 promoter driven pcDNA3 vector. Mouse PHD3 expression was found to be weaker compared to other PHD isoforms with both rabbit reticulocyte (RR) (Fig 7, *) and wheat germ (WG) (Fig 7, **) IVTT's. pcDNA3 vector lacking a cDNA insert was used as a negative control in the final lane. (Representative of 2 immunoblots).

3.3 Testing the sensitivity and specificity of antibodies to mouse PHD proteins

Existing anti-human PHD antibodies were next tested for their ability to detect mouse counterparts. First, an in-house affinity purified rabbit polyclonal anti-serum to human PHD1 termed af 1.1 was tested for sensitivity to mouse PHD1. Immunoblots demonstrated that this antibody weakly detected mouse PHD1 (fig 8), while producing very few cross reacting bands.

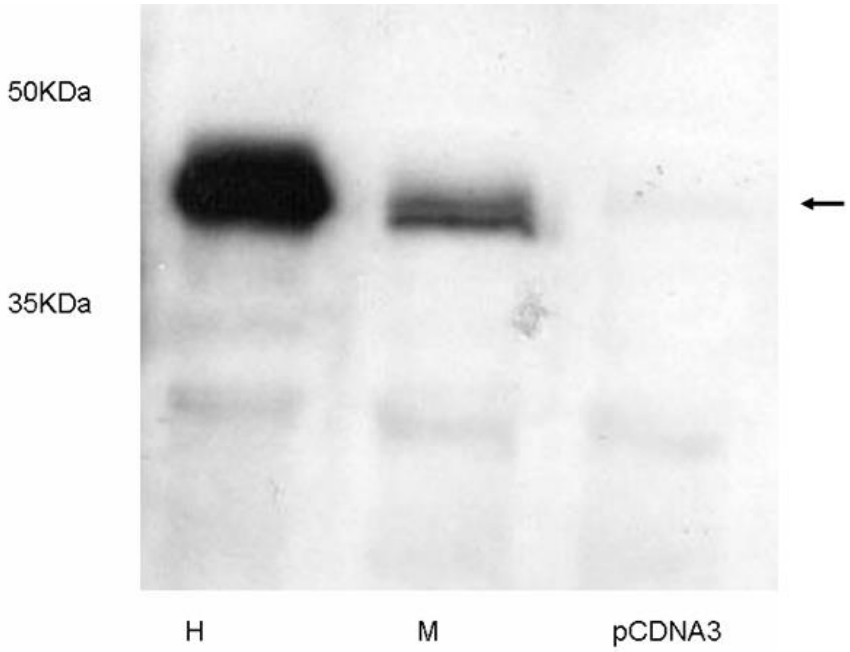


Figure 8. Testing the sensitivity of anti-human PHD1 antibody, af 1.1 to IVTT generated mouse PHD1

The in-house affinity purified rabbit polyclonal antibody to human PHD1 (af 1.1) was used to immunoblot equimolar amounts of human and mouse PHD1 on a 12% SDS-PAGE gel at a dilution of 1:500, overnight at 4ºC. HRP conjugated goat anti-rabbit secondary antibody was used at a dilution of 1:2000 at room temperature for 1 hr and bound antibody detected using a chemiluminescent reaction and 3 min radiographic exposure. This antibody strongly detected human PHD1 while producing a relatively weak signal against mouse PHD1 (fig 8, arrow) which appeared as a doublet. No signal was detected in the pcDNA3 empty vector control. (Representative of 2 immunoblots).

Using a 10% SDS-PAGE gel to allow better resolution of signal, further immunoblots were carried out with af1.1 to more clearly delineate the nature of the multiple species of mouse PHD1. Using this approach a number of species of mouse PHD1 (fig 9) were clearly visible and were in keeping with the species observed in earlier ^{35}S methionine PHD1 IVTT's. Two strong lower species of PHD1 were

detected with this antibody and after longer exposure; a fainter upper species was also detected.

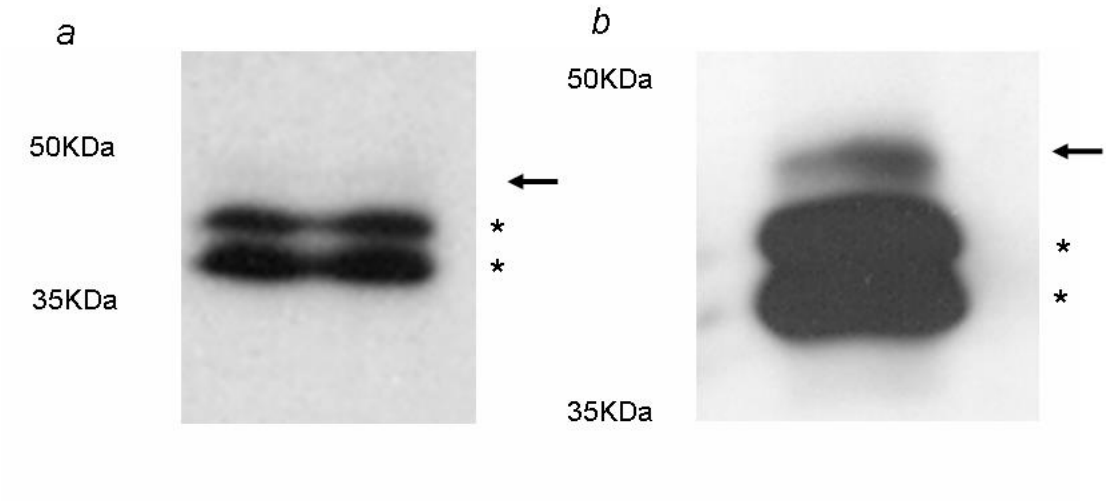


Figure 9. af 1.1 detects three species of mouse PHD1

Two strong lower species of mouse PHD1 were evident (fig 9 a, *). This immunoblot also hinted at the presence of a weaker upper species (fig 9 a, arrow). In order to study these species further, more sample (12µl compared to 8µl of extract) was resolved on a 7.5% SDS-PAGE gel, and immunoblotted with a higher concentration of secondary antibody (1:1000 compared to 1:2000 dilution) and exposed to radiographs for a longer period of time (10 min compared to 3 min). Using this approach, the third band which was faintly noted in earlier immunoblots became clearly visible (fig 9 b, arrow). These bands were not detected in control lanes (not shown). (Representative of 2 immunoblots).

Next, the specificity of antibody af 1.1 to mouse PHD1 was assessed. Equimolar amounts of mouse PHD1 to 3 were immunoblotted with antibody af 1.1. Immunoblots demonstrated that this antibody detected mouse PHD1 but not PHD2 or PHD3, thereby establishing its specificity to mouse PHD1 (fig 10).

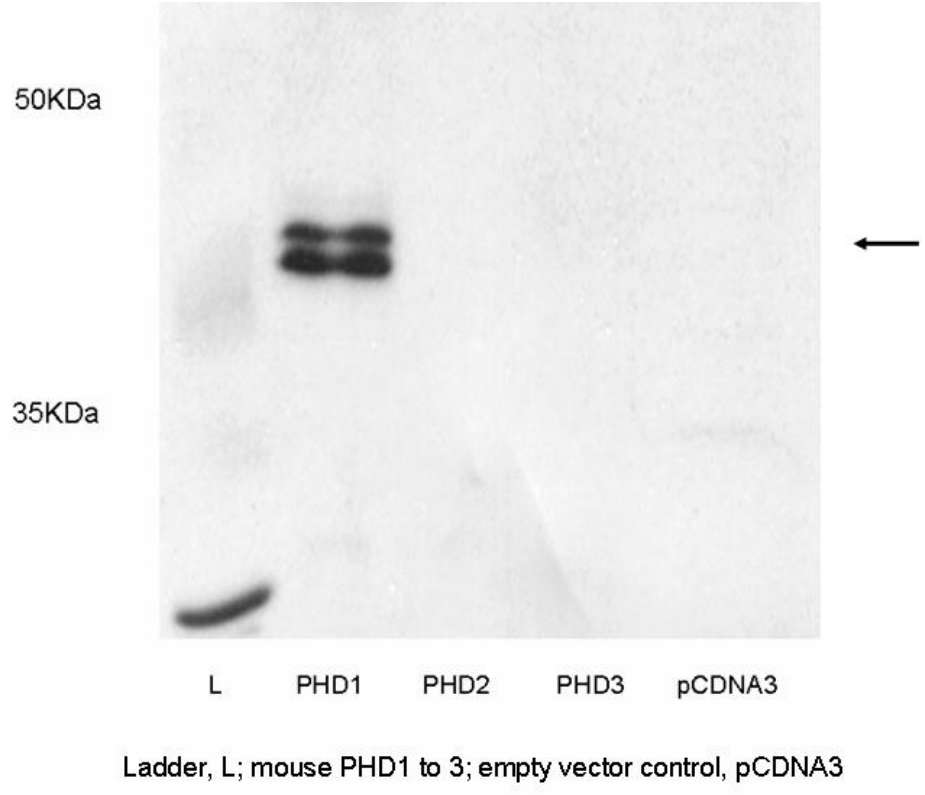


Figure 10. Testing the specificity of af 1.1 to mouse PHD1

Equimolar amounts of mouse PHD isoforms were immunoblotted with af 1.1 on a 10% SDS-PAGE gel. Af 1.1 detected mouse PHD1 but not mouse PHD2 or 3 (fig 10, arrow). (Representative of 2 immunoblots).

Further immunoblots demonstrated that an existing in-house mouse monoclonal antibody to human PHD1 (antibody 112) as well as a new anti-mouse PHD1 antibody, generated during this doctoral study, were both able to weakly detect mouse PHD1 (fig 11 and 12 respectively). A commercial polyclonal antibody to human PHD1 (NB100-310) detected human PHD1, but failed to detect mouse PHD1 (fig 13).

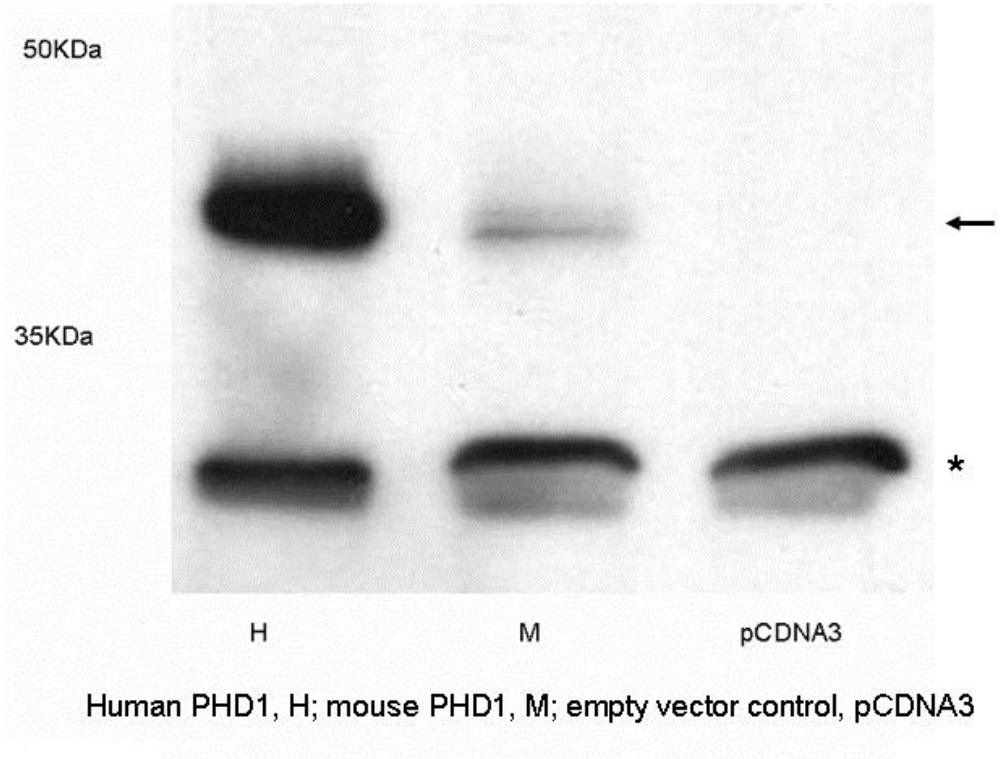


Figure 11. Testing the sensitivity of the in-house anti-human PHD1 antibody, 112 to mouse PHD1

Anti-human PHD1 mouse monoclonal antibody (112) (tissue culture supernatant at a dilution of 1:2) was used to immunoblot equimolar amounts of human (H) and mouse (M) PHD1 with an empty pcDNA3 vector negative control. Immunoblot demonstrated that this antibody was less sensitive at detecting mouse compared to human PHD1, but again a doublet was seen at this exposure (fig 11, arrow). No signal was detected in the pcDNA3 control lane. A strong cross reacting band was noted to migrate at a lower molecular weight than PHD1 (fig 11, *). (Representative of 2 immunoblots).

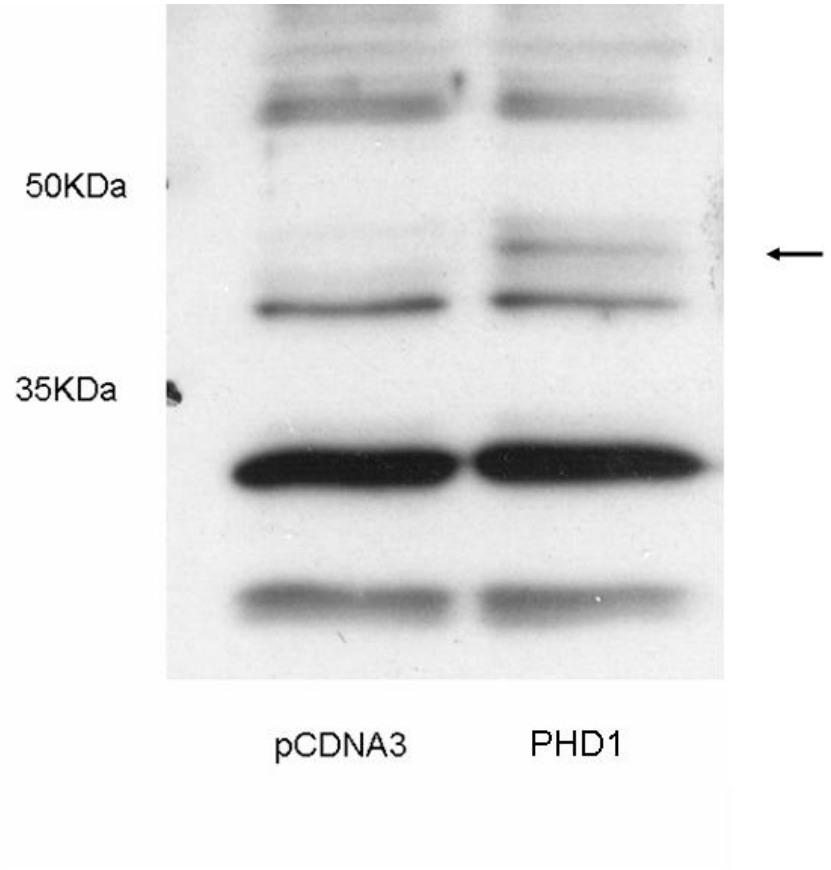


Figure 12. Testing the sensitivity of a new anti-mouse rabbit polyclonal antibody (generated from a 39KDa fusion protein of PHD1 and GST, indicated in Figure 1)

This antiserum was used at a concentration of 1:500 to immunoblot IVTT generated full-length mouse PHD1 as well as pcDNA3 control samples. Weak signal was detected after a 10min radiographic exposure. (fig 12, arrow). A number of cross reacting species were also noted to be present. (Representative of 2 immunoblots).

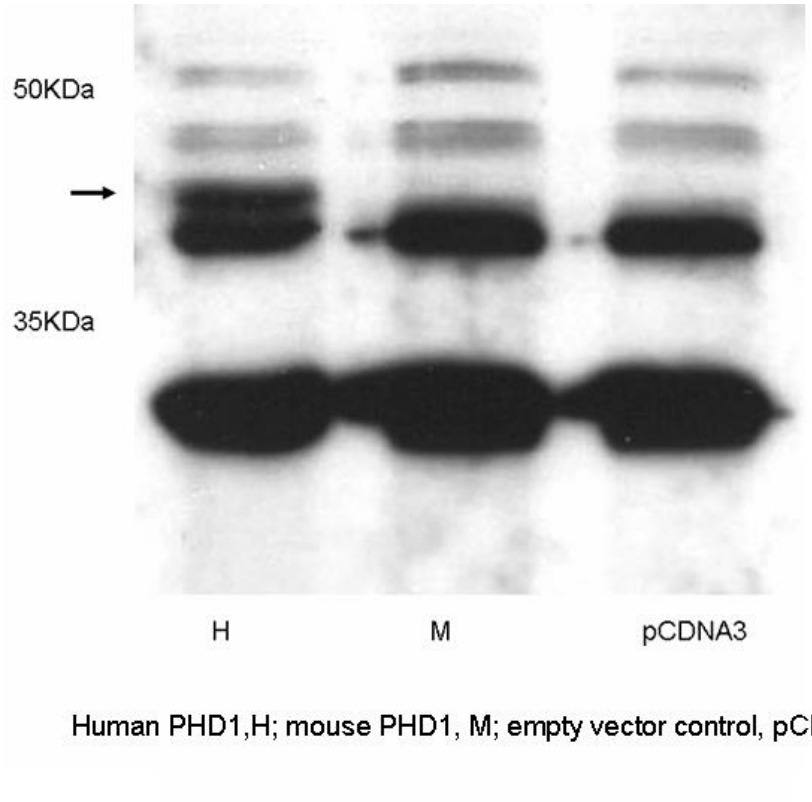


Figure 13. Testing the sensitivity of the commercial anti-human PHD1 antibody, NB100-310 to mouse PHD1

The commercial rabbit polyclonal antibody to human PHD1 (NB100-310) was used at a concentration of 1:1000 to immunoblot equimolar amounts of human and mouse PHD1 resolved on a 12% SDS-PAGE gel. After 3 min of radiographic exposure (fig 13, arrow) this antibody was able to weakly detect human but not mouse PHD1. (Representative of 2 immunoblots)

For mouse PHD2, a rabbit polyclonal antibody raised against mouse PHD2 produced by Prof Patrick Maxwell of University College, London, and termed PM-PHD2 was used. This antibody demonstrated both sensitivity and specificity to mouse PHD2 (fig 14).

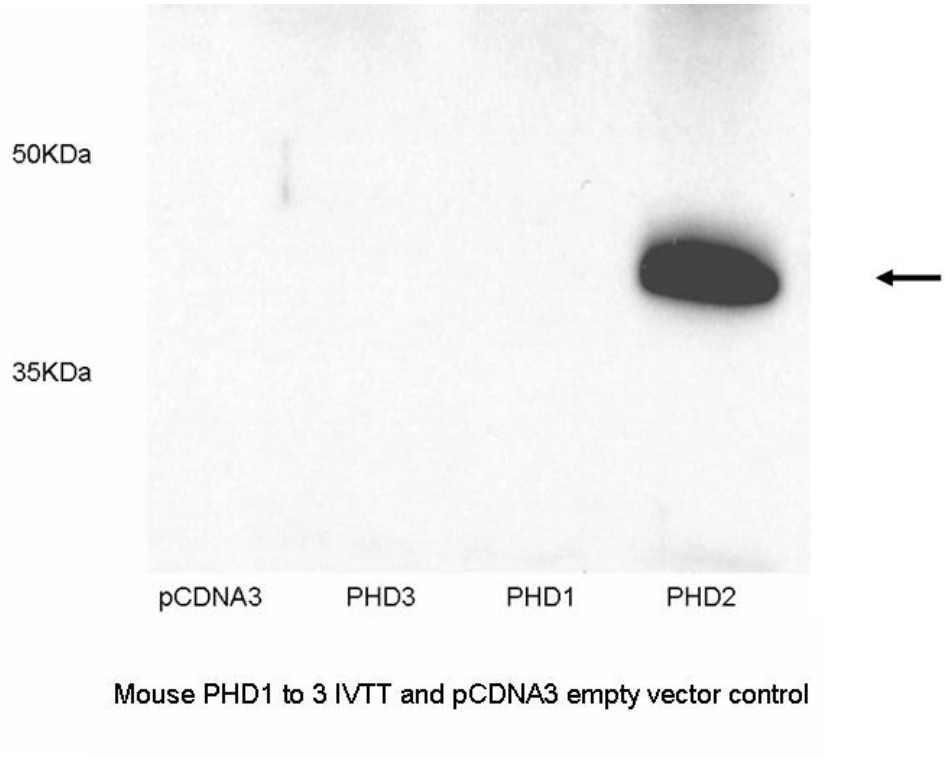


Figure 14. Testing the sensitivity and specificity of an anti-mouse PHD2 antibody to mouse PHD2(PM-PHD2)

PM-PHD2 was used at a dilution of 1:3000 to immunoblot equimolar amounts of mouse PHD isoforms resolved on a 12% SDS-PAGE gel. After 3 min of radiographic exposure, this antibody produced strong signal to mouse PHD2 IVTT (fig 14, arrow) while demonstrating no signal to PHD1, PHD3 or pcDNA3 empty vector control. (Representative of 2 immunoblots)

For mouse PHD3, the existing in-house mouse monoclonal antibody to human PHD3, termed antibody 188e, had a similar sensitivity to both human and mouse PHD3 (fig 15).

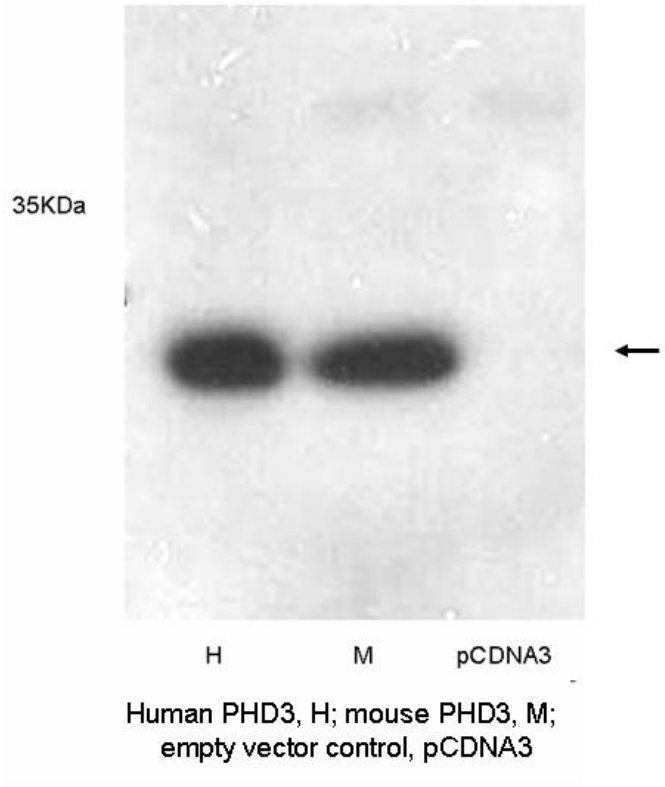


Figure 15. Testing the sensitivity of in-house anti-human PHD3 antibody, 188e to mouse PHD3

Hybridoma supernatant of antibody 188e was used at a concentration of 1:10 to immunoblot equimolar amounts of IVTT generated human and mouse PHD3, resolved on a 12% SDS-PAGE gel. After a 3 min radiographic exposure, this antibody produced signal of similar strength against mouse and human PHD3 (fig 15, arrow). No signal was detected in the pcDNA3 empty vector control. (Representative of 2 immunoblots)

The commercial anti-human rabbit polyclonal antibody NB100-303 was found to weakly detect mouse PHD3 (fig 16).

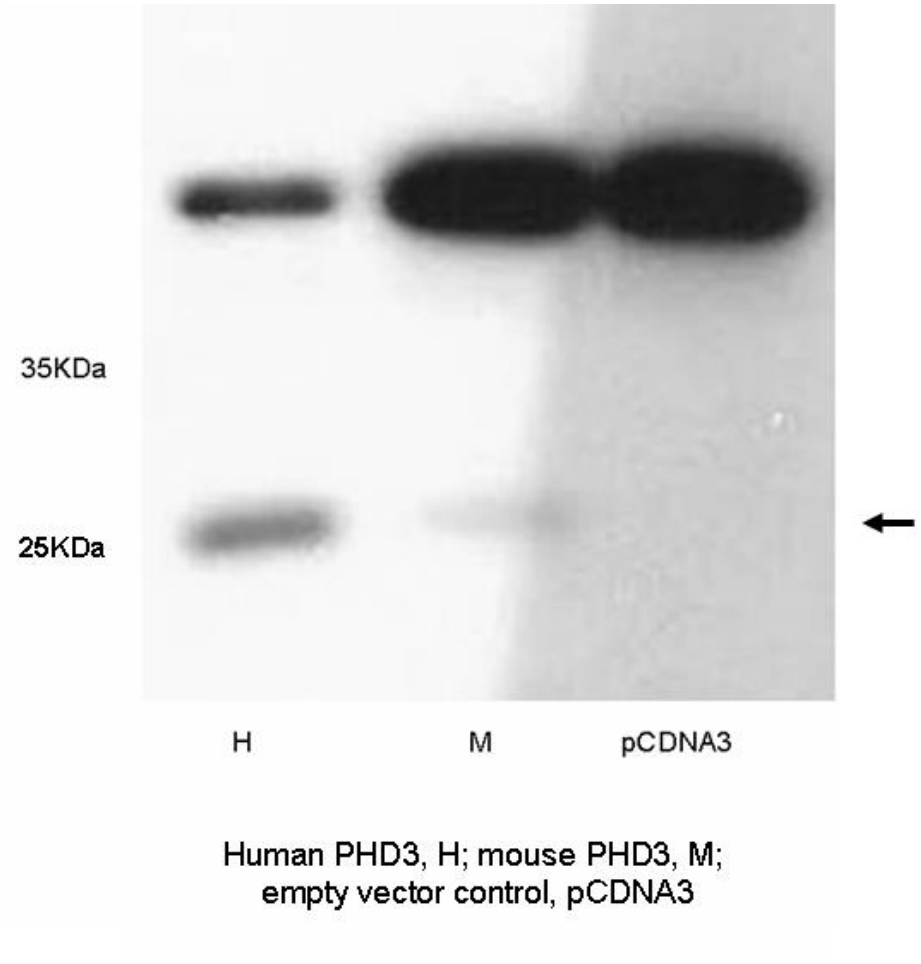


Figure 16. Testing the sensitivity of commercial anti-human PHD3 antibody, NB100-303 to mouse PHD3

Equimolar amounts of human and mouse PHD3 generated by programmed rabbit reticulocyte IVTT were resolved on a 12% SDS-PAGE gel and immunoblotted with a commercial anti-human PHD3 rabbit polyclonal antibody (NB100-303) at a concentration of 1:500. This antibody weakly detected both human and mouse PHD3 (fig 16, arrow). It produced a weaker signal against mouse PHD3 compared to human PHD3. A number of non-specific bands of a higher molecular weight were noted after 3 min of radiographic exposure. The intensity of these bands varied from one another in keeping with different amounts of IVTT loaded to achieve equimolar amounts of respective PHD3 (Representative of 2 immunoblots).

Because of the variable expression of IVTT programmed with mouse PHD3 cDNA, an alternative method was used to evaluate new anti-mouse PHD3 antibodies generated during this doctoral study. Using extracts from COS-7 cells transfected with PHD3 cDNA or empty vector pcDNA3 control (fig 17), all three new antisera were found to be capable of detecting over-expressed mouse PHD3. A number of cross reactive bands were noted with each antiserum

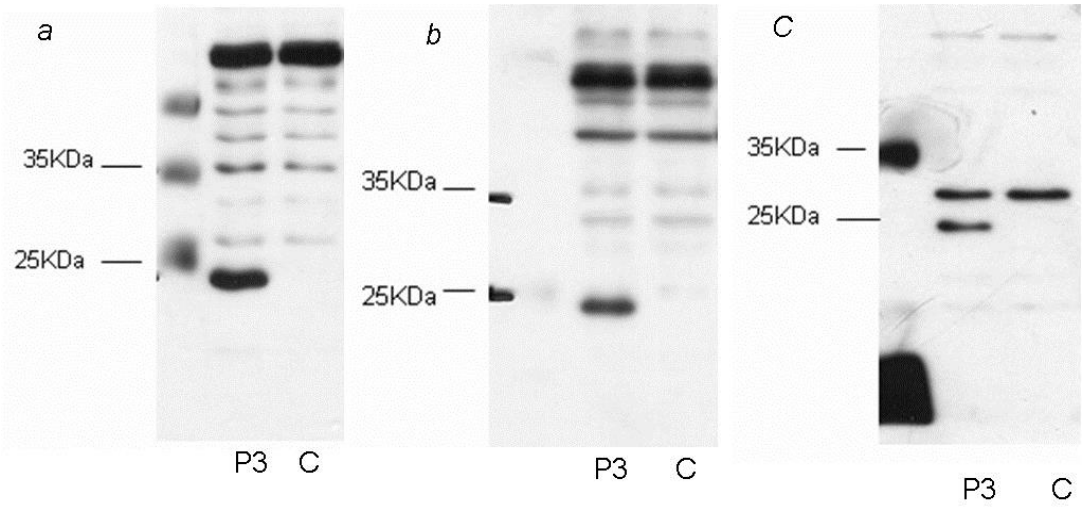


Figure 17. Testing the sensitivity of new rabbit anti-PHD3 antibodies to mouse PHD3

Immunoblots of 6µg of extracts from COS cells transfected with cDNA to mouse PHD3 (P3) or pcDNA3 empty vector control (C). Anti-sera were used at a dilution of 1:500 and radiographic exposure carried out for 3min for each anti-serum tested. Each of the three anti-sera was able to detect over expressed PHD3. *a*: Serum from a rabbit immunised with a fusion protein of GST and a 40 amino acid fragment of mouse PHD3 (amino acids 50 to 90). , *b*: Serum from a rabbit immunised with a fusion protein of GST and a 49 amino acid fragment of mouse PHD3 (amino acids 190 to 239). *c*: Serum from a rabbit immunised with a fusion protein of GST and a 50 amino acid fragment of mouse PHD3 (amino acids 110 to 160). (Representative of 2 immunoblots).

Chapter 4. Determining the relative expression of PHD protein in a range of different rodent tissues from healthy animals exposed to normal atmospheric oxygen levels

4.1 Characterising the expression of PHD proteins in mouse tissues

Having established a panel of antibodies which were both sensitive and specific to mouse PHD isoforms, the expression of each isoform in mouse tissues was next assessed.

4.1.1 Characterising the expression of PHD1 in mouse tissues

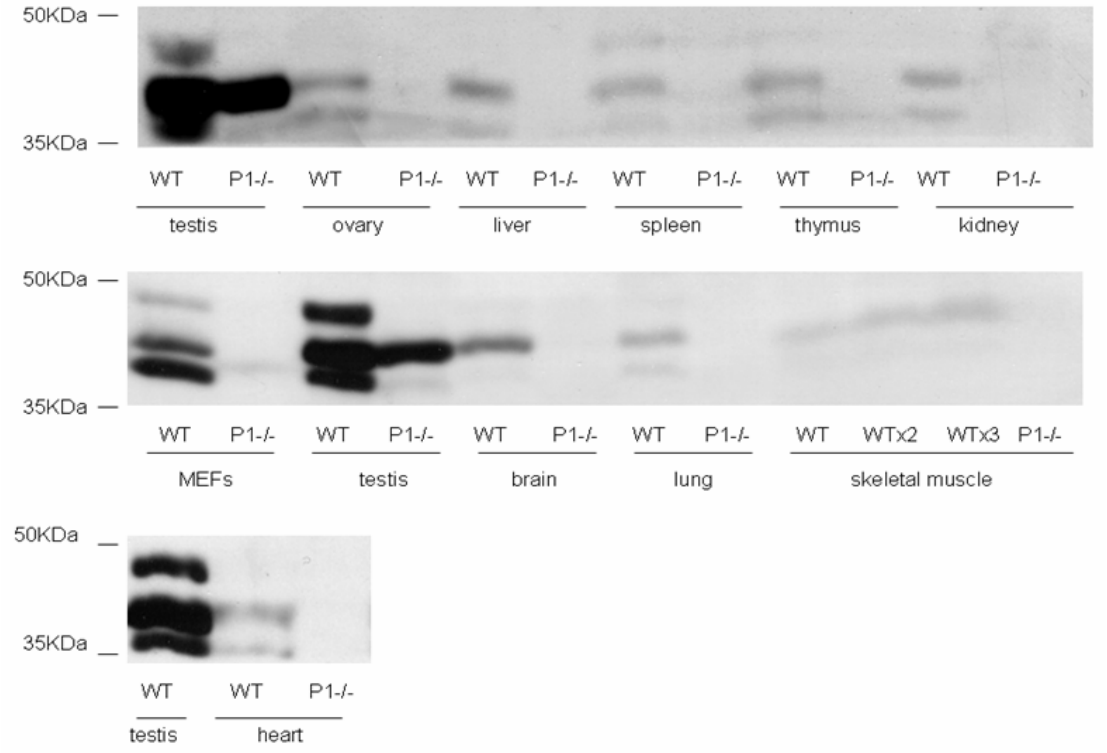
As previous studies had demonstrated an abundance of PHD1 mRNA in testis (Leib et al, 2002; Oehme et al, 2002), this tissue was chosen for the initial study of tissue PHD1 protein. Comparison between wild type and PHD1-/- testis demonstrated strong signal in wild type testis. In keeping with earlier mouse PHD1 IVTT immunoblots, tissue PHD1 was also detected as three closely migrating species. The middle species of this triplet migrated in close association with a non-specific species of a similar molecular weight (fig 18).



Figure 18. Expression of PHD1 in mouse testis

Immunoblot of whole testis homogenates from wild type and PHD1-/- animals with anti-PHD1 antibody af 1.1 was carried out. After a 20min radiographic exposure, three tissue species of PHD1 were observed. A non-specific band was noted to migrate at a similar molecular weight to the middle species of PHD1 as indicated by its presence in wild type and PHD1-/- tissues. (Representative of 2 immunoblots).

In comparison to testis, PHD1 was expressed at far lower levels in other mouse tissues (fig 19). In other tissues, PHD1 also consisted of one or more species which were weakly expressed. On the same immunoblot, a triplet signal was detected in cultured mouse embryonic fibroblasts (fig 19, MEFs), suggesting that it may have a role in certain developing tissues. The significance of these findings will be discussed later in this thesis.



Wild type, WT; homozygous PHD1 deletion, PHD1-/-

Fig 19. Expression of PHD1 in mouse tissues

30 µg of wild type and PHD1-/- tissue were immunoblotted with af 1.1. After a 40min radiographic exposure, strong PHD1 signal was noted in testis. Signal from other tissues was found to be far less intense. Three species of PHD1 were clearly visible in testis. In other tissues one, two or three species were weakly detected. The signal present in tissues was only marginally increased by loading more protein as exemplified by loading 30 µg, 60 µg and 90µg of skeletal muscle homogenate (fig 19: WT, WT x 2 and WT x 3 respectively). PHD1 expression in 15µg wild type and PHD1-/- extracts of cultured mouse embryonic fibroblasts (MEFs) was also compared and demonstrated a relatively strong signal, suggesting PHD1 was also expressed in developing mouse tissues. (Representative of 3 immunoblots).

The expression of PHD1 in mouse tissues was further assessed by immunohistochemistry in order to characterise those cell populations in which it was most abundant. In most tissues, no clear distinction in immunohistochemical signal was discernible between wild type and PHD1-/- tissues. However, in keeping with previous immunoblot findings, strong PHD1 signal was detected in wild type but not PHD1-/- testis sections (fig 20). Collaboration with Dr Tammie Bishop and the Department of Anatomy at Oxford University characterised the testis signal as originating from round spermatids. This finding gave rise to the possibility of a testis related PHD1 phenotype and led to a series of collaborative studies with Dr Tammie Bishop which will be described later.

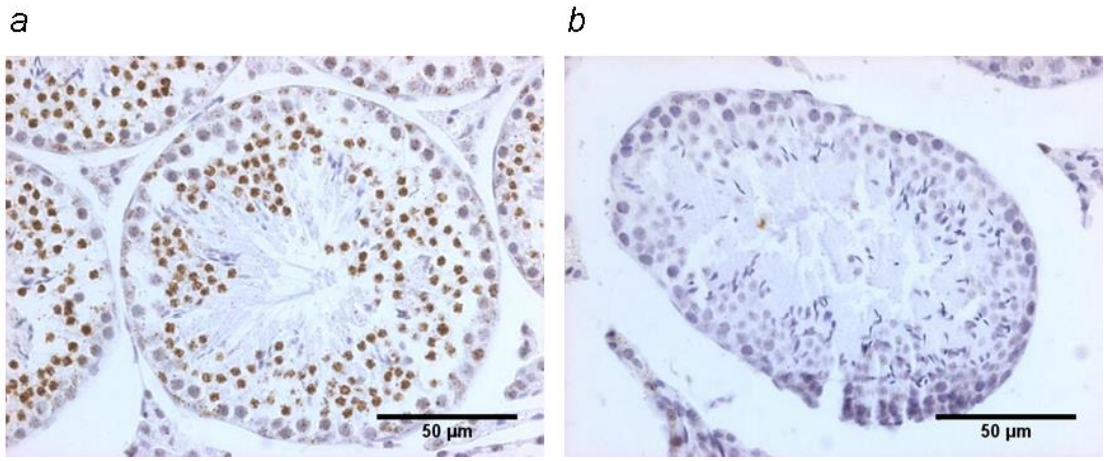


Figure 20. Characterising the expression of PHD1 in mouse testis

Sections of wild type and PHD1-/- testis were immunostained for PHD1 with af 1.1 at a concentration of 1:500, and counterstained with haematoxylin. PHD1 stain was noted in wild type (fig 20, a) but not PHD1-/- sections (fig 20, b). (Representative of three immunostains)

Immunohistochemistry with antibody af 1.1 also demonstrated signal in wild type but not PHD1-/- hepatocytes (fig 21). No difference in immunohistochemical signal was observed between wild type and PHD1-/- heart, kidney, spleen, thymus, brain, lung and skeletal muscle

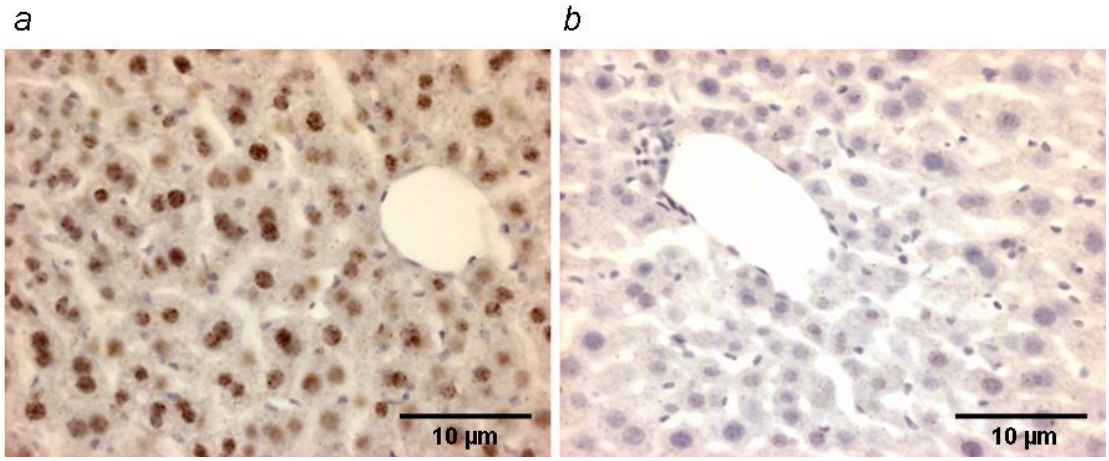


Figure 21. Characterising the expression of PHD1 in mouse liver

Sections of wild type and PHD1-/- liver were immunostained for PHD1 with af 1.1 at a concentration of 1:500, and counterstained with haematoxylin. PHD1 stain was noted in wild type hepatocytes (fig 21, a) but not PHD1-/- hepatocytes (fig 21, b). (Representative of three immunostains)

4.1.2 Characterising the expression of PHD2 in mouse tissues

The expression of PHD2 in mouse tissues was also studied using PHD2 heterozygous tissues as a specificity control. Heterozygous tissues were used because homozygous PHD2 deletion resulted in early intra-uterine death and were therefore not available. Using this approach, PHD2 signal was detected in the majority of mouse tissues which included heart, brain, lung, kidney, testis and ovary (fig 22, arrow). There was little detectable PHD2 in spleen. PHD2 was virtually absent from liver and skeletal muscle. Loading more skeletal muscle homogenate did not improve tissue signal. It was also noted that tissue PHD2 appeared as a closely migrating doublet. In heart, the prevalence of both doublet species was roughly equivalent whereas in other tissues there was a preponderance of the upper band (e.g. lung) or the lower band (e.g. brain). In PHD2 heterozygous tissues, there was a reduction in the intensity of these species which was in keeping with the heterozygous state. A particularly strong cross reacting species was noted in skeletal muscle, and to a lesser extent in heart and brain.

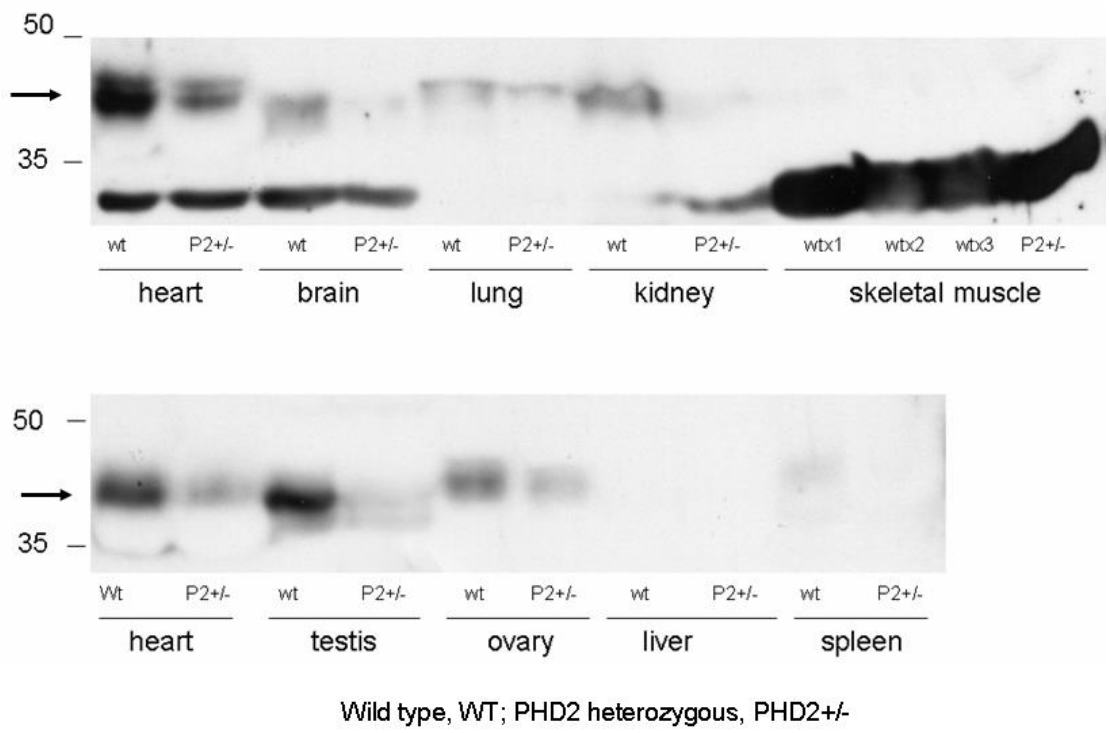


Figure 22. PHD2 expression in mouse tissues

30μg of wild type and PHD2+/- tissues were immunoblotted with an anti-mouse PHD2, PM-PHD2 antibody generated by Prof Patrick Maxwell of University College, London. After 10 min of radiographic exposure, PHD2 signal was noted in a number of different tissues (fig 22, arrow). A reduction in signal intensity was noted in heterozygous tissues. (Representative of 3 immunoblots.)

4.1.3 Characterising the expression of PHD3 in mouse tissues

The expression of PHD3 in mouse tissues was studied using the mouse monoclonal antibody 188e (fig 23). An initial survey focused on PHD3 expression in heart, skeletal muscle and liver, tissues in which an abundance of PHD3 mRNA had been demonstrated (Lieb et al., 2002; Oehme et al., 2002; Hirsila et al., 2003). The relatively low expression of PHD3 in normoxic cell lines (Appelhoff et al., 2004) gave rise to the possibility that its expression in normoxic tissue may also be poor. As such, tissues from animals exposed to varying lengths of 8% hypoxia were immunoblotted alongside those from normoxic animals.

Immunoblot with the 188e antibody demonstrated a number of strong signals in the regions of 50KDa and 25KDa (fig 23, a). The presence of these signals in wild type and PHD3-/- tissue indicated that they were non-specific. A secondary antibody only immunoblot was carried out in parallel and demonstrated an identical signal pattern (fig 23, b), confirming that this signal was non-specific, and due to cross-reaction between secondary antibody and endogenous tissue immunoglobulin.

In an attempt to identify tissue PHD3 signal, the 'True blot' secondary reagent was used (fig 23, c). This reagent preferentially detects non-denatured forms of immunoglobulin with intact disulphide bonds and therefore recognises primary antibody in preference to denatured endogenous mouse tissue immunoglobulin. Although this approach helped to alter cross-reacting signal, it did not allow reliable detection of tissue PHD3.

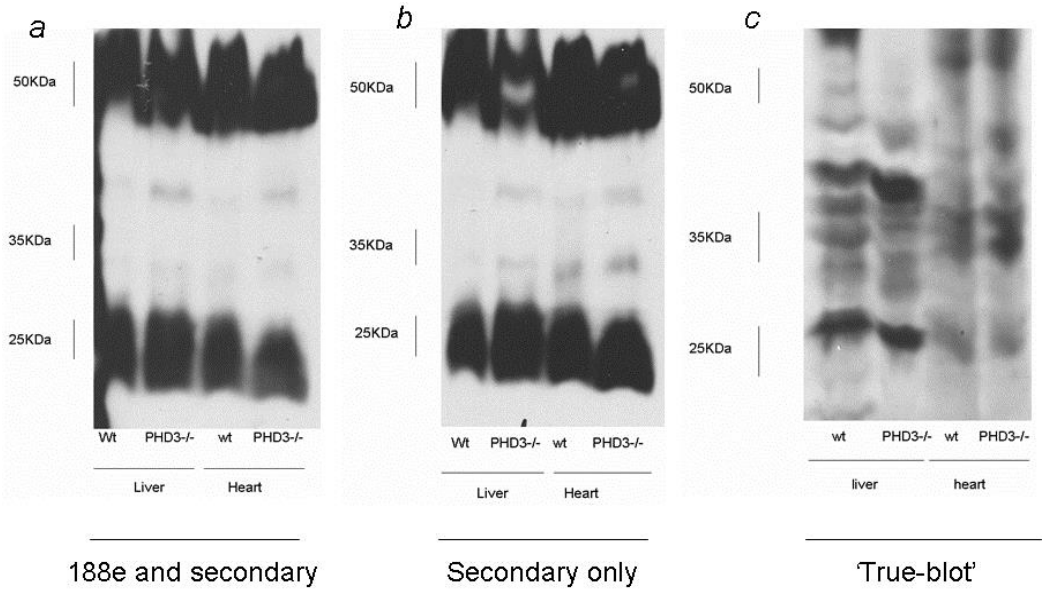


Figure 23. Cross reactive signal generated by immunoblot of mouse tissues with mouse monoclonal antibody to human PHD3 (188e)

Hybridoma supernatant of antibody 188e was used at a concentration of 1:10 to immunoblot wild type and PHD3-/- liver and heart extracts (fig 23, *a*). Immunoblots demonstrated strong signal of 50KDa and 25KDa in wild type and PHD3-/- tissues. An identical signal pattern was noted with secondary antibody only control (fig 23, b). The use of 'True-blot' reagent helped to reduce background signal but not to a level sufficient to allow detection of tissue PHD3 (fig 23,c). (Representative of 3 immunoblots)

In a further attempt to detect tissue PHD3, the 188e antibody was conjugated to FITC thus allowing an anti-FITC rather than anti-mouse IgG secondary reagent to be used. The conjugated antibody was able to detect PHD3 in extracts of mouse derived 3T3L1 cells using a conventional secondary antibody, thus confirming the conjugation process had not degraded the antibodies ability to detect PHD3 (fig 24). A similar signal to that produced by anti-IgG secondary antibody was produced by using an anti-FITC secondary antibody indicating that the conjugation process had also been successful (fig 24). Despite this, the conjugated antibody did not detect mouse tissue PHD3, even in tissues from hypoxia treated animals (fig 24 a and b). Extracts from 3 different wild type and PHD3-/- animal pairs was assessed, each producing similar results.

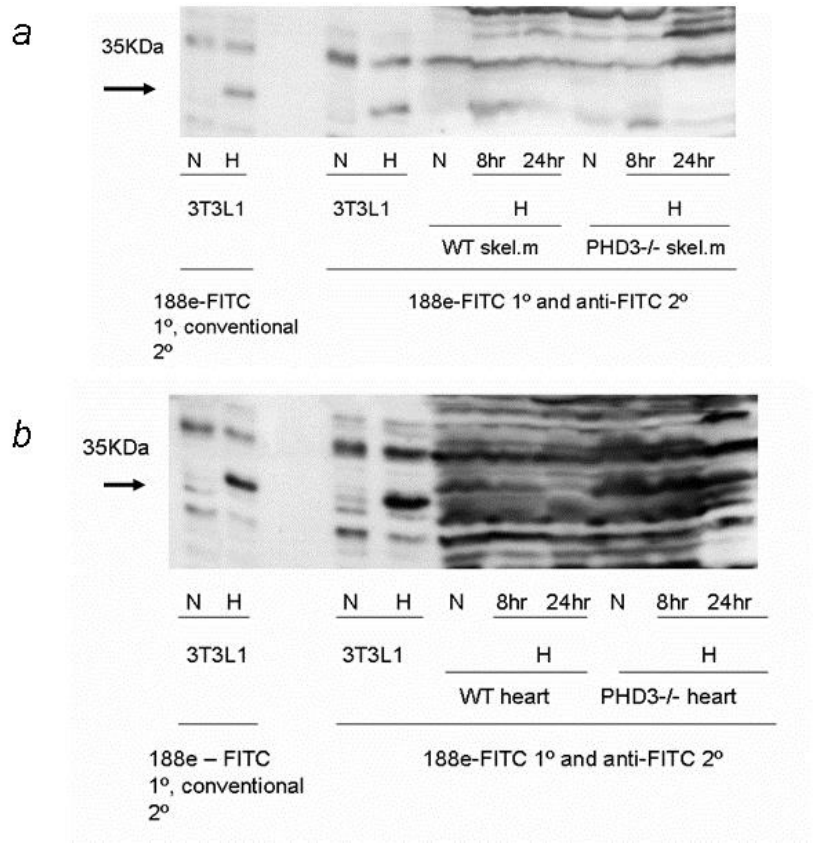


Figure 24. Testing sensitivity of FITC-conjugated mouse monoclonal antibody, 188e to mouse tissue PHD3

In order to test the ability of this antibody to detect physiologically relevant levels of mouse PHD3 rather than that in the context of over-expression, the signal from 4μg of 3T3L1 cells cultured in normoxia and after 6 hr of 1% hypoxia was compared. On the same membrane the signal from wild type and PHD3-/- tissues from normoxic and hypoxic mice (8 hr and 24 hr of 6% hypoxia) was also compared (N: normoxia; H: hypoxia). The FITC conjugated 188e antibody at a concentration of 1:500 was used to immunoblot 9μg of mouse skeletal muscle (fig 24, a) and heart (fig 24, b) extracts together with 3T3L1 extracts. A conventional goat anti-mouse secondary antibody was used at a concentration of 1:2000 at room temperature for 1 hr while the anti-FITC secondary antibody was used at a concentration of 1:2000 for the same length of time. Radiographs were exposed to chemiluminescent signal for 3 min. Immunoblot demonstrated that after FITC conjugation, the 188e antibody retained its ability to detect physiological levels of mouse PHD3 (fig 24, arrows). However the conjugated form was not able to improve signal to a level sufficient to allow detection of PHD3 in either normoxic or hypoxia mouse tissue extracts. (Representative of 3 immunoblots).

Next the three new anti-mouse PHD3 rabbit polyclonal antisera generated during this doctoral study were tested for their ability to detect endogenous tissue PHD3. Although capable of detecting over-expressed PHD3, these anti-sera did not detect endogenous tissue PHD3 (fig 25).

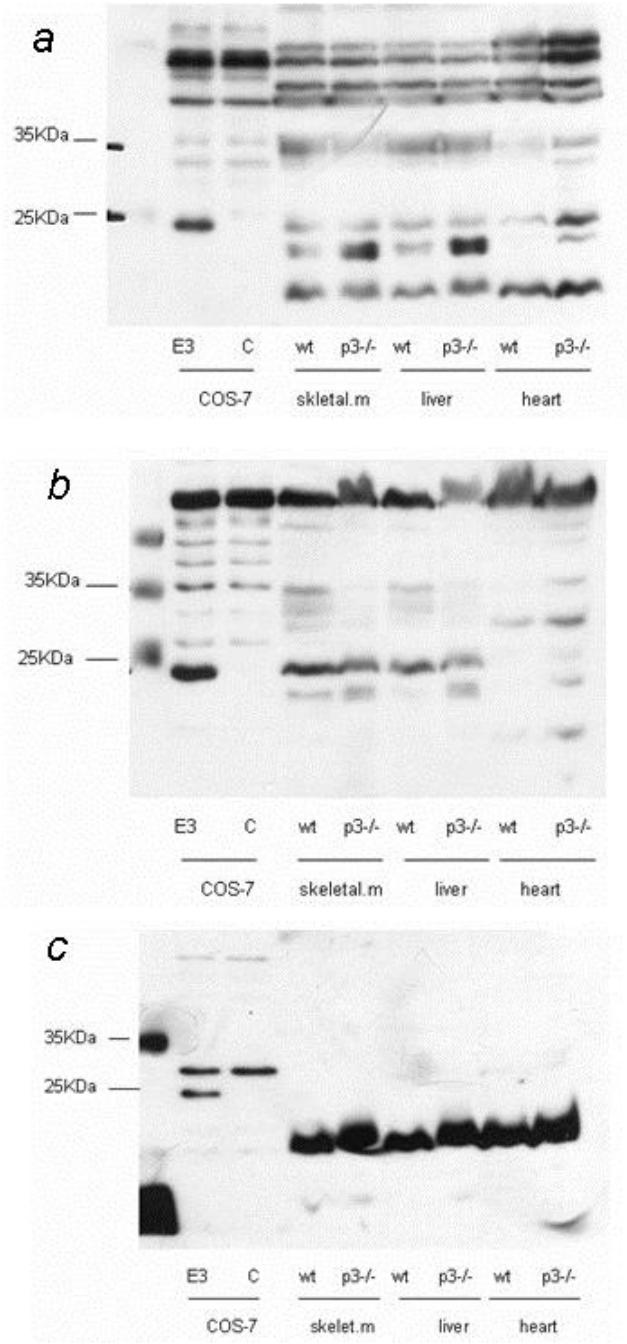


Figure 25. Testing the ability of new rabbit polyclonal anti-sera against mouse PHD3 to detect endogenous tissue

The three sets of anti-sera depicted (fig 25, a to c), although capable of detecting over-expressed mouse PHD3 as previously described (page 22), failed to detect endogenous tissue PHD3 at 1:500 dilution. (Representative of 2 immunoblots).

4.2 Characterising the expression of PHD isoforms in rat tissues

As part of this doctoral study, the tissue expression of PHD's in rat tissues was also assessed. This approach was particularly important because of the difficulties in detecting mouse tissue PHD3. Although this work was aimed primarily at characterising all PHD isoforms in a range of different tissues, the emerging role of PHD3 as a promoter of neuronal apoptosis favoured placing emphasis on its neuronal expression, particularly in the sympatho-adrenal axis. In contrast to the study of PHD isoforms in mouse tissues, the study of rat lacked the specificity control provided by animals deleted of individual PHD isoforms. The rat study was therefore validated by demonstrating largely concordant signal between independently raised antisera to respective PHD isoforms.

4.2.1 Characterising the expression of PHD1 in rat tissues

For rat PHD1, the in-house rabbit polyclonal antibodies R1 (fig 26, *a*) and af 1.2 (fig 26, b) produced similar signal. Both detected signal of the correct size in testis and also produced fainter signal in skeletal muscle.

Antibody R1 detected an additional band in heart which was too large to be PHD1. Antibody af 1.2 also produced faint additional bands in midbrain, brain stem and cerebellum. These bands were inconsistent between different immunoblots and could not be enhanced by loading more tissue extract or prolonging radiographic exposure ('blackening' after 5min exposure times). Although it is possible that these bands produced by antibody af1.1 represented true tissue PHD1 protein, their variability between different immunoblots and absence from immunoblots with the second anti-PHD1 antibody necessitated caution in their interpretation.

Nonetheless it was clear that both antibodies produced largely concordant signal in testis and skeletal muscle thereby validating PHD1 expression in these two tissues and suggesting that its expression in other tissues was at best significantly less. Because antibody R1 produced a more consistent tissue signal it was preferentially used for further quantitative studies of tissue PHD1 abundance which will be described later.

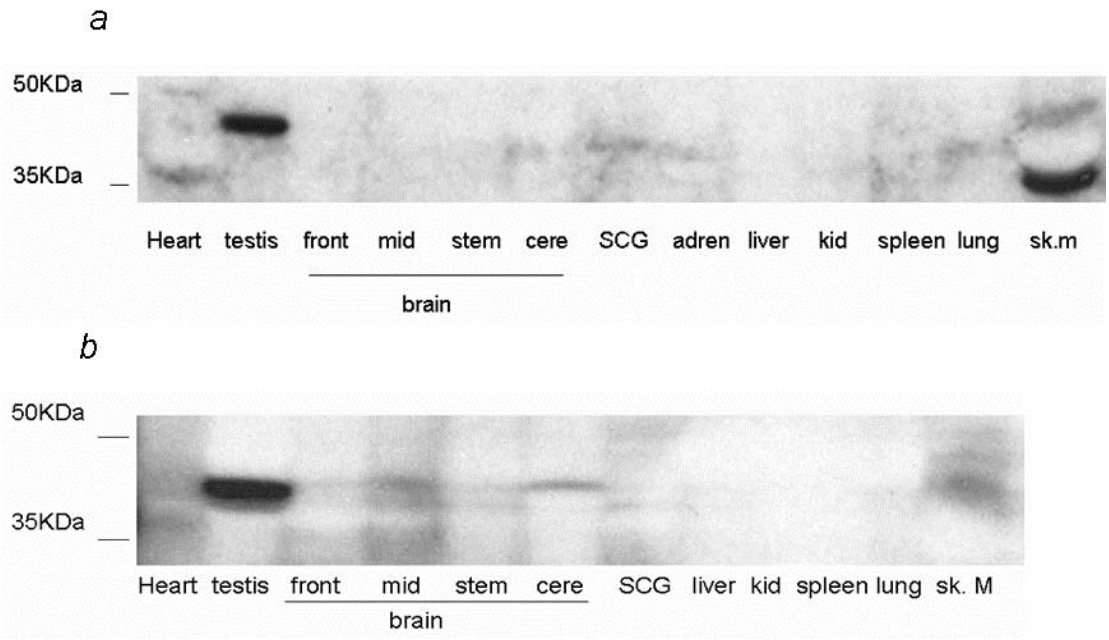


Figure 26. PHD1 expression in rat tissues as detected by two independent antibodies

Two independent antibodies were identified which produced largely concordant signal when used to immunoblot rat tissue. 9µg of each tissue homogenate was used apart from rat superior cervical ganglion (SCG) of which only 4µg was used, because of its small size. The in-house anti-rat PHD1 rabbit polyclonal antibody (R1) generated by Ya-Min Tian, was used at a concentration of 1:2000 (fig 26, a). After 3 min radiographic exposure, a single PHD1 species of the predicted molecular weight was detected in rat testis. A fainter signal was also noted in rat skeletal muscle which was of a similar molecular weight to that noted in testis. The in-house rabbit polyclonal antibody to human PHD1, af 1.2 was used at a concentration of 1:500 (fig 26, b). After 3 min of radiographic exposure, a single species of the predicted molecular weight for PHD1 was noted with this antibody in rat testis. Fainter signal of the same molecular weight was noted with this antibody in regions of the brain. It also produced a weak signal in skeletal muscle which was of a similar size to that present in testis. (Representative of 3 immunoblots).

As in mouse, the high level of PHD1 detected in rat testis was further assessed by immunohistochemistry. Staining with the R1 antibody demonstrated PHD1 in rat testis also localised to developing spermatozoa (fig 27).

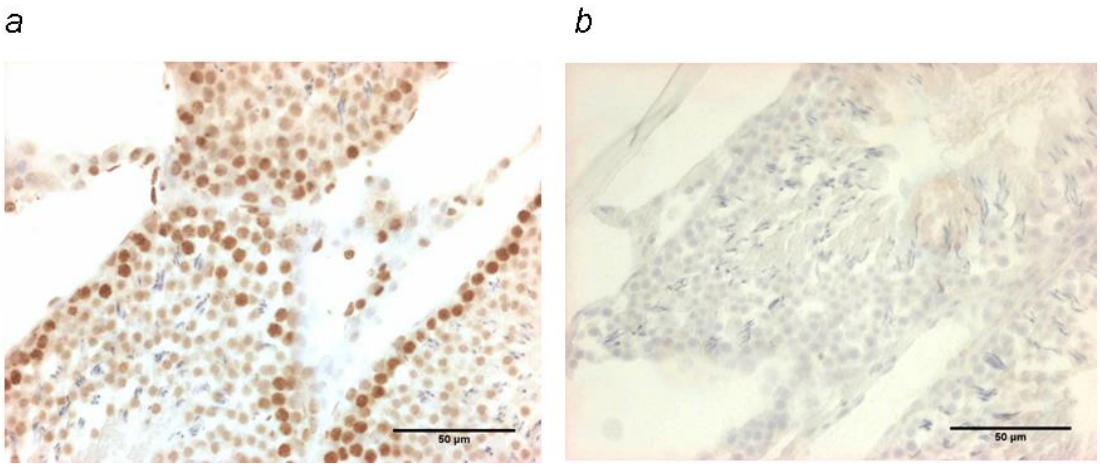


Figure 27. Characterising the expression of PHD1 in rat testis

PHD1 immunohistochemistry of rat testis sections were carried out with the rabbit polyclonal antibody to rat PHD1 (R1) at a concentration of 1:500 (fig 27, a). Normal rabbit serum control sections were immunostained in parallel (fig 27, b). Both sections were counterstained with haematoxylin. PHD1 signal was detected in developing spermatozoa. (Representative of 3 separate testis stains.)

4.2.2 Characterising the expression of PHD2 in rat tissues

As with PHD1, two independent antibodies to PHD2 were identified which produced largely concordant tissue signal. The commercial rabbit polyclonal antibody NB100-2219 produced strong signal in heart, liver, kidney, testis with weaker signal in forebrain, adrenal gland and skeletal muscle which appeared as a closely migrating doublet (fig 28, a), a further slower migrating band was detected by this antibody in liver. The second antibody used to immunoblot rat tissues was the anti-mouse PHD2 rabbit polyclonal antibody generated by Prof Patrick Maxwell (PM-PHD2) (fig 28, b). In keeping with NB100-2219, this antibody also produced strong signal in many tissues. Indeed the relative abundance of PHD2 signal was very similar with strongest signal noted in heart and weaker signal in forebrain, adrenal and skeletal muscle.

In contrast to the PHD2 doublet produced by NB100-2219 in many tissues, PM-PHD2 produces a single tissue species. However it is interesting to note that the same antibody produced a doublet signal in earlier immunoblots of mouse tissues. Taken together these findings may indicate that this antibody was less able to detect the doublet PHD2 species of rat compared to mouse.

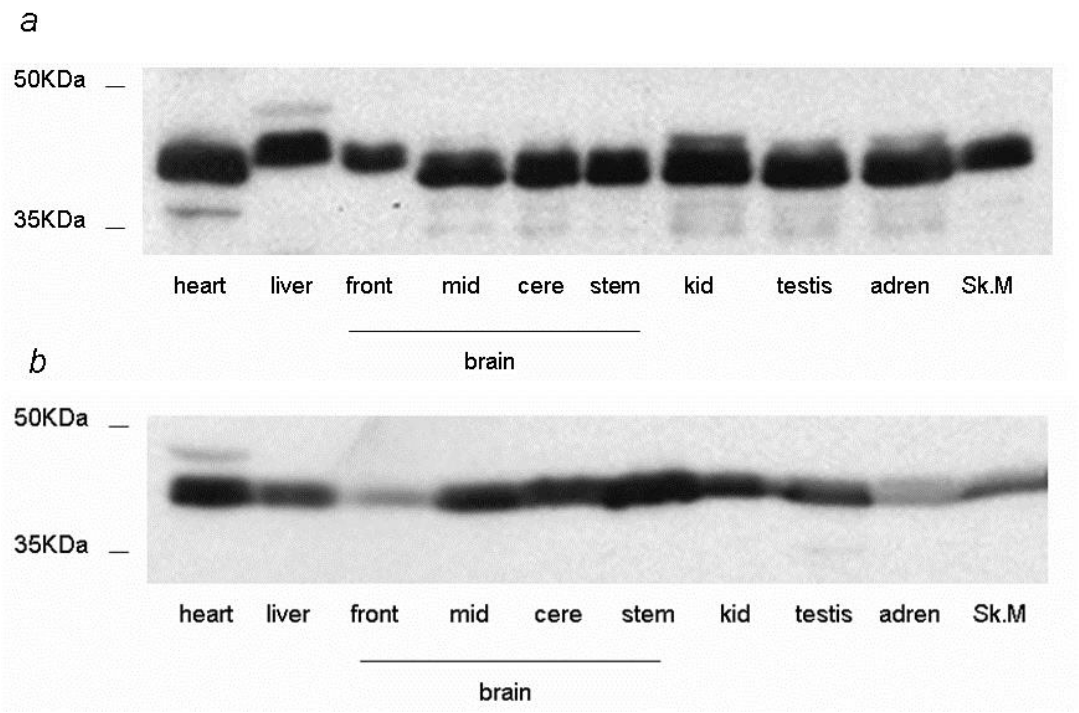


Figure 28. Characterising the expression of PHD2 in rat tissues

The expression of PHD2 in rat tissues was assessed by two independent antibodies. The commercial rabbit polyclonal antibody to mouse PHD2, NB100-2219 produced strong signal of the predicted size in many rat tissues (fig 28, a). A rabbit polyclonal antibody to mouse PHD2, generated by Prof Patrick Maxwell of University College London, termed PM-PHD2 also produced signal of the predicted size and similar relative intensity to that produced by NB100-2219. In contrast to NB100-2219, PM-PHD2 produced a single species in rat tissues (fig 28, b). (Representative of 3 immunoblots).

The stronger and cleaner signal generated by NB100-2219 in rat tissue meant that this antibody was used for further quantitative study of rat tissue PHD2 as will be described later.

4.2.3 Characterising the expression of PHD3 in rat tissues

In assessing the expression of PHD3 in rat tissues, it was important to consider the results of previous studies which had demonstrated that there were several protein species of rat PHD3 (Lipscomb et al., 1999; Lipscomb et al., 2001). A mitochondrial targeting peptide incorporating species of PHD3 had been demonstrated in sympathetic neurons, with a molecular weight of 40KDa. A further 33KDa species of PHD3 had also been demonstrated in sympathetic lineage cells. It was also possible that a conventional form of rat PHD3, similar in size to the 27KDa found in other species was also present in rat tissues.

Given the earlier difficulties relating to detection of mouse tissue PHD3, particular emphasis was placed on establishing the ability of anti-PHD3 antibodies to detect PHD3 in an endogenous rather than over-expressed state. Having established signal in the endogenous setting, each antibody was then further validated using an IVTT based approach.

In order to achieve this, putative anti-PHD3 antibodies were assessed for their ability to produce concordant signals when used to blot normoxic and hypoxic PC12 cell extracts. This cell line was chosen as previous studies had indicated that it expressed several forms of rat PHD3 (Straub et al., 2003; Lee et al., 2005).

Three antibodies were identified which produced concordant signals when used to immunoblot PC12 cell extracts. Each detected a lower molecular weight doublet signal in the region 27KDa which was strongly induced by hypoxia (fig 29). This species was of the correct size to be a rat homologue of human and mouse PHD3.

All three antibodies also detected a heavier species in the region of 50KDa which was not hypoxically induced and appeared much fainter than the lower molecular weight doublet. The fact that this 50KDa species was detected with three independent antibodies suggested that that it may represent a novel form of rat PHD3.

The two rabbit polyclonal antibodies, NB100-303 and NB100-137 detected an additional band in the region of 40KDa which was not induced by hypoxia. This species may represent the 40KDa species previously described (Wax et al., 1994). A further species which was also not induced by hypoxia was detected by NB100-303 alone in the region of 33KDa which may represent a previously described species of PHD3 (Lipscomb et al., 2001). However, a degree of caution was necessary in interpreting this signal as it was detected with only one antibody giving rise to the possibility that it could have been non-specific in nature.

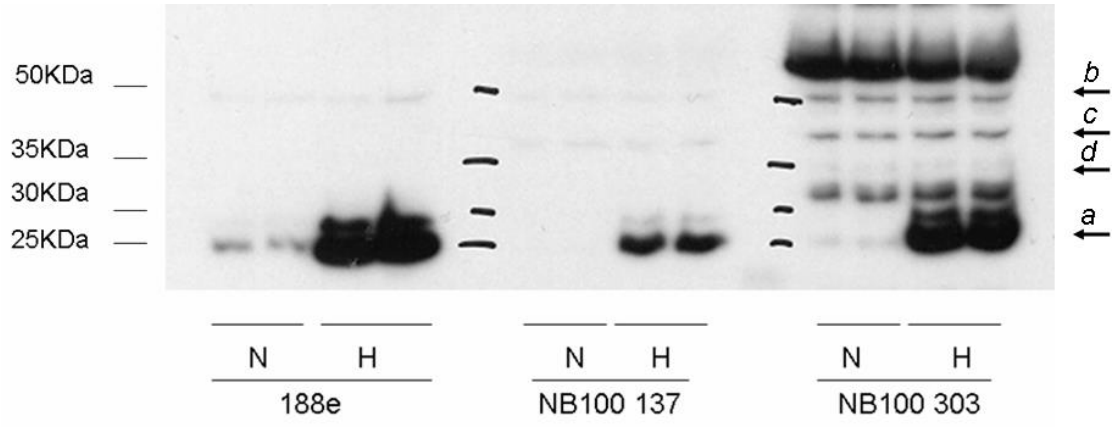


Figure 29. Testing the ability of anti-PHD3 antibodies to detect PHD3 in cultured PC12 cells

Extracts from PC12 cells cultured in normoxia and 6 hr of 1% hypoxia were immunoblotted with antibody 188e, NB100-137 and NB100-303. After 3 min of radiographic exposure, all three antibodies demonstrated an inducible doublet species of approximately 27KDa (fig 29, arrow a). A heavier species of 50KDa was also detected by all three antibodies (fig 29, arrow b). This species appeared as a single band. It was not induced by hypoxia and was weaker than the ~27KDa doublet species. NB100-137 and NB100-303 detected a species between 35KDa and 50KDa which may represent the 40KDa species of PHD3 detected by others (fig 29, arrow c). NB100-303 detected a further faint species between 30KDa and 35KDa which may represent the 33KDa species of PHD3 detected by others (fig 29, arrow d). (Representative of 3 immunoblots).

The ~27KDa species of PHD3 was likely to represent the rat counterpart of human and mouse PHD3. However unlike human and mouse PHD3, this form appeared as a doublet. In order to assess the nature of the doublet species further, immunoblots of PC12 cell extracts were carried out alongside those of mouse 3T3L1 cells and rat PHD3 protein generated by programming an IVTT with rat PHD3 cDNA (fig 30). The 27KDa doublet species of rat PHD3 was noted, and the lighter partner of this pair was found to migrate in parallel with mouse 3T3L1 PHD3. This suggested that this species did represent the rat homologue of mouse PHD3. The upper partner of this doublet, although heavier than mouse PHD3, migrated below the 30KDa marker indicating that it was not the 33KDa species described by others. This immunoblot also confirmed that the 50KDa species of PHD3 present in PC12 cells was greater in size to that of the known full-length rat PHD3 generated from cDNA programmed IVTT. It should be noted that immunoblots of extracts from a different batch of PC12 cells, carried out at a later stage of this study did demonstrate an additional 33KDa band (Fig 33), further supporting the novel nature of the rat PHD3 species identified here.

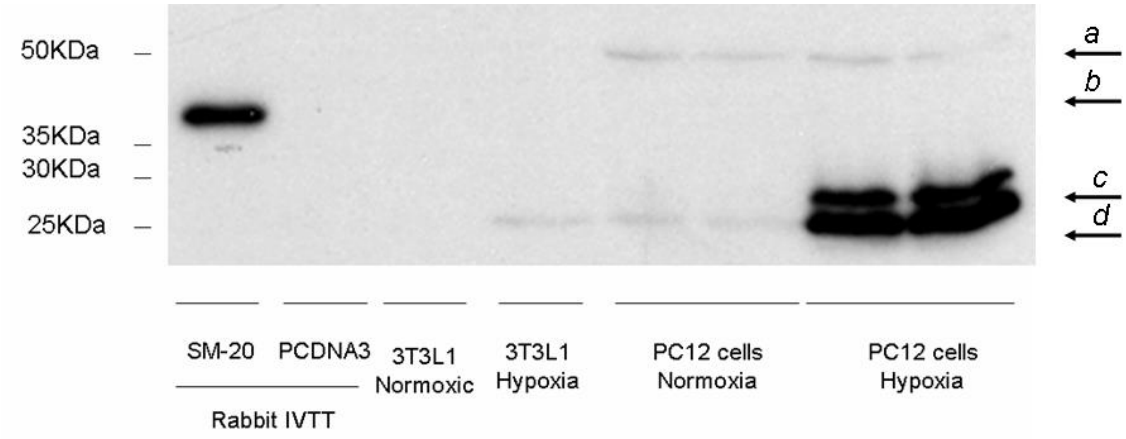


Figure 30. Comparing rat PC12 cell and IVTT generated PHD3(SM-20) with that of mouse

PHD3 signal from PC12 cells, IVTT programmed with rat PHD3 IVTT and mouse 3T3L1 cells was compared with antibody 188e. The 50KDa species was clearly present in PC12 cell extracts (fig 30, arrow, a). The IVTT generated form of PHD3 appeared as a single band of the predicted size of 40KDa (fig 30, arrow, b). The 27KDa doublet species of rat PHD3 was strongly induced by hypoxia. The lighter partner of his doublet migrated at the same mobility as its mouse counterpart in 3T3L1 cells (fig 30, arrow, d). (Representative of 3 immunoblots).

The ability of each antibody to detect PHD3 in rat tissues was next assessed. Because the mouse monoclonal antibody produced the cleanest and strongest signal, this antibody was initially tested on a limited number of rat tissues. The 30% homology shared between rat and mouse immunoglobulin gave rise to the possibility that as in mouse, cross-reaction between secondary antibody and endogenous tissue immunoglobulin could occur. In view of this, a secondary antibody only control immunoblot was carried out in parallel with primary and secondary antibody. Immunoblots demonstrated very similar signal between the primary and secondary antibody combination and the secondary antibody only control (fig 31).

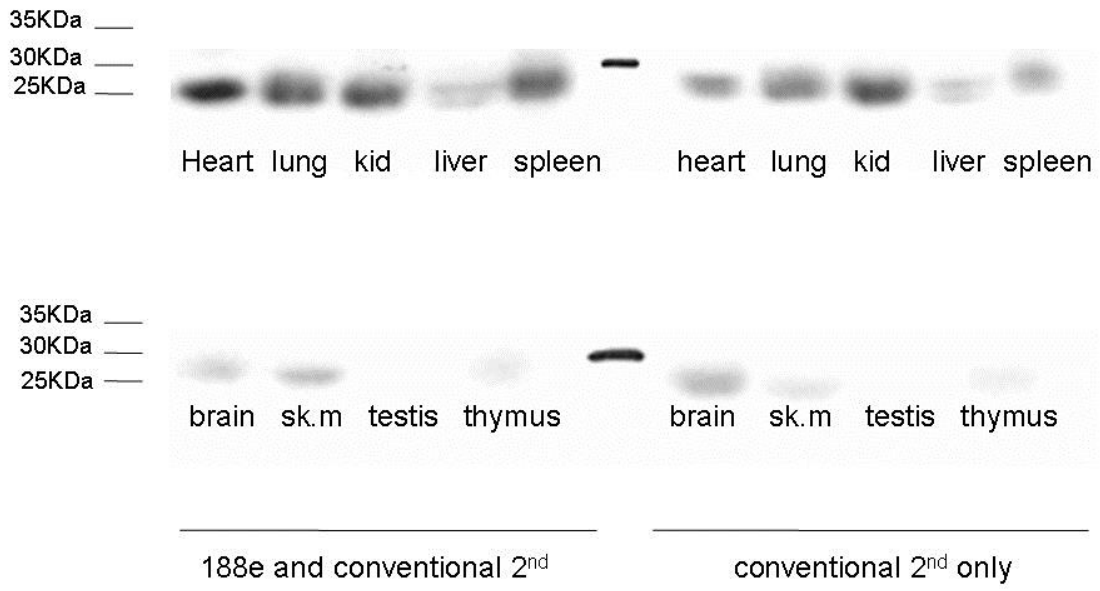


Figure 31. Testing the ability of the mouse monoclonal antibody, 188e to detect endogenous rat tissue PHD3

9µg of each rat tissue was loaded in duplicate sets onto a 10% SDS-PAGE gel as indicated. After transfer, the membranes were separated in two and immunoblotted with either 188e and goat anti-mouse secondary antibody or secondary antibody alone. Radiographs were exposed to chemiluminescent signal for 10 min. An almost identical signal was produced by both methods indicating that the anti-mouse secondary antibody detected immunoglobulin in rat tissues rather than tissue PHD3. (Representative of 3 immunoblot).

As a further measure to reduce cross-reacting signal, an isotype specific secondary antibody which preferentially detected mouse IgG1 was tested. Using this approach, a doublet signal in the region of 27KDa was detected in superior cervical ganglion (SCG) and heart, but not with the secondary antibody only control (fig 32). The appearance of this signal was very much in keeping with that detected previously in PC12 cell extracts, and as such was likely to represent tissue PHD3.

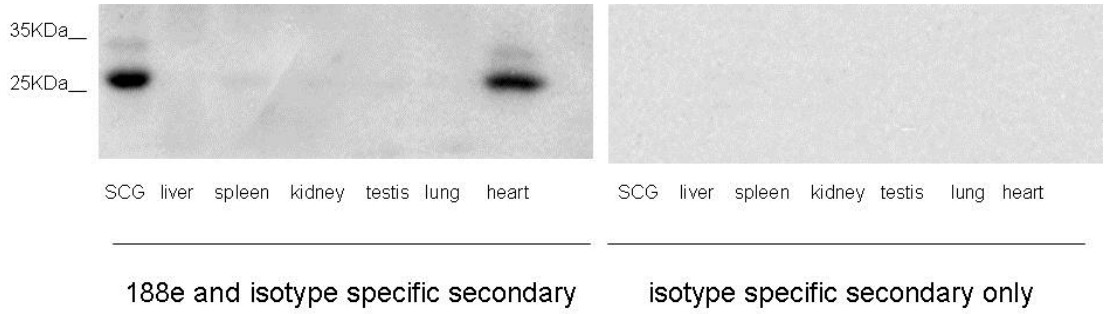


Figure 32. Combining 188e with an isotype specific secondary antibody to detect endogenous PHD3 in rat tissues

To overcome the cross-reactive signal between mouse and rat immunoglobulin, an isotype specific secondary antibody, specific to the IgG1 isotype of the 188e mouse monoclonal antibody, was used. 9µg of each rat tissue was loaded in duplicate sets onto a 10% SDS-PAGE gel as indicated. After transfer, immunodetection was carried out with 188e and isotype specific secondary antibody at a concentration of 1:1000 for 1 hr at room temperature or isotype specific antibody only, and radiographs exposed to chemiluminescent signal for 3min. Immunoblots demonstrated signal with 188e and isotype specific secondary antibody but not with isotype specific antibody alone. Using this approach a doublet signal of the predicted molecular weight for PHD3 was detected in SCG and heart. (Representative of three immunoblots).

This approach was next used to survey PHD3 expression in a range of rat tissues. Given the inducible nature of the lower species of PHD3 in hypoxic PC12 cells, tissues from hypoxia treated animals were immunoblotted alongside those from normoxic animals (fig 33). This immunoblot not only indicated the presence of the 27KDa doublet but also demonstrated the heavier 50KDa species. The doublet species was strongly expressed in SCG, heart and skeletal muscle, with lesser levels present in other tissues. In contrast to PC12 cells, this species was not induced in tissues by the hypoxic stimulus used and in fact appeared marginally reduced in hypoxic compared to normoxic skeletal muscle.

In lung, kidney, brain, liver, spleen and adrenal the 50KDa species was more abundant than the 27KDa species, while in SCG and heart the 27KDa species was dominant.

The 50KDa species was also strongly expressed in brain, skeletal muscle, kidney, spleen and adrenal gland. Lesser levels were present in other tissues. In skeletal muscle and to a lesser extent, testis and lung, the mobility of this species was marginally different. A doublet species in the region of 50KDa was detected in liver and skeletal muscle. This gave rise to the possibility that the signal in these tissues was non-specific or alternatively represented a 50KDa form of PHD3 which had undergone tissue specific post-translational modification. One way to assess these possibilities was to determine if a further anti-PHD3 antibody produced concordant tissue staining which was carried out next.

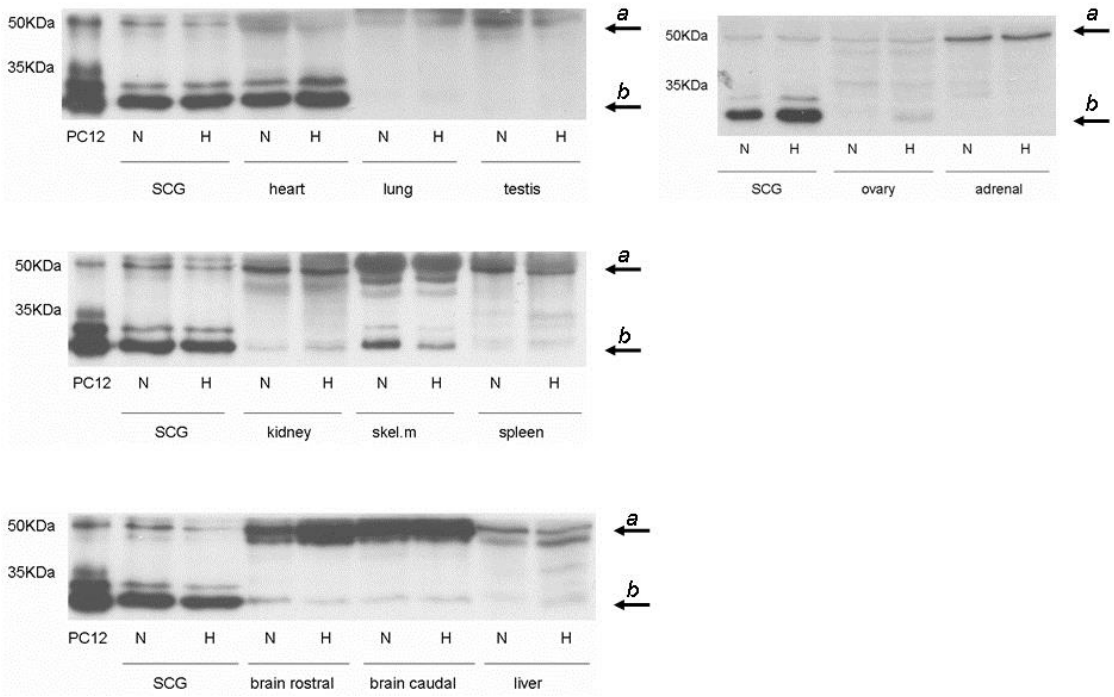


Figure 33. Expression of PHD3 in rat tissues

Using 188e with an isotype specific secondary antibody, the expression of PHD3 in tissues was assessed. Signal from normoxic rats and those treated for 8 hr with 8% hypoxia were compared. 9µg of each tissue was used apart from the SCG of which 4µg was used. 4µg of hypoxia treated PC12 cell extracts were loaded as a positive control. Membranes were incubated with 188e primary antibody followed by isotype specific secondary antibody. After 3min of radiographic exposure, a 50KDa species (fig 33 arrow a) and 27KDa species (fig 33, arrow b) were noted. (Representative of three immunoblots).

Next, the rabbit polyclonal antibody NB100-303 was tested for its ability to detect PHD3 in rat tissues (fig 34). This antibody produced a complex mixture of bands in different tissues. The dominant band detected in many tissues migrated at approximately 36KDa and did not correspond to any species of PHD3 previously reported or detected by the other antibodies used. A signal in the region of 27KDa was however seen in heart, SCG and skeletal muscle. In heart a 27KDa doublet signal was noted, in keeping with the doublet signal previously noted in PC12 cells and with antibody 188e in tissues, but in contrast only a single species of 27KDa was detected in SCG and skeletal muscle. A 50KDa species was also noted to be present which was particularly strong in heart, regions of the brain, adrenal, kidney and lung, tissues in which a similarly sized species had been detected with anti-PHD3 antibody 188e. In contrast to 188e very little of the 50KDa signal was detected in testis, spleen, lung and skeletal muscle. These differences may reflect the different antibody sensitivities to this form of PHD3.

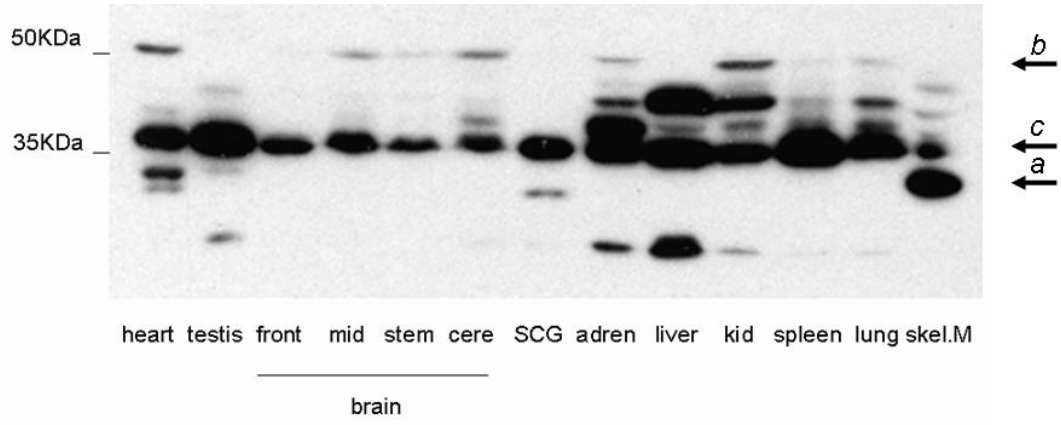


Figure 34. Determining the ability of NB100-303 to detect PHD3 in rat tissues

The rabbit polyclonal antibody, NB100-303 was used to immunoblot 9µg of each rat tissues, apart from rat SCG of which 4µg was used. After 3 min of radiographic exposure, a number of different species were detected. A species of 50KDa (fig 34, arrow b) and 27KDa (fig 34, arrow a) corresponding to those species previously detected with antibody 188e were observed. A non-specific dominant species of ~36KDa (fig 34, arrow c) was also present. (Representative of three immunoblots)

The second polyclonal antibody, NB100-137 was also assessed for its ability to detect rat tissue PHD3. This produced extensive non-specific tissue signal which meant that it was unsuitable for tissue immunoblotting.

4.2.4 Relative expression of different PHD isoforms in rat tissues

As part of collaborative work with Dr Tammie Bishop, ^{35}S radio-labelled rabbit reticulocyte IVTT programmed with cDNA for rat PHD1 to 3 and pcDNA3 empty vector control were prepared and their signal normalised (fig 35).

Rat PHD1 IVTT appeared as a doublet band of the predicted size. Rat PHD2 IVTT also produced a species of the predicted size which was somewhat diffuse, hinting at the possibility that it may consist of a number of closely migrating species. As with PHD1 and PHD2, a requirement for PHD3 signal quantitation was the generation of normalised IVTT species corresponding in size to those found in tissues. Dr Bishop successfully sourced rat PHD3 cDNA which generated a 27KDa species however a rat PHD3 cDNA capable of producing a 50KDa species was not available which meant that only the 27KDa could be reliably quantified.

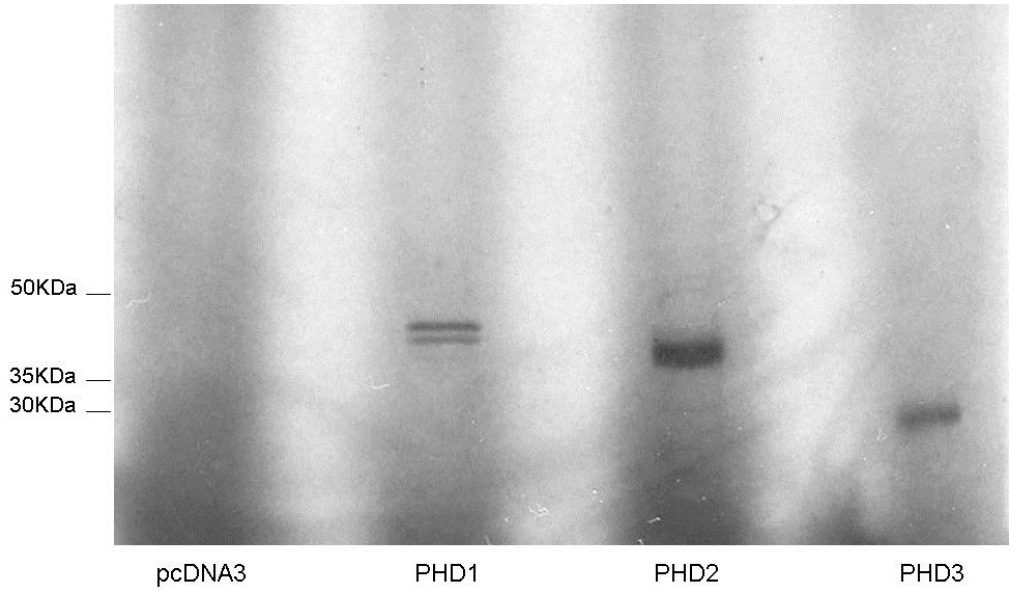


Figure 35. ^{35}S radio-labelled rabbit reticulocyte IVTT programmed with cDNA for rat PHD1 to 3 and pcDNA3 empty vector control – by Dr Tammie Bishop

Normalised ^{35}S radio labelled IVTT for rat PHD1 to 3 demonstrated similar signal intensity. A doublet PHD1 signal was seen for PHD1, while PHD2 and 3 appear as diffuse bands, suggesting the presence of one or more closely migrating species.

Antibodies R1, NB100-2219 and 188e were considered to produce the strongest and cleanest tissue immunoblot signals for PHD1 to 3 respectively and were used for further study. The binding of these antibodies to equimolar amounts of IVTT generated PHD protein was assessed (by Dr Tammie Bishop) and each antibody was found to be both sensitive and specific to respective rat PHD isoforms.

In order to quantify tissue PHD's it was necessary to determine the relative strength of each antibody to respective PHD isoforms and to correct tissue immunoblot signal accordingly. To achieve this, the immunoblot signal against equimolar amounts of each PHD isoform was quantified using ImageJ software (NIH, USA). This demonstrated that the anti-PHD2 antibody (NB100-2219) produced 5 fold stronger signal than either anti-PHD1 (R1) or anti-PHD3 (188e) antibodies. Furthermore antibody R1 and 188e produced similar signal to one another.

As only the 27KDa species of rat PHD3 was generated from programmed IVTT, it was not possible to quantify the relative strength of the 50KDa form detected in tissues with antibody 188e. Nonetheless, it was possible using this approach to quantify the expression of other PHD isoforms.

Immunoblots for PHD1 to 3 were carried out in parallel. 9μg of each tissue was used apart from SCG which, because of its small size, allowed only 4μg to be used. Tissue immunoblot signal was quantified using ImageJ software (NIH, USA) and SCG signal corrected for loading by multiplying the SCG signal 2.25 times. A further correction was then carried out for the sensitivity of each PHD antibody to its respective isoform. This was achieved by multiplying tissue PHD1 and PHD3 signal 5

times thereby normalising it to that of PHD2. Normalised tissue signal for each PHD isoform is graphically represented (fig 36).

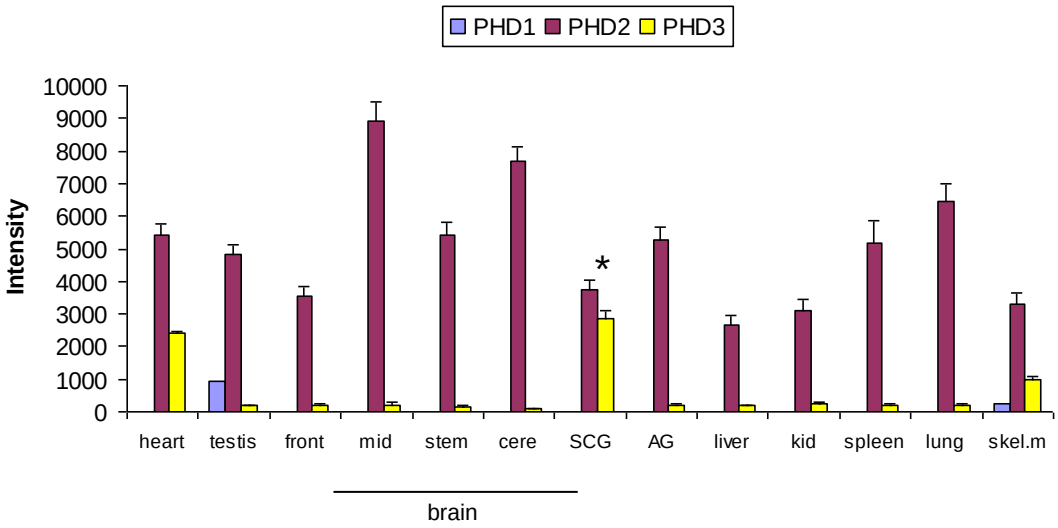


Figure 36. Relative expression of rat tissue PHD's

9µg of each tissue was immunoblotted apart from SCG, of which 4µg was used. The intensity of immunoblot signal for each PHD protein was quantified and SCG signal corrected to take into account the lesser amount loaded (*). Signal was further corrected according to the sensitivity of each antibody for its respective protein, and the relative tissue abundance of each PHD graphically represented as indicated. Only the 27KDa species of PHD3 was quantified. (Signal from two immunoblots was quantified and represented as mean optical density ± SEM).

After normalisation, PHD2 was found to be the dominant tissue PHD isoform in all tissues studied. PHD2 was most abundant in brain and least abundant in liver. In other tissues it was expressed at intermediate levels. A threefold difference was noted between the amount of PHD2 expressed in liver and midbrain. In testis, regions of the brain, lung, liver, spleen, kidney and adrenal gland the abundance of PHD2 was between 20 and 30 fold greater than that of the 27KDa species of PHD3.

PHD3 was most abundantly expressed in SCG, heart and skeletal muscle. SCG contained most PHD3 but even here PHD2 was 1.3 fold in excess. The absence of detectable levels of PHD1 in most rat tissues meant that a similar comparison could not be made, although clearly PHD2 expression was many fold more than PHD1. In contrast to most other tissues, PHD1 was of greater abundance in testis where it was found to be only 5 fold less than testis PHD2. Skeletal muscle also expressed detectable amounts of PHD1 and here its abundance was 12 fold less than that of PHD2.

The relative expression of PHD1 and 3 was also assessed. The lack of any detectable PHD1 signal in most tissues meant that PHD3 was the dominant of these two forms. PHD1 was however expressed in skeletal muscle where it was 3 fold less abundant than PHD3. In testis however PHD1 was 4.5 fold in excess of PHD3. Testis and skeletal muscle were unusual amongst tissues by expressing detectable levels of all three PHD's.

Chapter 5. Characterising the expression of PHD3 protein in tissues of the sympatho-adrenal axis.

The abundance of PHD3 detected in adult rat superior cervical ganglion (SCG) was an interesting finding. It gave rise to wider questions about the expression of PHD3 in other sympatho-adrenal tissues such as the carotid body and adrenal medulla.

While PHD3 immunoblot signal was detected in whole adrenal gland extracts, it was unclear if this arose from medullary or cortical tissues or both. Furthermore because the adrenal medulla represented only 10% of the volume of the adrenal gland as a whole (Tomlinson et al., 1987) any immunoblot signal derived from adrenal medullary tissue was likely to be significantly underrepresented in immunoblots of whole-gland extracts. With regards to the SCG, its PHD3 immunoblot signal could also have arisen from a number of different cell populations which included sympathetic neurons, small intensely fluorescent cells and SCG stromal cells (Davies et al., 1978; Smolen et al., 1983). Further study was therefore necessary to identify the specific cellular source of PHD3 signal within different sympatho-adrenal tissues.

This was achieved by immunohistochemistry, and the semi-quantitative approach used for this analysis allowed immunohistochemical signal from different sympatho-adrenal cell populations to be compared. Co-localisation studies with tyrosine hydroxylase (TH), a marker of the sympathetic lineage was used to determine if PHD3 signal arose from sympathetic or non-sympathetic lineage cell types of each tissue. For comparison, PHD3 signal in non-sympathetic lineage peripheral sensory neuronal populations of the trigeminal, dorsal root and nodose ganglia was also assessed.

Immunoblot analysis also indicated expression of PHD3 within brain extracts. CNS cell populations of the substantia nigra, locus coeruleus and brain stem catecholamine producing cardiorespiratory nuclei are known to express TH. The emerging role of PHD3 in sympathetic-lineage tissues of the peripheral nervous system gave rise to the possibility that it had similar roles in CNS sympathetic-lineage cell types.

Several TH expressing CNS regions are known to express HIF1 (Pascual et al., 2001), setting a precedent for their expression of HIF regulatory PHD enzymes. As a first step to testing this hypothesis, the expression of PHD3 in CNS sympathetic neurons was assessed. As in the study of the peripheral nervous system, an immunohistochemical approach was used.

5.1 Testing the ability of rat anti-PHD3 antibodies to detect tissue PHD3 by immunohistochemistry

Initially, the panel of anti-PHD3 antibodies used to immunoblot rat tissues were tested for their ability to detect rat PHD3 by immunohistochemistry. COS-7 cells transfected with rat PHD3 expression vector were pelleted and immunostained with these antibodies (fig 37). A similar pattern of immunohistochemical signal was produced by both antibodies thereby validating the ability of these antibodies to detect tissue PHD3 by immunohistochemistry. The rabbit polyclonal antibody (NB100-303) produced more background signal, a finding in keeping with its use in earlier immunoblots of rat tissues.

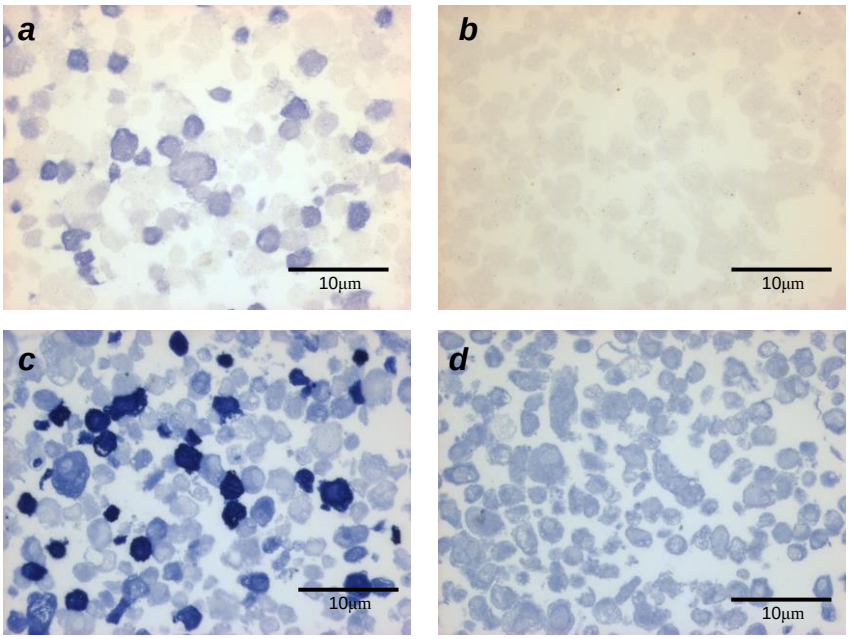


Figure 37. Testing the ability of anti-PHD3 antibodies to detect PHD3 by immunohistochemistry of transfected COS-7 cell pellets

COS-7 cells transiently transfected with rat PHD3 cDNA were immunostained with anti-PHD3 antibodies 188e (fig 37, a) and NB100-303 (fig 37, c). COS-7 cells transfected with pcDNA3 empty vector were immunostained in parallel with respective antibodies (fig 37, b and fig 37, d). Immunostaining using vector blue chromogen (shown) and DAB chromogen (not shown) produced concordant signal with both antibodies. (Representative of 2 immunostains).

5.2 Characterising the cellular expression of PHD3 in sympathetic tissues of the peripheral nervous system

5.2.1 Superior cervical ganglion and carotid body

Next, these antibodies were used to determine the cellular source of SCG PHD3 signal. Block tissue sections incorporating adult rat SCG and carotid body (CB) were carefully dissected from perfusion fixed animals and after processing, immunostained for PHD3. Largely concordant staining patterns were observed with two independent anti-PHD3 antibodies in the SCG (fig 38). The signal produced by these antibodies differed marginally at the subcellular level with antibody 188e producing strong nuclear and weaker cytoplasmic signal compared to equal signal in both compartments produced by antibody NB100-303.

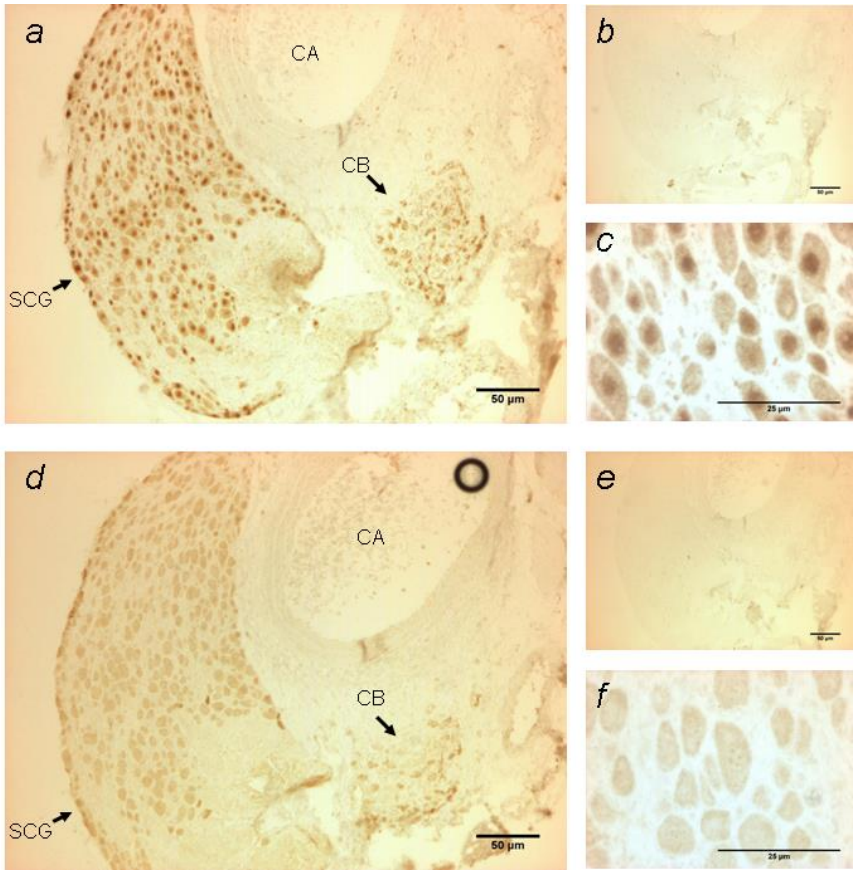


Figure 38. PHD3 staining of rat superior cervical ganglion (SCG)

Block sections incorporating adult rat SCG, carotid body (CB) and carotid artery (CA) were obtained. Immunostaining with the mouse monoclonal antibody, 188e and DAB chromogen demonstrated signal in the SCG and CB (fig 38, a). A serial section from the same tissue block immunostained with an anti-trinitrophenol IgG1 Kappa isotype matched control antibody demonstrated no significant staining (fig 38, b). At high power magnification, antibody 188e produced strong nuclear and weaker cytoplasmic signal in the SCG (fig 38, c). Further serial sections stained with the rabbit polyclonal antibody NB100-303 produced signal which localised to the same cell populations, but was weaker compared to the signal produced by antibody 188e (fig 38, d). No significant signal was detected in a serial section immunostained with normal rabbit serum (fig 38, e). At high power magnification, this antibody produced equal nuclear and cytoplasmic signal in SCG cells (fig 38, f). (Representative of two immunostains).

Given that antibody NB 100-303 did not detect a 50KDa SCG extract immunoblot band and produced equal cytoplasmic-nuclear Immunohistochemical staining, whereas antibody 188e did detect a 50KDa band and produced dominantly nuclear staining, the 50KDa band may represent a nuclear form of PHD3. Future studies could assess this by testing each antibody against separate nuclear and cytoplasmic SCG extracts and this will be discussed further at a later stage of this thesis.

5.2.2 Assessing PHD3 mRNA in the rat SCG

In view of the difference in subcellular PHD3 signal produced by these antibodies, further evidence was sought to confirm the expression of PHD3 in these tissues. This was achieved by in situ hybridisation of SCG sections using a probe to exon 1 of rat PHD3 which also demonstrated PHD3 signal within the SCG (fig 39). PHD3 is known to be expressed in both nuclear and cytoplasmic compartments (Metzen et al., 2003) and the difference in subcellular staining pattern observed with antibodies 188e and NB100-303 were likely to represent differences in their specificity to different PHD3 epitopes.

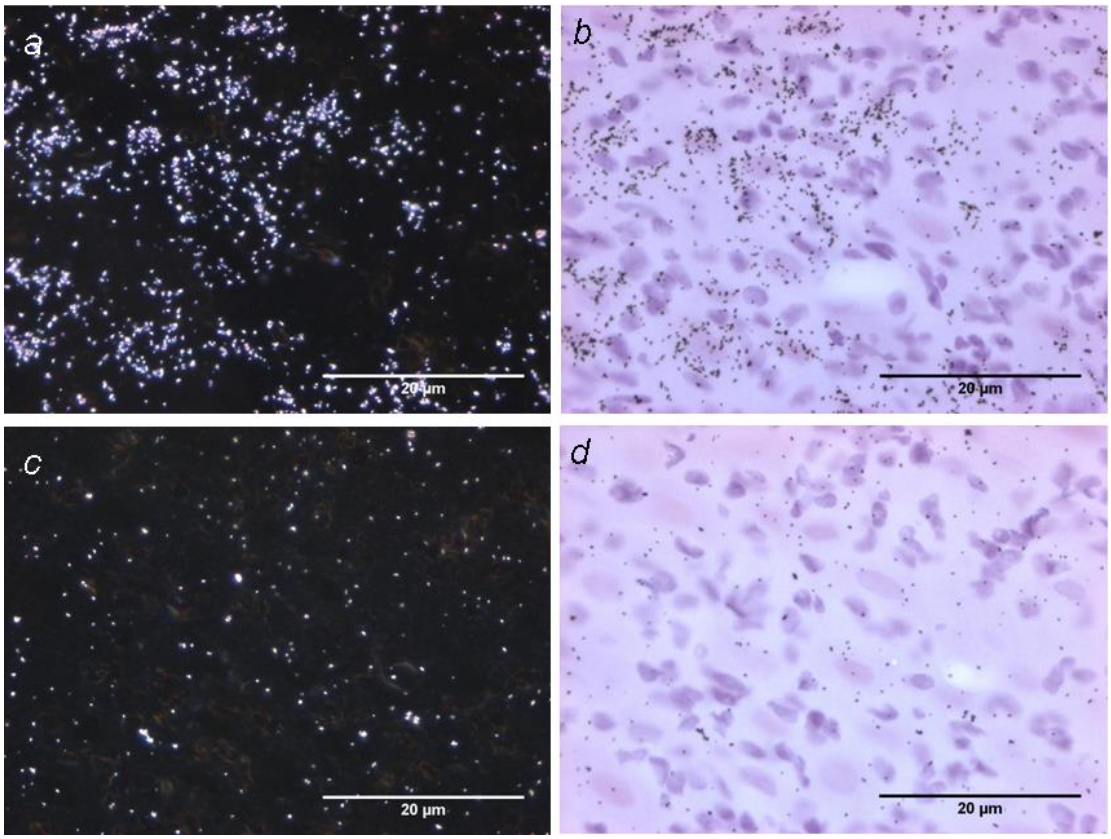


Figure 39. In situ hybridisation with a probe against exon 1 of rat PHD3

Dark field image of SCG sections hybridised with an anti-sense probe to exon 1 of rat PHD3 demonstrated strong signal (fig 39, a). Bright field images of the same section demonstrated signal predominantly over cell clusters (fig 39, b). Dark field image of SCG sections hybridised with a sense control probe to exon 1 of rat PHD3, demonstrated no significant signal (Fig 39, c). Bright field images of sense control probe section (fig 39, d). (Representative of three In situ hybridisations).

5.2.3 Co-localisation studies of PHD3 and TH in rat SCG

Having established that PHD3 was expressed in SCG cell populations, co-localisation studies with TH were next carried out to establish if PHD3 signal arose from sympathetic lineage cell types (fig 40). This demonstrated that PHD3 and TH localised to the same cell population thereby confirming that PHD3 was expressed in sympathetic-lineage cell types of the SCG. The majority of these cells were large in size with pale oval shaped nuclei, characteristic of sympathetic neurons.

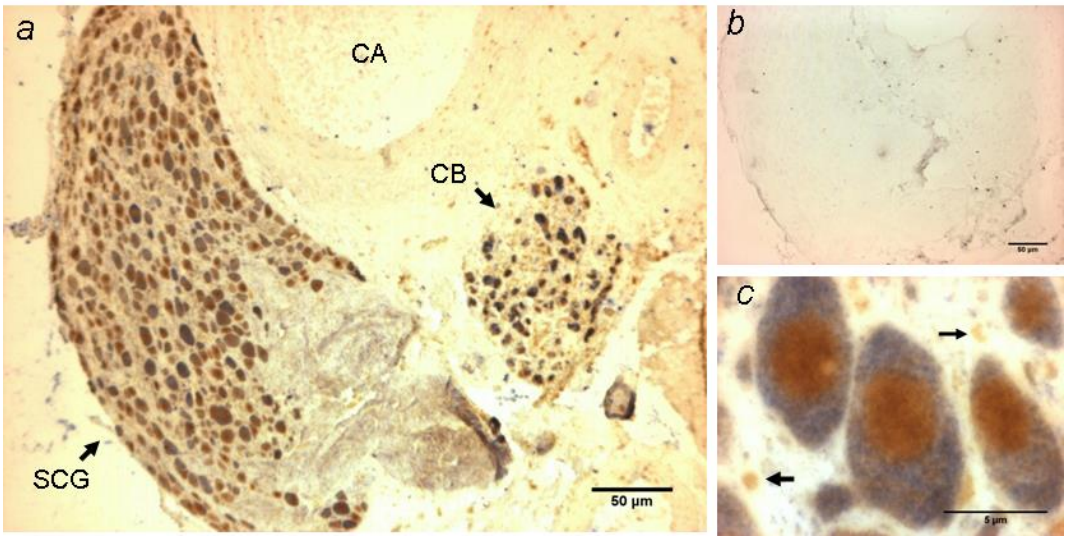


Figure 40. Double immunostaining for PHD3 (DAB) and TH (Vector blue).

Double staining was carried out with anti-PHD3 mouse monoclonal antibody 188e with DAB chromogen, and a commercial anti-TH rabbit polyclonal antibody with vector blue chromogen. Extensive staining was observed throughout the SCG (fig 40, a). Staining was also noted in the carotid body (fig 40, a). No significant staining was detected in the double negative control section double stained with isotype matched (anti-trinitrophenol, IgG1 Kappa) and normal rabbit serum control antibodies (fig 40, b). At high power, a representative cluster of four sympathetic neurons are depicted with strong nuclear PHD3 DAB signal, and cytoplasmic TH vector blue signal, thereby confirming that PHD3 was expressed in sympathetic neurons of the SCG (fig 40, c). Additional PHD3 signal was detected in smaller, TH lacking cell types (fig 40, c arrows). (Representative of 3 immunostains)

Additional punctate PHD3 staining was noted in-between sympathetic neurons and counter stained sections demonstrated that this arose from the nuclei of small cells scattered between larger sympathetic neurons (fig 41). This finding indicated that although the vast majority of PHD3 signal arose from sympathetic lineage SCG cell types, additional PHD3 expressing non-sympathetic lineage cell populations were also present. Further studies will be necessary to characterise these cell types.

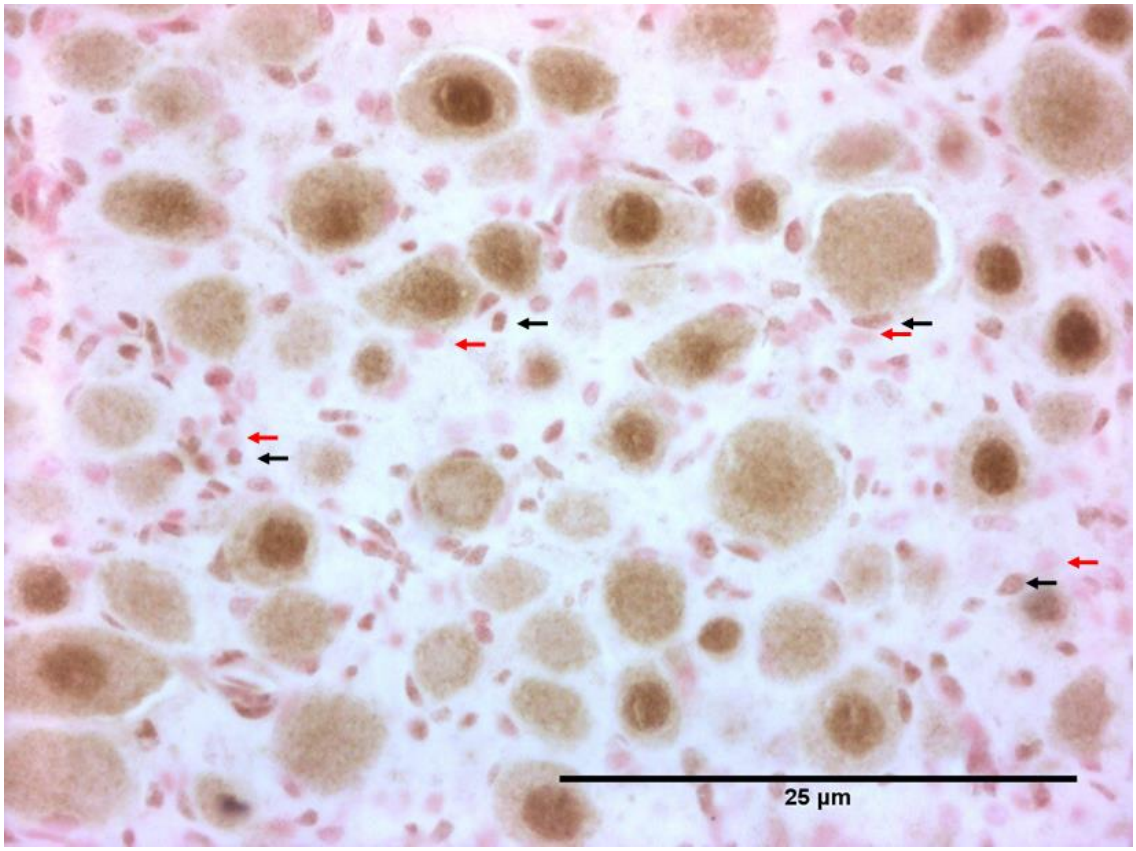


Figure 41. SCG stained with PHD3 and counterstained with nuclear fast red

SCG sections were stained for PHD3 with antibody 188e and DAB chromogen before Counter staining with nuclear fast red. Large PHD3 expressing sympathetic neurons were noted (fig 41). Counter staining also demonstrated additional clusters of smaller nuclei scattered between sympathetic neurons, some of which stained with nuclear fast red alone (red arrows), while others stained with nuclear fast red and PHD3 (black arrows). (Representative of 2 immunostains).

PHD3 expression in adult sympathetic neurons of the SCG was therefore confirmed. Its expression in other elements of the adult sympathetic nervous system was next assessed.

5.2.4 Characterising PHD3 expression in the adult rat carotid body

The small size of the carotid body, another key element of the sympathetic nervous system, meant that it was not amenable to immunoblot analysis in the same way as the SCG. Therefore an immunohistochemical approach was chosen to characterise its expression of PHD3. The tissue blocks used to characterise PHD3 in the SCG were carefully generated to incorporate rat carotid body allowing carotid body and SCG PHD3 signal to be simultaneously studied.

Tyrosine hydroxylase is known to be expressed in oxygen sensing type 1 cells of the carotid body (Czyzyk-Krzeska et al., 1992), and double staining for TH and PHD3 demonstrated co-localisation of signal to clusters of cells within the carotid body (fig 40, fig 42). The expression of PHD3 in oxygen sensing cells of the carotid body also provided a potentially important link between molecular and physiological oxygen sensing. As in the SCG, punctate PHD3 staining was also noted in non-sympathetic lineage carotid body cell types (fig 42). The identity of these cells remains unknown.

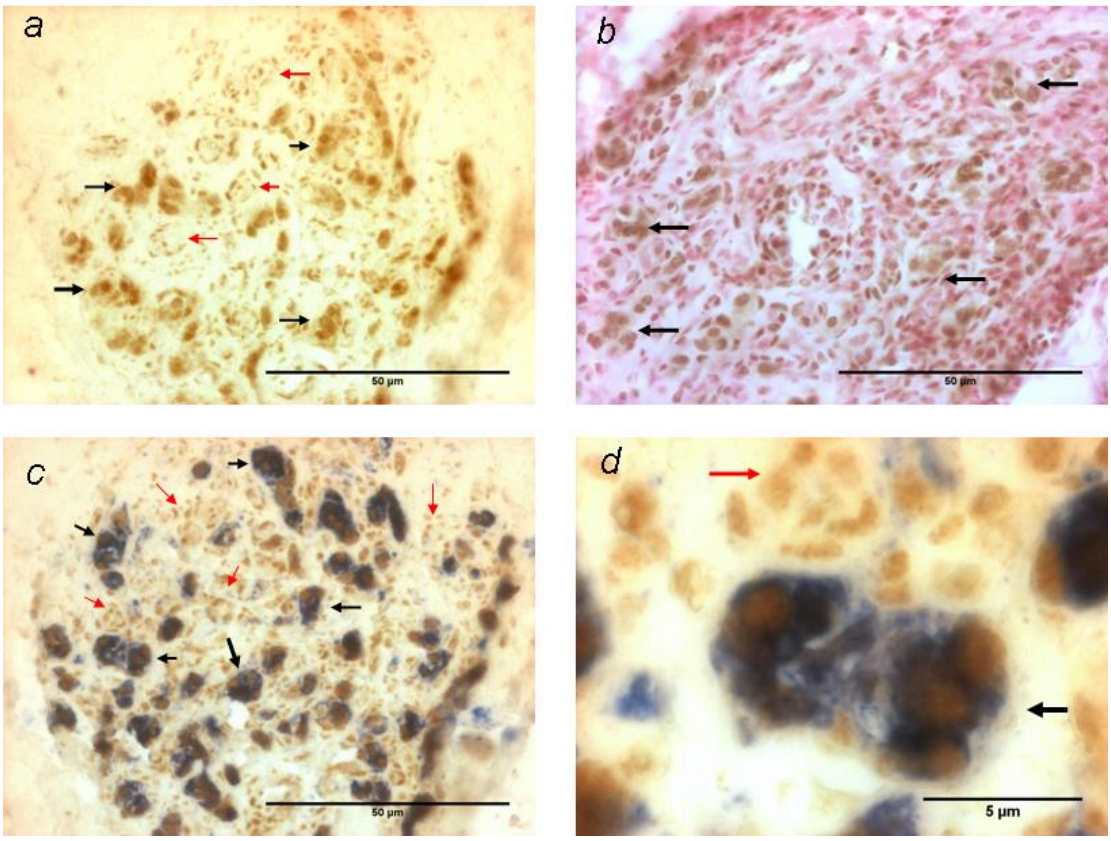


Figure 42. Characterising the expression of PHD3 in the adult rat carotid body

PHD3 immunostaining with DAB chromogen demonstrated diffuse (black arrows) and punctate (red arrows) staining within the carotid body (fig 42, a). A serial section stained for PHD3 and counterstained with nuclear acid red demonstrated that the diffuse PHD3 staining noted before originated from cell clusters (fig 42, b, black arrows). Furthermore counterstaining also demonstrated that the previously noted punctate staining originated from cell nuclei (fig 42, b, dark-pink stain). Nuclei which lacked PHD3 stain were also present (fig 42, b, light-pink stain). Double immunostaining for PHD3 with antibody 188e (DAB chromogen) and TH (vector blue chromogen) demonstrated that the majority of cell clusters which diffusely stained PHD3 also expressed TH (fig 42, c, black arrows). TH stain did not co-localise with punctate PHD3 stain (fig 42, c, red arrows). High power magnification of a double stained cell cluster confirmed that PHD3 was present in type I cells (fig 42, d, black arrow). In this cluster, PHD3 was strongly expressed within type I cell nuclei. Punctate PHD3 staining was also noted in non-sympathetic lineage cell types (fig 42, d, red arrow). A negative control section stained with an isotype matched antibody and normal rabbit serum is shown in figure 40, b. (Representative of 2 immunostains).

5.2.5 Characterising PHD3 expression in the adult rat adrenal gland

PHD3 immunostaining of whole adrenal gland sections with two anti-PHD3 antibodies, 188e and NB100-303 demonstrated staining which localised to the centre of the gland (fig 43). This suggested that PHD3 was likely to be expressed in the adrenal medulla, however the possibility remained that it was also expressed in more central regions of the adrenal cortex. In order to address this possibility, co-localisation studies with PHD3 and TH were carried out and will be described in the next section. In order to standardise signal, sections of rat SCG were immunostained in parallel with sections of adrenal tissue.

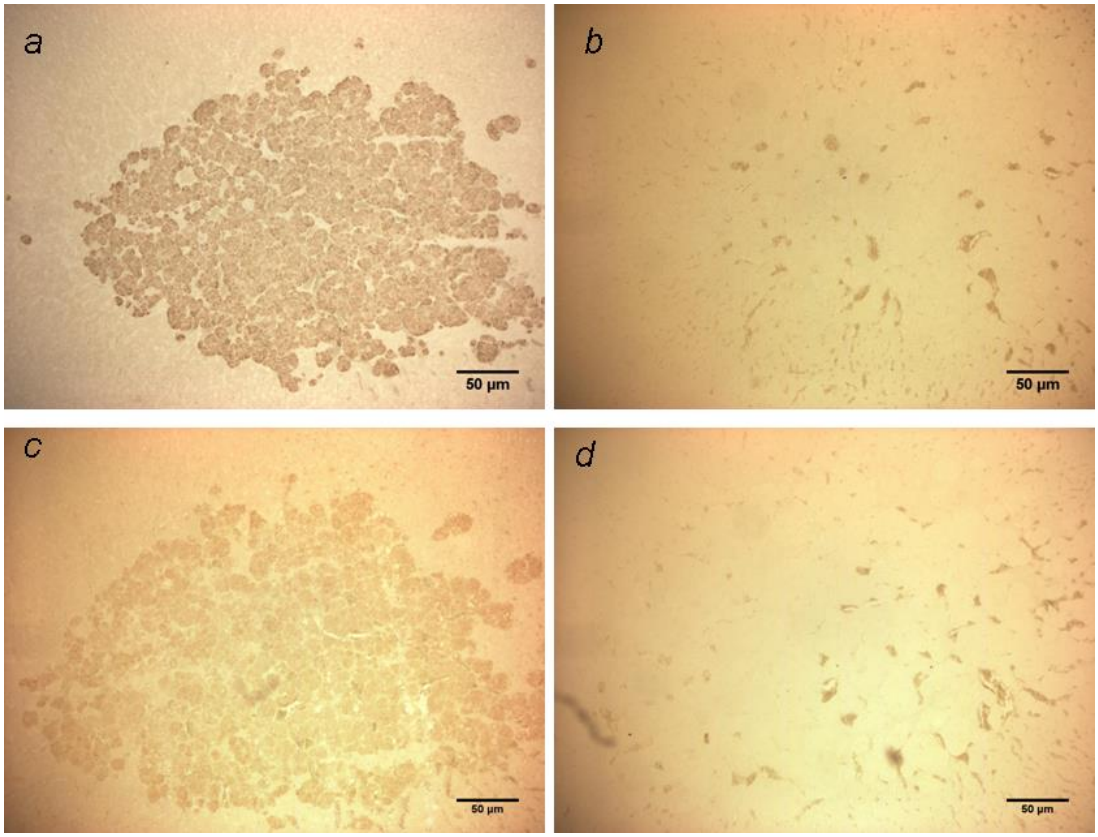


Figure 43. PHD3 immunostaining of the adrenal gland with two anti-PHD3 antibodies

Immunostaining for PHD3 with antibody 188e and DAB chromogen indicated staining towards the centre of the adrenal gland (fig 43, a, dark brown region). No staining was detected in a serial section stained with an isotype matched IgG1 Kappa control antibody directed against Trinitrophenol (fig 43, b). A serial section immunostained with the rabbit polyclonal antibody to PHD3, NB100-303 produced a weaker but similar pattern of staining (fig 43, c). No significant staining was detected in a serial section stained with normal rabbit serum (fig 43, d). (Representative of 3 immunostains).

The adrenal medulla contains TH expressing chromaffin cells. To determine if PHD3 was expressed in chromaffin cells, double immunostaining for PHD3 and TH was carried out. This demonstrated co-localisation of PHD3 and TH signal to the same cell population (fig 44), confirming that PHD3 was expressed in adrenal medullary chromaffin cells. In contrast PHD3 appeared to be virtually absent from adrenal cortical cells (fig 44). Immunostaining also suggested that chromaffin cells of the adrenal medulla contrasted with those of the SCG by expressing predominantly cytoplasmic as opposed to nuclear PHD3.

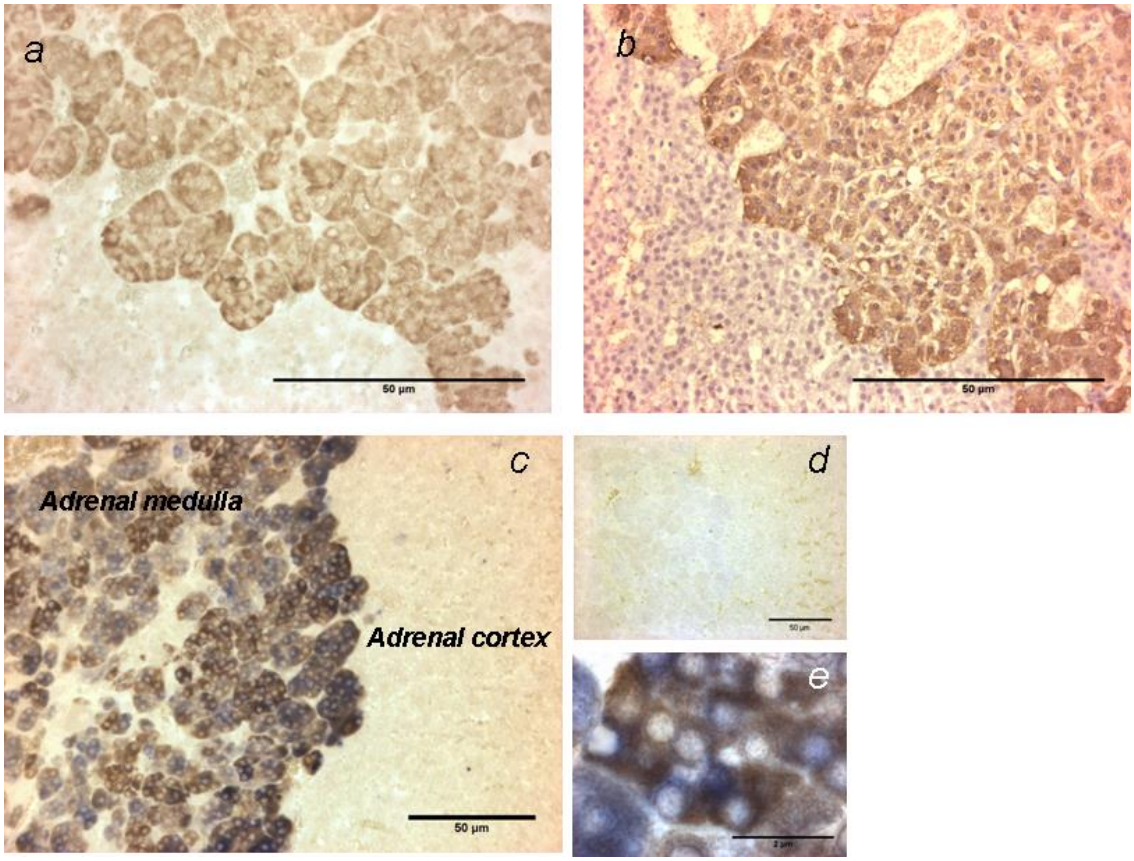


Figure 44. Characterising the expression of PHD3 in the adult rat adrenal gland

PHD3 immunostaining with antibody 188e and DAB chromogen demonstrated a 'halo' type staining pattern with brown DAB stain surrounding a central areas of pallor (fig 44, a). A serial section stained for PHD3 and counter stained with haematoxylin demonstrated that these regions of central pallor represented cell nuclei indicating that PHD3 was expressed predominantly in the chromaffin cell cytoplasm (fig 44, b). Double staining for PHD3 (DAB chromogen) and TH (vector blue chromogen), demonstrated that PHD3 was expressed in the adrenal medulla and was virtually absent from the adrenal cortex (fig 44, c). A control slide stained with isotype matched antibody and isotype matched antibody with vector blue and DAB chromogens demonstrated no significant staining (fig 44, d). Double stained sections at higher power demonstrate co-localisation of PHD3 to the majority of TH expressing cells, indicating that PHD3 was expressed in adrenal chromaffin cells (fig 44, e). (Representative of 3 immunostains).

5.3 Assessing the subcellular expression of PHD3 in different sympathetic lineage cell populations of the adult rat

Although care was taken to ensure that each set of tissues immunostained was derived from the same perfusion fixed animal, and duplicate sets demonstrated comparable staining, the possibility remained that systematic errors could account for the differences in subcellular PHD3 distribution observed between sympathetic neurons and adrenal chromaffin cells. For example, difference in fixative flow rates, cell to vessel distance, permeability of connective tissue to fixative, as well as differences in size of neurons compared to chromaffin cells had the potential to lead to systematic errors sufficient to artefactually produce the subtle difference in subcellular staining observed.

One approach to circumvent these potential confounders was to compare signal between cells of a single tissue; ideally between adjacent cell groups. In this respect, approximately 5% of the adrenal medulla is known to consist of sympathetic neurons (Tomlinson et al., 1987) and this provided an approach to enable direct signal comparison to be carried out.

The rat adrenal gland was finely sectioned and alternate adrenal medullary slides stained for TH. Each TH stained section was visualised under light microscope to identify scattered sympathetic neurons and the next tissue section immunostained for PHD3. In keeping with earlier results, PHD3 signal from chromaffin cells was predominantly cytoplasmic, while that of adrenal medullary sympathetic neurons was predominantly nuclear (fig 45).

Using this approach it became apparent that there were genuine differences in the subcellular staining pattern of PHD3 between different sympathetic lineage cell populations, both within and between sympathetic nervous system tissues.

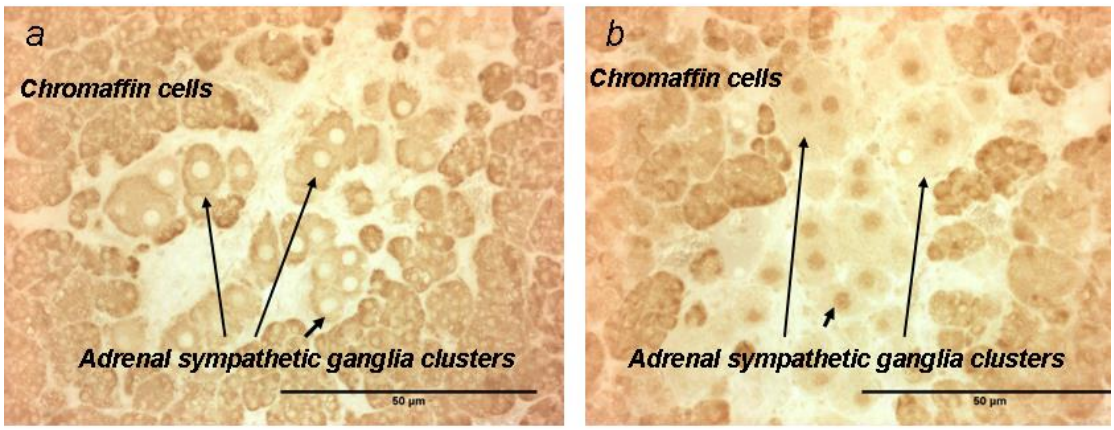


Figure 45. Differences in the subcellular distribution of PHD3 within chromaffin cells and sympathetic ganglia of the adrenal medulla

TH stain with DAB chromogen identified scattered sympathetic ganglia of the adrenal medulla, surrounded by adrenal chromaffin cells (fig 45, a). The next section in the series was immunostained for PHD3 and demonstrated differences in the subcellular distribution of PHD3 between adrenal medullary sympathetic neurons and chromaffin cells (fig 45, b). PHD3 was predominantly expressed in the cytoplasm of chromaffin cells, while being predominantly nuclear in adrenal medullary sympathetic neurons. (Representative of 3 immunostains).

5.4 Characterising the expression of PHD3 in extra-adrenal chromaffin cells

Populations of extra-adrenal chromaffin cells are also known to exist. The largest of these is the organ of Zukerkandle which constitutes a cluster of chromaffin cells located at the aortic bifurcation which acts as a source of catecholamines in the developing rat (Langercrantz and Marcus, *Prenatal and neonatal physiology*, Saunders 1992). Other clusters of extra-adrenal chromaffin cells, termed 'paraganglia' are recognised and located predominantly adjacent to large blood vessels particularly of the neck (Böck. P, *The paraganglia*, Springer, 1982.). All extra adrenal chromaffin cells undergo atrophy as animals' mature (Coupland R, *The Natural History of the Chromaffin cell*, Longmans, 1965) and therefore are not readily detectable in adult animals. Extra-adrenal chromaffin cells therefore need to be studied in developing tissues and during this doctoral study, neck paraganglia of the P2 rat were identified and their PHD3 expression studied (fig 46). P2 rat sections incorporating SCG and carotid body were identified and alternate sections in the series stained for PHD3. Using this approach it became clear that unlike other sympathetic lineage tissues, extra-adrenal chromaffin cell populations expressed very little PHD3.

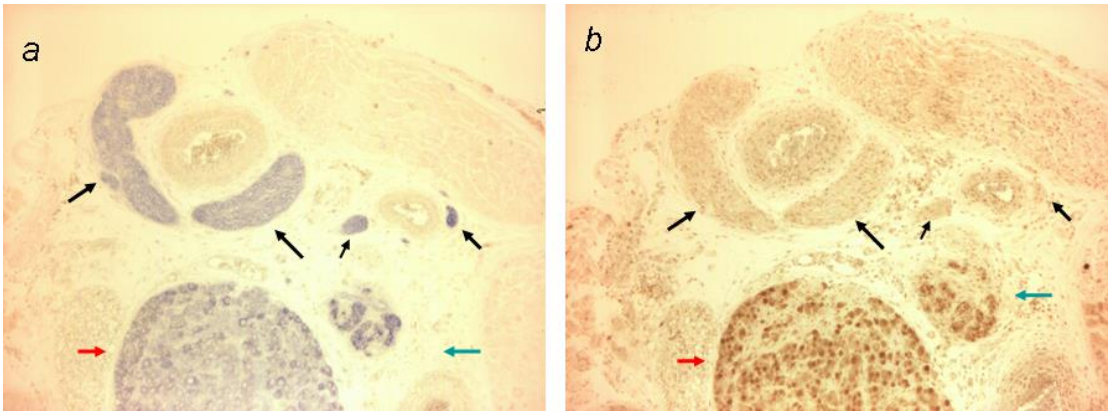


Figure 46. Characterising the expression of PHD3 in developing paraganglia of the P2 rat

Paraganglia of the P2 rat were identified by their anatomical position adjacent to large vessels and positive immunostaining for TH (vector blue chromogen), (fig 46, a, black arrows). The SCG and CB were also noted in the same tissue section (fig 46, a, red and blue arrows respectively). Immunostaining of alternate sections in the series demonstrated that PHD3 was present in the SCG and carotid body but not in paraganglia of the P2 rat (fig 46, b). (Representative of 3 immunostains).

Chapter 6. Establishing if neuronal populations apart from those of the sympatho-adrenal axis also expressed PHD3

6.1 Expression of PHD3 in non-sympathetic ganglia of the peripheral nervous system

In order to determine the relative expression of PHD3 in different neuronal tissues of the adult peripheral nervous system, PHD3 expression in the nodose and trigeminal ganglia were next assessed.

6.1.1 Characterising the expression of PHD3 in the nodose ganglion

The nodose ganglion forms part of the parasympathetic nervous system receiving sensory visceral afferents mainly from the heart, pharynx and upper intestine. PHD3 immunostaining of rat nodose ganglion sections demonstrated strong nuclear and weaker cytoplasmic neuronal staining (fig 47). Further punctate PHD3 staining was also noted to be present in nodose cells. The nodose ganglion is also known to contain scattered tyrosine hydroxylase expressing neuronal populations (Katz et al., 1983; Kummer et al., 1990). Double staining for PHD3 and TH demonstrated that PHD3 was also expressed in these nodose cells (fig 47).

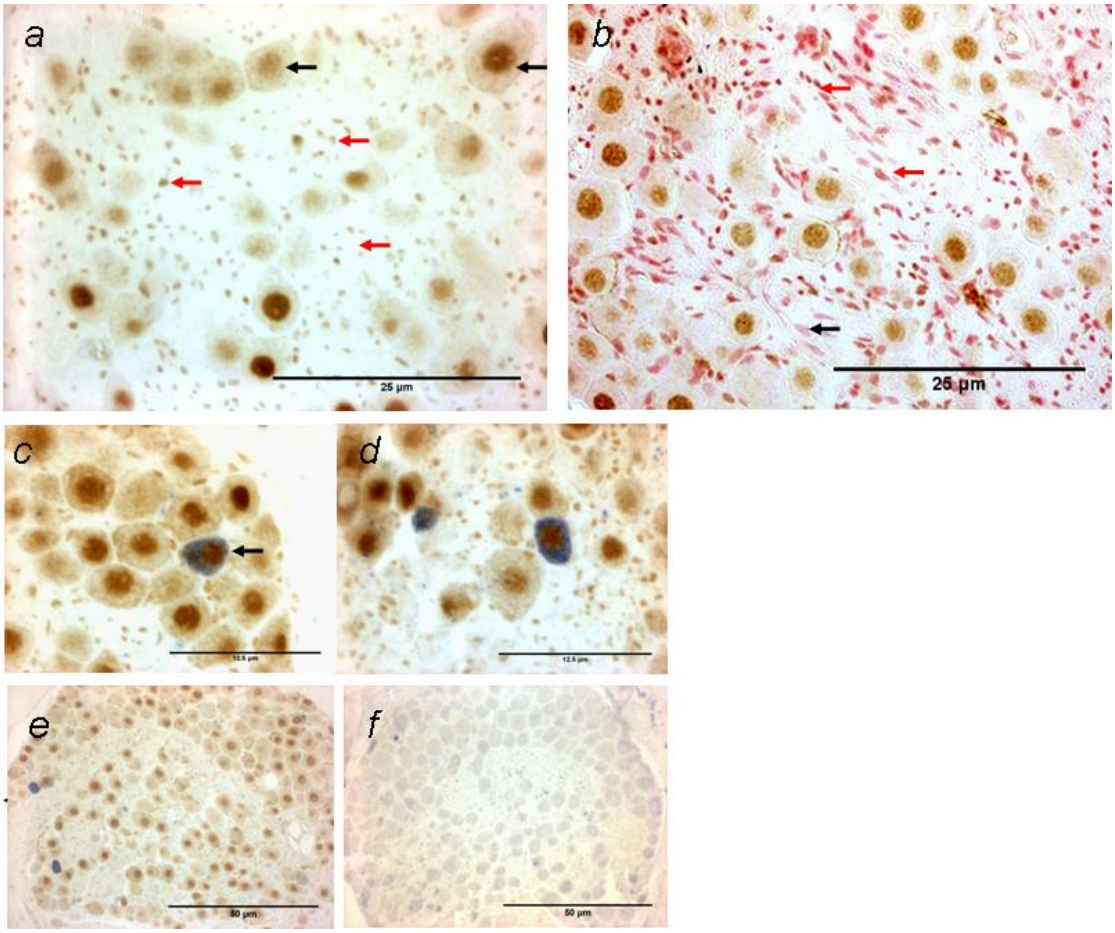


Figure 47. Characterising the expression of PHD3 and TH in adult rat nodose ganglia

Immunostaining for PHD3 with the mouse monoclonal antibody 188e and DAB chromogen demonstrated signal in the nodose ganglia (fig 47, a). PHD3 was strongly expressed in the nuclei of nodose neurons (fig 47, a, black arrows). Weaker PHD3 stain was noted in the cytoplasm of these neurons. Punctate PHD3 staining was noted between these neurons (fig 47, a, red arrows). Serial sections stained for PHD3 and counterstained with nuclear acid red demonstrated that the punctate stain originated from the nuclei of stromal cells (47, b, red arrow). Not all stromal cell nuclei expressed PHD3, as indicated by light pink stain produced by nuclear red stain alone (fig 47, b, black arrow). Double immunostaining with PHD3 (DAB chromogen) and TH (vector blue chromogen) demonstrated scattered TH expressing neurons within the nodose ganglia (fig 47, c & d, black arrows). Low power images of nodose

ganglion double stained for PHD3 and TH (fig 47, e). A further nodose section double stained with normal rabbit serum and IgG1 Kappa antibody to Trinitrophenol, served as a double negative control and demonstrated no significant staining (fig 47, f). N=3.

6.1.2 Characterising the expression of PHD3 in the trigeminal ganglion

PHD3 immunostaining also demonstrated that it was expressed in the trigeminal ganglion (fig 48). As in the SCG and nodose ganglion, PHD3 was detected predominantly in the nuclei of TG neurons.

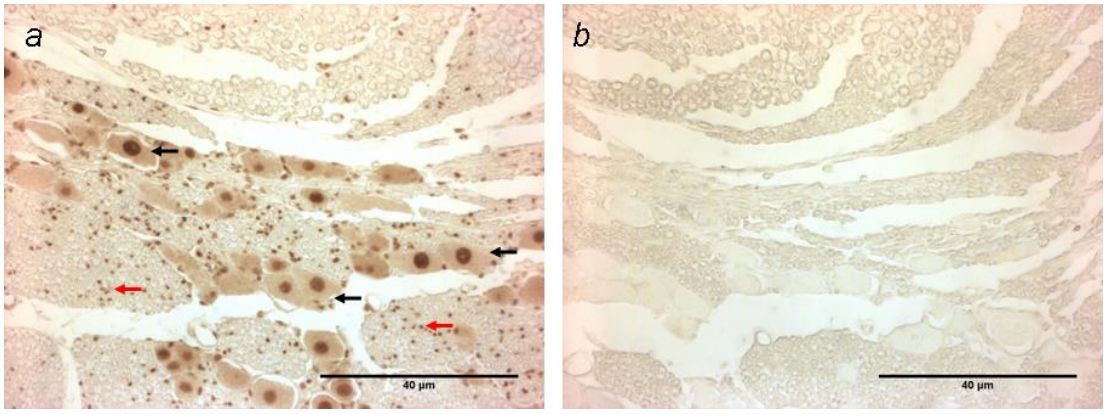


Figure 48. Characterising the expression of PHD3 in rat trigeminal ganglion (TG)

PHD3 immunostaining with antibody 188e and DAB chromogen demonstrated scattered TG neurons which expressed strong nuclear and weaker cytoplasmic PHD3 staining (Fig 48, a, black arrows). Punctate staining was also noted (fig 48, a, red arrows). A negative control TG section immunostained with an IgG1 Kappa antibody against Trinitrophenol showed no significant staining (fig 48, b). (Representative of 3 immunostains).

6.1.3 Characterising the expression of PHD3 in the dorsal root ganglion

Next the expression of PHD3 in rat dorsal root ganglia (DRG) was assessed. Because dorsal root ganglia are deep seated structures in close association with dense muscle groups and bony vertebrae, extracting them intact from adult rats proved technically challenging. In contrast the softer, less dense tissues of the P2 rat were more amenable to dissection allowing intact dorsal root ganglia to be obtained and immunostained for PHD3 (fig 49). Virtually no PHD3 was expressed in P2 rat dorsal root ganglia.

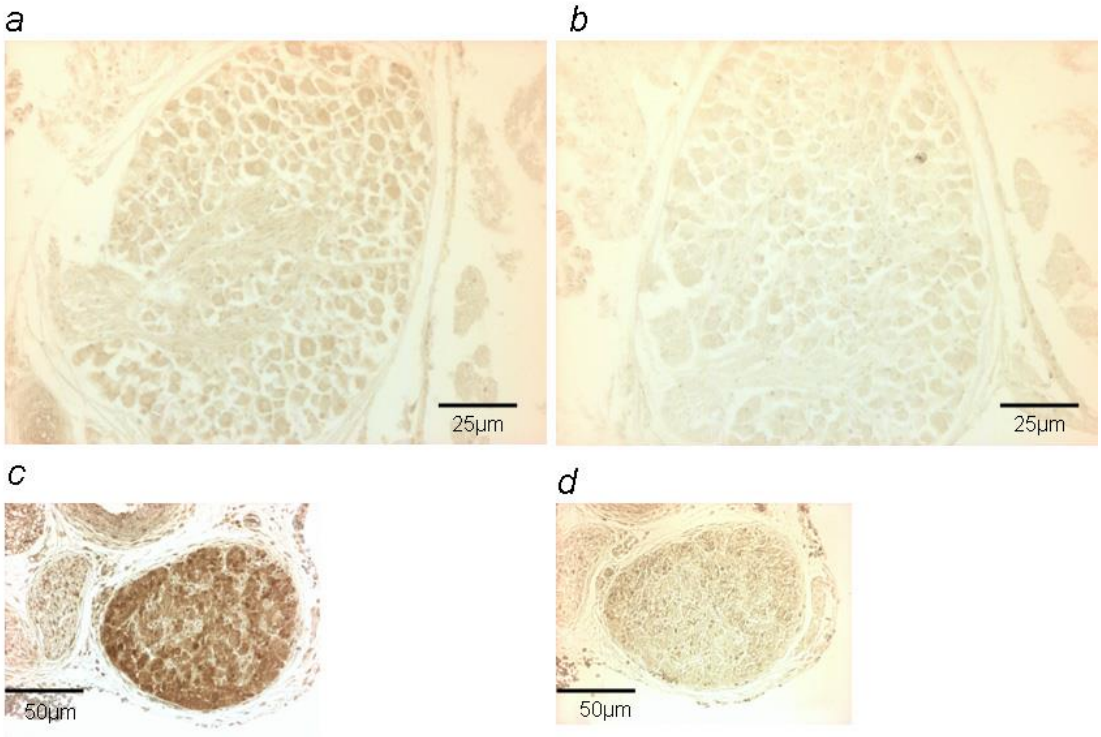


Figure 49. Characterising the expression of PHD3 in the P2 rat dorsal root ganglia (DRG)

P2 rat DRG demonstrated virtually no PHD3 signal using antibody 188e (fig 49, a), which contrasted with the strong signal detected in P2 rat SCG positive control sections stained with the same antibody (fig 49, c). No signal was detected in DRG and SCG sections stained with an isotype matched negative control antibody to Trinitrophenol (fig 49, b and d respectively). (Representative of 3 immunostains).

6.2 Relative PHD3 abundance in sympathetic and non-sympathetic rat ganglia

The small size of many nervous system ganglia precluded sufficient extract being generated for immunoblot; however, the semi-quantitative immunohistochemical approach used in this study, whereby SCG section standards were immunoblotted alongside those of respective nervous system tissues, allowed IHC signal from different tissues to be compared. Using this approach, nuclear and cytoplasmic PHD3 signal from each cell population was quantified using ImageJ software and average signal from 10 cells graphically represented (fig 50). PHD3 was found to be similarly expressed in the nuclei of sympathetic neurons of the SCG, sympathetic neurons of the adrenal medulla, type 1 cells of the carotid body (CB), visceral sensory neurons of the nodose ganglion (NG) as well as somatic sensory neurons of the trigeminal ganglion (TG). In contrast virtually no PHD3 could be detected in the nuclei of adrenal chromaffin cells.

The abundance of cytoplasmic PHD3 appeared more variable between different peripheral nervous system populations. Chromaffin cells expressed more cytoplasmic PHD3 compared to other cell types while nodose ganglion neurons expressed relatively less. The cytoplasmic PHD3 content of sympathetic neurons of the SCG, sympathetic neurons of the adrenal medulla, type 1 cells of the CB and somato-sensory neurons of the TG, were similar.

The small size of P2 rat paraganglia and DRG did not allow signal from individual subcellular compartments to be quantified; however, as previously described these tissues appeared to express virtually no PHD3 at least at this developmental time-point.

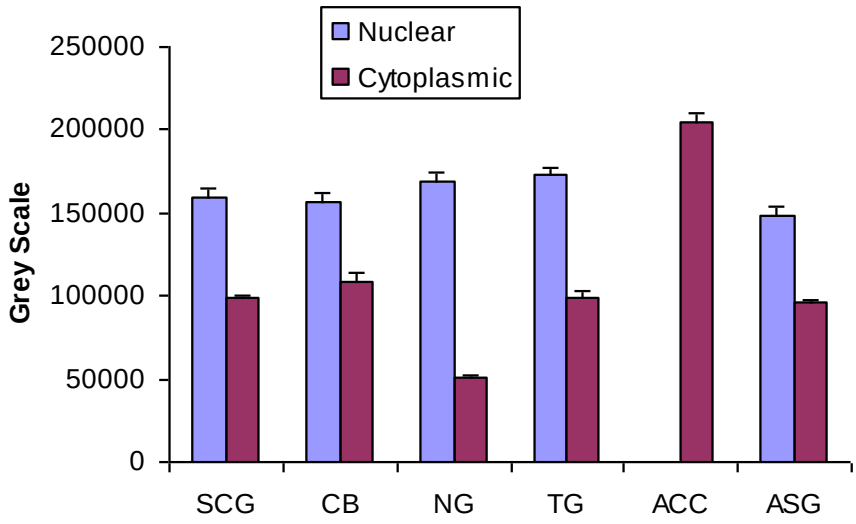


Figure 50. Relative expression of PHD3 in tissues of the adult rat peripheral nervous system

Semi-quantitative PHD3 immunostaining of the peripheral nervous system was carried out using SCG sections as standards. Nuclear and cytoplasmic PHD3 signal was compared between rat superior cervical ganglion (SCG); carotid body (CB); nodose ganglion (NG); trigeminal ganglion (TG); adrenal chromaffin cells (ACC) and adrenal sympathetic ganglia (ASG).

6.3 Characterising the expression of PHD3 in the CNS

In contrast to the peripheral nervous system, PHD3 immunostaining of the CNS could only be reliably carried out with antibody NB100-303. This was because the monoclonal antibody to PHD3 (188e), while producing good signal in the peripheral nervous system, resulted in extensive non-specific staining in the cerebellum (fig 51). Factors apart from the ability of antibody 188e to recognise PHD3 were responsible for this cerebellar signal. Such factors may include an interaction between cerebellar tissue and regions of antibody 188e not critical in antigen recognition or interaction. The possibility of similar interaction with other CNS tissues became a genuine concern and it was therefore decided not to use antibody 188e for further CNS staining. In the absence of a third anti-PHD3 antibody capable of detecting PHD3 in rat tissues, CNS immunostaining was carried out with only antibody NB100-303.

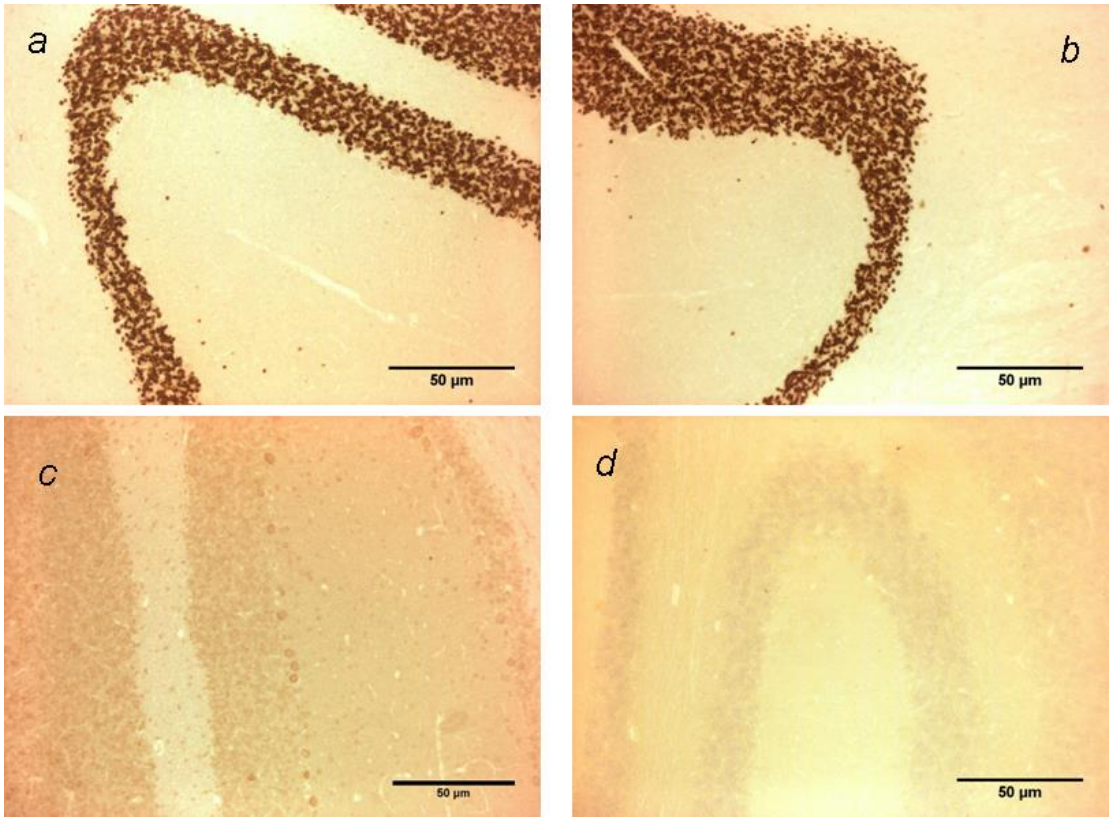


Figure 51. Strong cross-reactive signal with the mouse monoclonal antibody 188e in adult rat CNS tissues

Immunostaining of adult rat cerebellum sections with 188e (fig 51, a) and isotype matched antibody control to Trinitrophenol (fig 51, b) demonstrated identical staining patterns. In contrast, NB100-303 did not produce any significant cerebellar signal (fig 51, c). No significant staining was observed with a normal rabbit serum control (fig 51, d). (Representative of 3 immunostains).

Immunostaining demonstrated that antibody NB100-303 produced a generally low level of signal throughout the brain which in most regions was not clearly discernible from that produced by sections stained with normal rabbit serum. Given this subtle difference between NB100-303 and its control, a number of measures were used to optimise CNS signal. These included increasing the duration and number of washes between primary and secondary antibody as well as increasing the duration of avidin and biotin blocks. The endogenous brown colour of some brain tissue sections was also found to impact on signal resolution, particularly when brown DAB chromogen was used. In this respect, the use of vector blue chromogen helped to improve signal resolution.

6.3.1 Characterizing the expression of PHD3 in tyrosine hydroxylase expressing cell populations of the CNS

Given the role of PHD3 in sympathetic lineage cell types, particular emphasis was placed on identifying and characterising PHD3 expression within TH expressing CNS cell populations. Predefined anatomical coordinates (Rat Brain Atlas, Paxinos and Watson) and TH immunostaining were used to identify the substantia nigra, locus coeruleus (LC), ventro-lateral (A1C1) and dorso-medial (A2C2) nuclei of the brain stem.

6.3.1.1 PHD3 expression in the substantia nigra

Double staining for TH and PHD3 demonstrated that PHD3 was expressed in the substantia nigra (fig 52). In the substantia nigra, some cell populations expressed both TH and PHD3 while others expressed TH alone (fig 52, fig 53). These differences were detectable in cell populations directly adjacent to one another as observed more clearly at higher magnification (fig 53).

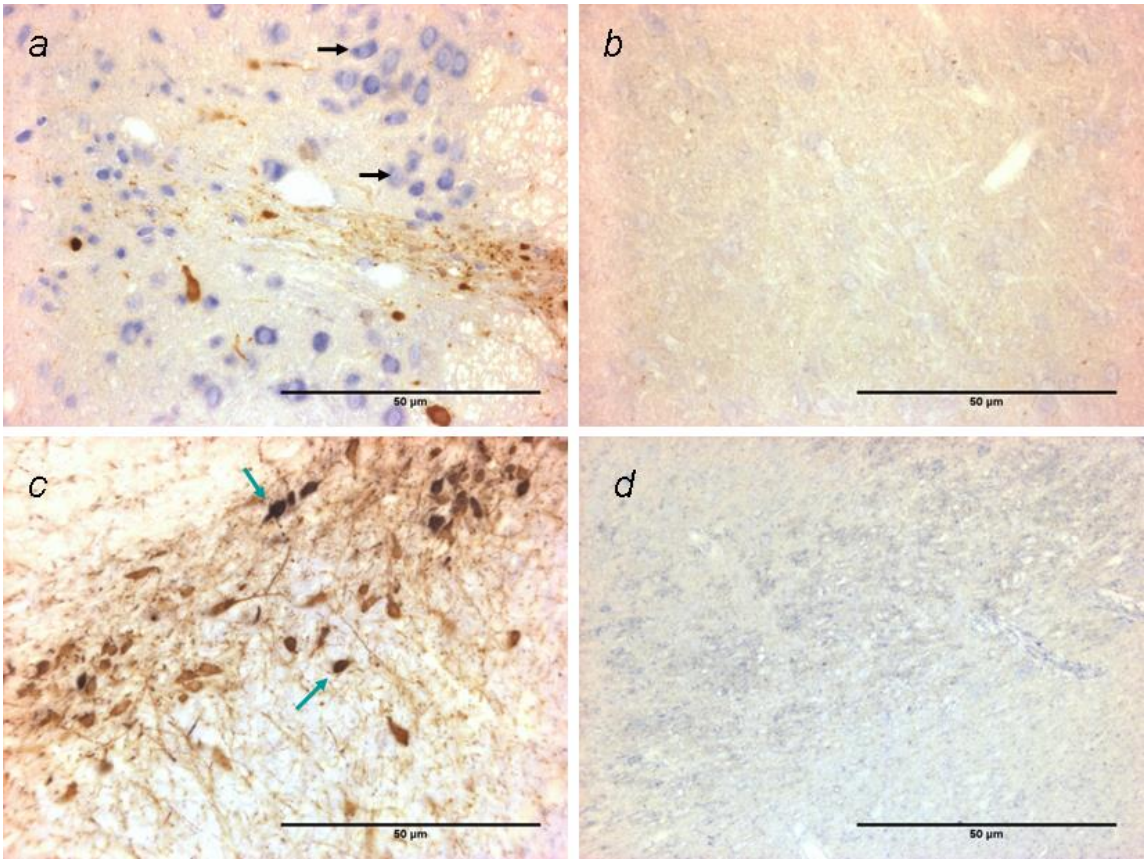


Figure 52. Expression of PHD3 in the adult rat substantia nigra

Double staining for PHD3 (NB100-303 antibody and vector blue chromogen) and TH (TH mouse monoclonal antibody and DAB chromogen), demonstrated the presence of PHD3 within the substantia nigra. Towards the medial boarder of the substantia nigra, cell populations expressed PHD3 (fig 52, a, black arrows). No significant staining was noted in sections double stained with normal rabbit serum and isotype matched antibody (fig 52, b). Towards the centre of the substantia nigra PHD3 appeared to be co-expressed with some TH expressing cells as indicated by cells staining black (fig 52, c blue arrows), and was more evident at higher power magnification as will be shown next. No significant staining was noted in the double negative control slide (fig 52, d). (Representative of 3 immunostains).

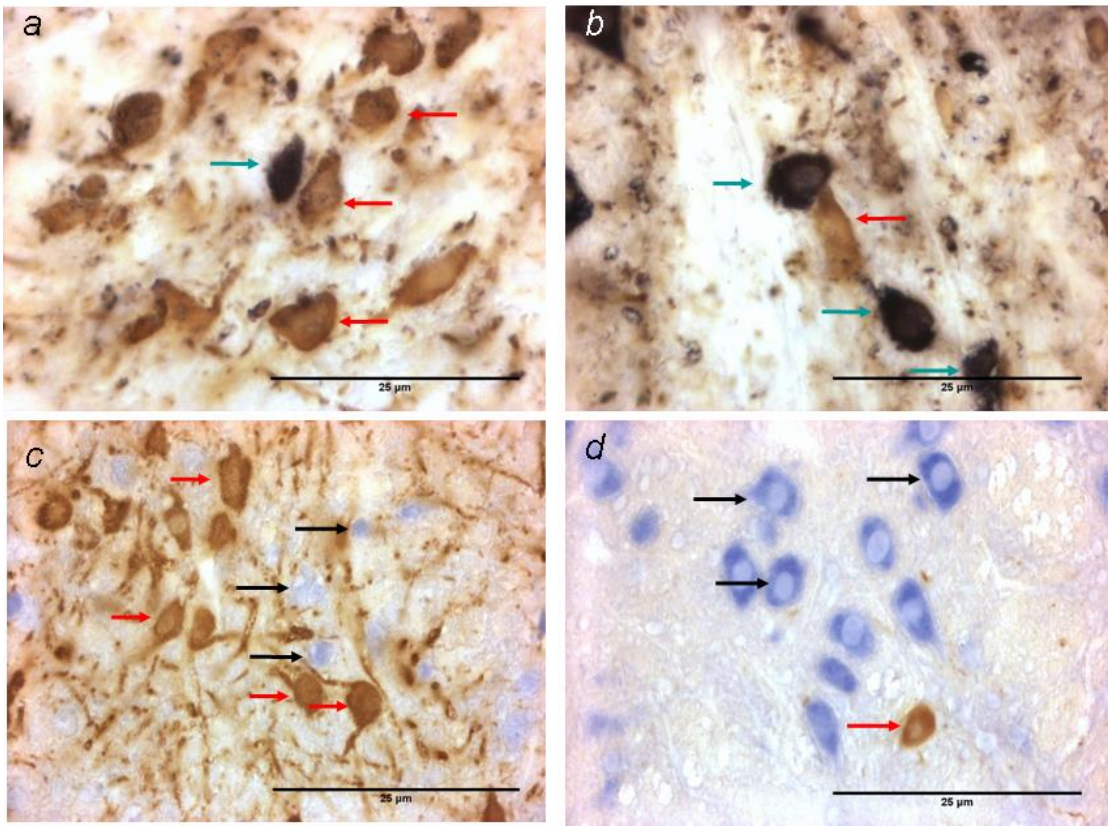


Figure 53. Characterising the expression of PHD3 in the adult rat substantia nigra

Higher power magnification demonstrated more regional differences in the expression of PHD3 in the substantia nigra. Towards its centre, PHD3 was co-expressed with TH in some but not all cells (fig 53, a and b, blue arrows). Cells expressing TH alone were also present in this region (fig 53, a and b, red arrows). PHD3 and TH were expressed in separate cell types in the lateral region of the substantia nigra {fig 53, c, black arrow (PHD3); red arrow (TH)}. At its lateral border, PHD3 and TH were also expressed separately {fig 53, d, black arrow (PHD3); red arrow (TH)}. Double negative control slides are depicted in fig 52.

6.3.1.2 Assessing PHD3 expression in other CNS sympathetic lineage cell types

Next, the expression of PHD3 in other TH expressing regions of the brain was assessed. In contrast to the substantia nigra, PHD3 was not detected in the locus coeruleus (LC), A1C1 or A2C2 catecholamine expressing regions (fig 54). The ventro-lateral medulla is known also to contain the pre-Botzinger complex, a region essential for generating mammalian respiratory rhythm (Smith et al., 1991) and known to express the HIF-1 target gene erythropoietin and its receptor (EPO-R) (Soliz et al., 2005) giving rise to the possibility that HIF-1 and its regulatory proteins may play a role in this region. The pre-Botzinger complex was identified by immunostaining for substance P, as previously described (Soliz et al., 2005) but did not express PHD3 (fig 54).

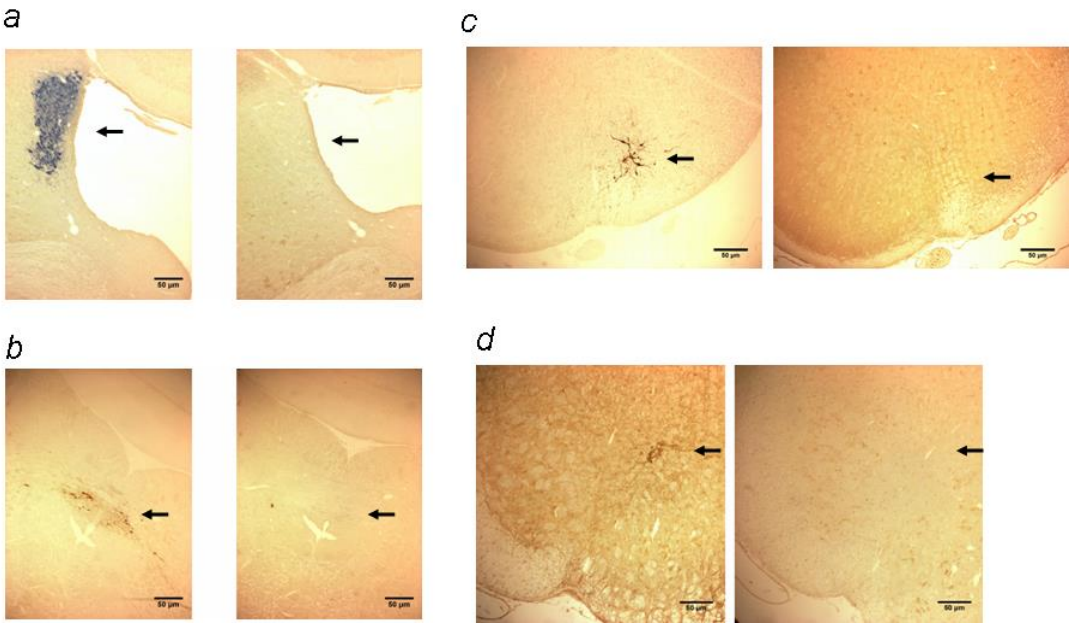


Figure 54. Absence of PHD3 from catecholamine producing brain stem regions (LC, A1C1, A2C2) and Pre-Botzinger complex

The locus coeruleus was immunostained with TH and vector blue chromogen (fig 54, a, left panel, arrow). Immunostaining of serial sections with anti-PHD3 rabbit polyclonal antibody, NB100-303 and DAB chromogen failed to demonstrate any signal in the LC (fig 54, a, right panel, arrow). A1C1 and A2C2 brain stem nuclei were identified by anatomical position and TH stain with DAB chromogen (fig 54, b, left panel, arrow; fig 54, c, left panel, arrows). PHD3 was not detected on serial sections (fig 54, b, right panel, arrow; fig 54, c, right panel, arrow). The Pre-Botzinger complex was identified by substance P stain with DAB chromogen (fig 54, d, left panel, arrow), and serial sections stained for PHD3 also did not demonstrate any significant signal (fig 54, d, right panel, arrow). (Representative of 2 immunostains).

6.3.2 PHD3 expression in other regions of the CNS

6.3.2.1 PHD3 expression in the trigeminal and facial cranial nuclei

Other regions of the brain were also surveyed, and PHD3 signal was identified in the fifth (trigeminal) and seventh (facial) cranial nerve nuclei, where double staining with a neuronal marker (NeuN) confirmed this signal arose from neuronal as well as glial cells (fig 55).

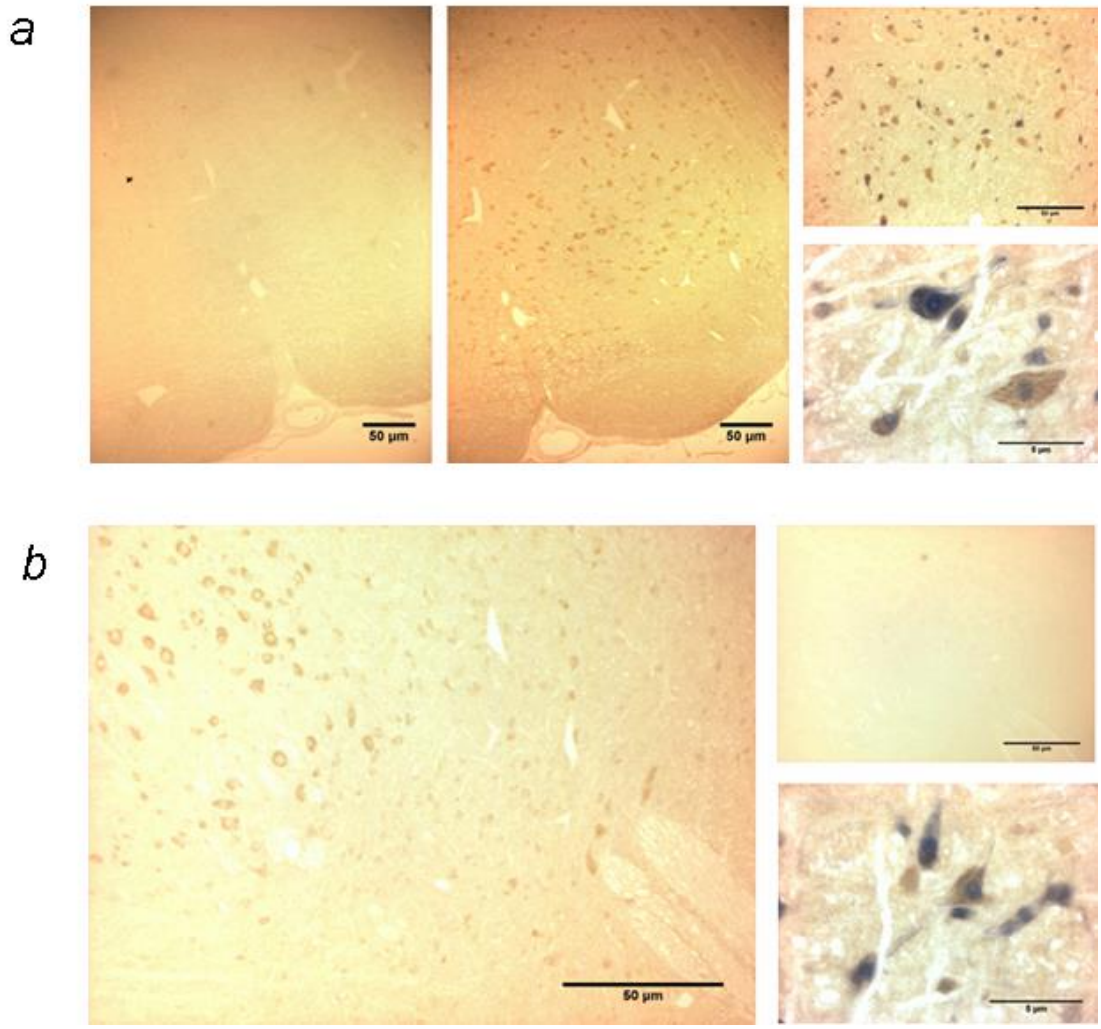


Figure 55. Expression of PHD3 in regions of the trigeminal and facial cranial nerve nuclei

PHD3 immunostain of the trigeminal cranial nerve nucleus with NB100-303 and DAB chromogen demonstrated staining of scattered cell types (fig 55, a, middle panel). No significant signal was detected on a serial section stained with normal rabbit serum (fig 55, a, left panel). Double staining of serial sections with the neuronal marker NeuN (vector blue chromogen) and PHD3 (DAB chromogen) demonstrated PHD3 was expressed in neuronal rather than glial cell types (fig 55, a, right panel - low and high power magnification). PHD3 was also detected in the facial cranial nerve nucleus with NB100-303 and DAB chromogen (fig 55, b left panel). No signal was detected with normal rabbit serum control (fig 55, b right upper panel). Double staining with NeuN (vector blue chromogen) and PHD3 (DAB chromogen) also demonstrated that PHD3 was expressed in CNS neuronal populations (fig 55, b right, lower panel). (Representative of 2 immunostains).

6.3.2.2 PHD3 expression in the hippocampus

PHD3 was found to be regionally expressed in the hippocampus (fig 56). Immunostain demonstrated PHD3 signal in cortical area (CA) 1, 2 and dentate with less signal in CA3. The hippocampus has a central role in learning, memory and behaviour. The role of PHD3 in such processes was assessed by a series of psychometric studies as will be described later in the results section of this thesis.

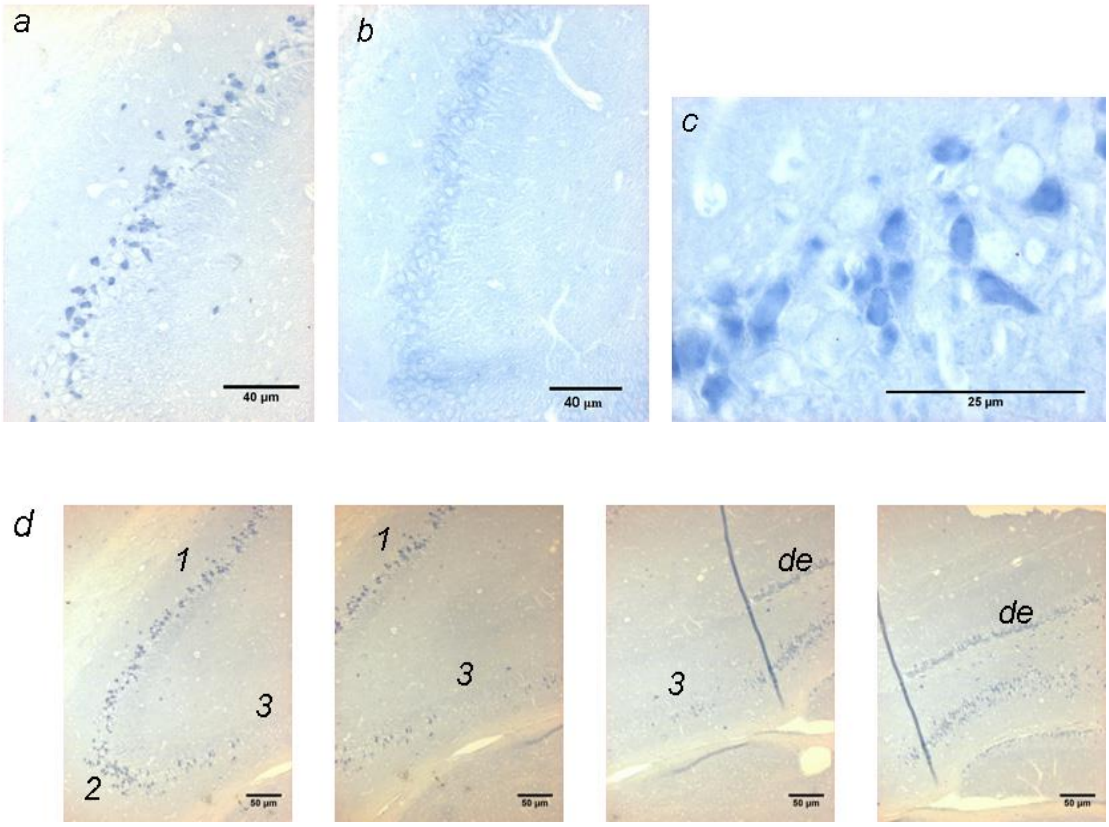


Figure 56. PHD3 expression in the adult rat hippocampus

PHD3 immunostaining with NB100-303 and vector blue chromogen demonstrated distinct signal in the hippocampus (fig 56, a), which was significantly more and different in distribution to that noted on a slide stained in parallel with normal rabbit serum (fig 56, b). High power magnification demonstrated heterogeneous PHD3 expression within hippocampal cells (fig 56, c). PHD3 was detected in CA1 (1), CA2 (2) and dentate (de) regions but not in CA3 (3). (Representative of 2 immunostains).

These finding indicated that unlike in the peripheral nervous system, there were relatively few CNS TH expressing cell populations which co-expressed PHD3. PHD3 was detected only in scattered TH positive cell populations of the substantia nigra, which gave rise to the possibility that it may have a role in neuro-degenerative disorders such as Parkinson's disease. Indeed, its expression in the substantia nigra and sympathetic chain may suggest a possible role in disease of the nervous system involving the substantia nigra and sympathetic nervous system such as the Parkinson's plus group of disorders. Further studies will be needed to assess PHD3's role in these disorders. Abnormal protein aggregation has been implicated in the development of neurodegenerative disorders such as Alzheimer's disease and Parkinson's disease and it is interesting to note that recent studies have implicated PHD3 in protein aggregation (Rantanen et al., 2008). These findings will be discussed later in this thesis.

The expression of PHD3 in the hippocampus may also have implications for cerebro-vascular disease, particularly because some regions of the hippocampus are more prone to ischaemic injury than others. It has been established that following transient global cerebral ischaemia the hippocampal CA1 region is more sensitive to ischaemic injury compared to region CA3 and the basis for this difference remains unknown (Mitani et al., 1995; Sugawara et al., 2000, Sugawara et al., 1999; Kirino et al., 1982). In this context, the relative absence of PHD3 from the CA3 region may have implications for its resistance to ischaemic injury. The mechanism by which a protective process could take place is not clear. The effects of HIF activation have been shown to promote pro-apoptotic as well as pro-survival neuronal pathways (Ratan et al., 2007), and further studies will be required to determine the impact of

PHD3 deletion on cerebral ischaemia. An in depth discussion of these findings will take place at a later stage in this thesis.

6.4 Reconciling the expression of PHD3 in adult sympatho-adrenal lineage tissues with its role as a promoter of apoptosis

The abundance of PHD3 detected in the adult rat sympathetic nervous system was in many ways an unexpected finding. A number of previous studies had indicated that PHD3 promoted apoptosis of sympathetic lineage cell types not only under NGF poor conditions, but also in a variety of other settings. This proven pro-apoptotic property of PHD3 would argue in favour of it being expressed at relatively low levels in adult sympathetic nervous system tissues. However the results of immunoblot and semi-quantitative immunohistochemistry carried out during this doctoral study demonstrated that PHD3 was abundantly expressed in a number of these tissues. Several possible explanations were considered and further studies carried out accordingly as outlined below.

1. ***The relative rather than absolute amount of PHD3 was important in determining which cells undergo apoptosis.***

One possible explanation was that although PHD3 was clearly expressed in adult sympathetic tissues, its level of expression was not sufficient to reach the threshold required to promote apoptosis. Instead its expression may be higher still in neurons undergoing apoptosis. To address this possibility the abundance of PHD3 in adult sympathetic neurons needed to be compared with those undergoing apoptosis. Rather than inducing apoptosis under conditions of cell culture, comparison was made between adult neurons and those undergoing 'naturally occurring neuronal apoptosis'. In rat, naturally occurring neuronal apoptosis is well characterised and occurs as part

of normal development, extending from late embryonic period into the second postnatal week (Wright et al., 1983). Rat SCG's were harvested from animals at different time points during this period and their PHD3 content compared with that of adult SCG.

2. Distinct pro-apoptotic forms of PHD3 existed which were different to those expressed in adult tissues.

A further explanation for the abundance of PHD3 detected in adult tissues related to the possibility that there were different forms of PHD3 in adult and developing tissues. While forms of PHD3 with pro-apoptotic properties were expressed in developing tissues, adult tissues may express other PHD isoforms which lacked the ability to promote apoptosis, thereby allowing adult forms of PHD3 to be expressed in abundance without apoptosis taking place. The study of PHD3 expression in adult and developing sympathetic neurons was carried out with this possibility in mind and a range of molecular weights were surveyed by PHD3 immunoblot to detect known as well as novel forms of PHD3 expressed in these two settings.

3. Difference in the nuclear and cytoplasmic localisation of PHD3 may influence its ability to promote apoptosis

The study of tissues of the adult sympatho-adrenal axis indicated that there were differences in the subcellular distribution of PHD3 between different sympathetic lineage cell types. PHD3 mediated apoptosis was shown to be dependent on mitochondrial function (Lipscomb et al., 2001) which gave rise to the possibility that the relative lack of cytoplasmic PHD3 in adult sympathetic neurons could result in reduced interaction between PHD3 and mitochondrial proteins, thereby failing to

reach the threshold required to promote apoptosis. Conversely this scenario would argue in favour of there being relatively more PHD3 in the cytoplasm of developing sympathetic neurites undergoing apoptosis, and would provide a mechanism whereby changes in subcellular rather than total cellular PHD3 content would be sufficient to promote apoptosis. In order to explore this possibility the subcellular distribution of PHD3 in sympathetic neurons undergoing apoptosis needed to be assessed. With this in mind, the proposed immunoblot study of developing and adult SCG sympathetic neurons was complemented with an immunohistochemical analysis of the subcellular distribution of PHD3 during the same period.

SCG's from P0, P2, P5, P7 and P14 rats were harvested under dissecting microscope and after removal of surrounding connective tissue, snap frozen in liquid nitrogen along with similarly harvested adult samples. Tissue homogenates were prepared as previously described and immunoblotted on a single membrane (fig 57).

Immunoblots demonstrated that the 50KDa and 27KDa adult species of PHD3 identified earlier in this doctoral study were expressed at similar levels in developing SCG's; furthermore, the ratio between 50KDa and 27KDa PHD3 species appeared similar throughout development and adult SCG extracts. Immunoblot of postnatal SCG extracts also demonstrated an additional 50KDa doublet, the abundance of which increased in intensity during the course of development and was most noticeable from P14 onwards. An additional higher molecular weight species was detected in the region of 109KDa which was strongly expressed during the period of naturally occurring cell death. Its intensity gradually decreased during this period and was at a very low level in adult SCG.

P14 nodose ganglia were more amenable to micro-dissection compared to those of adult, and these extracts were immunoblotted alongside those of developing nodose and SCG. The nodose ganglia was found to express the same species of PHD3 as SCG, however the relative abundance of these species was different. While the 50KDa PHD3 species was expressed at similar levels in SCG and nodose, both 27KDa and 109KDa species were of lesser abundance in nodose compared to SCG (Fig 57).

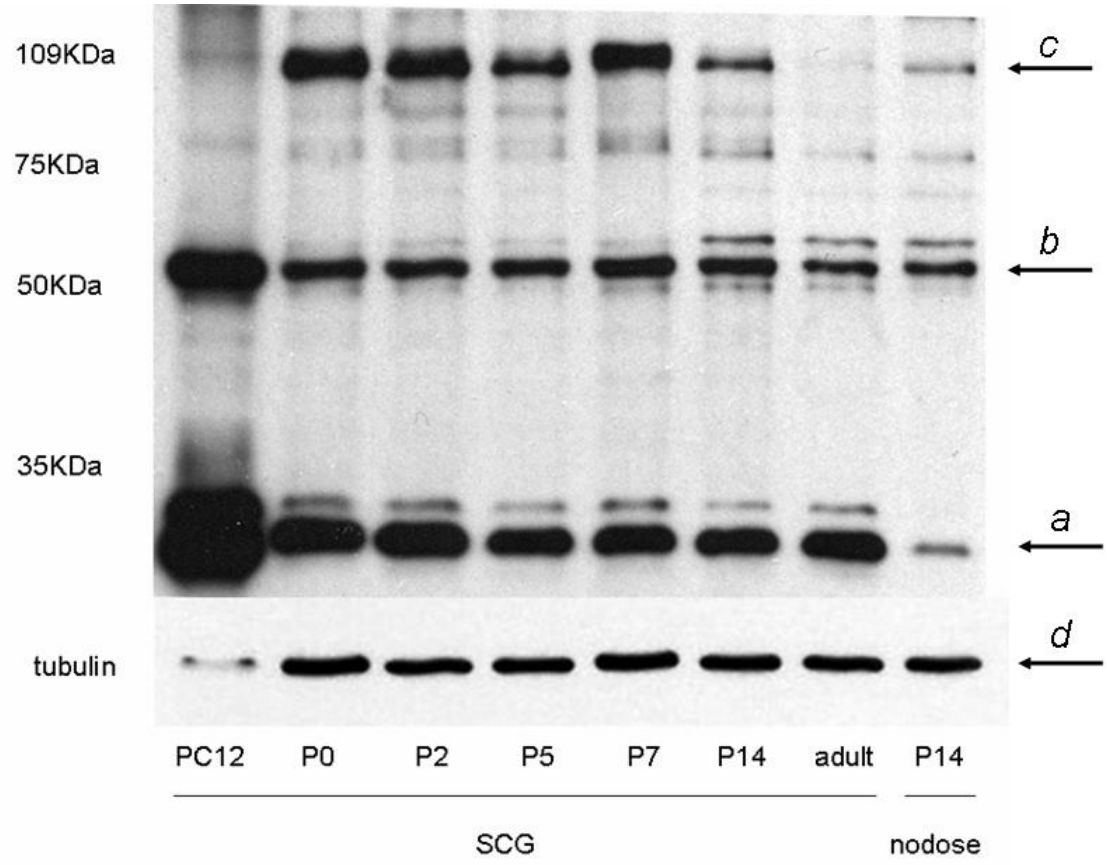


Figure 57. PHD3 expression in developing ganglia

Rat SCG extracts from P0, P2, P5, P7 and P14 animals was immunoblotted for PHD3 alongside P14 nodose extracts with antibody 188e. Immunoblot demonstrated that the 27KDa (fig 57, arrow a) and 50KDa (fig 57, arrow b) species of PHD3 were similarly expressed in developing and adult SCG. In developing SCG's, a higher molecular weight species of 109KDa was detected (fig 57, arrow c), which became less abundant at later time points. These three species were also present in extracts of P14 nodose ganglion, but were of different abundance. PC12 cells were once again noted to express both the 27KDa and 50KDa PHD3 species. Expression of the 109KDa species of PHD3 in PC12 cells was noted to be very weak. Tubulin immunoblot confirmed equal sample loading of the tissue extracts (fig 57, arrow d). (Representative of two immnostains).

Immunohistochemical analysis of developing and adult SCG's was also carried out and demonstrated a gradual decline in the cytoplasmic PHD3 content of sympathetic neurons during this period of developmental apoptosis (fig 58). At E18 and P2, the vast majority of developing neurites expressed an abundance of cytoplasmic PHD3. However, by P14 the majority of neurites expressed more nuclear PHD3. In order to gain further insights into processes underlying changes in cytoplasmic PHD3 signal the nuclear and cytoplasmic PHD3 signal from developing sympathetic neurons was quantified as previously described (fig 58). This demonstrated that there was a decline in both nuclear and cytoplasmic PHD3 but that the rate of decline was greater in the cytoplasmic fraction.

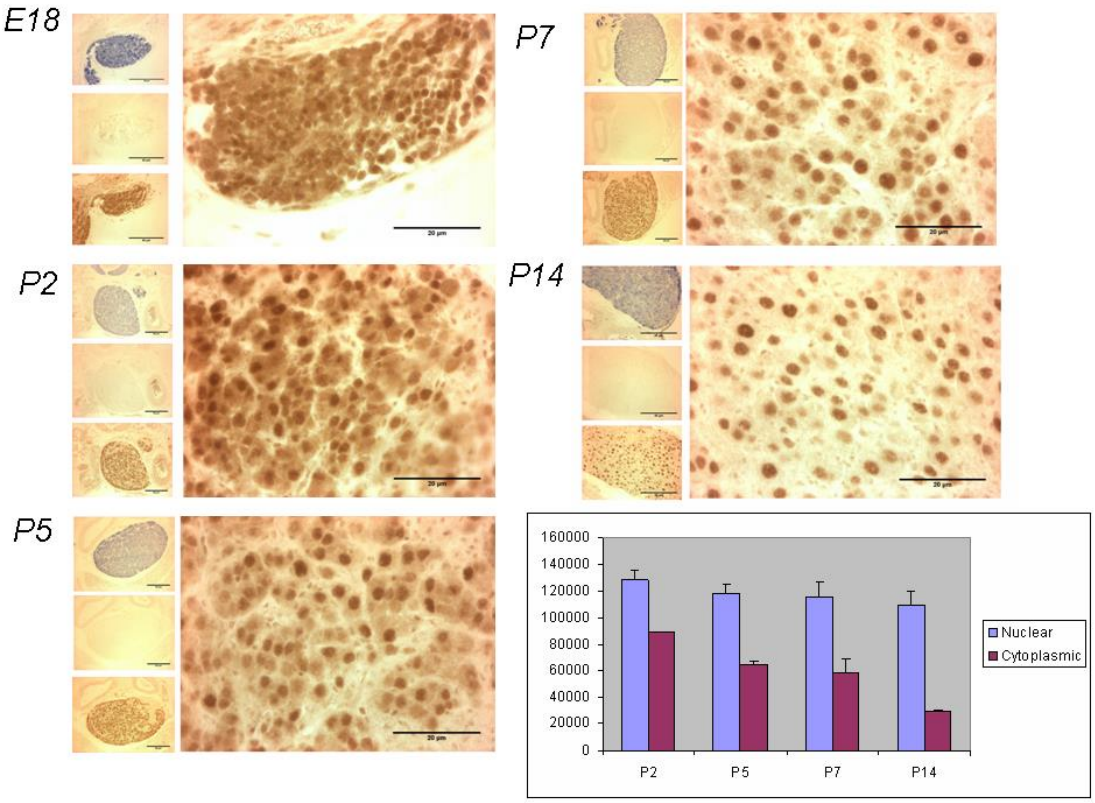


Figure 58. Changes in the subcellular expression of PHD3 during rat SCG development

Immunostaining demonstrated a gradual decline in cytoplasmic PHD3 signal from E18 to P14. Each immunoblot panel includes SCG sections for TH with vector blue chromogen (upper panel), isotype matched control with DAB chromogen (middle panel), and low power magnification of PHD3 with DAB chromogen (lower panel). Semi-quantitative analysis demonstrated a decline in nuclear as well as cytoplasmic PHD3. The rate of cytoplasmic PHD3 signal decline was greater than the rate of nuclear signal decline. (Representative of two immunostains).

6.5 PHD3 expression in rat lung

Recent studies give rise to the possibility that PHD3 is involved in hydroxylation dependent regulation of the β2 adrenoreceptor (Xie et al., 2009). β adrenoreceptor dysregulation is known to be involved in the pathogenesis of many disease states which include hypertension, heart failure and airways disease (Johnson et al., 1998; Lefkowitz et al., 2000; Iaccarino et al., 2002). This doctoral study demonstrated that there was an abundance of different PHD3 isoforms in heart, skeletal muscle and SCG compared to other tissues, which would be in keeping with a potential role for PHD3 in β2 adrenoreceptor regulation.

β2 adrenoreceptor stimulation is also known to enhance bronchodilation and alveolar fluid clearance (Johnson et al., 1998), suggesting that PHD3 might be expressed in bronchial epithelium and smooth muscle; however, immunoblot of whole lung demonstrated relatively little PHD3, giving rise to the possibility that its expression may be restricted to specific lung regions and under-represented in whole tissue immunoblots. In order to address this possibility an immunohistochemical approach was taken to study PHD3 in adult rat lung.

6.5.1 Characterising the expression of PHD3 in adult rat lung

PHD3 immunohistochemistry demonstrated that in addition to being expressed in the walls of pulmonary arteries, PHD3 was also strongly expressed in bronchial epithelial lining (fig 59). Further studies will be required to determine if this signal is derived from ciliated or goblet cells as well as the degree to which it co-localises with bronchial adrenoreceptors.

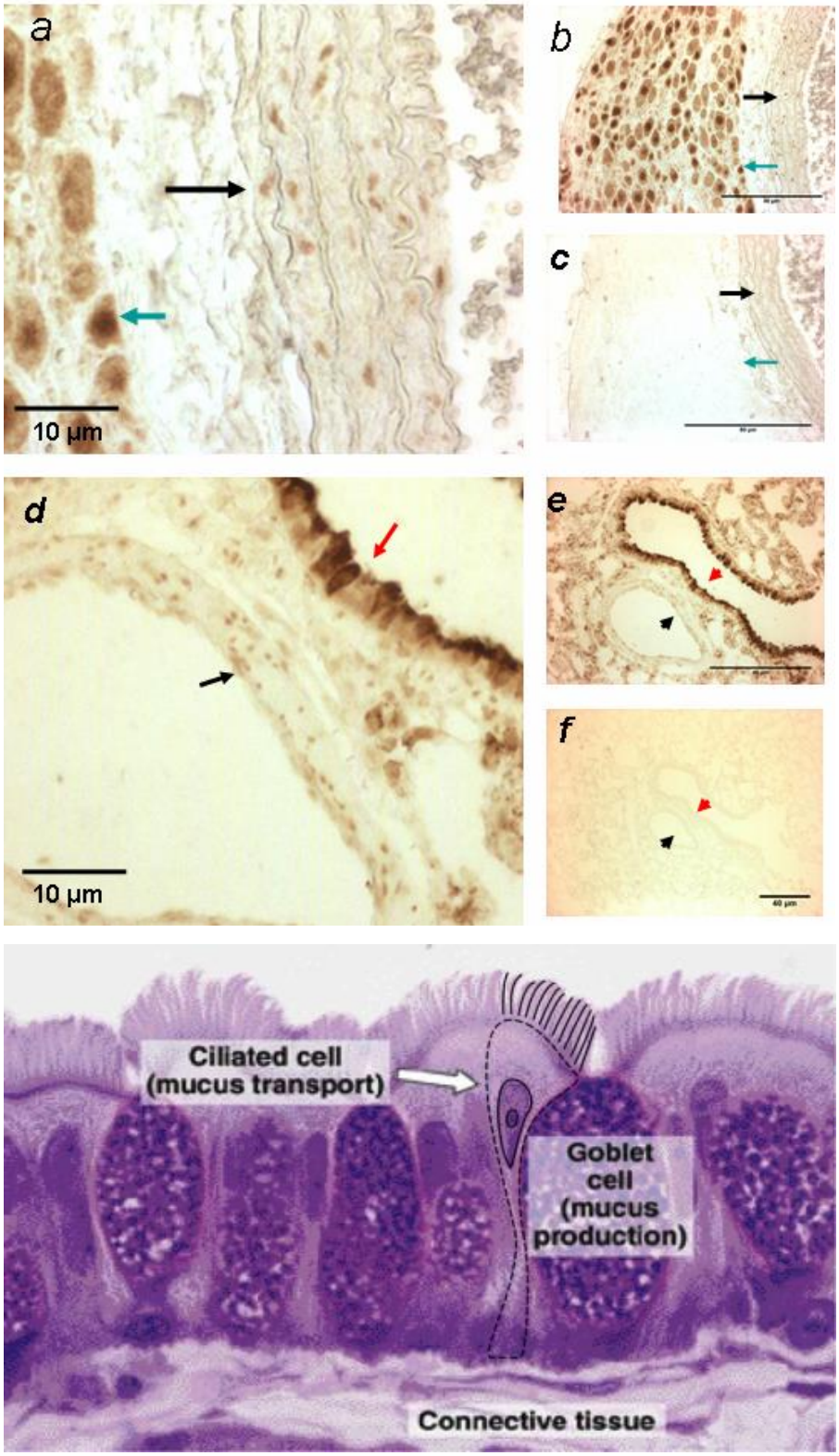


Figure 59. Characterising the expression of PHD3 in lung and carotid artery

PHD3 immunostaining with DAB chromogen confirmed expression of PHD3 in smooth muscle of the carotid artery (fig 59, a, black arrow). These tissue sections also contained the adjacent SCG (fig 59, a, blue arrow). At lower power magnification the SCG is more clearly demonstrated adjacent to the carotid artery (fig 59, b). No

staining was detected with an isotype matched control antibody (fig 59, c). PHD3 signal was also detected in the walls of pulmonary arteries which was punctate in nature (fig 59, d, black arrow). Strong PHD3 signal was noted in the adjacent bronchial epithelial lining (fig 59, d, red arrow). At lower power, PHD3 is noted to be widely expressed in bronchial epithelial lining (fig 59, e). No staining was noted with an isotype matched control antibody (fig 59, f). H&E stain of bronchial epithelium (*Taken from Junqueira and Carneiro, Basic Histology, a text and atlas, p350)*, indicates different ciliary cell and goblet cell populations of the bronchial epithelium. DAB stain was most strongly detected on the luminal boarder which may indicate its expression in cilia and further studies will be required.

6.5.2 Characterising the expression of PHD3 in developing rat lung

Adrenoreceptors are thought to play an important role in lung maturation (Reinhardt et al., 1989). In view of this, PHD3 expression in the developing lung was also assessed and was found to be expressed in developing bronchial epithelial lining of the E14 rat embryo (fig 60).

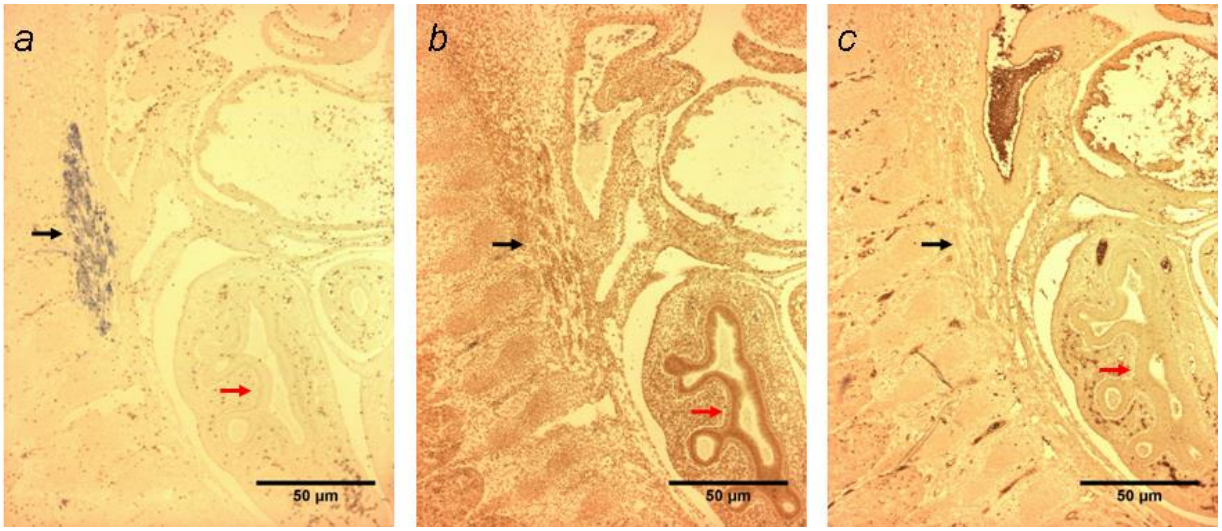


Figure 59. Characterising the expression of PHD3 in developing lung

TH immunostain of E14 rat embryo identified the rat SCG with vector blue stain (fig 60, a, black arrow). The developing bronchi are noted (fig 60, a, red arrow). Immunostaining of serial sections for PHD3 with DAB chromogen demonstrated staining in the SCG (fig 60, b, black arrow), and also in the lining of the developing bronchial epithelium (fig 60, b, red arrow). No staining was noted with an isotype matched control antibody (fig 60, c). (Representative of two immunostains).

6.6 Putative relationships between PHD3 expression and tumourigenesis within the sympatho-adrenal lineage

During the course of this doctoral study evidence emerged for interplay between genes linked to sympatho-adrenal tumour syndromes and PHD3 (Lee et al., 2005). These findings are schematically represented in figure 61.

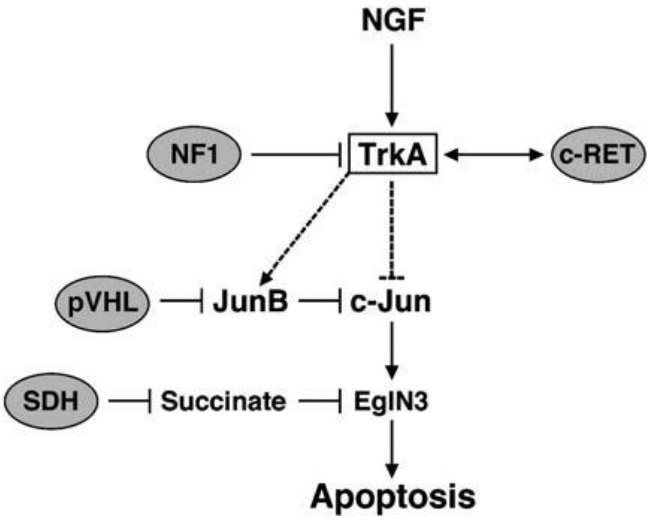


Figure 61. Interplay between PHD3 (EglN3) and familial phaeochromocytoma and paraganglioma linked genes. (Lee et al., 2005).

These studies speculated that this interplay could result in impaired PHD3 dependent apoptosis thereby providing a mechanism whereby rogue neurites could survive and undergo neoplastic transformation in later life. This gave rise to the possibility that processes which altered the function of PHD3 could have an impact on sympatho-adrenal disease.

6.6.1 Differences in the species of PHD3 expressed in PC12 cells and sympathetic lineage tissues and possible implications for tumour biology

In order to assess this possibility PHD3 from the rat PC12 phaeochromocytoma cell line was studied and compared with that of normal tissues (fig 62). Prolonged SDS PAGE electrophoresis demonstrated that the 27KDa doublet species of PHD3

was of different mobility in PC12 cells compared to SCG extracts. The lower species of the 27KDa PHD3 doublet was found to migrate further in PC12 cells compared to SCG extracts, suggesting that this species was marginally smaller in size (fig 62).

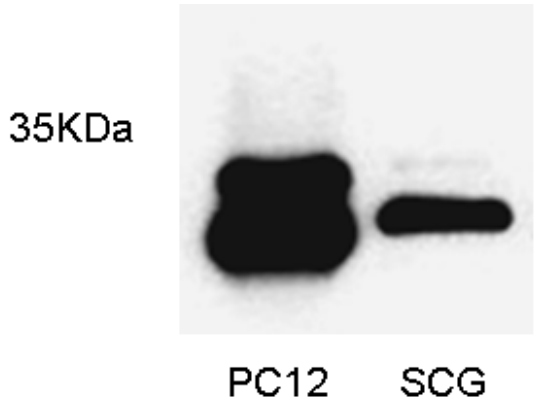


Figure 62. Differences in PHD3 species expressed in PC12 cells and sympathetic lineage tissues

Immunoblot comparison of PHD3 signal from PC12 cells and SCG extracts. The lower species of the 27KDa form of PHD3 was found to migrate further in PC12 cells compared to normal SCG derived PHD3. (Representative of three immunoblots).

Difference in mobility of this nature could arise from altered post-translational modification, splice variation, alternative methionine translation initiation or sequence mutation, and each will be described further in the discussion part of this thesis.

Determining the nucleotide sequence of the 27KDa species of PHD3 from PC12 cells allowed the possibility of splice variation and gene mutation to be simultaneously considered and was therefore carried out as part of this doctoral study.

A PCR based approach was used to sequence the 27KDa species of PC12 cell PHD3 (fig 63, 64). Primers indicated in the methods sections of this thesis were used to PCR amplify specific regions of rat PC12 cDNA. When the nucleotide sequence of PC12 cell PHD3 was compared to that of rat PHD3, no differences in nucleotide

sequence was observed arguing against roles for splice variation and sequence mutation to account for the difference in immunoblot. Instead, these findings suggested that post-translational modification or altered translation initiation may be responsible and further studies will be required to assess these possibilities.

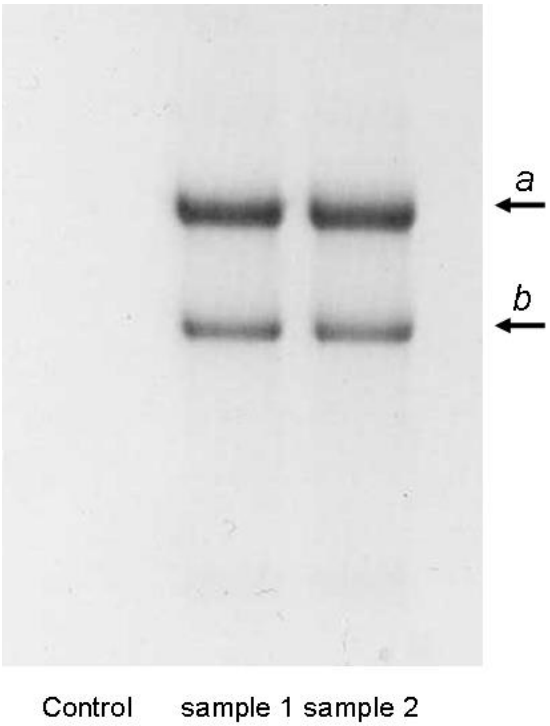


Figure 63. Assessing PC12 cell RNA extracts for degradation

RNA extracted from PC12 was assessed for degradation by agarose gel electrophoresis under RNase free conditions. This demonstrated the presence of discrete 28S (fig 63, arrow a) and 18S (fig 63, arrow b) bands indicating that degradation had not taken place. A negative control lane consisting of RNA extraction buffer did not demonstrate any signal.

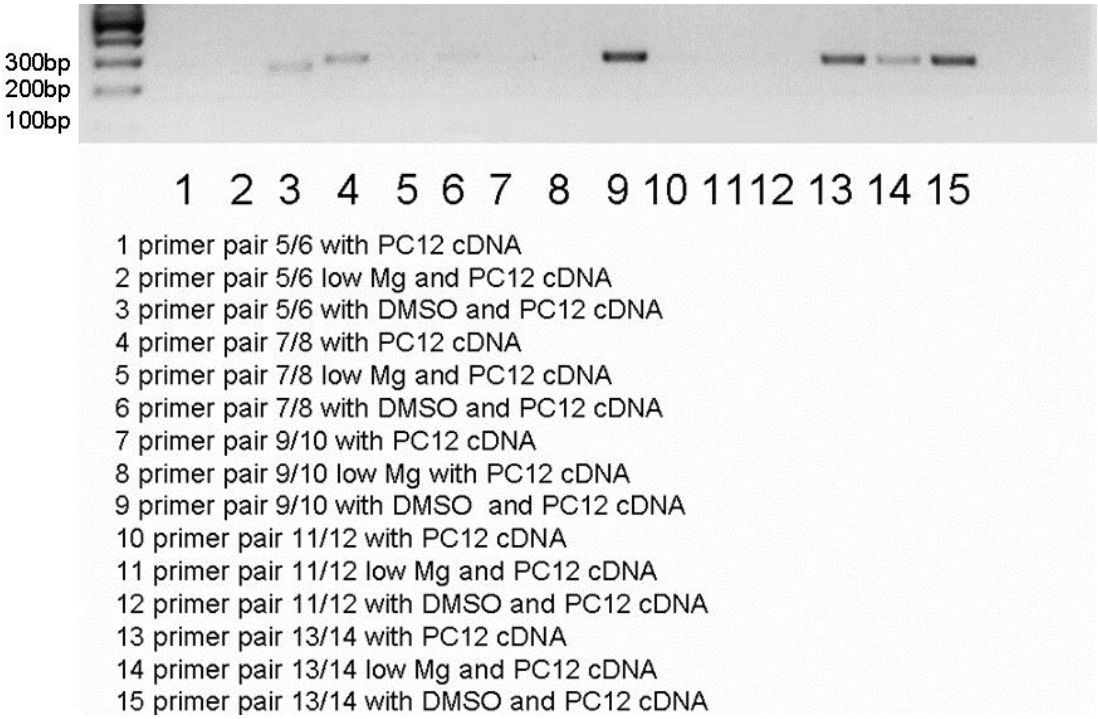


Figure 64. PCR amplification of rat PHD3 from PC12 cells under different reaction conditions

Illustrative blot of PCR amplification of cDNA generated from normoxic and 6hr of 0.5% hypoxia treated PC12 cells was carried out using the primer pairs indicated. A series of reactions were carried out for each primer pair to optimise PCR conditions which included the use of low Mg^{+2} and DMSO as well as combinations thereof.

Chapter 7. Understanding the relationship between expression and function of PHD isoforms in tissues

7.1 Phenotypic studies of mice with constitutional deletion of individual PHD isoforms

7.1.1 Assessing the significance of PHD3 expression within the rat sympatho-adrenal axis

This doctoral study clearly demonstrated that PHD3 was abundantly expressed in adult and developing tissues of the rat sympatho-adrenal axis. These findings gave rise to questions regarding the role of PHD3's in sympatho-adrenal tissues. The demonstration that PHD3 was an essential requirement for the apoptosis of sympathetic neurons (Lipscomb et al., 1999; Lipscomb et al., 2001; Straub et al., 2003; Lee et al., 2005) set a precedent for PHD3 acting as a promoter in sympathetic lineage apoptosis. Given that during normal development over 50% of sympathetic neurites undergo developmental apoptosis (Wright et al., 1983), it was felt that loss of PHD3 may result in increased cell numbers (hyperplasia) of sympatho-adrenal tissues.

The development of mice with constitutional deletion of PHD3 provided a means by which studies could be carried out to gain further insights into PHD3's role in sympatho-adrenal axis and other neuronal populations of the peripheral nervous system. These findings have now been reported in a paper of which I was a co-author (Abnormal sympatho-adrenal development and systemic hypotension in PHD3-/- mice, Bishop et al., 2008).

During these studies, comparison of the sympatho-adrenal axis of wild type and PHD3-/- animals was carried out and demonstrated an increase in cell numbers in the SCG, adrenal medulla and carotid body of PHD3-/- compared to wild type mice. These findings, particularly in relation to the SCG were in keeping with the loss of

PHD3's known role as a promoter of sympathetic lineage apoptosis. Importantly, further work carried out in parallel with this doctoral study went on to demonstrate lower resting systolic blood pressure and reduced cardiovascular responses in PHD3 homozygous deleted compared to wild type mice.

7.1.2 Psychometric studies of hippocampal function

My finding of an abundance of PHD3 in the CA1 subfield of the hippocampus may have implications for the know vulnerability of this regions to ischaemic injury (Schmidt-Kastner et al., 1991). Studies of brain ischaemia using wild type and PHD3-/- mice were considered to be of importance; however, the specific methodology required to carry out this work was not readily available at the time of this doctoral study.

The hippocampus also has an important role in learning and memory (Jarrard et al., 1993; Galani et al., 1998). Considerable expertise in the field of hippocampal function was available in the Department of Psychology at Oxford University. A number of pilot collaborative psychometric tests were therefore carried out to assess for a PHD3 related hippocampal phenotype.

Mouse strains are known to differ in their ability to carry out different psychometric tests. For example hippocampal functions such as burrowing behaviour are known to be better in mouse strains C57BL6, BALB/c, DBA/2 compared to strains CBA and 129S2/Sv (Deacon., 2006). Mouse strains may over-perform in certain tasks, completing them in advance of useful measurements being obtained. To avoid such 'ceiling effects', the work load or time interval between measurements can

be altered within the boundaries of any given test. This inherent variability in drive of different mouse strains necessitates using a number of different behavioural tests when assessing mouse hippocampal function. This is particularly true when animals are bred onto a mixed genetic background such as the 129/SvEv background of PHD3-/- mice.

Following discussion with colleagues in the Department of Psychology the following psychometric tests were considered as appropriate to assess for a hippocampal phenotype: Food hoarding behaviour, burrowing behaviour, nest building behaviour and spontaneous 'T' maze alternation. The study design followed a format specified by the Oxford University Department of Psychology and was sufficiently powered to detect significant phenotypic differences which could be further dissected by more complex in vivo studies such as that of long term potentiation.

7.1.2.1 Psychometric assessment of food hoarding

Food hoarding represented an effort related species typical behaviour influenced by hippocampal function. Hoarding behaviour varies between mouse strains, however a validated protocol for its study had been established at the Oxford University Department of Psychology, which was followed during this doctoral study. The ability of animals to hoard 100g of food overnight was compared between wild type and PHD3-/- animals (fig 65). Both were found to be vigorous hoarders with PHD3-/- animals hoarded a mean of 95.5g ± 2g compared to 94 ± 3g hoarded by wild type animals, a non-significant difference (n = 8 PHD3-/-; 8 wt animals; amount of food hoarded in grams as mean ± SEM; t-test $p > 0.05$).

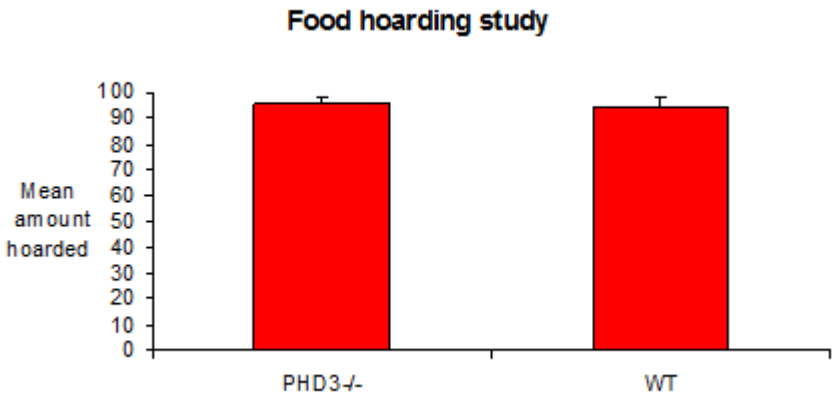


Figure 65. Psychometric study comparing the food hoarding behaviour of PHD3-/- and wild type mice. Error bars indicate mean ± SEM. No difference was observed between hording behaviour of PHD3-/- and wild type mice.

Given this result, the option of modifying the study protocol to increase its sensitivity was considered. This could be achieved by either loading more food or reducing the duration of time allowed for animals to hoard. Hoarding behaviour occurs sporadically at night which necessitated an overnight period of study to allow undisturbed hoarding to take place. Altering the duration of time allowed for hoarding would have altered this behaviour pattern and negated the test and was therefore not carried out; furthermore, the architecture of the study apparatus did not allow loading of more than 100g of food which precluded the study protocol being modified by providing more food to hoard.

In order to minimise the risk of similar ceiling effects compounding other studies, subsequent psychometric tests were chosen on the basis of open end points ('T'-Maze spontaneous alternation), studies involving subjective measurements (study of nest building behaviour) or a number of different time points during which assessment could be carried out (study of burrowing behaviour).

7.1.2.2. 'T' maze spontaneous alternation

T-maze spontaneous alternation is a test of recall during which an animal recalls the path taken in a T-maze apparatus. During the second visit to the apparatus, an animal with intact hippocampal function normally recalls the side first visited and chooses the opposite side. Each animal was allowed to choose 10 times and the mean number of correctly made choices calculated. The number of times PHD3-/- chose correctly was 7±0.5 compared to 8.125±0.39 for the wild type, a non-significant difference (fig 66). (*n* = 8 PHD3-/-; 8 wt animals; expressed as mean ± SEM; Mann-Whitney U test $p > 0.05$).

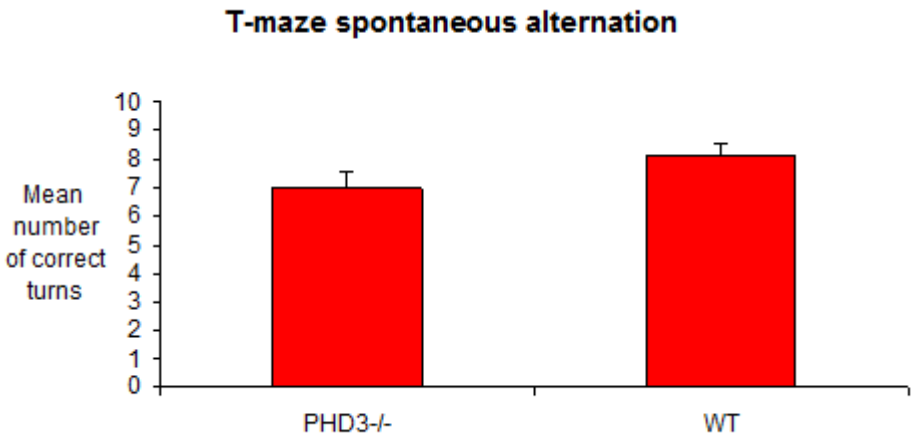


Figure 66. Psychometric studies comparing the T-maze spontaneous alternation behaviour of PHD3-/- and wild type mice. Error bars indicate mean ± SEM.

7.1.2.3 Psychometric study of nest building

Nest building is considered to be a species typical hippocampal function. Nest building, in addition to providing shelter from the elements, is important to the successful rearing of pups. Nest building is usually carried out during the initial phase of a 12hr night cycle. The nest building ability of PHD3-/- and wild type animals was compared overnight and scored independently by two observers (fig 67). PHD3-/- animals obtained mean scores of 3 ± 0.6 compared to 4.5 ± 0.25 for wild type animals, which was a non-significant difference (n = 8 PHD3-/-; 8 wt animals; nest building scores expressed as mean ± SEM; Mann-Whitney U test $p > 0.05$).

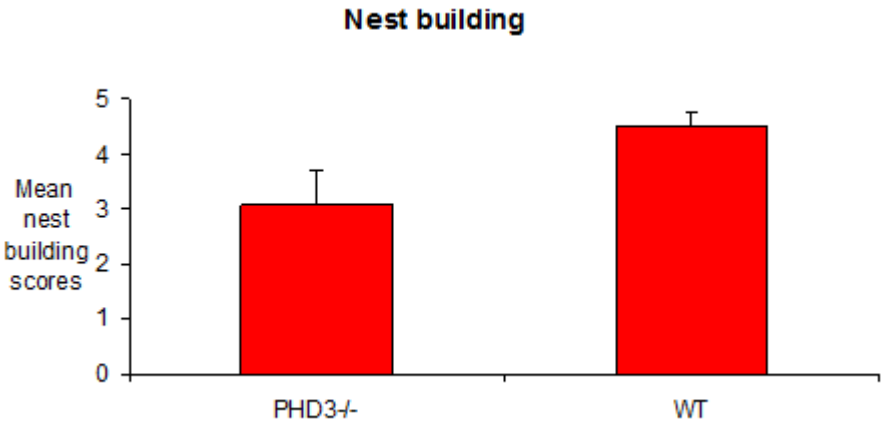


Figure 67. Psychometric studies comparing the nest building behaviour of PHD3-/- and wild type mice. Error bars indicate mean ± SEM. No significant difference between PHD3-/- and wild type mice was observed.

7.1.2.4 Psychometric assessment of burrowing behaviour

Burrowing behaviour is an effort related species typical behaviour influenced by hippocampal function. The study of burrowing behaviour involves comparing amounts burrowed after 2hr and overnight periods of study. Two time points are used because vigorous burrowers can empty the burrow of all material during the longer study period, leading to a loss of sensitivity in detecting differences in burrowing

activity. The burrowing behaviour of PHD3-/- and wild type animals was compared after 2hr (Fig 68, a) and overnight (Fig 68, b) periods of study. Of the 200g of material available, PHD3-/- and wild type animals burrowed mean amounts of 57 ± 24g and 114 ± 20g respectively after 2hr; (*n* = 8 PHD3-/-; 8 wt animals; t-test, p>0.05); 164 ± 10g and 154 ± 12g respectively after the overnight study,(*n* = 8 PHD3-/-; 8 wt animals; t-test p>0.05). Although neither set of results were significantly different, the amounts burrowed at 2hr approached a significant difference.

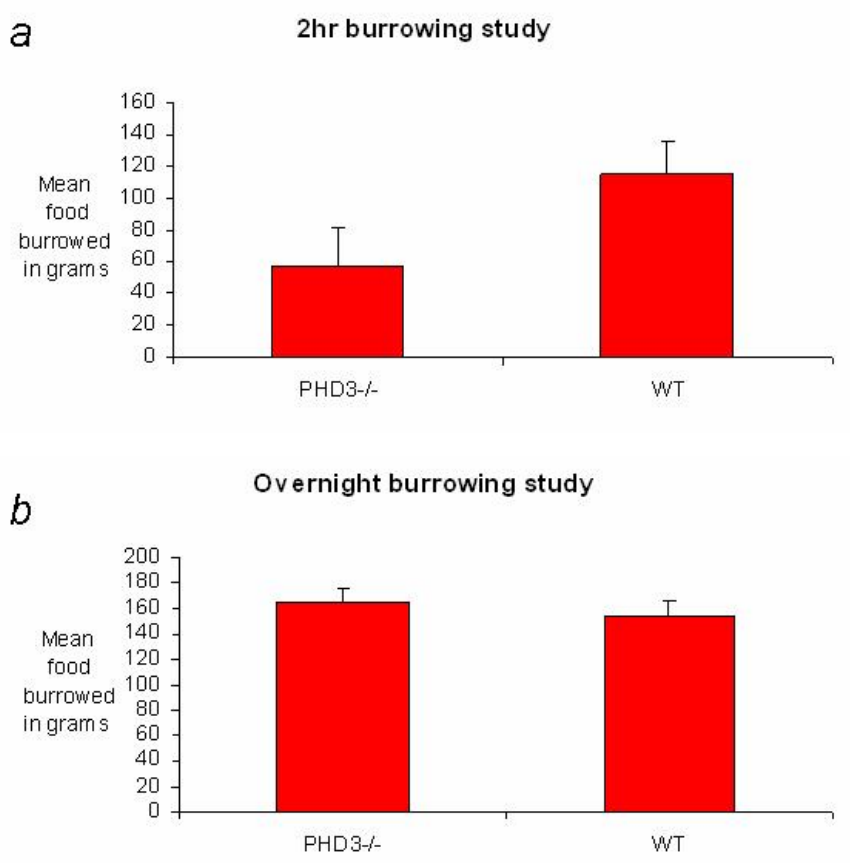


Figure 68. Burrowing studies comparing PHD3-/- and wild type mice

Animals were provided with 200g of food pellets to burrow and the amount burrowed measured after 2hr (fig 68, a), and an overnight period of study (fig 68, b). Amount of food burrowed in grams as mean ± SEM. No significant differences were detected between PHD3-/- and wild type mice.

Studies carried out in parallel with this work demonstrated a phenotype of sympatho-adrenal hyperplasia and cardiovascular hypofunction in PHD3-/- compared to wild type mice. A reduction in systemic blood pressure could impact on the exercise capacity of an animal which gave rise to the possibility that the borderline differences in effort related psychometric tests, instead of representing a behavioural phenotype, reflected a lack of ability of PHD3-/- mice to carry out sustained physical activity.

Despite the possible confounding effects of impaired cardiovascular function on effort related psychometric tests, the non-effort related test of 'T'-maze spontaneous alternation, also demonstrated non-significant differences between wild type and PHD3-/- animals. This argued against the differences observed at the 12hr time point of the hoarding study, being solely due to impaired cardiovascular function.

The similarity in amounts burrowed overnight suggested that given time, PHD3-/- animals were able eventually to achieve the same total amount of work despite potentially being cardiovascularly disadvantaged. Therefore psychometric tests requiring a degree of effort carried out over a 12hr period were likely to negate the potential confounding effects of cardiovascular hypofunction. As such the trend towards significance observed in the overnight nest building study was also more likely to reflect differences in hippocampal than cardiovascular function.

Following discussion with the Department of Psychology, it was felt that the non-exertional study differences could be explained by a weak underlying PHD3-/- hippocampal phenotype. However these differences were too small to assess further

by further psychometric tests. Given the inherent variances of more complex and invasive tests such as the study of long term brain potentiation, which would be required to directly compare the function of wild type and PHD3-/- hippocampal neurons, this work was not taken further forward.

7.2.3 Characterising the testicular phenotype of PHD1-/- mice

Immunoblot analysis of both mouse and rat demonstrated an abundance of PHD1 within testis. Immunohistochemical analysis demonstrated strong signal from developing spermatozoa in both species giving rise to the possibility of a possible reproductive phenotype, which was studied further in collaborative with Dr T Bishop. Testis weights of PHD-/- and wild type animals were normalised to that of the whole animal and compared. PHD1-/- testis weight was 0.079±0.005g compared to 0.11±0.007g for wild type animals (fig 69, a). This indicated that wild type testes were significantly heavier (n=10 PHD3-/-; n = 11 wt animals; weights expressed in grams as mean ± SEM; t-test p<0.05).

Epididymal sperm counts normalised for testis size, of PHD1-/- mice were also compared with wild type mice (fig 69, b). The mean epididymal sperm count of PHD1-/- mice was $12.5x10^6$ $\pm5x10^6$ compared with $19x10^6$ ± $4x10^6$ for wild type animals which indicated a non-significant difference (n = PHD3-/- ; n = 3 wt animals; sperm counts expressed as mean ± SEM; t-test p > 0.05).

Further studies carried out by Dr Bishop did not demonstrate a difference in PHD1-/- litter sizes or male to female pup ratio suggesting that despite the abundance of PHD1 in developing spermatids, its loss did not appear to have a significant impact

on reproduction in the setting of the normal laboratory environment. These findings will be discussed later in this doctoral study.

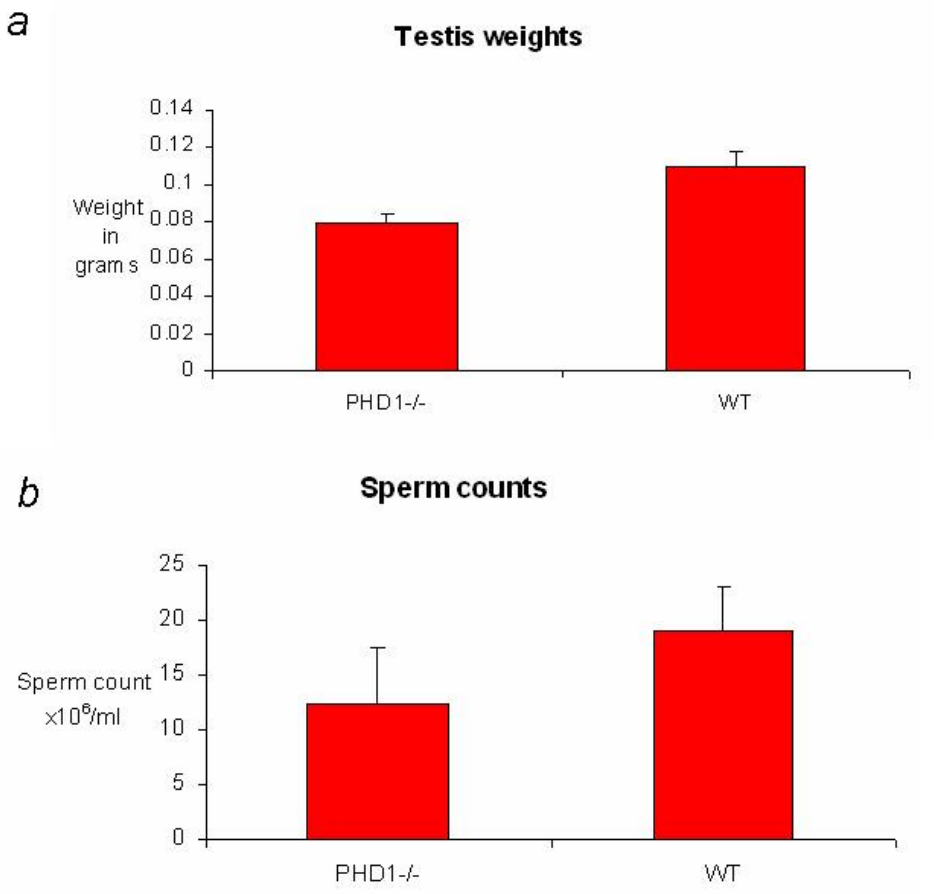


Figure 69. Characterising the testicular phenotype of PHD1-/- compared to wild type mice

The testis weights, normalised to body weight, of 10 week old PHD1-/- male mice and age matched wild type mice (fig 69, a) were compared. Sperm counts, normalised to testis volume, of PHD1-/- mice were also compared with those of age matched wild type animals (Fig 69, b). A significant difference in testis size between PHD1-/- and wild type mice was observed, however sperm counts were no different between the two.

Section 4: Discussion

Chapter 8. Discussion

8.1 Discussion relating to the relative expression of PHD isoforms in rodent tissues

HIF is a master regulator of cellular adaptation to hypoxia (Pugh et al., 2003; Semenza et al., 2001). Hypoxia has been implicated in the pathogenesis and progression of a range of human diseases which include stroke, cardiovascular disease, obstructive airways disease, neoplasia, inflammatory arthritis and inflammatory bowel disease (Semenza., 2007). Altering the expression of HIF may provide new therapeutic avenues for treating these and other human diseases (Semenza., 2007; Semenza., 2002).

Oxygen sensitivity is rendered to HIF through the action of PHD enzymes (Kaelin and Ratcliffe., 2008; Metzen and Ratcliffe., 2004). Therefore understanding the biology of PHD enzymes may provide new insights into HIF regulation and also into putative therapeutic targets for manipulating the HIF system.

One facet of PHD enzyme biology involves understanding the way these enzymes are expressed in tissues. A number of studies sought to address this question by assessing the levels of PHD mRNA in different tissues. However the functional outcome of a gene is determined through protein expression and although often representative of one another, protein and mRNA levels can vary. It was therefore important to characterise the abundance of PHD proteins in tissues, particularly because the non-equilibrium reaction kinetics of these enzymes (Hirsila et al., 2003) means that their abundance determines the amount of HIF hydroxylation which occurs at a given oxygen tension.

Several studies demonstrated that PHD proteins were expressed in a number of different mammalian tissues (Willam et al., 2006; Rohrbach et al., 2005; Soilleux et al., 2005). However, despite these insights, a quantitative assessment of the relative abundance of each PHD isoform in normal mammalian tissues remained an outstanding goal. Achieving this in normal adult rodent tissues, under standard laboratory conditions, was one of the central aims of this doctoral study.

I achieved this aim in rat tissues and demonstrated that PHD2 was the most abundant protein isoform in all tissues studied. In the tissues studied, PHD2 abundance was found to be between 41 and 1.3 fold in excess of the next most abundant tissue PHD isoform. Brain contained the largest amount of PHD2 while the least amount was found in liver. Its abundance in brain was found to be 3.3 fold greater than that of liver.

PHD1 and PHD3 were found in fewer tissues compared to PHD2. In rat tissues, detectable amounts of PHD1 were present only in testis and skeletal muscle. The abundance of PHD1 in testis was 3.5 fold greater than that of skeletal muscle. PHD2 abundance was between 5 and 12 fold greater than the respective amounts of PHD1 found in testis and skeletal muscle.

PHD3 was most abundantly expressed in heart, skeletal muscle and SCG. Although SCG contained most PHD3, PHD2 remained the dominantly expressed SCG isoform being 1.3 fold in excess of PHD3.

8.1.1 Relationship between the abundance of tissue PHD protein and mRNA

The dominance of PHD2 protein in rat tissues was very much in keeping with that of previous cell line based studies (Appelhoff et al., 2004) and several mRNA studies of tissue PHD expression (Oehme et al., 2002; Lieb et al., 2002; Cioffi et al., 2003; Willam et al., 2006). The relatively low level of liver PHD2 was also in keeping with studies of tissue PHD mRNA (Oehme et al., 2002; Willam et al., 2004; Willam et al., 2006). However the expression of PHD2 mRNA in brain was more variable. While some studies demonstrated its abundance in brain (Oehme et al., 2002), others indicated either similar or lesser levels of PHD2 compared to other tissues (Lieb et al., 2002; Hirsila et al., 2003). Because of such differences, further proof was sought to validate the abundance of PHD2 protein levels detected during this doctoral study in rat tissues. In addition to demonstrating concordant signal with two independently raised anti-rat PHD2 antibodies further proof of the dominance of brain PHD2 protein was achieved by studying PHD2 abundance in mouse brain. Although only one antibody capable of detecting mouse tissue PHD2 was available at the time of this doctoral study, the extra specificity control provided by PHD2 mouse heterozygous tissues allowed mouse PHD2 expression to be characterised. The expression of PHD2 protein in mouse tissues was found to be very much in keeping with that of rat. In particular, mouse brain contained most PHD2 while mouse liver expressed least PHD2 further validating the PHD2 protein signal detected in rat.

There are a number of possible reasons for the difference between PHD2 mRNA levels demonstrated in previous studies of tissue PHD expression. In one study which demonstrated no difference between the amount of PHD2 expressed in brain and other tissues, human cadaver tissue was used (Hirsila et al., 2003), and it is possible that

factors such as differences in tissue age, method of preparation, influence of disease and drug therapies may have individually or in combination served to reduce the amount of PHD2 mRNA detected in brain. A second study demonstrated relatively low PHD2 mRNA in mouse brain and other mouse tissues (Lieb et al., 2002). While this study was free of the limitations of human cadaver material it used RNA probes directed against unique regions of the 3' untranslated region of mouse PHD2 and it is possible that polyadenylation downstream of this site may have served to reduce probe binding resulting in brain PHD2 signal being under represented.

In this doctoral study, the abundance of rat PHD1 immunoblot signal was validated by using two independent antibodies and complemented with a study of mouse tissue PHD1 with homozygous PHD1 deleted mouse tissues as specificity controls. While strong PHD1 signal was demonstrated in mouse testis, generally weak signal was present in most other mouse tissues including skeletal muscle. The abundance of PHD1 protein in testis was found to mirror mRNA levels described in previous studies (Lieb et al., 2002; Erez et al., 2002; Oehme et al., 2002; Willam et al., 2004). The same studies indicated lesser amounts of PHD1 mRNA in other tissues which was in keeping with the weaker PHD1 tissue immunoblot signal observed in this doctoral study.

It is of interest that while PHD2 protein in testis was found to be in excess of PHD1, the opposite was true of the mRNA levels of these two isoforms (Lieb et al., 2002; Oehme et al., 2002). Such findings serve to highlight the differences in relative abundance between PHD protein and mRNA.

During this doctoral study a relative abundance of the 27KDa species of PHD3 was detected in SCG, heart and skeletal muscle, which was in keeping with the abundance of PHD3 mRNA previously reported in these tissues (Willam et al., 2004; Willam et al., 2004; Lieb et al., 2002). SCG contained the highest amount of PHD3 protein but SCG mRNA PHD3 levels had not been previously quantified and therefore no comparison between protein and mRNA levels could be made. This species of PHD3 protein was found at relatively low levels in other rat tissues, a finding which was in keeping with previous mRNA based studies (Lieb et al., 2002; Oehme et al., 2002; Cioffi et al., 2003).

8.1.2 Discussion relating to the different protein species of each PHD isoform

Immunoblot analysis of rodent tissues demonstrated that there were several protein isoforms of each PHD. Three tissue species of PHD1 were identified in wild type mouse tissues. Analysis of PHD1-/- tissues demonstrated a species which co-migrated with the middle band of the wild type triplet, giving rise to the possibility that the middle band was cross-reactive. However higher resolution immunoblot analysis demonstrated that the wild type middle band was composed of two separate species, the smaller of which co-migrated with that detected in PHD1-/- tissues. Therefore the wild type middle band did represent a species of PHD1 which was partly obscured by an additional cross-reacting band. In contrast two species of PHD1 were detected in rat tissues. Their identity was confirmed by the demonstration of concordant signal with two independent antibodies capable of detecting rat tissue PHD1.

Two closely migrating species of PHD2 were detected in mouse tissues which were validated by the demonstration of a correspondingly reduced signal in PHD2 heterozygous tissues. Two closely migrating species of PHD2 were also detected in rat tissues and validated by concordant signal with two independent anti-PHD2 antibodies.

The absence of an antibody capable of detecting mouse tissue PHD3 meant that PHD3 expression in mouse tissues could not be assessed. PHD3 expression in rat tissues was however studied and validated with two independent anti-PHD3 antibodies. Rat tissue immunoblots demonstrated a 27KDa doublet as well as ~50KDa form of rat PHD3. The ~33KDa species of PHD3 described by others was also detected in some tissues.

In cell culture, the 27KDa form of PHD3 was found to be strongly induced in PC12 cells treated with hypoxia while the ~50KDa form remained stably expressed under the same conditions. A ~50KDa band was strongly detected in many rat tissues, while the 27KDa form was expressed in relatively few tissues. Taken together these findings suggest that there are constitutive and dynamic forms of PHD3 present in rat tissues.

The aetiology of these tissue PHD forms was next considered. A number of different processes can account for different species of a given protein. These include splice variation, alternative translation start sites, post-translational modification and alternative promoter translation initiation.

In relation to PHD1, IVTT programmed with rodent PHD1 cDNA generated three mouse and two rat species which were of very similar mobility to corresponding tissue forms. These findings suggested that different tissue species of PHD1 originated from processes acting on a single cDNA. Alternative methionine translation initiation and post-translational modification can lead to generation of several species of protein from a single cDNA. Two species of human PHD1 are known to exist and previous studies indicated that these were derived from first and second methionine translation initiation (Tian et al., 2006). Given that these translation initiation sites are conserved between human, mouse and rat with an optimal Kozak sequence of a guanine at position +4 and purine at -3 (Tian et al., 2006), second methionine translation initiation is likely to contribute towards two of the three rodent PHD1 species detected here. Site directed mutagenesis of specific mouse and rat residues could, as in the study of human PHD1 species, be used to confirm their aetiology. The aetiology of the third PHD1 species, uniquely found in mouse, is less clear. Sequence analysis demonstrated that the third mouse methionine was located 149 amino acids downstream of the first. Translation initiation from this site would therefore generate a 15KDa difference in size between the second and third species. The observed difference between second and third and even first and third PHD1 species was considerably less than 15KDa and it was therefore highly unlikely that third methionine translational initiation was a contributory factor to the PHD1 triplet. Instead, it was more likely that a form of post-translational modification accounted for the third mouse species of PHD1. Phosphorylation is a common form of post-translational modification. Within the time frame of this doctoral study it was not possible to assess the role of this form of post-translational modification although it

may be possible to do so in the future by comparing tissue PHD1 signal for a change in bands, before and after phosphatase treatment.

In contrast to PHD1, IVTT programmed with PHD2 cDNA generated a single species. Therefore second methionine translation initiation was unlikely to contribute to the two species of rodent PHD2. Instead, post-translational modification or splice variation could have accounted for the two species of PHD2 observed in rodent tissues. Several splice forms of PHD2 have been reported. In mouse, two PHD2 mRNA species were detected at 2Kb and 4Kb (Lieb et al., 2002). Further studies indicated that there were two splice variants of human PHD2 which lacked exon 3 and 4 (Hirsila et al., 2003). The small size of these exons in both rat and mouse, may account for the small difference in mobility observed between the two species of PHD2, as could post-translational modification. The role of different splice forms could be tested by transfecting cells with cDNA for each PHD2 splice variant and comparing the PHD2 immunoblot signal generated to that of wild type tissues. Phosphatase treatment could also be used to assess if the second PHD2 species arose from post-translational phosphorylation.

In relation to PHD3, the 27KDa doublet was of a size in keeping with human PHD3. However, while human PHD3 was reported as a single species (Appelhoff et al., 2004), its rat counterpart was clearly a doublet. Sequence comparison of human and rat PHD3 would suggest the 27KDa form is generated from second methionine translation initiation as this position equates to methionine one of human PHD3. Future studies could use site directed mutagenesis to test this possibility. Interestingly the third rat PHD3 methionine is only 6 amino acids down-stream of the second and

initiation of translation from second and third methionines could potentially account for the 27KDa doublet observed in rat. Site directed mutagenesis could be used to test the relevance of the third rat methionine towards the 27KDa doublet species as well. The fourth rat methionine is located 140 amino acids down-stream of the second and translation initiation from this site would produce a peptide which was 14KDa smaller in size. Such a difference would clearly be too large to account for the small difference in size observed between the 27KDa doublet bands.

Human and mouse counterparts of rat PHD3 second and third methionines exist which give rise to questions as to why, if a doublet species is a consequence of translation initiation from these sites, a corresponding doublet form of human PHD3 has not been detected. The rat leader sequence, absent from mouse and human, may be of relevance and contribute towards promoting additional translation in rat. Other processes in rat such as post-translational modification may also contribute towards generating the 27KDa PHD3 doublet. A phosphatase reaction could be used to explore the role of this common form of post-translational modification towards generating the doublet species observed.

During this doctoral study a ~50KDa species of PHD3 was also observed in rat tissues. Rat PHD3 has an open reading frame of 355 amino acids (Wax et al., 1996), and is predicted to produce a protein of 35KDa. Rat PHD3 cDNA generated species of 40KDa but also a further 33KDA processed form (Lipscomb et al., 2001). Therefore a peptide generated from this open reading frame would not by itself account for the 50KDa species detected in tissues. It is of interest that tissue immunoblots failed to demonstrate PHD3 tissue species of 40KDa or 33KDa and it is

possible that the ~50KDa species represents a tightly bound complex of smaller forms of PHD3 with other proteins. Such a complex would need to be tightly bound, possibly through covalent bonds, in order to resist the denaturating conditions used for tissue immunoblot. Complexes of PHD3 with the TRiC chaperonin have been described (Masson et al., 2004). However the TRiC complex is large, with a molecular weight of 900KDa, and any complex formed between it and PHD3 would migrate more slowly than the ~50KDa band demonstrated here. Recently a hydroxylation dependent interaction between PHD3 and the aggresome was demonstrated (Rantanen et al., 2008). In this study PHD3 aggregates were found to complex with components of the 26S proteasome, HSP70 and ubiquitin. It is possible that such aggregates may contribute towards formation of the ~50KDa band demonstrated here in rat tissues.

A number of splice forms of PHD3 have also been described. 2.7Kb and 2Kb splice forms of PHD3 were demonstrated to be present in mouse tissues (Lieb et al., 2002). A further splice form of PHD3 lacking amino acids 26 - 119 has also been identified in human PHD3 (Hirsila et al., 2003). It would be possible to explore the role of these splice forms in relation to the tissue protein species observed here by isolating and transfecting individual spliced cDNA forms and comparing the immunoblot size of the peptides generate to those found in tissues. An alternative approach would be to retrieve protein from tissues and analyse by proteomics or to analyse mRNA from tissues for different splice forms of PHD3.

8.1.3 Implications of differences in the abundance of each PHD isoform for PHD deletional mouse models

8.1.3.1 Direct versus indirect nature of deletional models

A direct phenotype relates to one in which the deleted protein is normally abundantly expressed in the tissue manifesting a given phenotype, while an indirect one is when protein expression occurs in a different tissue to that which develops a deletional phenotype. A number of PHD deletional models have been described and their direct versus indirect nature was assessed by studying PHD mRNA abundance. Given the potential disparity between mRNA and protein levels, the study of PHD tissue protein is likely to provide a greater degree of certainty as to the direct or indirect nature of each PHD phenotype. An appreciation of the direct or indirect nature of a phenotype may also help with future drug design, allowing therapeutic agents to be targeted specifically to those tissues expressing an abundance of the relevant PHD isoform.

PHD1 dependent resistance to ischaemic stress has been described in skeletal muscle (Aragones et al., 2007). A PHD3 dependent phenotype of sympatho-adrenal hyperplasia and hypofunction was also described (Bishop et al., 2008). The latter study was collaboratively carried out during the course of this doctoral study. My finding of an abundance of PHD1 in skeletal muscle and abundance of PHD3 in sympatho-adrenal tissue, favoured both these phenotypes being 'direct' in nature.

In contrast, immunoblots failed to demonstrate an abundance of PHD1 in liver suggesting that the PHD1 dependent liver phenotype of ischaemic resistance (Schneider et al., 2009) may be 'indirect' in nature. However the possibility remained

that there may be a liver specific form of PHD1, not readily detected by immunoblot. This is because immunohistochemical analysis with an antibody capable of detecting mouse PHD1 demonstrated nuclear staining in wild type but not PHD1-/- mouse liver. In this respect, it is possible that processes such as altered first methionine translation initiation, as observed of human PHD1 (Tian et al., 2006); liver-specific post-translational modification, or PHD1 splice variation may contribute towards a liver specific form of PHD1 which is poorly recognised by the two anti-rat PHD1 antibodies and single anti-mouse PHD1 antibody used in this doctoral study.

In the absence of a second antibody capable of detecting mouse tissue PHD1, in situ hybridisation of wild type and PHD1-/- liver was carried out to corroborate PHD1 immunohistochemical signal. Intermediate levels of liver PHD1 mRNA were detected by several earlier studies (Erez et al., 2002; Lieb et al., 2002; Hirsila et al., 2003). However despite the strong PHD1 in situ hybridisation signal detected in mouse testis positive control sections used in this doctoral study, no signal was detected in sections of mouse liver. Several explanations for this finding were considered. Firstly, the lesser levels of PHD1 mRNA demonstrated by previous studies in liver may be at too low a level to be detected by the in situ hybridisation protocol used here. Alternatively liver may express a unique splice form of PHD1 which lacked the region of exon 1 to which the in situ probe was directed. In the limited time available for this doctoral study, these possibilities were not addressed but insights into liver PHD1 could be gained either by generating new anti-PHD1 antibodies or using in situ probes directed against exons 2 to 5 of PHD1. In this respect previous mRNA studies may help direct the design of new anti-PHD1 mRNA probes; in a study of mouse tissue PHD1 by northern blot (Erez et al., 2002), a probe was used against the 5' untranslated region of

PHD1 and it may be possible to use this probe in future studies. A further PCR based approach used primers against the 3' untranslated region of mouse PHD1 (Lieb et al., 2002), however a probe based on this runs the risk of signal under representation if the region contained multiple polyadenylation sites.

Different tissues consist of different cell populations and it is possible that the functionally significant amount of a given PHD isoform may vary from one cell type to another. Therefore it could be argued that although immunoblots failed to demonstrate any significant level of PHD1 in rat liver, it may nonetheless, still be present at physiologically significant yet low levels. In favour of this is the finding that of all the tissue surveyed, liver expressed the least amount of PHD2. Given the dominant role of PHD2 in normoxic HIF1 regulation, other PHD isoforms may play a greater role in HIF1 regulation in tissues which express lesser amounts of PHD2. The relative dearth of PHD2 in liver may therefore allow for relatively low levels of PHD1 to become functionally important and to dictate development of a phenotype when deleted. It may be possible to test this scenario by crossing PHD1-/- animals onto a PHD2+/- genetic background. Such animals would, according to this scenario, be expected to have greater liver ischaemic resistance compared to PHD1-/- animals alone because they would contain even lesser quantities of PHD2 compared to wild type mice. They may also show a greater reversal of phenotype compared to PHD1-/- animals when crossed onto a HIF2+/- background. At this stage it still remains unclear if the PHD1 deletional liver phenotype of resistance to ischaemic stress is 'direct' or 'indirect' in nature.

The study of abundance may also help to shed light on the 'direct' versus 'indirect' nature of PHD2 deletional models. A number of PHD2 deletional phenotypes have been described. Homozygous germ line deletion of PHD2 but not PHD1 or PHD3 resulted in early embryonic death (Takeda et al., 2006), while somatic deletion of PHD2 but not PHD1 or PHD3 resulted in phenotypes of exaggerated angiogenesis (Takeda et al., 2007) and severe polycythaemia with congestive cardiac failure (Minamishama., 2008). A PHD2 heterozygous phenotype of vascular normalisation and reduced tumour metastasis (Mazzone et al., 2009) has also been described. The differences in somatic PHD2 deletional phenotypes were likely to reflect the different cell populations targeted for PHD2 deletion. In the former study PHD2 flox/flox; Cre-Rosa26 were used to delete PHD2 in a ubiquitous manner while the latter used PHD2 flox/flox; Cre-erythropoietin (ER) to enable deletion in erythropoietin producing cells. Such potent PHD2 dependent phenotypes may well be in keeping with the finding that PHD2 was by far the most abundant PHD isoform in all tissues studied.

The ubiquitous expression of Rosa26 locus meant that it was more difficult to gain insights into the 'direct' or 'indirect' in nature of the pro-angiogenic phenotype. Interestingly angiogenesis in brain occurred despite its PHD2 content being incompletely deleted suggesting that circulating rather than local pro-angiogenic factors contributed more towards brain angiogenesis. It is also possible that brain is more sensitive compared to other tissues to the effect of PHD2 and that even partial PHD2 loss was sufficient to allow a 'direct' phenotype to develop. In contrast, the PHD2 deletional phenotype of severe polycythaemia is more likely to be direct in nature. This is because the PHD2 flox/flox; Cre-erythropoietin (ER) mice used in this

study enabled PHD2 deletion to be targeted to erythropoietin producing cells alone resulting in excessive kidney EPO production.

8.1.3.2 Implications of PHD abundance for 'true' and 'functional' PHD levels

The 'true' and 'functional' amount of a given PHD isoform would be considered to be similar if the isoform in question were abundantly expressed in tissues manifesting a phenotype when deleted. If however the isoform was expressed at a low level but was nonetheless capable of producing a corresponding deletional phenotype its 'true' and 'functional' level would be different. An appreciation for the 'true' and 'functional' level of a protein is of importance from a therapeutic perspective because it would suggest that tissues expressing relatively low levels of a given isoform may still prove to be valuable therapeutic targets.

The precedent set by the demonstration that PHD enzyme kinetics were unidirectional (Hirsila et al., 2003), and the central role of PHD2 abundance in regulating normoxic HIF1 (Appelhoff et al., 2004), suggested that the abundance of PHD enzymes was likely to be of importance in determining their tissue function. These studies therefore suggested that there would be a close relationship between 'true' and 'functional' amounts of PHD enzymes in tissues. However the possibility remained that in the complex environment of tissues, this relationship could be modulated by factors such as changes in PHD activity (e.g. relating to oxygen or co-factor availability and/or the presence of endogenous inhibitors such as fumarate), cellular compartmentalisation, post-translational modification and non-HIF hydroxylation targets, resulting in differences between 'true' and 'functional' PHD abundance. Indeed recent studies demonstrated that the activity of PHD3 can be influenced by factors other than its abundance (Lee et al., 2005). Although differences

in the subcellular distribution of PHD isoforms have been demonstrated (Metzen et al., 2002; Soilleux et al., 2005), only recently has the significance of subcellular distribution in relation to the ability of PHD2 to regulate HIF1 been established (Yasumoto et al., 2009). Furthermore the suggestion that the β2 adrenoreceptor is regulated by PHD3 in a hydroxylase dependent manner (Xie et al., 2009) demonstrated the presence of non-HIF PHD3 targets. These recent findings added further weight to the possibility of there being a difference between 'true' and 'functional' tissue levels of PHD proteins. In this respect correlating the findings of this doctoral study with those of PHD deletional mouse models, may allow a means to gain further insights into 'true' and 'functional' levels of tissue PHD. These studies will be discussed next in relation to each PHD isoform.

8.1.3.2.1 Insights gained into the 'true' and 'functional' amounts of tissue PHD2 from the study of PHD2 deletional phenotypes

A number of PHD2 deletional studies have been described. Constitutional PHD2 deletion resulted in a phenotype of severe placental vascular abnormalities and intrauterine death (Takeda et al., 2006). Conditional deletional phenotypes of vascular hyperplasia (Takeda et al., 2007), polycythaemia and congestive cardiac failure (Takeda et al., 2008; Minamishima et al., 2008) and the PHD2 heterozygous phenotype of vascular normalisation with reduced tumour metastasis (Mazzone et al., 2009) has also been described. The study of abundance carried out during this doctoral study demonstrated that PHD2 was expressed far in excess of other tissue PHD's. This dominance in PHD2 expression would be in keeping with an inability for either PHD1 or PHD3 to adequately compensate for the loss of PHD2 and with the emergence of PHD2 deletional phenotypes. Further understanding of 'true' and 'functional' PHD2 levels can be gained through the study of PHD2 heterozygous

states. Such studies are of importance because they may indicate that partial loss of PHD2 is sufficient to allow certain phenotypes to manifest, a finding likely to relevant to the design of putative PHD2 modulators. These studies will be discussed next.

Non-functional heterozygous mutations of PHD2 have been linked to familial polycythaemia syndromes (Percy et al., 2006). In this study a C to G mutation at position 950 of the coding sequence of human PHD2 resulted in a proline to arginine change at codon 317, a region in close proximity to the iron binding domain of PHD2. A further PHD2 mutation which results in a change in arginine to histidine at codon 371 of PHD2 has also been described and shown to reduce HIF hydroxylation (Percy et al., 2007). Such studies suggest that even PHD2 heterozygosity is sufficient to allow polycythaemia phenotypes to develop.

Interestingly however PHD2 heterozygous animals, despite expressing substantially lesser tissue PHD2 compared to wild types were not reported to demonstrate a polycythaemia, a finding which would appear at odds with those relating to human PHD2 polycythaemia syndromes. Several of the human kindred were smokers, and this together with other environmental factors may be sufficient to promote a profound polycythaemia response when combined with PHD2 mutation. Yet other PHD2 mutations have been described in non-smokers and mechanisms underlying development of polycythaemia in relation to such mutations remains unclear. Although it has been suggested that a dominant negative effect of PHD2 mutation on either the remaining PHD2 allele or PHD1 and PHD3, may contribute towards the polycythaemia response (Percy et al., 2006) there is currently little

evidence in support of this. Indeed several of the PHD2 mutations described have been shown not to exert dominant negative effects (Percy et al., 2007).

The relative normality of laboratory PHD2 heterozygous animals may therefore at least in part reflect their isolation from physiological stressors to which human subjects were exposed and it is possible that under conditions aimed to mimic smoke inhalations, such as intermittent carbon monoxide exposure, PHD2 heterozygote mice may also manifest a similarly exaggerated polycythaemia response, compared to wild type animals. It is also possible that other genetic factors, possibly relating to PHD1 and PHD3 could have impacted on the human phenotypes and further studies will be necessary to characterise these isoforms in the reported kindred.

PHD2 heterozygous animals may therefore be 'normal' under standard laboratory conditions. This is in itself interesting because it would suggest that the amount of PHD2 in heterozygous animals, although reduced compared to wild types would nonetheless still be sufficient to allow a normal phenotype to occur. It would also suggest that under standard laboratory conditions, wild type tissues were 'programmed' to express an excess of tissue PHD2.

It is possible to speculate as to why wild type tissues may express an excess of PHD2. Metabolic demands relating to activities such as fight or flight would, at the cellular level, pose considerable hypoxic stress on tissues such as heart or skeletal muscle. Although rapid cardiovascular reflexes are designed to minimise fluctuation in tissue oxygenation, there would nonetheless be a time lag before such adaptations take effect. During such periods, cellular hypoxia may be sufficient to transiently

stabilise HIF and promote transcription of adaptive hypoxic genes. Given the transient nature of such hypoxic stressors, activation of HIF mediated transcription could be envisaged as wasteful and it is therefore possible that an excess of tissue PHD2 may act as a 'physiological buffer', preventing or limiting HIF stabilisation under conditions of transient low oxygen pending adaptive physiology from re-establishing the normal cellular milieu. In contrast prolonged hypoxic stress, as may occur at altitude, diving or long distance running, could saturate a putative PHD2 buffering mechanism and promote HIF driven hypoxic responses in a more appropriate manner. An individual moving to altitude would for example experience greater acute tissue hypoxia which in turn would promote an adaptive cardiovascular response sufficient to re-establish normal tissue oxygenation. However more vigorous activity carried out at this altitude or moving to higher altitude could potentially saturate adaptive physiological responses thus driving tissue oxygenation below the capacity of the putative PHD2 'buffer'. Under such circumstances, promotion of HIF driven gene transcription would be deemed appropriate and subsequent angiogenesis in particular would aid normalisation of tissue oxygenation. Such a scenario would favour PHD2 having an important role in adaptive physiology to intermittent or long term hypoxia rather than the transient acute episodes of hypoxia relating to activities of daily living. Further studies could be carried out to test the adaptive capabilities of wild type compared to PHD2 heterozygous animals subject to prolonged hypoxia or graded exercise. The lesser abundance of PHD2 in heterozygous tissues would be predicted to promote greater HIF stabilisation, producing a greater adaptive response in the form of angiogenesis compared to wild types.

8.1.3.2.2 Insights gained into the 'true' and 'functional' amounts of tissue PHD1 and PHD3 from the study of corresponding deletional mouse models

Phenotypes arising from deletion of PHD1 and PHD3 cannot readily be reconciled through scenarios in which their abundance held precedence in determining phenotype. This is because PHD2 was more abundant then PHD1 and PHD3 in all tissues studied and as such, predicted to compensate for their loss (at least with respect to the HIF pathway).

Our analysis demonstrates that those tissues manifesting a PHD1 or PHD3 deletional phenotype appeared also to express relatively less PHD2 protein. Of the tissues surveyed in this doctoral study liver was found to contain the least PHD2 while skeletal muscle and SCG had the 3rd and 5th lowest PHD2 content. Taken together these findings may suggest that although the phenotypes manifested were clearly the result of loss of PHD1 or PHD3, the reason they occurred in specific tissues, may in part reflect the relative lack of PHD2 within these tissues.

The study of abundance may also help to provide additional insights into processes underlying development of the recently described double PHD deletional phenotypes. PHD1/3 double knock-out mice demonstrated an interesting phenotype of moderate polycythaemia secondary to hepatic Epo production (Takeda et al., 2008). This phenotype is of interest because as previously discussed, PHD1 in liver may be atypical while PHD3 in liver was expressed at relatively low levels. These features of liver PHD1 and PHD3 may have bearing on why their combined deletion was sufficient to generate a phenotype which was not evident through single deletion alone. Of all the tissues studied, liver was also found to express the least amount of PHD2, at a level which may be insufficient to compensate for the loss of both PHD1

and 3 thereby allowing a liver phenotype to develop in the resting state. These findings would point towards the liver being particularly sensitive to either therapeutic or detrimental effects of putative PHD modulators.

Taken together the findings of this doctoral study and those of previous studies would suggest that the dominant expression of tissue PHD2 demonstrated here did play a central role in influencing PHD2 deletional phenotypes. This role would be very much in keeping with that previously demonstrated for PHD2 in cell lines, as being the principal regulator of normoxic HIF1. Indeed taken further, it would suggest that PHD2 deletional phenotypes were likely to be more closely linked to tissue HIF1 than HIF2. This link could be tested further by demonstrating greater reversal of phenotype by breeding onto a HIF1 compared to HIF2 heterozygous background.

In contrast, the abundance of tissue PHD1 and 3 was less clearly linked to respective deletional phenotypes. This was because even in those tissues manifesting PHD1, PHD3 or PHD1/3 deletional phenotypes, the abundance of these isoforms remained well below that of PHD2. This finding suggested that despite their common ability to hydroxylate HIF, PHD2 was unable to compensate for the loss of PHD1 and PHD3 in selected tissues and other factors apart from abundance contributed to development of PHD1 and PHD3 deletional phenotypes.

The question remains as to why, despite being of greater abundance, PHD2 was insufficient to compensate for the loss of these isoforms. It is possible to speculate that processes such as differences in cellular or subcellular localisation, post-translational modification, complex formation or interaction with yet to be defined

non-HIF hydroxylation targets serve to suppress PHD2 activity or indeed promote the activity of PHD1 or PHD3 resulting in a difference between 'true' and 'functional' PHD abundance. The reversal of many of the PHD1 and PHD3 deletional phenotypes by crossing onto HIF2 but not HIF1 heterozygotes indicates that HIF2 remains a key factor in determining these phenotypes.

8.1.3.3 Implications of PHD abundance for 'hidden' tissue phenotypes

The study of abundance may also help to identify those tissues prone to developing other PHD dependent phenotypes which are either undeclared or unnoticed in existing PHD deletional models.

A PHD1 deletional phenotype was described in skeletal muscle (Aragones et al., 2007), and comparison of its PHD1 content with that of testis demonstrated a 3 fold excess in testis. This finding favoured there being a testis specific PHD1 phenotype which was undeclared under standard laboratory conditions. Such a phenotype remains elusive and this may in part relate to the greater abundance of PHD2 in testis which was 1.5 fold greater than its level in skeletal muscles. The greater abundance of PHD2 in testis may therefore mean that it is better placed to compensate for the loss of PHD1.

However the relative as well as absolute amounts of PHD isoforms may also be important determinants of phenotype and in this respect the excess of PHD2 over PHD1 in testis was only 4.5 fold compared to 24 fold in skeletal muscle. This would suggest that PHD1 made a greater contribution towards the total HIF hydroxylase capacity of testis compared to skeletal muscle, and also that relatively less PHD2

would be available to compensate for the loss of relatively more PHD1 in testis compared to skeletal muscle, favouring there being a testis specific PHD1 deletional phenotype.

Clearly testis and skeletal muscle are different tissues and the impact of relative or absolute PHD isoform abundance on phenotype development may vary between different tissues. Nonetheless the study of abundance would strongly favour there being a testis dependent PHD1 phenotype which has yet to be declared. In this context it is interesting to note that the PHD1 skeletal muscle phenotype was not recognised under resting conditions and became evident only under ischaemic stress. It is possible that a testis dependent phenotype may be revealed under conditions of ischaemic stress. Testicular ischaemia occurs in the context of testicular torsion and assessment for a PHD1 related phenotype of ischaemic resistance may be of medical relevance.

The study of abundance may indicate the existence of a PHD2 deletional phenotype which remains undeclared in skeletal muscle. This is because skeletal muscle expressed only marginally more PHD2 than kidney. While kidney did develop a PHD2 deletional phenotype, the same was not true of skeletal muscle and this may be due to the compensatory effects of a 4 fold greater amount of PHD3 in skeletal muscle compared to kidney, as well as its expression of PHD1. This possibility could be assessed further by assessing PHD1/3 deletional animals for a skeletal muscle phenotype.

The study of abundance may also provide insights into hidden PHD3 related phenotypes. The findings of this doctoral study indicated that in addition to the SCG, PHD3 was also abundantly expressed in heart and skeletal muscle however while SCG developed a PHD3 deletional phenotype, none have been reported in heart or skeletal muscle. Comparing skeletal muscle, heart and SCG the abundance of PHD2 was 3.4, 2.3 and 1.3 fold more than PHD3 in each. Therefore although PHD3 was of abundance in all three tissues its contribution towards total tissue hydroxylation capacity was greatest in SCG and its loss would therefore be more likely to have a greater impact in SCG leading to sympathetic but not cardiac or skeletal muscle phenotypes. This relationship could be further tested by cross breeding PHD3-/- animals onto a PHD2 heterozygous background. The lesser levels of PHD2 in crossed animals may be insufficient to compensate for PHD3 loss thereby allowing additional PHD3 dependent cardiac and skeletal muscle phenotypes to manifest. The greater expression of PHD1 in skeletal muscle compared to heart may also provide a degree of compensation favouring a cardiac rather than skeletal muscle phenotype on this genetic background. Another approach to determining the significance of each PHD isoform would be to use Cre-recombinase methods, under control of the α-Myosin Heavy Chain promoter or skeletal muscle actin promoter to enable specific targeted deletion of given isoforms in cardiac and skeletal muscle respectively.

The study of abundance may also help to identify tissues more prone to developing double deletional phenotypes such as those reported in relation to PHD1/3 (Takeda et al., 2008). In this study PHD1/3 double deletion resulted in a phenotype of moderate erythropoiesis secondary to increased Epo production in the liver. The abundance of PHD1 and PHD3 in testis and skeletal muscle would suggest these

tissues may contain hidden double deletional phenotypes, and it is possible that the reason they failed to manifest is due to compensation by PHD2. The study of abundance demonstrated that skeletal muscle and testis contained respectively 1.3 and 1.8 fold more PHD2 compared to liver, which may have proved sufficient to compensate for the loss of PHD1 and PHD3. It would be possible to test this hypothesis by further reducing tissue PHD2 content in these tissues by breeding PHD1/3 deletional animals onto a PHD2 heterozygous background. Under such conditions, the further reduction in skeletal muscle and testis PHD2 may be sufficient to prevent PHD2 compensation from taking place, thereby allowing double deletional phenotypes to manifest in these tissues.

8.1.4 Speculation regarding the impact of tissue PHD abundance on tissue HIF regulation

Given the central role of PHD's in HIF regulation the differences in their relative abundance demonstrated here is at some level, likely to impact on tissue HIF regulation. In cultured cells all PHD's contribute towards regulation of HIF1 and HIF2 but preferences do exist. PHD2 was shown to favour degradation of HIF1 over HIF2, whereas PHD 1 and 3 favour HIF2 degradation over that of HIF1 (Huang et al., 2003; Appelhoff et al., 2004).

8.1.4.1 PHD2 abundance and tissue HIF regulation: a speculative analysis

The demonstration that transient knock down of PHD2 was sufficient to promote expression of normoxic HIF1 in cell lines defined PHD2 as the principal regulator of normoxic HIF1 (Berra et al., 2003; Appelhoff et al., 2004). The abundance of tissue PHD2 demonstrated in this doctoral study may therefore have a greater impact on

tissue HIF1 compared to HIF2 regulation in a manner in keeping with that previously described in cell lines. It would be possible to test this hypothesis by demonstrating greater reversal of the previously described PHD2 dependent phenotypes, on a HIF1+/- compared to HIF2+/- background.

8.1.4.2 Impact of PHD2 abundance in relation to tissue HIF2: a speculative analysis

The abundance of tissue PHD2 may also have implications for tissue HIF2. Throughout the range of tissue oxygen tensions PHD2, by virtue of its greater specificity for HIF1, may lead to there being a relative excess of tissue HIF2 over HIF1. Such a scenario is very much in keeping with early findings in the field which demonstrated that in cell lines HIF2 was expressed more abundantly than HIF1 under conditions of mild to moderate hypoxia (Wiesener et al., 1998).

We speculate that in such a scenario the relative abundance of HIF2, if left unchecked, would more readily promote HIF2 dependent gene activation and argue in favour of a need for additional processes specifically aimed at suppressing HIF2 gene transcription. The simplest approach to achieve this would be for tissues to express more PHD1 or PHD3, which by virtue of their greater specificity for HIF2 (Appelhoff et al., 2004), would promote its degradation over that of HIF1. However the findings of this doctoral study indicate that these isoforms were expressed in relatively few tissues and at relatively low levels arguing against this method of HIF2 regulation. This dearth of tissues expressing PHD1 and 3 would favour there being other mechanisms aimed specifically at limiting HIF2 activity. In this context it is interesting to note that in many cell lines HIF2 specific regulatory processes have

been described such as the titratable HIF2 transcriptional repressor (Hu et al., 2006), as well as reduced HIF2 nuclear localisation (Park et al., 2003). It is possible that such HIF2 specific repressor elements may serve as 'physiological buffers' to limit the impact of a relative excess of HIF2.

The greater abundance of tissue PHD2 may also hint at a scenario in which hydroxylation has a greater impact on tissue HIF1 compared to HIF2. While hydroxylation clearly also regulates HIF2, the relative dearth of tissues expressing PHD1 and 3 may favour a lesser role for hydroxylation in ultimately determining HIF2 compared to HIF1 gene activation in tissues. Instead, the activity of HIF2 titratable repressor mechanisms described may have a greater impact on which HIF2 dependent genes are transcribed in any given tissue. This hypothesis could be tested once the molecular identity of the titratable repressor has been determined.

8.1.4.3 Impact of PHD1 and PHD3 abundance on tissue HIF: a speculative analysis

The study of abundance demonstrated that both PHD1 and PHD3, while not achieving the levels of expression of PHD2, were of abundance in selected tissues. In such tissues it could be argued that the presence of these isoforms, by virtue of their greater specificity for HIF2, would allow hydroxylation to play a greater role in HIF2 regulation. The findings of this doctoral study demonstrated that sympatho-adrenal axis, testis, skeletal muscle and heart expressed a greater abundance of either PHD1 or 3 and it is of interest that the HIF2 deletional phenotypes described to date relate mostly to this cluster of tissues. Constitutional HIF2 deletion resulted in a sympatho-adrenal phenotype (Tian et al., 1998), a finding which was pertinent to the abundance

of PHD3 in this tissue. Furthermore the sympatho-adrenal phenotype of PHD3-/- mice was reversed by crossing onto a HIF2 but not HIF1 heterozygous background (Bishop et al., 2008). The PHD1 dependent phenotype of skeletal muscle resistance to ischaemic stress was also reversed on a HIF2 but not HIF1 heterozygous background (Aragones et al., 2007) and together with the findings of this doctoral study would suggest that the abundance of tissue PHD1 and PHD3 formed the basis for the close relationship between HIF2 and these tissue phenotypes.

These findings would therefore allude to a central role for HIF2 in generating the PHD1 and PHD3 deletional phenotypes discussed. Such a scenario would necessitate HIF2 having a greater role in gene transcription in the setting of tissues with a greater abundance of PHD1 or PHD3. Mechanistically however the greater abundance of PHD1 and PHD3 in these tissues would be expected to promote HIF2 degradation through the range of oxygen tensions arguing in favour of there being relatively low levels of HIF2. Nonetheless the demonstration of reversal of PHD1 and PHD3 phenotypes by crossing onto HIF2 heterozygous genetic backgrounds would argue, that HIF2, despite being of a lesser abundance, would remain functionally significant. Such a scenario of low HIF2 levels promoting phenotypically significant levels of gene transcription would be difficult to reconcile if the HIF2 titratable repressor previously described were active. Indeed a prerequisite for this scenario would be for HIF2 repressor mechanisms to be specifically reduced in tissues expressing an abundance of PHD1 or PHD3.

8.1.5 Implications of PHD abundance for drug design and therapeutics

Deletional models have helped to clearly demonstrate the therapeutic potential and tolerability of PHD modulation and the use of PHD modulation for the treatment of

anaemia, liver and skeletal muscle disease will no doubt become an area of intense scientific study. There are considerable differences between manipulating a protein at the genetic level and through drug based strategies. While genetic manipulation of a protein can, on the whole, achieve considerable protein knock-down in a number of different tissues, the ability of a drug to achieve a similar effect will depend on a number of factors. These include drug absorption, first pass metabolism, lipid solubility, renal excretion, half-life and tissue expression of the target protein.

From the perspective of tissue expression, this doctoral study has identified a number of important characteristics of PHD enzymes that are likely to be of importance for future drug design strategies. Firstly a number of different tissue isoforms of each PHD were demonstrated and it remains to be established if each isoform equally regulates HIF or indeed non-HIF hydroxylation targets. Establishing this would be of particular importance from a therapeutic perspective as PHD modulators may need to be designed against each isoform to optimise a given therapeutic effect.

A further important finding was that PHD2 was the most ubiquitously and abundantly expressed PHD isoform. Therefore modulation of PHD2 may affect a range of other tissues in either a detrimental or therapeutic way. The study of abundance would therefore support a dedicated programme to assess for such effects. PHD2 abundance was found to vary between different tissues and this finding may help to predict those tissues which may be most prone to such changes in the context of PHD2 modulation. Liver and kidney expressed the least amount of PHD2 which may make them particularly prone to the effects of PHD2 modulation. In this respect

it is interesting that a recent trial of a PHD modulator was discontinued due to a death resulting from fulminant hepatic failure (C. Pugh, personal communication, 2011), but after investigation the study has been resumed.

The relative normality of the PHD2 heterozygous state, which occurred despite a reduction in PHD2 protein abundance, would suggest that PHD2 may be expressed in excess of the amount required for baseline function of a laboratory animal. From a therapeutic perspective this finding would suggest that considerable suppression of PHD2 is likely to be required to achieve a biological effect. This is an area which requires further study particularly given that PHD2 heterozygous mutation associated polycythaemia has been reported in a number of human kindred.

The study of abundance would suggest that further therapeutic strategies may be designed around modulation of PHD3 in skeletal muscle, heart and tissues of the sympatho-adrenal axis. Similarly skeletal muscle, testis and liver are likely to be influenced by PHD1 modulators. A PHD1 related testicular and PHD3 related myocardial and skeletal muscle phenotypes may be 'hidden' but may become declared either in a therapeutic or detrimental manner through the use of PHD modulators. Modulators of PHD1 activity would be predicted to have an effect on PHD1 function in liver and skeletal muscle but because of the abundance of PHD1 in testis, may also have untold effects on male fertility. As such the use of PHD1 modulators in particular may need to be generated to specifically target liver and/or skeletal muscle forms of PHD1.

Therapeutic strategies based on co-modulation of PHD isoforms are being devised. Proof of the viability of PHD1 and PHD3 co-deletion has been demonstrated in an animal model (Takeda et al., 2008) and further studies will be needed to assess if combined deletion of other isoforms can also be achieved. Such combined deletions may impact on 'hidden' phenotypes, particularly those which may fail to manifest due to the compensatory effects of other PHD isoforms. PHD1/3 deletional animals may be more prone to developing a cardiac and skeletal muscle phenotype and studies of duel chemical modulators may choose to place particular emphasis on these tissues.

The abundance of PHD2 in tissues may also have implications for phenotypes detected in the context of PHD1 or 3 deletional models. Several tissues which develop a phenotype in the context of PHD1 or 3 deletion also appear to express relatively less PHD2. This gives rise to the possibility that the PHD1 dependent resistance of skeletal muscle and liver to ischaemic stress and PHD3 dependent phenotype of sympatho-adrenal hyperplasia and hypofunction may be further modulated by co-altering PHD2 expression.

8.2 Discussion relating to the expression of PHD3 in rat sympatho-adrenal tissues

During this doctoral study, a number of forms of PHD3 were found to be abundantly expressed in developing and adult rat sympathetic nervous system tissues. These included previously characterised adult forms of PHD3 as well as a number of other species which may represent novel forms of PHD3. The significance of these findings will be discussed in the following sections.

8.2.1 Discussion relating to stable expression of adult forms of PHD3 during the period of naturally occurring neuronal death

Previous studies demonstrated that induction or over-expression of PHD3 was sufficient to promote apoptosis of sympathetic neurons (Lipscomb et al., 1999; Lipscomb et al., 2001; Straub et al., 2003). Therefore my finding that there was an abundance of adult forms of PHD3 during the period of postnatal developmental apoptosis was unexpected. It gave rise to the possibility that the adult forms of PHD3 identified here lacked the pro-apoptotic properties which had been previously assigned to rat PHD3 as a whole. This may either be because these forms were different to the apoptosis promoting forms identified in previous studies or because their activity could be altered without concomitant changes in abundance.

Recent studies demonstrated that a reduction in activity of the mitochondrial enzyme SDH, through build-up of succinate, could inhibit the activity of PHD3 (Lee et al., 2008). It is therefore possible that although the abundance of PHD3 was similar in developing and adult SCG, its activity may be altered through interactions with other enzyme pathways. The promotion of PHD3 mediated apoptosis without a concomitant change in abundance would necessitate a pathway leading to its activity being increased and while processes leading to a reduction of PHD3 activity have now been described (Lee et al., 2008), it remains unknown if enzyme pathways capable of promoting PHD3 activity exist. Instead of interplay with enzyme pathways, it is also possible that tissue oxygenation *per se* may influence the activity of PHD3 during this developmental window. Processes such as transition from foetal to adult circulation, lung maturation, and conversion from foetal to adult haemoglobin could serve to improve neurite oxygenation, in turn enhance PHD3 activity to a level sufficient to promote apoptosis while maintaining stable PHD3 protein abundance. It

is interesting that a change in oxygenation is a recognised trigger for developmental apoptosis of retinal photoreceptors during the postnatal period (Maslim et al., 1997) and it is possible that similar changes in oxygenation may play a role in the context of sympathetic neurite development. This possibility could be tested using the tetracycline induced PHD3 PC12 cell line (Straub et al., 2003) to achieve stable levels of PHD3 and compare rates of apoptosis under different oxygen tensions. An animal model could also be used by assessing SCG cell number from postnatal animals delivered and maintained under conditions of hypoxia, the expectation being that they would have greater numbers of sympathetic neurons compared to animals from a parallel study in normoxia.

8.2.2 Discussion relating to the developmental expression of additional bands in proximity to the 50KDa species of PHD3

Two further bands were noted to emerge in close proximity to the 50KDa species of PHD3. The intensity of these bands increased with maturity and were static from P14 into adult life. It is interesting that these changes correlate well with the time course of rat sympathetic neurone developmental apoptosis which declines after the first postnatal week (Wright et al., 1983) and may therefore also have bearing on processes which lead to PHD3 mediated apoptosis. In particular, it is possible that these additional 50KDa species may function to reduce PHD3 activity towards the end of developmental apoptosis and provide a further explanation for how apoptosis could be affected in the context of relatively stable PHD3 abundance.

As discussed earlier in relation to mature tissues, a number of processes such as alternate start sites, post-translational modification or multiple promoter activity can produce different species of a protein. It is possible that these processes also have

bearing on the developmental species of PHD3 detected here. Although several splice forms of human PHD3 have been described (Hirsila et al., 2003), as yet, none have been described in rat. It is however possible that there may exist PHD3 splice forms expressed only in developing rat tissues. Further assessment of this possibility would require generating cDNA libraries of developing tissues with particular emphasis on those of the sympathetic lineage. It is of interest that bioinformatics analysis predicts 2 tyrosine phosphorylation sites, within exons 2 and 3 of rat PHD3, which may also contribute towards different species of PHD3. This could be tested by immunoblot analysis for a loss of additional bands after phosphatase treatment of developing SCG extracts. There may also exist other PHD3 promoters apart from those already described (Menzies et al., 2004) which may be particularly active in developing tissues, leading to additional developmental forms of PHD3.

8.2.3 Discussion relating to the expression of 109KDa species in PHD3 immunoblots of developing tissues

Another explanation for the stable expression of adult forms of PHD3 in developing sympathetic tissues relates to the possibility that they may be relatively weak promoters of apoptosis and instead there exist other apoptosis promoting forms of PHD3. Although previous studies relating to sympathetic lineage apoptosis demonstrated that induction of adult forms of PHD3 occurred during apoptosis and their knock-down suppressed it (Lipscomb et al., 1999; Lipscomb et al., 2001; Lee et al., 2005), they do not preclude the possibility of other functionally significant forms of PHD3 occurring in tissues.

In this context it is interesting to note that immunoblots using a single anti-PHD3 antibody demonstrated the presence of 109KDa species in developing sympathetic neurons. The second anti-PHD3 antibody used on the same developing tissue extracts produced extensive cross-reactive signal which limited its use on these extracts. As such it remains unknown at this stage if this 109KDa species represents a form of PHD3 or non-specific signal. It is however of interest that the expression of this species gradually decreased as neurons matured, and was present at very low levels in adult tissues as well as in extracts of PC12 cells which were used as a positive control. The decrease in expression of this species correlates well with that described for the postnatal decline in rate of developing neurite apoptosis (Wright et al., 1983) and such correlative findings give rise to the possibility that the 109KDa species may be another developmental form of PHD3. Further studies will be required to determine the exact nature of this species, and the demonstration of a concordant signal with a new anti-rat PHD3 antibody may allow it to be formally assigned to PHD3. A number of other approaches could be used in future work to validate this signal. These include immunoblot comparison of wild type and PHD3-/- mouse tissues, once an anti-PHD3 antibody capable of detecting mouse tissue PHD3 becomes available. Another approach would be to repeat the previously described cell culture demonstrating sympathetic neuronal apoptosis in the context of NGF withdrawal and assessing for expression of 109KDa species. Finally, mass spectrometry of developing rat tissue extracts could be compared with that of adult tissues to determine if the 109KDa species represent a novel form of PHD3, although generating sufficient extracts of developing SCG for mass spectrometry analysis may prove challenging. Recent studies have indicated that PHD3 is part of the aggreasome like structures (Rantanen et al., 2008), and as such it is possible that the 109KDa species could represent a

tightly bound complex of PHD3 and other proteins which have the ability to promote neuronal apoptosis.

8.2.4 Discussion relating to changes in the subcellular expression of PHD3 during development

The immunoblot study of PHD3 in developing SCG was complemented with an immunohistochemical analysis of the same tissues. This study demonstrated that in contrast to adult sympathetic neurons, developing sympathetic neurites strongly expressed cytoplasmic PHD3 signal. The intensity of this signal was found to gradually decline with maturity and correlated with the time course of naturally occurring apoptosis. In this context the demonstration that subcellular localisation of PHD2 could impact on its ability to regulate HIF1 (Yasumoto et al., 2009), was an important finding. It sets a precedent for the possibility that the activity of other PHD enzymes could be similarly altered. In this regard the finding that PHD3 mediated apoptosis is dependent on mitochondrial function (Lipscomb et al., 2001; Straub et al., 2003) may also be of relevance. A scenario could therefore be envisaged whereby developing sympathetic neurons, with a greater cytoplasmic PHD3 abundance could, by virtue of greater interplay with mitochondria, be more prone to PHD3 dependent apoptosis. In contrast the relative lack of cytoplasmic PHD3 in adult sympathetic neurons may render their PHD3-mitochondrial protein interaction below the threshold required to achieve apoptosis. A change in PHD3 subcellular localisation may provide another mechanism to reconcile how apoptosis could occur despite the relatively stable expression of recognised forms of PHD3.

Although a number of previous studies had established the ability of PHD3 to be expressed in different cellular compartments (Soilleux et al., 2005; Willam et al.,

2006; Metzen et al., 2002), temporal changes in PHD3 subcellular expression had not been reported and as such these findings represent a novel aspect of PHD3 biology. Mechanistically the changes in subcellular distribution could occur from cytoplasmic to nuclear PHD3 shuttling, turnover of a cytoplasmically expressed form of PHD3 or a combination of the two. A mitochondrial localisation signal has already been identified in the first 25 amino acids of rat PHD3 (Lipscomb et al., 2001) and it is possible that the forms of PHD3 reported here may contain localisation signals to other cellular compartments. The presence of different forms of PHD3 in different cellular compartments may also be in keeping with its reported role in formation of subcellular aggregates (Rantanen et al., 2008).

The semi-quantitative approach taken during my Immunohistochemical study of developing rat SCG allowed PHD3 signal to be quantified and compared at different developmental time points. In addition to demonstrating a clear decline in cytoplasmic PHD3, quantitation also indicated that there was a less rapid decline in nuclear PHD3 content over the same time course. If the decline in cytoplasmic PHD3 was predominantly due to shuttling from cytoplasm to nucleus then nuclear PHD3 content would be expected to have increased. Therefore these findings would argue in favour of a dominant role for PHD3 turnover rather than compartmental shuttling to account for the temporal changes in subcellular expression. It is possible to speculate that such a process of turnover may also relate to the observed reduction in developmental forms of PHD3 noted by immunoblot. These hypotheses could be assessed further by generating nuclear and cytoplasmic extracts of developing rat SCG's and comparing changes in their PHD3 content over time. This approach however may prove technically challenging because of the limited amount of tissue

extract that can be generated from a developing SCG. An alternative approach would be to assess these effects in a cell line. In this context the PC12 cell line could be assessed to determine if there was evidence of changes in its nuclear and cytoplasmic PHD3 content under different NGF concentrations and if blockade of nuclear localisation or inhibition of protein turnover would alter the PHD3 content of nuclear and cytoplasmic compartments. It should however be borne in mind that such cell lines have been generated specifically through selective pressures against apoptosis and their response to apoptotic triggers may differ from that of normal sympathetic lineage cell types.

8.3 Insights gained into the development of sympatho-adrenal neoplasia from the study of PHD3 expression

The study of PHD3 expression may also provide additional insights into PHD3's role in tumourigenesis as outline in figure 3 of the introduction to this thesis. Mutations of SDH, FH, VHL and NF1 were shown to suppress the activity of PHD3 and thereby PHD3 mediated apoptosis. Reduced sympathetic neuronal apoptosis was hypothesised to promote survival of rogue neurites which had the potential to undergo neoplastic transformation in later life (Lee et al., 2005). This work demonstrated a functional interaction took place and it remains to be established if direct protein-protein contact or protein co-localisation is also necessary for these functional outcomes.

The importance of this pathway lies in its ability to link genes with known sympatho-adrenal tumour potential through a single common pathway. The recent demonstration that PHD3 has a central role within this pathway gives rise to the possibility that it too could impact on tumourigenesis of sympatho-adrenal tissues.

However, unlike the other tumour syndromic genes depicted here, mutations of PHD3 have not so far been identified in or been linked to sympatho-adrenal neoplasia.

The study of PHD3 abundance carried out during this doctoral study demonstrated several tissues species which may represent novel forms of PHD3. A dynamic change in the expression of several of these species was noted to take place during the period of naturally occurring developmental apoptosis. Although these findings are purely correlative, they give rise to the possibility that these forms may have a role as mediators of PHD3 dependent apoptosis. They highlight the need to characterise more clearly the species identified here, and also give rise to the possibility that a selection bias may have contributed towards the lack of identifiable mutant PHD3 forms linked to sympathetic lineage tumourigenesis.

One way to address this possibility would be to compare and contrast the expression of all discernible PHD3 species in normal and pathological sympathetic lineage tissues. Differences in the expression of potentially novel forms of PHD3 between normal tissues and those derived from phaeochromocytomas and paragangliomas may suggest more than a correlative relationship. As part of this doctoral study an immunohistochemical assessment of PHD3 in a selection of archival human phaeochromocytomas was carried out. This demonstrated heterogeneous patterns of subcellular PHD3 localisation, and it was not clear if, and the degree to which, such differences were due to differences in sample preparation and storage or a reflection of underlying disease processes. While immunoblot comparison was considered more quantitative, sourcing pathological samples suitable for immunoblot analysis proved challenging. The PC12 cell rat phaeochromocytoma

cell line was an alternative source of sympathetic lineage neoplastic study material and studies relating to PC12 cell PHD3 will be discussed next.

8.3.1 Insights gained into the biology of sympatho-adrenal neoplasia from the study of PC12 cell PHD3

The subtle differences observed between the mobility of doublet 27KDa species of PHD3 in rat SCG and PC12 extracts were of interest from the perspective of altered PHD3 function. In an attempt to gain insights into processes underlying this difference, the sequence of the 27KDa species of PHD3 in PC12 cells was assessed and compared to that of the known wild type rat PHD3 sequence. No differences in sequence were detected arguing against splice variation or sequence mutation as the cause of the observed difference in mobility. Alternative translation initiation was a further process which could account for a difference in mobility and in this respect, the third rat PHD3 methionine is known to be located 6 amino acids downstream of the second and could act as a site for translation initiation, producing a predicted difference in molecular weight of 680Da, compatible with the subtle difference in size of the 27KDa species of PHD3 observed here. Future studies could assess this possibility further by using site directed mutagenesis to alter the second translation initiation site and assess if this leads to correction of migration of immunoblot species. A further process which could account for this difference in size could be post-translational modification and it may be possible that a form of modification occurs in normal tissues which was absent or reduced in PC12 cells. Phosphorylation is a common form of post translational modification and its role in producing a difference in mobility could be assessed by phosphatase treatment of PC12 cells to assess for a change in immunoblot mobility.

8.3.2 Insights gained into the predisposition of different autonomic nervous system tissues to neoplastic transformation through the study of PHD3 expression

Although united by development of phaeochromocytomas and paragangliomas, the frequency of each neoplasm varies from one tumour syndrome to another. Mutations of RET, NF1 and VHL are associated primarily with phaeochromocytomas while those of SDHB, C and D predominantly develop paragangliomas (Dahia et al., 2006). Furthermore paragangliomas, despite consisting of sympathetic nervous system tissues, can arise from the parasympathetic Jugular-nodose ganglion complex (Ellison et al., 2001). The basis for these different predispositions to tumourigenesis remains unclear, particularly because many tumour genes are broadly expressed within the sympatho-adrenal axis as well as other tissues (Takaya et al., 1996; Santoro et al., 1990).

8.3.2.1 PHD3 expression in relation to neoplasms of parasympathetic tissues and carotid body

The nodose ganglion is known to contain scattered NGF sensitive neurons (Forgie et al., 2000), however lack of a nodose related phenotype in mice with constitutional NGF deletion (Crowley et al., 1994), suggests that this population was relatively small. The nodose ganglion is also known to contain scattered tyrosine hydroxylase expressing cell populations (Kummer et al., 1993). We observed that PHD3 was broadly expressed throughout nodose neurons in both TH expressing and lacking neuronal populations. Given the interplay between PHD3 and pathways leading to tumourigenesis, it may be possible that those nodose neurons co-localising PHD3 and TH may form the nidus for neoplastic transformation within this ganglion.

PHD3 and TH were also found to co-localise in type I cells of the carotid body. It is therefore possible that in keeping with that of the nodose ganglion, PHD3 and TH co-localising cells in the carotid body, may also form a nidus for neoplastic transformation.

8.3.2.2 PHD3 expression in relation to syndromic neoplasms of the autonomic nervous system

Immunoblot of SCG and adrenal gland extracts demonstrated that a 50KDa species of PHD3 was predominantly expressed in adrenal gland while the 27KDa species was more strongly expressed in SCG. It is possible to speculate that VHL, RET and NF-1 mutations may have greater interplay with the 50KDa than 27KDa PHD3 species, thereby increasing the tumourigenic potential of chromaffin cell rich tissues of the adrenal gland over those of the chromaffin cell poor, sympathetic chain. Conversely, SDH mutation may impact more on the 27KDa species of PHD3 favouring tumourigenesis in sympatho-neuronal lineage rich tissues of the sympathetic chain over those of chromaffin cell rich tissues.

Further insights into such preferential interplay could be assessed in future studies by a number of different methods. A direct interaction between different PHD3 forms and syndromic tumour genes could be evaluated by co-localisation studies in PC12 cells, assessing if VHL, RET and NF-1 co-localised more with the 50KDa form of PHD3, while SDH co-localised more with the 27KDa form. The impact of gene mutation on any putative co-localisations could also be assessed by transfecting PC12 cells with mutant cDNA's for each tumour gene and assessing for a change from the wild type pattern of putative co-localisation.

The possibility that modulation of apoptosis may occur through indirect, functional interactions between these gene products and different forms of PHD3 also needs to be considered. This possibility could be explored in future studies by assessing the impact on apoptosis rates of specific siRNA against each tumour gene, the expectation being that SDH knock down may have greater effect in cell lines rich in the 27KDa form of PHD3, while VHL, NF-1 and RET gene product knock-down may modulate apoptosis more in cell lines expressing predominantly the 50KDa form of PHD3.

8.3.2.3 PHD3 expression in relation to development of adrenal and extra-adrenal phaeochromocytomas

The study of PHD3 localisation may help to shed light on other elements of chromaffin-lineage neoplasia. The vast majority of phaeochromocytomas are known to originate from adrenal compared to extra-adrenal sites. This finding is likely to reflect the greater abundance of adrenal compared to extra-adrenal chromaffin cells. It is nonetheless interesting that immunohistochemical analysis demonstrated very little PHD3 in extra-adrenal chromaffin cell populations of the P2 rat. The absence of PHD3 from extra-adrenal chromaffin cells may render them less prone to the effects of mutagenic genes linked to PHD3 mediated apoptosis and may hint at another reason for phaeochromocytomas occurring less frequently at extra-adrenal sites.

In the future it may be possible to study this possibility by comparing rates of apoptosis after transfection of PHD3 cDNA into an extra-adrenal chromaffin cell derived cell lines. To the best of our knowledge, such cell lines do not currently exist. Difficulties generating and maintaining primary extra-adrenal chromaffin cell cultures are likely to make such studies using primary cells, extremely challenging.

8.3.2.4 PHD3 expression in relation to syndromic tumour predispositions of tissues outside those of the sympatho-adrenal axis

Tissues outside the sympatho-adrenal axis can also be involved in these tumour syndromes. VHL disease is linked to formation of haemangioblastomas and renal cell carcinomas, while mutation of RET results in the syndrome of multiple endocrine neoplasia (MEN) which is also associated with hyperparathyroidism in the type 2A variants while being linked to Marfanoid habitus in type 2B. Mutations of NF1 are additionally associated with neurofibroma formation, CNS tumours and leukaemias (Dahia et al., 2006) and the reason for these additional tumour predispositions remain unclear. The study of PHD abundance provides a number of other correlative observations which may have bearing on these findings. Haemangioblastomas and renal cell carcinomas form part of the spectrum of VHL disease, and the study of PHD abundance demonstrated that of the tissues studied, liver and kidney expressed least amounts of PHD2. The central role of PHD2 in setting normoxic HIF levels has been established (Appelhoff et al., 2004) and it is possible to speculate that the lesser abundance of PHD2 in these tissues combined with their known regional hypoxic gradients may, in the context of VHL mutation, be sufficient to favour HIF dysregulation leading to neoplastic transformation in these compared to other tissues. Haemangioblastoms also occur in the cerebellum and retina and the basis for their predisposition remains unclear.

The abundance of PHD2 noted in brain would be at odds with the proposed role of PHD2 in the process described, serving to highlight the complexity of the processes involved. The role of PHD2 in this process could be assessed at the whole animal level by cross-breeding PHD2 heterozygous or conditional knock-out mice with *VHL*

deleted mice and assessing for enhanced tumourigenesis in tissues outside the sympatho-adrenal axis.

8.4 Functional insights gained through collaborative animal studies into PHD3's role in the sympatho-adrenal axis

The abundance of PHD3 within tissues of the sympatho-adrenal axis led to a series of collaborative studies to characterise the function of PHD3 in this tissue. The production of mice with constitutional deletion of PHD3 allowed a putative PHD3 related sympatho-adrenal phenotypes to be studied. Comparison of wild type and PHD3-/- mice demonstrated hyperplasia of the SCG, adrenal medulla and carotid body of PHD3-/- mice, a finding very much in keeping with impaired developmental apoptosis. Further studies carried out in parallel with this doctoral study demonstrated systemic hypotension and impaired cardiovascular responses in PHD3-/- compared to wild type animals indicating that hyperplasia of key sympatho-adrenal tissues was linked with sympathetic hypo-function (Bishop et al., 2008). This was felt in part to be due to abnormal target organ innervation, possibly due to survival of those neurons which would normally undergo apoptosis in the presence of PHD3. Further studies demonstrated that this phenotype could be reversed by breeding onto a HIF2+/- but not HIF1+/- background. These findings would also be in keeping with the previously described phenotype of sympathetic hypofunction in HIF2 deletional mice (Tian et al., 1998), and taken together serve to strengthen the relationship between PHD3 and HIF2 at the whole animal level.

8.5 Other emerging roles for PHD3 within the sympatho-adrenal axis

The recent finding that PHD3 regulates the β2 adrenoreceptor (Xie et al., 2009) adds a further level of complexity to its role in sympathetic tissues. In this work, PHD3 activity in normoxia was found to promote degradation of the β2 adrenoreceptor thereby enhancing sympathetic neurotransmission under conditions of hypoxic stress. This receptor is predominantly expressed in vascular and bronchial smooth muscle but has also been reported in sympathetic neurons, where it augments signal transmission through the muscarinic receptor (Watson-Wright et al., 1991). It is therefore possible that PHD3 expressed in sympathetic lineage tissues may have additional roles in catecholamine receptor regulation. Such a scenario may hint at the existence of oxygen sensing feed-back loops at the level of chromaffin cells and sympathetic neurons which may serve to further modulate catecholamine responses during hypoxic stress. It is possible that the interplay between PHD3 and the β2 adrenoreceptor may also impact on the phenotype of sympathetic hypofunction in PHD3-/- mice, and this could be studied further by assessing cardiovascular responses in wild type and PHD3-/- animals during hypoxia.

8.6 The study of PHD3 expression in lung

Adrenergic transmission in the lung is known to be of importance particularly in relation to conditions associated with bronchospasm such as asthma. Given PHD3's emerging role in modulation of the β2 adrenoreceptor, its expression in lung was of interest and may hint at putative links between such disorders and PHD3. While the expression of PHD3 in vascular smooth muscle has been previously demonstrated, this doctoral study demonstrates that it is also expressed in pulmonary bronchial epithelium.

The role of PHD3 in bronchial epithelial lining could be studied by comparing the bronchodilator responses of wild type and PHD3-/- mice as well as their response to different forms of lung injury. Furthermore, expression of PHD3 in bronchial epithelium was also evident in E14 rat, suggesting that PHD3 could have an additional role in lung maturation which may merit future study. The relative abundance of PHD2 in lung, may indicate that a PHD3 related pulmonary phenotype is more likely to be evident on a mixed PHD3-/- and PHD2 +/- background.

8.7 Insights gained from the study of PHD3 expression in other peripheral nervous system tissues

Expression studies also demonstrated that PHD3 was abundantly expressed in neurons of the trigeminal ganglion (TG). Semi-quantitative IHC indicated that its expression within the trigeminal ganglion was very similar to that of sympathetic lineage neurons. The trigeminal ganglion is known to express an abundance of NGF sensitive neurons, and NGF deletional mice were found to have a significant reduction in TG size (Crowley et al., 1994). However, studies carried out in parallel with this doctoral study demonstrated that despite the abundance of TG PHD3, there were no differences in NGF dependent survival of explanted TG neurons from PHD3-/- and wild type mice (Bishop et al., 2008). Taken together these findings suggested that while apoptosis in the TG and sympathetic lineage were both NGF dependent, only the latter was also dependent on PHD3. Nonetheless the abundance of PHD3 in TG neurons gave rise to the possibility that PHD3 had functions in non-sympathetic lineage tissues which were distinct from its known role as a promoter of apoptosis. Such functions may relate to PHD3's role as a primary oxygen sensor and regulator of HIF. Recently the motor proteins KIF1Bα and KIF1Bβ were shown to be involved in the pathway leading to sympathetic neuronal apoptosis (Schlisio et al., 2008).

Interestingly, the KIF1B proteins are also known to be involved in more generic neuronal functions of mitochondrial and synaptic vesicle precursor transport (Nangaku et al., 1994; Zhao et al., 2001). The interplay between PHD3 and KIF1B proteins may therefore have multiple effects in different neuronal tissues and it is possible that in the context of TG, such a role may exist relating more towards synaptic vesicle function than apoptosis.

8.8 Insights gained from the study of PHD3 expression in the CNS

As part of this doctoral study the expression of PHD3 in CNS neuronal populations was also expressed. The finding that PHD3 was absent from TH expressing A1C1, A2C2 and locus coeruleus brain stem nuclei indicates that its expression was not generic to all sympathetic lineage neuronal types. However PHD3 was found to be expressed in some TH expressing cell populations of the substantia nigra, and further studies will be required to determine if PHD3 has an impact on pathologies of the substantia nigra such as Parkinson's disease. In this context it is interesting that multi-system atrophy is a neurological disorder characterised not only by Parkinsonian features but also by disturbances of autonomic function and the expression of PHD3 demonstrated during this doctoral study in the sympathetic nervous system and substantia nigra may be of relevance. It may be possible to assess the role of PHD3 in Parkinson’s disease by inducing parkinsonism in wild type and PHD3-/- mice using 1-methyl-4-phenyl-1,2,3,6-tetrahydropyridine (MPTP) based on previously established protocols (Jackson-Lewis & Przedborski., 2007).

PHD3 was also detected in regions of the hippocampus. Different hippocampal regions are known to have different sensitivities to ischaemic stress. In particular, the expression of PHD3 in the CA1 hippocampal subfield may have implications for the

know vulnerability of this region to ischaemic injury (Schmidt-Kastner et al., 1991). Studies of brain ischaemia using wild type and PHD3-/- mice could be used to study the effects of PHD3 in this and other brain regions further. The hippocampus is also affected in Alzheimer's disease. Abnormal protein aggregation has been implicated in the development of neuro-degenerative disorder such as Alzheimer's disease, Parkinson's disease, Huntingdon's chorea and amyotrophic lateral sclerosis (Ardley et al., 2004; Kopito et al., 2000; Garcia-Mata et al., 2002). Recent studies have demonstrated a role for PHD3 in aggresome formation (Rantanen et al., 2008), which may hint at a tentative mechanism to link PHD3 expression to these neurodegenerative disorders.

8.9 Achievements of this doctoral study and where they lead

This doctoral study validated a panel of antibodies with sensitivity and specificity for rodent PHD tissue proteins. Using these reagents it was possible to characterise PHD protein expression in different rodent tissues. The demonstration that PHD2 was by far the most abundant PHD protein isoform in tissues was in keeping with earlier studies of tissue PHD mRNA; the critical role of PHD2 demonstrated through gene deletional animal studies was also likely to be because of its ubiquitous distribution and greater tissue abundance.

This doctoral study also demonstrated selective expression of PHD1 and 3 proteins in rodent tissues and helped to guide phenotyping of respective tissues. These phenotypic studies in which I collaborated, demonstrated several novel phenotypes in skeletal muscle and sympathetic nervous system tissues. A psychometric analysis of hippocampal PHD3 expression was carried out in parallel with other PHD3 phenotypic studies and while a psychometric hippocampal PHD3 phenotype was not

observed, the possibility remains that hippocampal PHD3 may contribute to known regional differences in hippocampal resistance to ischaemic stress.

The study of PHD expression also provided insights into why, despite an abundance of specific PHD isoforms, testis and hippocampus failed to demonstrate deletional phenotypes and provided putative strategies to explore such 'hidden' phenotypes. The study of abundance suggests that both 'direct' and 'indirect' PHD deletional phenotypes exist, further serving to demonstrate the diverse roles of PHD isoforms in tissues. The findings of this study may in the future aid in drug design and therapeutics by identifying tissues in which putative PHD modulators may have therapeutic benefit.

The study of the developing sympathetic nervous system tissues has for the first time demonstrated temporal differences in PHD3 subcellular localisation which correlated with developmental apoptosis. This study went on to identify several species which may represent novel forms of PHD3 which may have bearing on developmental apoptosis and help to explain why conventional forms of PHD3 appeared stably expressed in developing and adult tissues. A difference in the relative abundance of different PHD3 isoforms was also observed between different sympatho-adrenal tissues, a finding which may have bearing on the different predispositions of sympatho-adrenal tissues to syndromic neoplasia.

The expression of PHD3 in the substantia nigra as well as sympathetic nervous system tissues may hint at a putative role in Parkinsons' disease and 'Parkinsons' plus' syndromes. Ways to explore these possibilities have been discussed. The expression of PHD3 in developing and adult bronchial epithelium was also

demonstrated, hinting at a potential role for PHD3 in disorders of bronchospasm such as lung allergy and asthma and. Ways to explore PHD3's role in lung have also been discussed.

Bibliography

Appelhoff, R., Tian, Y., Raval, R., Turley, H., Harris, A., Pugh, C., et al. (2001, September 10). Differential function of the prolyl hydroxylase PHD1, PHD2 and PHD3 in the regulation of hypoxia-inducible factor. *Journal of Biological Chemistry, 279*(37), pp. 38458-65.

Aragones, j., Schneider, M., Can Geyte, K., Fraisal, Bishop, T., Grosfeld, A., et al. (2008, Januray 6). Deficiency or inhibition of oxygen sensor Phd1 induced hypoxia tolerence by reprogramming basal metabolism. *Nature Genetics, 40*, 170-180.

Ardley, H., & Robinson, P. (2004). The role of ubiquitin-protein ligases in neurodegenerative disease. *Neurodegenerative Disease, 1*(2-3), 71-87.

Beckstead, R., More, J., & Norgren, R. (1980, March 15). The nucleus of the solitary tract in the monkey. *The Journal of Comparative Neurology, 190*(2), 259-82.

Berra, E., Benizri, E., Ginouves, A., Volmat, V., Roux, D., & Pouyssegur, J. (2003, August 15). HIF prolyl-hydoxylase 2 is the key oxygen sensor setting low steady-state levels of HIF-1alpha normoxia. *European Molecular Biology Organisation, 22*(16), pp. 4082-90.

Bishop, T., Gallager, D., Pascual, A., Lygate, C., de Bono, J., Nicholls, L. O.-S., et al. (2008, May). Abnormal sympathoadrenal development and systemic hypotension in PHD3-/- mice. *Molecular and Cellular Biology, 28*(10), 3386-400.

Blancher, C., Moore, J., & Talks, K. H. (2000, December 15). Relationship of hypoxia-inducible factor (HIF)-1alpha and HIF-2alpha expression to vascular endothelial growth factor induction and hypoxia survival in human breast cancer cell lines. *Cancer Research, 60*(24), pp. 7106-13.

Blouin, C., Page, E., Soucy, G., & Richard, D. (2004, February 1). Hypoxic gene activation by lipopolysaccharide in meacrophages: implication of hypoxia-inducible factor 1alpha. *Blood, 103*(3), pp. 1124-30.

Blouw, B., Song, H., Tihan, T., Bosze, J., Ferrara, N., Gerber, H., et al. (2003, August). The hypoxic response of tumours is dependent on their microenvironment. *Cancer Cell, 4*(2), pp. 133-46.

Bock. (1982). *Paraganglia.* Springer.

Bruick, R., & McKnight, S. (2001, November 9). A conserved family of prolyl-4-hydroxylases that modifiy HIF. *Science, 294*(5545), pp. 1337-40.

Bryant, J., Famer, J., Kessler, L., & Townsend, R. (2003). Phaeochromocytoma: The expanding Genetic Differential Diagnosis. *Journal of the National Cancer Institute, 95*(16), 1196-1204.

Bunn, H., & Poyton, R. (1996, July). Oxyten sensing and molecular adaptation to hypoxia. *Pysiology Reviews, 76*(3), pp. 839-85.

Carneiro, J. a. (1998). *Basic histopahology, a text and atlas.* (9th, Ed.) Appelton & Lange.

Cioffi, C., Liu, X., Kosinski, P. G., & Bowen, B. (2003, April aa). Differential regulation of HIF-1 alpha prolyl-4-hydroxylases genes by hypoxia in human cardiovascular cells. *Biochemical and Biophysical Research Communications, 303*(3), 947-53.

Cockman, M., Masson, N., Mole, D., Jaakkola, P., Chang, G., Clifford, S., et al. (2000, August 18). Hypoxia inducible factor-alpha binding and ubiquitylation by the von Hippel-Lindau tumour suppressor protein. *Journal of Biological Chemistry, 275*(33), pp. 25733-41.

Compernolle, V., Brusselmans, K., Acker, T., Hoet, P., Tjwa, M., Neck, H., et al. (2002, July). Loss of HIF-2 alpha and inhibition of VEGF impar fetal lung maturation , whereas treatement with VEGF prevents fatal respiratory distress in premature mice. *Nature Medicine, 8*(7), pp. 702-10.

Couland, R. (1965, April). Electron microscopic observation on the structure of the rat adrenal medulla. *Journal of Anatomy, 99*(Pt2), pp. 255-72.

Coupland. (1965). *The Natural History of the Chromaffin Cell.* Longmans.

Coupland, R. (1968). Development of chromaffin tissue in the rabbit. *Journal of Anatomy, 102,* pp. 425-455.

Cramer, T., & Johnson, R. (2003, June). A novel role for the hupoxia inducible transcription factor HIF-1 alpha: critical rgulation of infalmmatory cell function. *Cell Cycle, 2*(3), pp. 192-3.

Crowley, C., Spencer, S., Nishimura, M., Chen, K., Pitts-meek, S., Armaninl, M., et al. (1994, March). Mice lacking nerve growth factor display perinaal loss of sensory and sympathetic neurons yet develop basal forebrain cholinergic neruons. *Cell, 76*(6), 1001-1011.

Czyzyk-Krzeska, M., Bayliss, D., Lawson, E., & Milhorn, D. (1992, April). Regulation of tryosine hydroxylase gene expression in the rat carotid body by hypoxia. *Journal of Neurochemistry, 58*(4), 1538-46.

Dahia, P. (2006, January). Evolving concepts in phaeochromocytoma and paraganglioma. *Current Opinions in Oncology, 18*(1), 1-8.

Davies, D. (1978). Neuronal number inthe superior cervical ganglion of the neonatal rat. *Journal of Anatomy, 127*(Pt 1), 43-51.

Deacon, R. (2006, August). Assessing nest building in mice. *Nature protocols*, pp. 1117-1119.

Deacon, R. (2006, June). Burrowing in rodents: a sensitive method for detecting behavioral dysfunction. *Nature Protocols*, pp. 118-121.

Deacon, R. (2006, June). T-maze alternation in the rodent. *Nature Protocols*, pp. 7-12.

Dupuy, D., Aubert, I., Duperat, V., Petit, J., Taine, L., Stef, M., et al. (2000, November 1). Mapping, characterisation and expression analysis of the SM-20 human homologue, c1orf12 and identification of a novel related gene, SCAND2. *Genomics, 69*(3), pp. 348-54.

Ellison, D., & Paraham, D. (2001). Tumours of the autonomic nervous system. *American Journal of Clinical Pathology, 115*(S1), S46-S55.

Ema, M., Taya, S., Yokotani, N., Sogawa, K., Matsuda, Y., & Fujii-Kuriyama, Y. (1997, April 29). A novel bHLH-PAS factor with close sequence similarity to hypxia-inducible factor 1alpha regulates the VGEF expression and is potentially involved in lung and vascular development. *Proceedingings of the National Acadamy of Sciences, 94*(9), pp. 4273-8.

Epstein, F., Agmon, Y., & Brezis, M. (1994, April). Physiology of renal hypoxia. *Annals of the New York Academy of Science, 15*(718), pp. 72-81.

Epstein, A., Gleadle, J., McNeill, L., Hewtison, K., O'Rourke, J., Mole, D., et al. (2001, October 5). C. Elegans EGL-9 and mammalian homologs define a faimily of dioxygenases that regualte HIF by prolyl hydroxylation. *Cell, 107*(1), pp. 43-54.

Erez, N., Milyavsky, M., Goldfinger, N., Peles, E., Gudkov, A., & Rotter, v. (2002, October 3). Falkor, a novel cell growth regulator isolated by a functional genetic screen. *Oncogene, 21*(44), pp. 6713-21.

Erez, N., Stambolsky, P., Shats, I., Milyavasky, M., Kachko, T., & Rotter, V. (2004, June 4). Hypxia-dependent regulation of PHD1: cloning and characterisation of the human PHD1/EGLN2 gene promoter. *Final Short Reports in teh Fields of Molecular Biosciences Lett, 567*(2-3), 311-5.

Ernesberger, U., Reissmann, E., Mason, I., & Rohrer, H. (2000). The expression of dopamine beta-hydroxylase, tyrosien hydroxylase and Phox2 transcription factors in sympathetic neurons. *Mechanims of Development, 92*(2), pp. 169-77.

Estus, S., Zaks, W., Freeman, R., Gruda, M., Bravo, R., & Johnson, E. (1994, December). Altered gene expression in neurons during programmed cell death: identification of c-jun as necessary for neuronal apoptosis. *Journal of Cell Biology, 127*(6), 1717-27.

Feldser, D., Agani, F., Iyer, N., Pak, B., Ferreira, G., & Semenza, G. (1999, August 15). Reciprocal postitive regulation of hypoxia-inducible factor 1alpha and insulin-like growth factor 2. *Cancer Research, 59*(16), pp. 3915-8.

Finley, J., & Katz, D. (1992, February). The central organisation of the carotid body afferent projections to the brainstem of the rat. *Brain Research, 14*(572 (1-2)), 108-16.

Forgie, A., Kuehnel, F., Wyatt, S., & Davies, A. (2000, February). in vivo survival requirement of a subset of nodose ganglion neurons for nerve growth factor. *European Journa of Neurosicence, 12*(2), 670-6.

Formenti, F; Constantin-Teodosiu, D; Emmanuel, Y; Cheeseman, J; Dorrington, KL; Edwards, LM; Humphreys, SM; Lappin, TR; McMullin, MF; McNamara, CJ; Mills, W; Murphy, JA; I'Connor, DF; Percy, MJ; Ratcliffe, PJ; Smith, TG; Treacy, M; Frayn, KN; Robbins, PA. (2010, July 13). Regulation of human metabolism by hypoxia inducible factor. *Proceedings of the Nationatl Acadamy of Sciences, 107*(28), pp. 12722-7.

Galani, R., weiss, I., Cassel, J., & Kelche, C. (1998, November). Spatial memory, habituation and reactions to spatial and nonspatial changes in rat with selective lesions of the hippocampus, the entorhinal cortex or the subiculum. *Behavioral Brain Research, 96*(1-2), 1-12.

Kummer, W; Gibbins, IL; Stefan, P; Kapoor, V. *Cell Tissue Research, 261*(3), 595-606.

Garcia-Mata, R., Gao, Y., & Sztul, E. (2002, June). Hasseles with taking out the garbage: aggravating aggresomes. *Traffic, 3*(6), 388-96.

Gelderblom, M., Eminel, S., Herdegen, T., & Waetzig, V. (2004). c-Jun N-terminal kinases (JNKs) and the cytoskeleton - functions beyound neurodegeneation. *Internation Jounral of Developmental Neurosicence, 22*(7), 559-64.

Giaccia, A., Simon, M., & Johnson, R. (2004, September 15). The biology of hypoxia: the role of oxygen sensing in development, normal function and disease. *Genes and Development, 18*(18), pp. 2183-94.

Gorlach, A., Diebold, I., Schini-Kerth, V., Berchner-Pfannschmidt, U., Roth, U., Brandes, R., et al. (2001, July 6). Thrombin activates the hypoxia-inducible factor-1 signaling pathway in vascular smooth muscle cells: Role of the p33(phox0-containing NADPH oxidase. *Circulation Research, 86*(1), pp. 47-54.

Gray, H. (2008). *Gray's Anatomy of the Human Body.* Churchill Livingstone.

Ham, j. B., Whitfield, J., Pfarr, C., Lallemand, D., Yaniv, M., & Rubin, L. (1995, May). a c-Jun dominant negative mutant protects symapthetic neurons against programmed cell death. *Neuron, 14*(5), 927-39.

Hara, S., Hamada, J., Kobayaashi, C., Kondo, Y., & Imura, N. (2001, October 5). Expression and characterisation of hypoxia-inducible factor (HIF)-3alpha in human kidney:

suppression of HIF-mediated gene expression by HIF-3alpha. *Biochemical and Biophysical research Communications, 287*(4), pp. 808-13.

Hellwig-Burgel, T., Rutkowski, K., Metzen, E., Fandrey, J., & Jelkmann, W. (1999, September 1). Inerleukin-1beta and tumour necrosis factor-alpha stimulate DNA binding of hypoxia-inducible factor-1. *Bood, 94*(5), pp. 1561-7.

Herdegen, T., & Leah, J. (1998, December). Inducible and constitutive trnascription factors in the mammalian nervous system: control of gene expression by Jun, Fos, Krox and CREB/ATF proteins. *Brain Research Reviews, 28*(3), 370-490.

Hirsila, M., Koivunen, P., Gunzler, V., Kivirikko, K., & Myllyharju, J. (2003, August 15). Characterisation of the human prolyl 4-hydroxylase that modify the hypoxia-inducible factor. *Journal of Biological Chemistry, 278*(33), pp. 30772-80.

Hogenesch, J., Chan, W., Jackiw, V., Brown, R., Gu, Y., Pray-Grant, M., et al. (1997, March 28). Characterisation of a subset of the basic-helix-loop-PAS superfamily that ineracts with components of the dioxin signaling pathway. *Journal of Biological Chemistry, 272*(13), pp. 8581-93.

Hu, C., Iyer, S., Sataur, A., Covello, K., Chodosh, L., & Simon, C. (2006, May). Differential regulation of the transcriptional activities of HIF-1 alpha and HIF-2 alpha in stem cells. *Molecular and Cellular Biology, 26*(9), 3514-3526.

Huang, L., & Bunn, H. (1995, March). Regulation of eryethropoietin gene expression. *Current opinion in Heamatology, 2*(2), pp. 125-31.

Huang, Y., Hickery, R., Yeh, J., Liu, D., Dadak, A., Young, L., et al. (2004, July). Cardiac myocyte-specfic HIF-1alpha deletion alters vascularisation, energy availability, calcium flux and contractility in the normoxic heart. *Federation of American Societies For Experimental Biology, 18*(10), pp. 1138-40.

Iaccarino, G., Cipolletta, E., Fiorillo, A. A., Ciccarelli, M., Cimini, V., Koch, W., et al. (2002, July 16). Beta(2)-adrenergic receptor gene delivery to the endothelium corrects impaired adrenergic vasorelaxation in hypertension. *Circulation, 106*(3), 349-55.

Ivan, M., Kondon, K., Yang, H., Kim, W., Valiando, J., Ohh, M., et al. (2001, April 20). HIF alpha targted for VHL-medicated destruction by proline hydroxylation: implications for Oxygen sensing. *Science, 292*(5516), pp. 464-8.

Iyer, N., Koth, L., Agani, F., Leung, S., Laughner, E., Wenger, R., et al. (1998, January 15). Cellular and developmental control of oxygen homeostasis by hypoxia-inducible factor 1 alpha. *Genes and Development, 12*(2), pp. 149-62.

Jaakkola, P., Mole, D., Tian, Y., Wilson, M., Gielber, J., Gaskell, S., et al. (2001, April 20). Targeting of HIF-alpha to von Hippel-Lindau ubiquitylation complex by oxygen regulated proly hydroxylation. *Science, 5516*, pp. 468-72.

Jackson-Lewis, V., & Przedborski, S. (2007, February 15). Protocol for the MTPT mouse model of Parkinson's disease. *Nature Protocols*, pp. 141-151.

Jarrard, L. (1993, July). On the role of the hippocampus in learning and memory in the rat. *Behavioral and Neural Biology, 60*(1), 9-26.

Johnson, M. (1998, November). The beta-adrenoceptor. *American Journal of Critical Care Medicine, 158*(5 Pt 3), S146-53.

Kaelin, W. J., & Ratcliffe, P. (2008, May 23). Oxygen sensing by metazoans: the central role fo the HIF hydroxylase pathway. *Molecular Cell, 30*(4), 393-402.

Karavanov, A., Sainio, K., Palgi, J., Saarma, M., L, S., & Sariolo, H. (1995, November 21). Neurotrophin 3 rescures neuronal precursors from apoptosis and promotes neuronal differentiation in the embryonic metanephric kidney. *Porceedings of the National Accadamy of Sciences, 92*(24), 11279-83.

Katz, D., Markey, K., Goldstein, M., & Black, I. (1983, June). Expression of catecholaminergic charateristics by primary sensory neurons in the normal adult rat in vivo. *Proceedings of the National Acadamy of Sciences, 80*(11), 3526-30.

Kim, W., & Kaelin, W. (2004, December 15). Role of VHL gene mutation in human cancer. *Journal of Clinical Oncology, 22*(24), pp. 4991-5004.

Kirino, T. (1982, May 6). Delayed neuronal death in the gerbil hippocampus following ischaemia. *Brain Research, 239*(1), 57-69.

Kirjaka, O., Eranko, O., & Hervonen, A. (1973). Find structure o fthe rat carotid body after 6-methylprendisolone treatment. *International Journal of Neurosciences, 6*(3), 109-15.

Koivunen, P., Hirsila, M., Remes, A., Hassinen, I., Kivirikko, K., & Myllyharju, J. (2007, February 16). Inhibition of hypoxia-inducible factor (HIF) hydroxylases by citric acid cycle intermediates: possible links between cell metabolism and stabilisation of HIF. *Journal Biological Chemistry, 282*(7), 4524-32.

Kopito, R., & Sitia, R. (2000, September). Aggresomes and Russell bodies. Symptoms of cellular indigestion? *EMBO reports, 1*(3), 225-31.

Korkala, O., Eranko, O., & Hervonen, A. (1973). Fine structure of the rat carotid body after 6-methlprednisolone treatment. *Iinternational Journal of Neuroscience, 6*(3), 2109-15.

Kummer, W., Bachmann, S., Neuhuber, W., Hanze, J., & Lang, R. (1993, January). Tyrosine hydroxylase containing vagal afferent neurons in the rat nodose ganglion are independent from neuropeptide-Y-containing populations and project to the oesophagus and stomach. *Cell Tissue Research, 271*(1), 135-44.

Lando, D., Peet, D., Gorman, J., Whelan, D., Whitelaw, M., & Bruick, R. (2002, June 15). FIH-1 is an asparaginyl hydroxyalse enzyme what regulates the granscriptional activity of hypoxia-inducible factor. *Genes and Development, 16*(12), pp. 1466-71.

Lando, D., Peet, D., Whelan, D., Gorman, J., & Whitelaw, M. (2002, February 1). Asparagine hydroxylation of the HIF transactivation domain a hypoxic switch. *Scienced, 295*(5556), pp. 858-61.

Lee, S., Nakamura, E., Yang, H., Wei, W, Linggi, M., et al. (2005, August). Neronal apoptosis linked to Egln3 prolyl hydroxylase and familial phaeochormocyoma genes: developmental culling and cancer. *Cancer Cell, 8*(2), 155-167.

Lefkowitz, RJ, Rockman, H., & Koch, W. (2000, April 11). Catecholamines, Cardiac beta-adrenergic receptors and heart failure. *Circulation, 101*(14), 1634-7.

Levi-Montalcini, R., & Angeletti, P. (1968). Nerve growth factor. *Physiology Reviews*, 534-569.

Lieb, M., Menzies, K., Moschella, M. N., & Taubman, M. (2002). Mammalian EGLN genes have distinct patterns of mRNA expression and regulation. *Biochemistry and Cell Biology, 80*(4), 421-6.

Lipscomb, E., Patrick, D., Sarmiere, R., Crowder, R., & Freeman, S. (1999). Expression of the SM-20 gener promotes death in nerve growth factor dependent sympathetic neurons. *Journal of Neurochemistry, 73*(1), 429-432.

Lipsocomb, E., Sarmiere, P., & Freeman, R. (2001, February 16). SM-20 is a novel mitochondrial protein that causes caspase-dependent cell death in nerve growth factor-dependent neurons. *The Jounal of Biological Chemistry, 276*(7), 5085-92.

Loring, J., & Erickson, C. (1987, May). Neural crest cell migratory pathways in the trunk of the chick embryo. *Developmental Biology, 121*(1), pp. 220-36.

Madden, S., Galella, E., Riley, D., Bertelsen, A., & Beaudry, G. (1996, December 1). Induction of cell growth regulatory genes by p53. *Cancer Research, 56*(23), pp. 5384-90.

Maher, E., & Eng, C. (2002, October). The pressure rises: update on the genetics of phaeochromocytoma. *Human Molecular Genetics, 1*(11), 2347-54.

Mahon, P., Hirota, K., & Semenza, G. (2001, October 15). FIH-1: a novel protein that interacts with HIF-1 alpha and VHL to mediate repression of HIF-1 transcriptional activity. *Genes and Development, 15*(20), pp. 2675-86.

Maranchie, J., Vasselli, J., Riss, J., Bonifacino, J., Linehan, W., & Klausner, R. (2002, April). The contribution of VHL substrate binding and HIF1-alpha to the phenotype of VHL loss in renal cell carcinoma. *Cancer Cel, 1*(3), pp. 247-55.

Marcus, L. a. (1992). *Prenatal and neonatal physiology.* Saunders.

Martin, T., Irving, R., & Maher, E. (2007). The genetics of paragnaliomas: a review. *Clinical Otolaryngology, 32*(1), 7-11.

Maslim, J., Valter, K., Egensperger, R., Hollander, H., & Stone, J. (1997, August). Tissue oxygen during a critical developemental period controls the death and survival of photoreceptors. *Investigative Ophthalmology and Visual Science, 38*(9), 1667-77.

Masson, N., Appelhoff, r., Tuckerman, R., YM, T., Demol, H., Puype, M., et al. (2004, July 16). The HIF prolyl hydroxylase PHD3 is a potential substrate of the TRiC chaperonin. *FEBS Lett, 570*(1-3), 166-70.

Masson, N., Willam, C., Maxwell, P., Pugh, C., & Ratcliffe, P. (2001, September 17). Independent function of two destruction domains in hypoxia-inducible factor-alpha activated by prolyl hydroxylation. *European Molecular Biology Organisation, 17*(20), pp. 5197-206.

Maxwell, P., Dachs, G., Gleadle, J., Nicholss, L. H., Stratford, I., Hankinson, O., et al. (1997, July 22). Hypoxia-inducible factor-1 modulates gene expressinin solid tumours and

inflences angiogenesis and tumour growth. *Proceedings of the National Acadamy of Sciences, 94*(15), pp. 8104-9.

Maxwell, P., Wiesener, M., Chang, G., Clifford, S. V., Cockman, M., Wykoff, C., et al. (1999, May 20). The tumour suppressor protein VHL targets hypoxia-inducible factors for oxgyen-dependent proteolysis. *Nature, 399*(6733), pp. 271-5.

Maynard, M., Qi, H., Chung, J., Lee, E., Kibdib, Y., Hara, S., et al. (2003, March 28). Multiple splice variants of the human HIF-3 alpha locus are targets for the von Hippel-Landau E3 ubiquitin ligase complex. *Journal of Biological Chemistry, 278*(13), pp. 11032-40.

Mazzone, M. D., Leite de Oliveira, R., Loges, S., Schmidt, T., Jonckx, B., YM, T., et al. (2009, March 6). Heterozygous deficiency of PHD2 restors tumour oxgyenation and inhibits metastiasis via endothelial normalisation. *Cell, 136*(5), 839-51.

McMullin, M., Bareford, D., Campbell, P., Green, A., Harrison, C., Hunt, B., et al. (2005, July). Guidelines for the diagnosis, investigation and mangement of polycythaemia/erythocytosis. *British Journal of Haematology, 130*(2), pp. 174-195.

Menzies, K., Liu, B., Kim, W., Moschella, M., & Taubman, M. (2004, May 7). Regulation of the SM-20 prolyl hydroxylase gene in smooth msucle cells. *Biochemical and Biophysical Research Communications, 317*(3), 801-10.

Metzen, E., & Ratcliffe, P. (2004, March-April). HIF hydroxylation and cellular oxygen sensing. *The Journal of Biological Chemistry, 385*(3-4), 223-30.

Metzen, E., Berchner-Pfannschmidt, U., Stengel, P., Marxen, J., Stolze, I., Klinger, M., et al. (2003, April 1). Intracellular localisationof human HIF-1 alpha hydroxylases implications for oxygen sensing. *Journal of Cell Science, 116*(Pt 7), pp. 1319-26.

Minamishima, Y., Moslehi, J., Bardeesy, N., Cullen, D., Bronson, R., & Jr, K. W. (2008, March 15). Somatic inactivation of the PHD2 prolyl hydroxylase causes polycythemia and congestive heart failure. *Blood, 111*(6), 3236-44.

Percy, M., Beer, P., Campbell, G., Dekker, A., Green, A., Oscier, D., et al. (2008, June 1). Novel exon 12 mutaions in the HIF2 alpha gene associated with erythrocytosis. *Blood, 111*(11), pp. 5400-2.

Moon, E., Jeong, C., Jeong, J., Kim, K., Yu, D., Murakami, S., et al. (2004, February 18). Hepatitis B virus X protein induces angiogenesis by stabilising hypoxia-inducible factor 1alpha. *Federation of American Societies For Experimental Biology, 18*(2), pp. 382-4.

Nakayama, K., & Ronzai, Z. (2004, November). Siah: new players in the cellular response to hypoxia. *Cell Cycle, 3*(11), pp. 1345-7.

Nangaku, M., Sato-Yoshitake, R., Okada, Y., Noda, Y., Takemura, R., Yamazaki, H., et al. (1994, December 30). KIF1B, a novel microtubule plus end-directed monomeric motor protein for transport of mitochondria. *Cell, 79*(7), 1209-20.

Natarajan, R., Salloum, F., Fisher, B., Kukreja, R.. (2006, January 6). Hypoxia inducible factor-1 activation by prolyl 2-hydroxylase-2 silencing attenuates myocardial ishaemia reperfusion injury. *Circulation Research, 98*(1), 133-40.

Oehme, F., Ellinghaus, P., Kolkhof, P., Smith, T., Ramakrishanan, S., Hutter, J., et al. (2002, August 16). Overexpression of PH-4, a novel putative proline 4-hydroxylase modulates activity of hypoxia-inducible transcription faccotrs. *Biochemical and Biophysical Research Communications, 296*(2), 343-9.

Oehme, F., Ellinghaus, P., Kolkhof, P., Timothy, J., Shyam, R., Joachim, H., et al. (2002, August). Overexpression of PH-4, a novel putative proline 4-hydroxylase modulates

activity of hypoxia-inducible transcription factors. *Biochemical and Biophysical Research Communications, 296*(2), pp. 343-349.

Ohh, M., Park, C. I., Hoffman, M., Kim, T., Huang, L., Pavletich, N., et al. (2000, July). Ubiquitination of hypoxia-inducible facotr requires direct binding to the beta-domain of the von Hippel-Lindau protein. *Nature Cell Biology, 2*(7), pp. 423-7.

Onita, T., Ji, P., Xuan, J., Sakai, H., Kenetake, H., Maxwell, P., et al. (2002, February). Hypoxia-induced, perinecrotic expression of endothelial per-ARNT-Sim domain protein-1/hypoxia-inducible factor-2alpha correlates with tumour progression, vascularisation and focal macrophage infiltration in bladder cancern. *Clinical Cancer Research, 8*(2), pp. 471-80.

Oppenheim, R. (1991, March). Cell death during development of the nervous system. *Annual Reviews of Neuroscience, 14*, 453-501.

Paranen, M., Rapoport, S., Reis, D., Joh, T., Stolk, J., Linnoila, I., et al. (1984). Catecholamine-synthesising enzymes in the paraganglia of aged Fischer-344 rats. *Cell Tissue Research, 238*(2), pp. 217-20.

Park, S., Dadak, A., Haase, V., Fontana, L., Giaccia, A., & Johnson, R. (2003, July). Hypoxia-induced gene expression occurs soleyl through the action of hypoxia-inducible factor 1alpha: role of cytoplasmic trapping of HIF-2 alpha. *Molecular and Cellular Biology, 23*(14), 4959-71.

Partanen, M., Hervonen, A., & Rapoport, S. (1984). The ultrastructure of hypertrophied paraganglia in aged rats. *Journal of Anatomy, 139*(Pt4), pp. 619-626.

Pascual, O., Denavit-Saubie, M., Dumas, S., Kietzmann, T., Ghilini, G., Jacques, M., et al. (2001). Secective cardiorespiratory and catecholaminergic areas express the hypoxia-

inducible factor -1 alpha under in vivio hypoxia in rat brainstem. *European Journal of Neruoscience, 14*(12), 1981-1991.

Pastore, Y., Jelinek, J., Ang, S., Guan, Y., Liu, E., Jedlickova, K., et al. (2003, February 15). Mutations in the VHL gene in sporadica apparently congenital polycythemia. *Blood, 101*(4), pp. 1591-5.

Paxinos, G., & Watson, C. (1982). *Rat Brain Atlas.* Elsevier.

Peng, J., Zhang, L., Drysdale, L., & Fong, G. (2000, July 18). The transcription factor EPAS-1/hypoxia-inducible factor 2alpha plays and improtant role in vascular remodeling. *Proceedings of the National Acadamy of Sciences, 97*(15), pp. 8386-91.

Percy, M., Mooney, S., McMullin, M., Flores, A., Lappin, T., Lee, F. (2003, September 9). A common polymorphism in the Oxygen-dependent degradation (ODD) domain of hypoxia inducible factor-1 alpha (HIF-1 alpha) does not impair Pro-564 hydroxylation. *Molecular Cancer, 2*(31), pp. 1-7.

Percy, M., Furlow, P., Beer, P., Lappin, T., McMullin, M., Lee, S. (2007, September 7). A novel erythrocytosis-associated PHD2 mutation suggest the location of a HIF binding groove. *Blood, 110*(6), pp. 2193-6.

Percy, M.., Furlow, P., Lucas, G., Li, X., Lappin, T., McMullin, M., et al. (2008, January). A gain-of-function mutation in the HIF2A gene in familial erythrocytosis. *New Engleand Journal of Medicine, 77*(2), pp. 86-8.

Percy, M.., Zhao, Q., Flores, A., Harrison, C., Lappin, T., Maxwell, P., et al. (2006, January 17). A family with erythrocytosis establishes a role for prolyl hydroxylase domain protein 2 in oxygen homeostasis. *Proceedings of the National Acadamy of Sciences, 103*(3), 654-9.

Pugh, C., & Ratcliffe, P. (2003, June). Regulation of angiogenesis by hypoxia: role of the HIF system. *Nature Medicine, 9*(6), 677-84.

Rantanen, K., Pursiheimo, J., Hogel, H., Himanen, V., Metzen, E., & Jaakkola, P. (2008, May). Prolyl hydroxylase PHD3 activates oxygeg-dependent protein aggregation. *Molecular Biology of the Cell, 19*(5), 2231-40.

Ratan, R., Sddiq, A., Smirnova, N., Karpisheva, K., Haskwr-Layton, R., McConoughey, S., et al. (2007, December). Harnessing hypoxic adaptation to prevent, treat and repair stroke. *Journal of Molecular Medicine, 85*(12), 1331-8.

Raval, R., Lau, K., Tran, M., Sowter, H., Mandriota, S., Li, J., Li, J., Pugh, C., Maxwell, P., Harris, A., Ratcliffe, P. (2005, July). Contrasting properties of hypoxia-inducible factor (HIF-1) and HIF-2 in von Hippel-Lindau-associated renal cell carcinoma. *Molecular and Cellular Biology, 25*(13), pp. 5675-86.

Reinhardt, D. (1989, January). Adrenoceptors and the lung: their role in health and disease. *European Journal of Paediatrics, 148*(4), 486-93.

Richard, D., Berra, E., & Pouyssegure, J. (2000, September 1). Nonhypoxic pathway mediated induction of hypoxia-inducible factor 1alpha in vascular smooth muscle cells. *Journal of Bological Chemistry, 275*(35), pp. 26765-71.

Rohrbach, S., Simm, A., Pregla, R., Franke, C., & Katschinski, D. (2005). Agd-dependent increase of prolyl-4-hydroxylase domian (PHD) 3 expression in human and mouse heart. *Biogerontology, 6*(3), 165-71.

Rumsey, W., Pawlowski, M., Lejavardi, N., & Wilson, D. (1994, April). Oxygen pressure distribution in the heart in vivo and evalution of the ischaemic "border zone". *American Journal of Physiology, 266*(4 Pt 2), pp. H1676-80.

Ryan, H., Lo, J., & Johnson, R. (1998, June 13005-15). HIF-1alpha is required for solid tumour formation and embryonic vascularisation. *European Molecular Biology Organisation, 17*(11).

Sagawara, T., Fujimura, M., Morita-Fujimura, Y., Kawase, M., & Chan, P. (1999, November 15). Mictochondrial release of cytochrome c corresponds to the seletive vulnerability of hippocampla CA1 neurons in rats after transient global cerebral ischaemia. *Journal of Neuroscience, 19*((22)), RC39.

Santoro, M., Rosati, R., Grieco, M., Berlingieri, M., D'Amato, G., Franciscis, V., et al. (1990, October). The ret proto-oncogene is consistently expressed in human phaeochromocytoms and thyroid medullary carcinomas. *Oncogene, 5*(10), 1595-8.

Saulian, E., & Karin, M. (2002, May). AP-1 as a regulator of cell life and death. *Nature Cell Biology, 4(5)*, E131-6.

Schlisio, S., Kenchappa, R., Vredeveld, L. G., Stewart, R., Greulich, H., K, S., et al. (2008, April 1). The kinesin KIF1B beta acts downstream from EglN3 to induce apoptosis and is a potential 1p36 tumour suppressor. *Genes and Development, 22*(7), 884-93.

Schmidt-Kastner, R., & Freund, T. (1991). Selective vulnerability of the hippocampus in brain ischaemia. *Neurosicence, 40*(3), 599-636.

Schneider, M; Van Geyte, K; Fraisl, P; Kiss, J; Aragones, J; Mazzone, M; Mairbaurl, H; De Bock, K; Jeoung, NH; Mollenhauer, M; Georgiadou, M; Bishop, T; Roncal, C; Sutherland, A; Jordan, B; Gallez, B; Weitz, J; Harris, RA; Maxwell, P; Baes, M;. (2010, March). Loss of silencing of the PHD1 prolyl hydroxylase protects livers of mice against ischaemia/reperfusion injury. *Gastroenterology, 138*(3), 1143-54.

Schurek, H., Jost, U., Baumgartl, H., Bertram, H., & Heckmann, U. (1990, December). Evidence for a preglomerular oxygen diffusion shunt in rat renal cortex. *American Journal of Physiology, 259*(6 Pt 2), pp. F910-5.

Scortegagna, M., Ding, K., Oktay, Y., Gaur, A., Thurmond, F., Yan, L., et al. (2003, December). Multiple organ pathology, metabolic abnormalities and impaired homeostasis of reactive oxygen species in Epas1-/- mice. *Nature Genetics, 35*(4), pp. 331-40.

Seagal, R., & Greenberg, M. (1996). Intracellular signaling pathways activated by neurotrophic factor. *Annual reviews of Neuroscience, 19*, 463-89.

Selak, M., Armour, S., MacKenzie, E., Boulahbel, H., Watson, D., Mansfield, K., et al. (2005, January). Succinate links TCA cycle dysfunction to oncogenesis by inhibiting HIF-alpha prolyl hydroxylase. *Cancer Cell, 7*(1), 77-85.

Selak, MA, Duran, R., & Gottlieb, E. (2006). Redox stress is not essential for pseudo-hypoxic phenotype of succinate dehydrogenase deficient cells. *Biochim Biophys Acta, 1157*(5-6), 567-72.

Semenza, G. (2001, April). HIF-1 and mechanisms of hypoxia sensing. *Current Opinions in Cell Biology, 13*(2), 161-71.

Semenza, G. (2002). HIF-1 and tumour progression: pathophysiology and therapeutics. *Trends in Molecular Medicine, 8*(4 Suppl), S62-7.

Semenza, G. (2007, December). Hypoxia and human disease. *The Journal of Molecular Medicine, 85*(12), 1293-4.

Seth, P., Krop, I., Porter, D., & Polyak, K. (2002, Januray 24). Novel oestrogen and tamoxifen induced gene identification by SAGE Serial Analysis of Gene Expression. *Oncogene, 24*(5), pp. 836-46.

Shaimad, H., Umehara, S., Monobe, Y., Hachitanda, Y., Nakagawa, A., Goto, S., et al. (2001, November). International neuroblastoma pathology classification for prognostic evaluation of patients with peripheral neuroblastomic tumours: a report from the Childrens' Cancer Group. *Cancer, 92*(9), 2451-61.

Shaulian, E., & Karin, M. (2002, May). AP-1 as a regulator of cell life and death. *Nature Cell Biology, 4*(5), E131-6.

Shimanda, H., Ambros, I., Dehner, L., Hata, J., Joshi, W., Roald, B., et al. (1999, July). The International Neuroblastoma Pathology Classification (th Shimada system). *Cancer, 86*(2), 364-72.

Smith, J., Ellenberger, H., Ballanyi, K., Richter, D., & Feldman, J. (1991, November 1). Pre-Botzinger comples: a brainstem region that may generate respiratory rhythm in mammals. *Science, 254*(5032), 726-9.

Smolen, A., Wright, L., & Cunningham, T. (1983). Neruon number in the superior cervical symapthetic ganglion of the rat: a critical comparison of methods for cell counting. *Journal of Neurocytology, 12*(5), 739-750.

Soilleux, E., Turley, H., Tian, Y., Pugh, C., Gatter, K., & Harris, A. (2005, December). Use of novel monoclonal antibodies to determine the expression and distribution of the hypoxia regulatory factors PHD-1, PHD-2, PHD-3 and FIH in normal and neoplastic human tissues. *Histopathology, 47*(6), 602-10.

Soliz, J., Joseph, V., Soulage, C., Becskei, C., Vogel, J., Pequignot, J., et al. (2005, October 15). Erythropoietin regulates hypoxic ventilation in mice by interacting with brainstem and carotid bodies. *Journal of Physiology, 568*(Pt 2), 559-71.

Straub, J., Lipscomb, E., Yoshida, E., & Freeman, R. (2003, April). Induction of SM-20 in PC12 cells leads to increased cytochrome c levels, accumulation of cytochrome c in

the cytosol and caspase-dependent cell death. *Journal of Neurochemistry, 82*(2), 318-28.

Stroka, D., Burkhardt, T., Desbaillets, I., Wenger, R., Neil, D., Bauer, C., et al. (2001, November). HIF-1 is expressed in normoxic tissue and displays an organ-specific regulation under systemic hypoxia. *Federation of American Societies For Experimental Biology, 15*(13), pp. 2445-53.

Sugawara, T., Kawase, M., Lewen, A., Noshita, N., Gasche, Y., Fujimura, M., et al. (2000, September 22). Effect of hypotension severity on hippocampal CA1 neuros in rat global ischaemia model. *Brain Research, 877*(2), 281-7.

Takaya, K., Yoshimasa, T., Arai, H., Tamura, N., Miyamoto, Y., Itoh, H., et al. (1996, October). Expression of the RET proto-oncogene in normal human tissues, phaeochromocytomas and other tumours of neural crest origin. *Journa of Molecular Medicine*, 617-21.

Takeda, K. C., & Fong, G. (2007, August 14). Essential role for prolyl hydroxylase domain protein 2 in oxygen homeostasis of the vasuclar system. *Circulation, 116*(7), 774-81.

Takeda, K., Ho, V., Takeda, H., Duan, L., Nagy, A., & Fong, G. (2006, November). Placental but not heart defects are associated with elevated hypoxia-inducible factor alpha levels in mice lacking prolyl hydroxylase domain protein 2. *Molecular and Cellular Biology, 26*(2), 8336-46.

Talks, K., Turley, H., Gatter, K., Maxwell, P., Pugh, C., Ratcliffe, P., et al. (2000, August). The expression and distribution of hypoxia-inducible factors HIF-1alpha and HIF-2alpha in normal human tissues, cancers and tumour-associated macrophages. *American Journal of Pathology, 157*(2), pp. 411-21.

Taylor, M. (2001, September 5). Characterisation and comparative analysis of EGLN gene family. *Gene, 275*(1), pp. 125-32.

Tian, H., Hammer, R., Matsumoto, A., Russell, D., & McKnight, S. (1998, Novmember 1). The hypoxia-response transcritpion factor EPAS 1 is essential for catecholamine homeostasis and protection against heart failure during embryonic development. *Gens and Development, 12*(21), pp. 3320-4.

Tian, H., McKnight, S., & Russell, D. (1997, January 1). Endothelial PAS domian protein 1 (EPAS1), a transcription factor selectively expressed in endothelial cells. *Genes and Development, 11*(1), 72-82.

Tian, Y., Mole, D., Ratcliffe, P., & Gleadle, J. (2006, July 1). Characterisation of different isoforms of the HIF prolyl hydroxylase PHD1 generated by alternative initiation. *Biochemical Journal, 397*(1), 179-86.

Tian, Y., Mole, D., Ratcliffe, P., & Gleadle, J. (2006, July 1). Characterisation of different isoforms of the HIF prolyl hydroxylase PHD1 generated by alternative initiation. *Biochemical Journal, 397*(1), 179-86.

Tomlinson, A., Durbin, J., & Coupland, R. (1987, March). A quantitative analysis of rat sdrenal chromaffin tissue: morphometric analysis at tissue adn cellular level correlates with cathecholamine content. *Neuroscience, 20*(3), 895-904.

Tomlinson, A., Durbin, J., & Coupland, R. (1987, March). A quantitative analysis of rat adrenal chrmoaffin tissues: morphometic analysis at tissue and cellular level correlated with catecholamine content. *Neruoscience, 20*(3), 895-904.

Tuckerman, J., Zhao, Y., Hewitson, K., Tian, Y.-M., Pugh, C., Ratcliffe, J., et al. (2004, October 576). Determination and comparision of the specific activity of the HIF-Prolyl hydroxylases. *FEBBS Letters, 576*(1-2), pp. 145-150.

Verwoerd, C., & Van Oostrom, C. (1979). Cephalic neural crest and placodes. *Advances in Anatomy Embryology and Cell Biology, 58*, pp. 1-75.

Vogel, K., Brannan, C. J., Copeland, N., & Parada, L. (1995, September 8). Loss of neurofibromin resuls in neurotrphin-independent survival of embyonic sensory and sympathetic neurons. *Cell, 82*(5), 733-42.

Wang, G., & Semenza, G. (1993, December). Desferrioxamine induces erythropoietin gene expression and hpoxia-inducible factor 1 DNA-binding activity: implications for models of hypoxia signal transduction. *Blood, 82*(12), pp. 3610-3615.

Wang, G., & Semenza, G. (1995, January 20). Purification and characterisation of hypoxia-inducible factor 1. *Journal of Biological Chemistry, 270*(3), pp. 1230-7.

Watson-Wright, W., Boudreau, G., Cardinal, R., & Armour, J. (1991, November). Beta 1- and beta 2-adrenoceptor subtypes in canine intrathoracic efferent sympathetic nervous system regulating the heart. *American Journal of Physiology, 261*(5 Pt 2), R1269-75.

Wax, S., Rosenfield, C., & Taubman, M. (1994, April 29). Identification of a novel growth factor-responsive gene in vascular smooth muscle cells. *Journal of Biological Chemistry, 269*(17), pp. 13041-7.

Wenger, R., & Gassmann, M. (1997, July). Oxygen(es) and the hypoxia-inducible factor-1. *The Journal of Biological Chemistry, 378*(7), pp. 609-16.

Whalen, W., Ganfield, R., & Nair, P. (1970, May-June). Effects of breathing oxygen or oxygen and carbon dioxide and of the injection of neurohumors on the PO2 of cat cerebral cortex. *Stroke*, pp. 194-200.

Wiesener, M., Jurgensen, J., Rosenberger, C., Scholze, C., Horstrup, J., Warnecke, C., et al. (2003, February). Widespread hypoxia-induced expression of HIF-2alpha in distinct cell populations of different organs. *17*(2), pp. 271-3.

Wiesener, M., Turley, H., Allen, W., Eckardt, K., Talks, K., Wood, S., et al. (1998, October 1). Induction of the endothelial PAS domian protein-1 by hopoxia: characterisation and comparison with hpoxia-inducible factor-1 alpha. *Blood, 92*(7), 2260-8.

Willam, C., Maxwell, P., Nichols, L., Lygate, C., Tian, Y., Bernhardt, W., et al. (2006, July). HIF prolyl hydroxylase in the rat; organ distribution and changes in expression following hypoxia and coranary artery ligation. *Journal of Molecular and Cellular Cardiology, 41*(1), 68-77.

Willam, C., Nicholss, L., Ratcliffe, P., Pugh, C., & Maxell, P. (2004). The prolyl hydroxylase enzymes that act as oxygen sensors regulating destruction of hypoxia-inducible factor alpha. *Advances in Enzyme Regulation, 44*, 75-92.

Wolfle, D., Schmidt, H., & Jungermann, K. (1983, October 3). Short-term modulation of glycogen metabolism, glycolysis and gluconeogenesis by physiological oxygen concentrations in hepatocyte cultures. *European Journal of Biochemistry, 135*(3), pp. 405-12.

Wright, L., Cunningham, T., & Smolen, A. (1983). Developmental neuron death in the rat superior cervical sympathetic ganglion: cell counts and ultrastructure. *Journal of Neurocytology, 12*(5), 727-38.

Xie, L., Xiao, K., Whalen, E., Forrester, M., Freeman, R., Fong, G., et al. (2009, July 7). Oxygen-regulated beta (2)-adrenergic receptor hydroxylation by EGLN3 and ubiquitylation by pVHL. *Science Signaling, 2*(78), RA33.

Yasumoto, K., Kowata, Y., Yoshida, A., Torii, S., & Sogawa, K. (2009, May). Role of the intracellular localisation of HIF-prolyl hydroxylases. *Biochmimica et Biophysica Acta, 1793*(5), 792-7.

Zhang, Z., Ren, J., Stammers, D., Baldwin, J., Harloss, K., & Schofield, C. (2000, February). Structural origins of the selectivity of the trifunctional oxygenases clavaminic acid synthase. *Nature Structural Biology, 7*(2), pp. 127-33.

Zhao, C., Takita, J., Tanaka, Y., Setou, M., Nakagawa, T., Takeda, S., et al. (2001, June 1). Charcot-Marie-Tooth disease type 2A caused by mutation in a microtubule motor KIF1B beta. *Cell, 105*(5), 587-97.

Zhou, J., Gunsior, M., Bachmann, B., Townsend, C., & Solomon, E. (1998). Substrate binding to the alpha-ketoglutarate-dependent non-heme iron enzyme clavaminate synthase 2: coupling mechanism of oxidative decarboxylation and hydroxylation. *Journal of American Chemical Society, 120*, pp. 13539-13540.